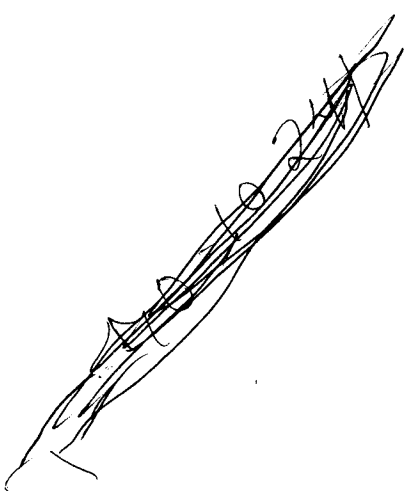


NORTHROP VENTURA

NASA CR-66879 S366A



WIND TUNNEL AND FREE FLIGHT
INVESTIGATION OF
ALL-FLEXIBLE PARAWINGS
AT SMALL SCALE

N70-19796

By

E. M. Linhart and W. C. Buhler

Distribution of this report is provided in the interest
of information exchange. Responsibility for the contents
resides in the author or organization that prepared it.

Prepared under Contract No. NAS 1-7467 by

NORTHROP CORPORATION, VENTURA DIVISION

Newbury Park, California 91320

for

NATIONAL AERONAUTICS AND SPACE ADMINISTRATION

June 1969

WIND TUNNEL AND FREE FLIGHT
INVESTIGATION OF
ALL-FLEXIBLE PARAWINGS
AT SMALL SCALE

Prepared by:

E. M. Linhart and W. C. Buhler
June 1969

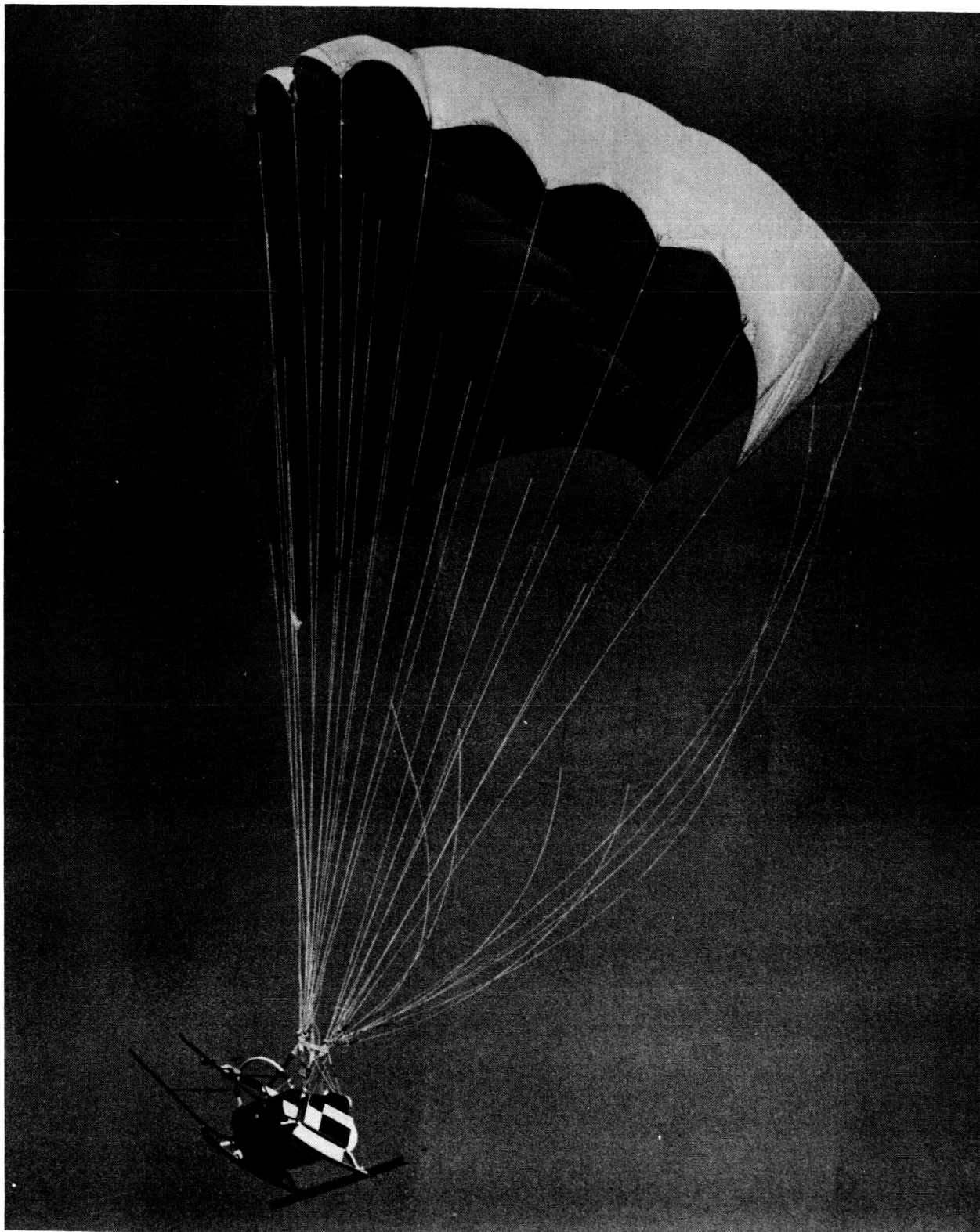
Approved:


R. G. Lemm, Chief
Systems Engineering Group


J. H. Moeller
Parawing Chief Project Engineer

NORTHROP CORPORATION, VENTURA DIVISION
1515 Rancho Conejo Boulevard
Newbury Park, California 91320

NVR-6366A



Small-Scale, Single-Keel Parawing In Controlled Flight

CONTENTS

<u>SUMMARY</u>	xi
<u>INTRODUCTION</u>	xii
<u>SYMBOLS</u>	xiii
<u>WIND TUNNEL TEST PROGRAMS</u>	1
INTRODUCTION.....	1
LANGLEY WIND TUNNEL TEST PROGRAM.....	2
Basis for Selecting Reefing Sequences for Test....	2
Reefing System Design Criteria.....	3
Test Model Configurations.....	5
Materials.....	15
Wind Tunnel Test Procedure.....	29
Summary of Wind Tunnel Gliding Performance Characteristics.....	35
General Discussion and Evaluation of the Reefed Configurations.....	38
Selection of Reefing System for Further Testing.....	49
Detailed Description of the Selected Reefing Systems.....	50
Representative Data for the Selected Reefing Systems.....	54
AMES WIND TUNNEL TEST PROGRAM.....	64
General.....	64
Test Model Configurations.....	66
Ames Wind Tunnel Test Procedures.....	71
Summary of Test Results.....	72
<u>GENERAL DISCUSSION OF TETHERED FLIGHT CHARACTERISTICS OBSERVED DURING WIND TUNNEL TESTS</u>	80
Single Keel Parawing.....	80
Twin Keel Parawing.....	83
<u>APPROACH USED FOR DYNAMIC SCALING</u>	86
<u>FREE FLIGHT GLIDING PERFORMANCE TESTS</u>	91
TEST MODELS.....	91
Description of Twin Keel Parawings.....	92
Description of Single Keel Parawings.....	92
Parawing Materials.....	100
Harness and System Rigging.....	100

CONTENTS
(Continued)

TEST PROCEDURES FOR FREE FLIGHT GLIDING	
PERFORMANCE TESTS.....	100
General.....	100
Trim Verification Tests.....	106
Flight Performance and L/D Modulation Tests.....	106
Turn Rate Tests.....	108
SUMMARY OF SMALL SCALE FREE FLIGHT TESTS.....	109
TEST RESULTS.....	109
L/D Performance Test Results.....	109
Discussion of Free Flight L/D Performance Test Results.....	115
Free Flight Turn Rate Tests.....	119
Discussion of Free Flight Turn Rate Test Data.....	124
Discussion of Flight Handling Qualities.....	126
Comparison of Performance in Free Flight and Wind Tunnel Tethered Flight.....	127
<u>FREE FLIGHT DEPLOYMENT TESTS.....</u>	131
PLANNED AND ACTUAL DEPLOYMENT TESTS.....	132
TEST PROCEDURE.....	132
TEST MODELS.....	135
PARAWING REEFING SYSTEMS.....	135
Single Keel Reefing System, Version I.....	138
Single Keel Reefing System, Version II.....	138
Single Keel Reefing System, Version III.....	141
Twin Keel Reefing System, Version I.....	143
Twin Keel Reefing System, Version II.....	143
VARIATIONS IN REEFING SYSTEMS USED DURING DEPLOYMENT TESTS.....	145
Single Keel Parawing Deployment Tests.....	145
Twin Keel Parawing Deployment Tests.....	148
DISCUSSION OF FLIGHT DEPLOYMENT TEST RESULTS.....	149
General Discussion of Parawing Behavior During the Reefing Sequence.....	149
Opening Loads.....	151
Parawing Geometry During the Opening Sequence..	165
Predicted Loads for Hypothetical 5000 Pound System.....	170
Suspension Line Loads.....	173
Reefing Line Loads.....	186

CONTENTS
(Continued)

<u>CONCLUDING REMARKS</u>	188
<u>APPENDIX A TEST VEHICLES AND INSTRUMENTATION</u>	191
<u>REFERENCES</u>	200
 TABLES	
1. Single Keel Reefed Configurations and Disreef Sequences.....	6
2. Twin Keel Reefed Configurations and Disreef Sequences.....	7
3. Summary of Parawing Model Configurations....	8
4. Summary of Performance Data from Wind Tunnel Tether Tests.....	36
5. Qualitative Evaluation of Single Keel Parawing Reefing Systems.....	46
6. Qualitative Evaluation of Twin Keel Parawing Reefing Systems.....	47
7. Single Keel Composite Line Load Distribution at Deployment.....	65
8. Twin Keel Line Load Distribution at Deployment.....	65
9. Summary of Gliding Performance Measured During Ames Wind Tunnel Tests.....	73
10. Dynamic Similitude Relationships.....	90
11. Suspension Line Lengths and Locations for Wings Flown in Gliding Performance Tests..	99
12. Parawing Materials.....	104
13. Small Scale Parawing Free Flight Test Program.....	110
14. Summary of Gliding Flight Data.....	116
15. Small Scale Parawing Deployment Tests.....	133
16. Deployment Test Preflight Suspension Line Lengths - Single Keel.....	136
- Twin Keel.....	137
17. Single Keel Deployment Tests.....	146
18. Twin Keel Deployment Tests.....	147
19. Summary of Small Scale Deployment Data.....	154
20. Summary of Load Factor Data.....	156
21. Summary of First Stage Filling Time.....	160
22. Intermediate Scale Opening Loads Predictions Based on Small Scale Test Data	172
23. Reefing Line Load Ratio Data.....	187

CONTENTS
(Continued)

FIGURES

Figure

1.	Single Keel Wind Tunnel Model Basic Planform and Model S-1 Canopy Construction ...	10
2.	Single Keel Wind Tunnel Model Basic Planform and Model S-2 Canopy Construction.....	11
3.	Single Keel Model S-3 Planform and Canopy Construction.....	13
4.	Twin Keel Wind Tunnel Model Basic Planform and Models T-1 and T-2 Canopy Construction....	14
5.	Twin Keel Model T-3 Planform and Canopy Construction.....	16
6.	Single Keel Wind Tunnel Model Line Location and Length Ratios.....	17
7.	Single Keel Wind Tunnel Model Line Location and Length Ratios.....	18
8.	Single Keel Wind Tunnel Model Line Location and Length Ratios.....	19
9.	Single Keel Wind Tunnel Model Line Location and Length Ratios.....	20
10.	Single Keel Wind Tunnel Model Line Location and Length Ratios.....	21
11.	Single Keel Wind Tunnel Model Line Location and Length Ratios.....	22
12.	Twin Keel Wind Tunnel Model Line Location and Length Ratios.....	23
13.	Twin Keel Wind Tunnel Model Line Location and Length Ratios.....	24
14.	Twin Keel Wind Tunnel Model Line Location and Length Ratios.....	25
15.	Twin Keel Wind Tunnel Model Line Location and Length Ratios.....	26
16.	Twin Keel Wind Tunnel Model Line Location and Length Ratios.....	27
17.	Twin Keel Wind Tunnel Model Line Location and Length Ratios.....	28
18.	Tethered Gliding Flight Test Setup.....	30, 31
19.	T-Bar Model Attachment Fixture.....	32
20.	Deployment Test Setup.....	34
21.	Single Keel Model S-1G Inflated in Langley full-scale tunnel.....	39
22.	Single Keel Model S-1G Aerodynamic Performance.....	40

CONTENTS
(Continued)**Figure**

23.	Single Keel Model S-2 Inflated in Langley full-scale tunnel.....	41
24.	Single Keel Model S-2 Aerodynamic Performance.....	42
25.	Twin Keel Model T-1E Inflated in Langley full-scale tunnel.....	43
26.	Twin Keel Model T-1E Aerodynamic Performance.....	44
27.	Planforms of Selected Single Keel Reefing System.....	51
28.	Planforms of Selected Twin Keel Reefing System.....	53
29.	Typical Single Keel Wind Tunnel Model First Stage C_D Histories.....	55, 56
30.	Typical Single Keel Parawing Wind Tunnel Model Disreef Sequence.....	57
31.	Typical Twin Keel Wind Tunnel Model First Stage C_D Histories.....	58
32.	Typical Twin Keel Parawing Wind Tunnel Model Disreef Sequence.....	59
33.	First Stage Reefed Drag Coefficient vs. Reefing Line Length Ratio.....	61
34.	First Stage Filling Time vs. Inverse of Reefing Ratio Squared.....	63
35.	Flat Pattern Details of the 15-ft ℓ_K Single Keel Parawing, Model S-2A.....	67
36.	Flat Pattern Details of the 24 ft ℓ_K Single Keel Parawing Model.....	68
37.	Flat Pattern Details of 22.7-ft ℓ_K Twin Keel Parawing Model Without Ripstop Tapes...	69
38.	Flat Pattern Details of 22.7-ft ℓ_K Twin Keel Parawing Model With Ripstop Tapes.....	70
39.	Performance Data for 15-ft ℓ_K Single Keel Parawing (Model S-2A).....	74
40.	Performance Data for 24 ft ℓ_K Single Keel Parawing.....	75
41.	Performance Data for 22.7 ft ℓ_K Twin Keel Parawing.....	76
42.	Performance Data for 22.7 ft ℓ_K Twin Keel Parawing With Ripstop Tapes.....	77
43.	Comparison of Data for a 15-ft ℓ_K Single Keel Parawing Tested in the Ames and Langley Full Scale Wind Tunnels (Model S-2A).....	78
44.	Comparison of Test Data for Two Twin Keel Parawings with Different Methods of Construction.....	79

CONTENTS
(Continued)

Figures

45.	L/D vs. Tip Line Length Ratio for 24 ft 1K Single Keel Model.....	82
46.	L/D vs. Dynamic Pressure for Two Typical Single Keel Models.....	82
47.	L/D vs. Tip Line Length Ratio for Typical Twin Keel Model.....	85
48.	L/D vs. Dynamic Pressure.....	87
49.	Twin Keel Parawing, 36 Line Version.....	93
50.	Twin Keel Parawing, 44 Line Version.....	94
51.	Canopy Seam Construction.....	95
52.	Suspension Line Attachment - Leading Edge, Trailing Edge and Keel.....	96
53.	Suspension Line Attachment - Tip.....	97
54.	Twin Keel Suspension Line Arrangement.....	98
55.	Single Keel Parawing 32-Line Version (8 Trailing Edge Lines).....	101
56.	Single Keel Parawing 40-Line Version (8 Trailing Edge Lines).....	102
57.	Single Keel Suspension Line Arrangement.....	103
58.	Wing/Test Vehicle Harness Rigging.....	105
59.	Helicopter Drop Sequence of Events.....	107
60.	L/D versus Rear Keel Line Control Deflection for 36-Line Twin Keel Model.....	111
61.	L/D versus Rear Keel Line Control Deflection for 44-Line Twin Keel Model.....	112
62.	L/D versus Rear Keel Line Control Deflection for 32-Line Single Keel Model.....	113
63.	L/D versus Rear Keel Line Control Deflection for 40-Line Single Keel Model.....	114
64.	Maximum L/D vs. Wing Loading for the Twin Keel Models.....	118
65.	Turn Rate versus Tip Control Line Deflection for Single Keel, 32-Line Model.....	120
66.	Turn Rate versus Tip Control Line Deflection for Single Keel, 40-Line Model.....	121
67.	Turn Rate versus Tip Control Line Deflection for Twin Keel, 36-Line Model.....	122
68.	Turn Rate versus Tip Control Line Deflection for Twin Keel, 44-Line Model.....	123
69.	Slope of Turn Rate vs. Tip Control Line Deflection as a Function of Test Weight....	125
70.	Comparison of Free-Flight and Wind Tunnel Gliding Performance for 32-Line Single Keel Parawing.....	128

CONTENTS
(Continued)

Figures

71.	Comparison of Free-Flight and Wind Tunnel Gliding Performance for 36-Line Twin Keel Parawing.....	129
72.	Sequence of Parawing Test Events.....	134
73.	Schematic of Single Keel Reefing Version I....	139
74.	Schematic of Single Keel Reefing Version II...	140
75.	Schematic of Single Keel Reefing Version III..	142
76.	Twin Keel Reefing Line Arrangement.....	144
77.	Force and Dynamic Pressure Histories for a Typical Single Keel Parawing Deployment Sequence (Test 105S).....	152
78.	Force and Dynamic Pressure Histories for a Typical Twin Keel Parawing Deployment Sequence (Test 105T).....	153
79.	First Stage Load Factor (C_K) vs. Reefing Ratio.....	158
80.	First Stage Filling Time vs. Inverse of Reefing Ratio Squared.....	161
81.	First Stage Load Factor (C_K) vs. Filling Time.....	162
82.	Filling Time vs. Line Stretch Velocity.....	164
83.	Disreefing Sequence Geometry, Test 105T.....	166
84.	Disreefing Sequence Geometry, Test 106S.....	167
85.	Drag-Area Ratio in First Reefed Stage vs. Filling Time, Test 105T.....	168
86.	Drag-Area Ratio in First Reefed Stage vs. Filling Time, Test 106S.....	169
87.	Single Keel, Stage 1 Suspension-Line Load Ratio Data.....	174
88.	Single Keel, Stage 2 Suspension-Line Load Ratio Data.....	175
89.	Single Keel, Stage 3 Suspension-Line Load Ratio Data.....	176
90.	Single Keel, Stage 4 Suspension-Line Load Ratio Data.....	177
91.	Single Keel, Stage 5 Suspension-Line Load Ratio Data.....	178
92.	Twin Keel, Stage 1 Suspension-Line Load Ratio Data.....	179
93.	Twin Keel, Stage 2 Suspension-Line Load Ratio Data.....	180
94.	Twin Keel, Stage 3 Suspension-Line Load Ratio Data.....	181
95.	Twin Keel, Stage 4 Suspension-Line Load Ratio Data.....	182
96.	Twin Keel, Stage 5 Suspension-Line Load Ratio Data.....	183

**CONTENTS
(Continued)**

Figures

97. Weight Vehicle.....	193
98. Controllable Vehicle - El Mirage Tests.....	195
99. L/D Indicator.....	197
100. Small Scale Bomb Vehicle - El Centro Tests....	199

WIND TUNNEL AND FREE FLIGHT INVESTIGATION
OF ALL-FLEXIBLE PARAWINGS AT SMALL SCALE

By E. M. Linhart and W. C. Buhler
Northrop Corporation, Ventura Division

SUMMARY

This report presents the results of several types of tests of small scale, all flexible parawings. These include wind tunnel tests conducted in the Langley Research Center's 30 ft by 60 ft full scale tunnel and the Ames Research Center's 40 ft by 80 ft tunnel, gliding flight tests conducted at El Mirage Dry Lake, California, and deployment tests conducted at the DOD Joint Parachute Test Facility, El Centro, California.

Two parawing designs were tested: the single keel and the twin keel models. Maximum lift-to-drag ratios measured in wind tunnel tests were in the range of 2.5 to 2.7 for the single keel models and 3.2 to 3.4 for the twin keel models. Free flight gliding tests indicated maximum lift-to-drag ratios 10 to 15 percent less than those measured in the wind tunnels, due at least in part to the added drag of the test vehicles. Wing tunnel tests showed that maximum lift-to-drag ratio is strongly influenced by the length of the tip suspension lines for a given line length rigging, both for single keel and twin keel models.

Deployment tests in the Langley wind tunnel and at El Centro showed the need for a five stage deployment process in order to maintain deployment decelerations at or below 3 g's for the specified deployment envelope. Furthermore, the El Centro tests demonstrated the practicality of multi-stage parawing reefing systems and confirmed by scaled testing, the feasibility of deploying larger parawings with payloads of 5000 pounds at dynamic pressures up to 100 psf and altitudes up to 18,000 ft.

INTRODUCTION

A deployable aerodynamic deceleration device capable of controllable gliding flight is a promising approach to the problem of making land landings with manned spacecraft. A candidate design for this use, called the "All-Flexible Parawing", has been developed by the NASA Langley Research Center. References 1 through 5 report the results of wind tunnel investigations of several single keel and twin keel parawing configurations. Further parawing technology development is being carried out by Ventura Division of Northrop Corporation under NASA Contract NAS 1-7467, administered by Langley Research Center. The overall plan is to develop progressively larger parawings, called "small", "intermediate", and "full" scale, respectively. The small scale parawing test phase of the program constitutes the subject of this report.

Two small scale parawing planforms were tested, a single keel model and a twin keel model. The small scale effort may be divided into four phases:

- a. Wind tunnel tests of 156 sq ft single and 174 sq ft twin keel parawings in the Langley Research Center full scale (30 ft by 60 ft) wind tunnel.
- b. Wind tunnel tests of a 156 sq ft single keel parawing and 400 sq ft single and twin keel parawings in the Ames full scale (40 ft by 80 ft) wind tunnel.
- c. Free flight gliding performance tests of 400 sq ft single keel and twin keel parawings at El Mirage Dry Lake (near Edwards AFB, California).
- d. Deployment and uncontrolled gliding tests of 400 sq ft single and twin keel parawings at El Mirage Dry Lake, California and at the DOD Para-Chute Test Facility, El Centro, California.

SYMBOLS

b_o	flat pattern wing span
c_D	drag coefficient - drag/ qS_W
c_K	load factor - peak stage force/(reference stage drag area) (q at start of stage)
c_L	lift coefficient - lift/ qS_W
c_R	resultant force coefficient - $\sqrt{c_L^2 + c_D^2}$
d	diameter
F	force
G	ratio of acceleration to earth gravity
h	height above mean sea level
ℓ	length of suspension line from bottom of skirt or keel band to center of top cross bar of link to which suspension line is attached
ℓ_K	reference keel length
ℓ_{RL}	effective reefing line length, including end attachments for non-continuous reefing lines
ℓ_{RL}/ℓ_K	effective reefing ratio
L/D	lift to drag ratio
L.E.	leading edge
p	differential air pressure across cloth porosity test specimen
q	dynamic pressure, psf
r	radius
SK	single keel parawing type
S_W	reference area of parawing = $0.69148 \ell_K^2$ for single keel models = $0.7726 \ell_K^2$ for twin keel models
T.E.	trailing edge
TK	twin keel parawing type
t	time
t_f	time from line stretch to maximum projected diameter of first reefed stage
t_{pl}	time from line stretch to peak load
W_t	total system weight
W_t/S_W	canopy unit loading (wing loading)

X	distance along leading edge or keel from theoretical apex of nose, or distance along trailing edge from rear end of keel
δ	movement of tip control line or aft keel control line from neutral position
Λ_0	flat pattern leading edge sweep
ρ	mass density of air

SUBSCRIPTS

\circ	initial condition, flat pattern dimension
RK	rear keel line(s)
RL	reefing line
T	tip suspension line
t	total
W	wing, parawing

NOTE: Symbols used in scaling relationships are defined in Table 10.

WIND TUNNEL TEST PROGRAMS

INTRODUCTION

This section of the report summarizes the results of two wind tunnel test programs. These test programs were conducted in the Langley full-scale tunnel and the Ames Research Center 40 ft by 80 ft wind tunnel. The primary objectives of the Langley tests were to:

1. Determine the effects of various structural features of the wing and rigging geometry on the aerodynamic performance of the basic single keel and twin keel parawing configuration.
2. Evaluate various reefing configurations in terms of such parameters as aerodynamic behavior, drag coefficients, opening characteristics, suspension line loads and reefing line loads.

Based on results of these tests, the type of parawing canopy structure and reefing method were selected for design of para-wings to be tested in free flight. These free flight designs were subsequently tested in a wind tunnel test program at the Ames Research Center with the following objectives:

1. To obtain additional data on the effect of structure on the gliding performance of the twin keel parawing.
2. To obtain wind tunnel measurements of L/D for comparison with L/D values measured during the free flight gliding performance tests using the same test models.

LANGLEY WIND TUNNEL TEST PROGRAM

Basis for Selecting Reefing Sequences for Test

The objective of the small scale tests in the Langley wind tunnel was to evaluate the performance of reefing systems and the effects of parawing construction on gliding performance.

The wind tunnel tests were intended to provide information relevant to the design of a hypothetical full scale parawing spacecraft recovery system with certain performance requirements. These performance requirements were:

1. Deployment altitude range of 3000 ft to 18,000 ft.
2. Deployment dynamic pressure at line stretch of 30 psf to 100 psf.
3. The maximum load imparted to the payload under any deployment condition not to exceed 3.0 g's including the 1-g gravitational force.
4. Maximum lift-drag ratio of greater than 2.0.
5. Vertical velocity at landing of 15 fps or less in a steady 1-g glide condition.
6. Minimum horizontal velocity of 30 fps.
7. Turn rate capability range of 0 degrees per second to 25 degrees per second.
8. All preceding requirements to be applicable to a 15,000 lb system weight.

In addition to performance requirements, inherent design characteristics of the parawing were considered. The parawing design features which had the greatest impact on the design of the reefing system to be tested were:

1. Low porosity canopy material.
2. Nonaxisymmetrical canopy planform.
3. Unequal length suspension lines.

Reefing System Design Criteria

Combination of the performance requirements and inherent design features of the parawing resulted in criteria for the design and evaluation of reefing systems. The following paragraphs discuss the primary criteria used in designing the reefing systems to be tested in the wind tunnel.

1. Multi-step drag area capability. - The combination of the requirement for a maximum of 3.0 g's during the deployment process and the low porosity of the canopy material resulted in reefing systems which provided a number of steps in drag area during inflation. Previous experience by Northrop Ventura with recovery systems similar to the parawing indicated that the low porosity of the wing surface would give the parawing certain inflation characteristics. It was expected that the first stage of the inflation process would result in a balloon-like inflated shape with a relatively long filling time and high drag coefficient. However, all stages following the first stage would probably have very short filling times.

Experience had indicated that a drag coefficient (based on the wing reference area S_W) of approximately .10 could be expected for the first stage. Also to maintain maximum deceleration below 3.0 g's during the remainder of the opening sequence, the drag coefficient of each successive reefing stage would have to be limited to a value approximately double that of the previous stage. To meet these requirements, it was anticipated that at least four stages of reefing would be necessary to decelerate a parawing recovery system from a dynamic pressure of 100 psf with a system weight of 15,000 lbs.

2. Reliable and repeatable inflation characteristics. - This requirement is self-explanatory; a reefing system to be useful must reliably and repeatably control the opening forces during each stage of the opening process.
3. Stable reefed aerodynamic characteristics. - Oscillating or spinning motions of the system could result in high dynamic loads. The low porosity material used for the wing surface and the nonaxisymmetrical planform of the wing surface could have resulted in reefed configurations that had strong spinning or gliding characteristics. A configuration that spins is unacceptable because of the danger of winding up the suspension lines or inducing high dynamic loads. Gliding configurations must be stable to avoid system oscillations which could cause high dynamic loads or collapse of the inflated wing.
4. Control of canopy material and suspension lines during deployment. - Typical fabric materials used for construction of gliding flexible decelerators such as parawing type devices are made of various forms of nylon and dacron. These materials have the characteristic that relative motion between two pieces of fabric in contact can result in friction burn damage to the material. The nonaxisymmetrical canopy planform and the non-uniform suspension line lengths of the para-wing increase the possibility of friction burn damage. It is therefore desirable that the reefing system be designed to control the canopy material and suspension lines during all stages and thus minimize the conditions which cause this type of damage.

5. Uniform load distribution in canopy and lines during the opening process. - The non-uniform suspension line lengths and nonaxisymmetrical planform of the wing make it difficult to meet this criterion. However, a reefing system that can satisfy this requirement is desirable from a design and weight standpoint.
6. No adverse effect on gliding performance. - In meeting the preceding five criteria it was possible that changes in canopy planform, suspension line lengths or arrangement would result in either degradation or improvement in performance during the opening process.

Any changes in the design should not result in a decrease in L/D performance of the wing.

Based on the preceding criteria, a series of reefing sequences was established. It should be noted that not all of the criteria were applied for each reefing sequence. Some of the reefing sequences were set up to investigate the effects of a criterion not being met, such as not controlling the length of suspension lines during the deployment sequence. Tables 1 and 2 list and describe the reefing sequences that were selected for testing in the Langley wind tunnel.

Test Model Configurations

A series of wind tunnel models was designed to test the previously discussed reefing systems and to determine the effects of variations in the number and diameter of suspension lines and basic canopy structure on gliding flight performance. Six models were designed and built. The following paragraphs describe the structure and design features of these models. The six models could be set up in a number of different configurations for gliding flight. These configurations are summarized in Table 3. Figures 1 through 5 are sketches showing the basic

Table 1
Single Keel Reefed Configurations and Disreef Sequences

	Stage 1 Reef	Stage 2 Reef	Stage 3 Reef
Trailing edges laced together. Reefing lines around periphery of wing. No control of suspension lines.	Same as Stage 1 except longer reefing line	Same as Stage 1 except longer reefing line	Reefing line removed
2. All peripheral suspension lines same length. Reefing lines around periphery of wing. No control of keel lines.	Same as Stage 1 except longer reefing line	Same as Stage 1 except longer reefing line	All suspension lines to gliding lengths
3. All peripheral suspension lines same length from circle laid out on wing surface. Reefing lines around circle on wing surface. No control of keel lines.	Same as Stage 1 except longer reefing line	Same as Stage 1 except longer reefing line	All suspension lines to gliding lengths
4. All suspension lines same length. Trailing edges laced together. Reefing lines around leading edges and keel to form two lobes.	Same as Stage 1 except longer reefing lines	Reefing line removed	Trailing edge lacing removed
5. All suspension lines same length. Reefing lines around leading edges. Keel and trailing edges to form two lobes.	Same as Stage 1 except longer reefing lines	Same as Stage 2 Reefing removed	All suspension lines to gliding lengths
6. All suspension lines same length. Trailing edges laced together.	Same as Stage 1 except longer reefing lines	Trailing edges free	All suspension lines to gliding lengths

Table 2
Twin Keel Reefed Configurations and Disreef Sequences

Basic Reefed Configuration (Stage 1 of Reefing Sequence)	Stage 2	Stage 3	Disreef Sequence
	Same as Stage 1 except longer reefing line	Reefing line removed	Keels unlaced
1. Keels laced together. All peripheral suspension lines same length to circle laid out on wing surface. Reefing lines around circle on canopy surface.			All suspension lines to gliding lengths
2. Trailing edges laced together. All suspension lines same length. Reefing lines around leading edges and keels to form three lobes.	Side lobe reefing removed	Center lobe reefing removed	Trailing edges released
3. Trailing edges gathered together. All suspension lines same length. Reefing lines around leading edges and keels to form three lobes.	Side lobe reefing removed	Center lobe reefing removed	Trailing edges released
4. All suspension lines same length. Reefing lines around leading edges, trailing edges and keels to form three lobes.	Center lobe reefing removed	Side lobe reefing removed	All suspension lines to gliding trim

TABLE 3
Summary of Parawing Model Configurations

Parawing (Keel) Planform	Model Number	Suspension Lines			Canopy Construction		Canopy Weight Lb-(8)	
		Number On T.E.	Strength (6) Pounds	Material	Lay of (1) Seams	Tape Pattern		
Single	S-1A	23	0	500	Dacron	Normal	None	2.73
Single	S-1B	43	0	250	Dacron	Normal	None	2.73
Single	S-1C	63	0	250	Dacron	Normal	None	2.73
Single	S-1D	29	6	250	Dacron	Normal	None	2.73
Single	S-1E	23	0	250	Dacron	Normal	None	2.73
Single	S-1F	23	0	185 ^{1/32 in(7)} Steel Cable	Dacron(2)	Normal	None	2.73
Single	S-1G	23	0	500	Dacron(2)	Normal	None	2.73
Single	S-2	23	0	500	Dacron	Parallel	None	3.39
Single	S-2A	24 (3)	0	500	Dacron	Parallel(4)	None	3.39
Single	S-3	29	6	500	Dacron	Normal (4)	Radial	4.26
Twin	T-1A	36	0	500	Dacron	Normal	None	3.30
Twin	T-1B	68	0	250	Dacron	Normal	None	3.30
Twin	T-1C	100	0	250	Dacron	Normal	None	3.30
Twin	T-1D	42	6	250	Dacron	Normal	None	3.30
Twin	T-1E	36	0	250	Dacron	Normal	None	3.30
Twin	T-2 (5)	36	0	500	Dacron	Normal (4)	None	3.80
Twin	T-3	42	6	500	Dacron	Normal (Outbd)(4) Parallel (Ctr)	Radial	4.75

- NOTE:
- (1) Relative to trailing edge.
 - (2) Same as S-1A with links, hold-down loops, etc. added to suspension lines.
 - (3) One keel line added.
 - (4) Reefing provisions added for deployment tests.
 - (5) This model not flight tested.
 - (6) Canopy material was 1.6 oz. acrylic coated nylon.
 - (7) Originally planned as 60 lb. dacron, however stretch of this material caused shift to steel cable.
 - (8) Canopy weight only, not including suspension lines.

canopy structure and Figures 6 through 17 give suspension line dimensions. These dimensions are from the bottom of the canopy skirt band to the center of the top cross bar of the link to which the lines were attached.

Single Keel Models. - Model S-1: This model was the basic single keel design previously tested by LRC, as reported in References 1 and 2. The wing material was oriented with the warp and seams normal to the trailing edges of the wing. Provisions were incorporated to permit the number of suspension lines to be changed. Four variations in numbers of lines were tested. Three line sets with different line diameters were provided for the 23 suspension line configuration. Model S-1 was used only for tethered performance and stability tests, since the suspension line attachment fittings were not designed for deployment loads. Figure 1 shows the wing planform and seam orientation.

Model S-2: This model was the basic 23 suspension line single keel planform, but with fabric seams parallel to the trailing edges of the wing. The model was designed with various reefing configurations for both deployment and gliding performance tests. Grommets were installed in the trailing edges, leading edges, and keel of the wing. Loops were installed in the suspension lines to permit all lines to be rigged at equal length from the line confluence point to the edge of the wing surface. "Daisy chain loops"^{*} were sewn on the trailing edges; for some reefing configurations additional loops were installed at grommets along the leading edges and keel. Figure 2 shows the wing planform and seam orientation of the S-2 model.

* A series of short, cord loops designed to be interwoven consecutively like chain stitching and locked at the open end with a reefing line cutter.

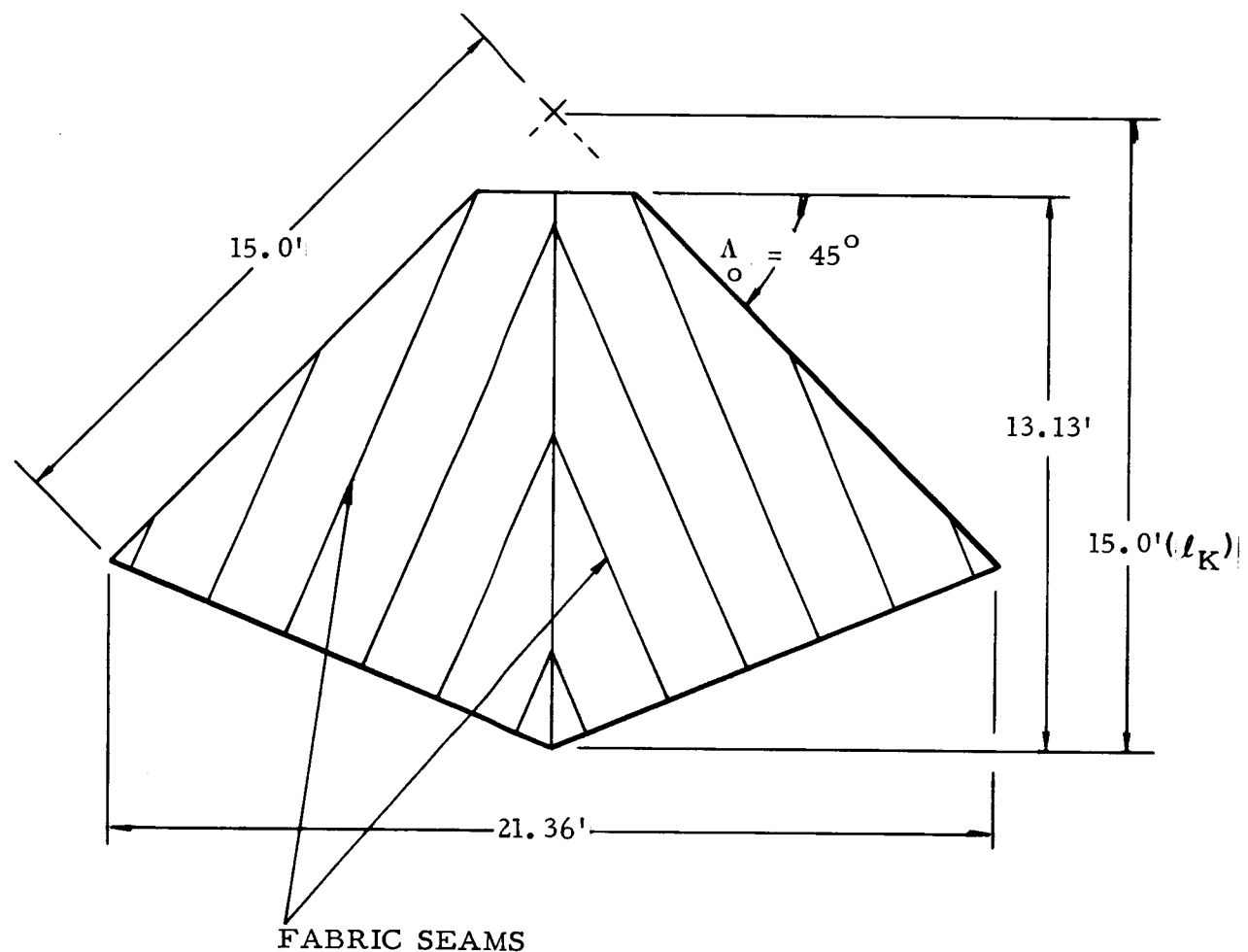


Figure 1. Single Keel Wind Tunnel Model Basic Planform and Model S-1 Canopy Construction

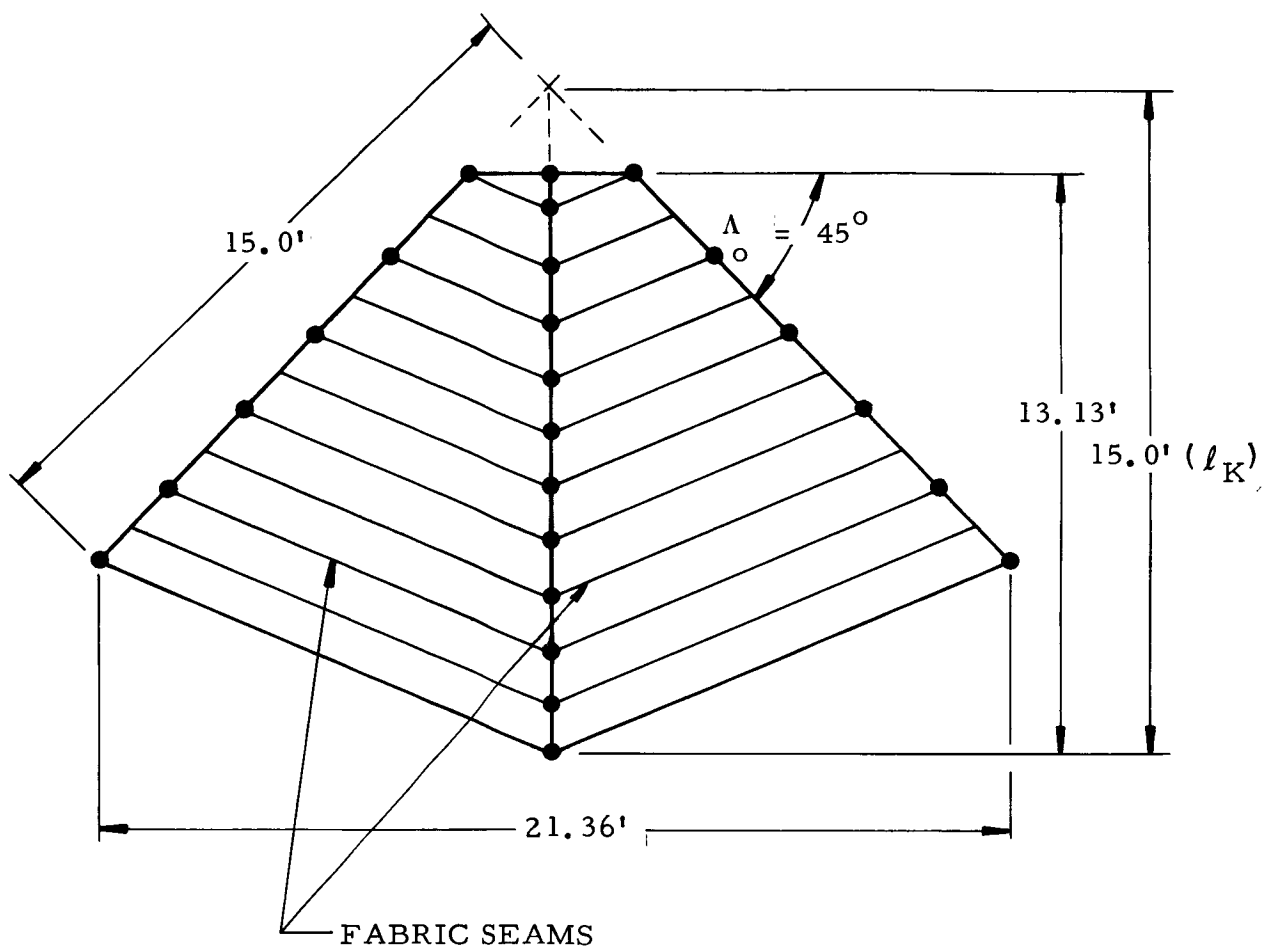


Figure 2. Single Keel Wind Tunnel Model Basic Planform and Model S-2 Canopy Construction

Model S-3: This model had a radial tape reinforcing network with the warp of the wing material oriented normal to the trailing edges. The model had 29 suspension lines, six of which were located along the trailing edges of the wings. A circular reinforcing band was attached to the wing surface. This served as a reference line from which all peripheral suspension lines were rigged to the same length, and on which reefing rings were located. Reefing rings were also located along the leading and trailing edges and the keel. Figure 3 shows the wing planform and seam orientation of the S-3 model.

Twin keel models. - Model T-1: This model was the basic twin keel design previously tested by Langley Research Center. It was designed for use only in the tethered flight performance and stability tests. The wing fabric was oriented with seams chordwise in the center section of the wing and normal to the trailing edges in the outboard sections of the wing. The number of suspension lines was variable with provisions for the basic 36 line arrangement and three other line configurations having 42, 68 and 100 lines. Three sets of suspension lines of different diameters were provided in the 36 suspension lines configuration. Figure 4 shows the wing planform and seam orientation of the T-1 model.

Model T-2: This model was designed for deployment tests and had provisions for investigation of various types of reefing. It had the same planform and wing construction as Model T-1. Provision was made for rigging all suspension lines to equal lengths. Grommets were mounted around the leading edges, the keels and the trailing edges, and "daisy chain loops" were located along the trailing edges. Figure 4 shows the wing planform and seam orientation of the T-2 model.

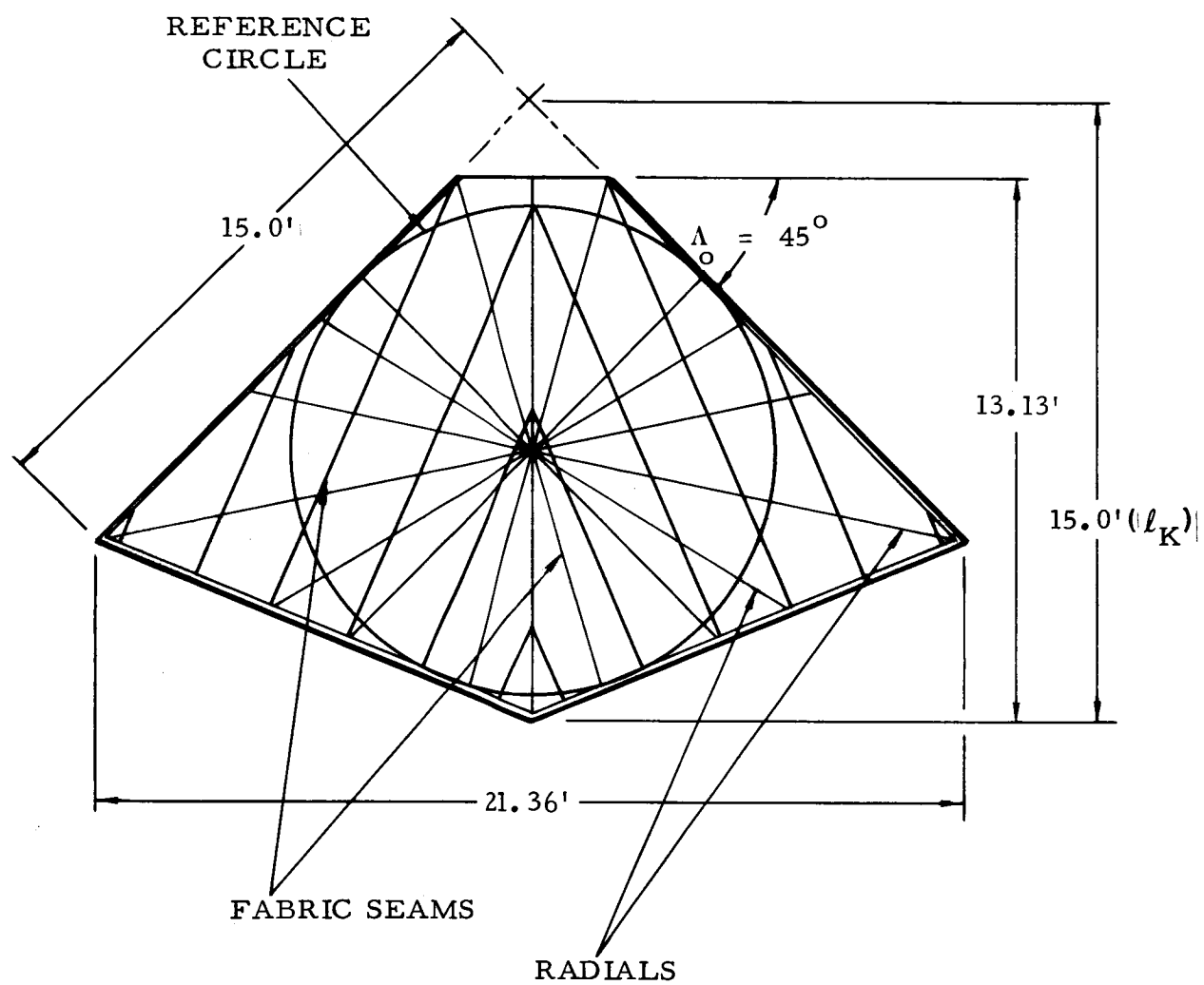


Figure 3. Single Keel Model S-3 Planform and Canopy Construction

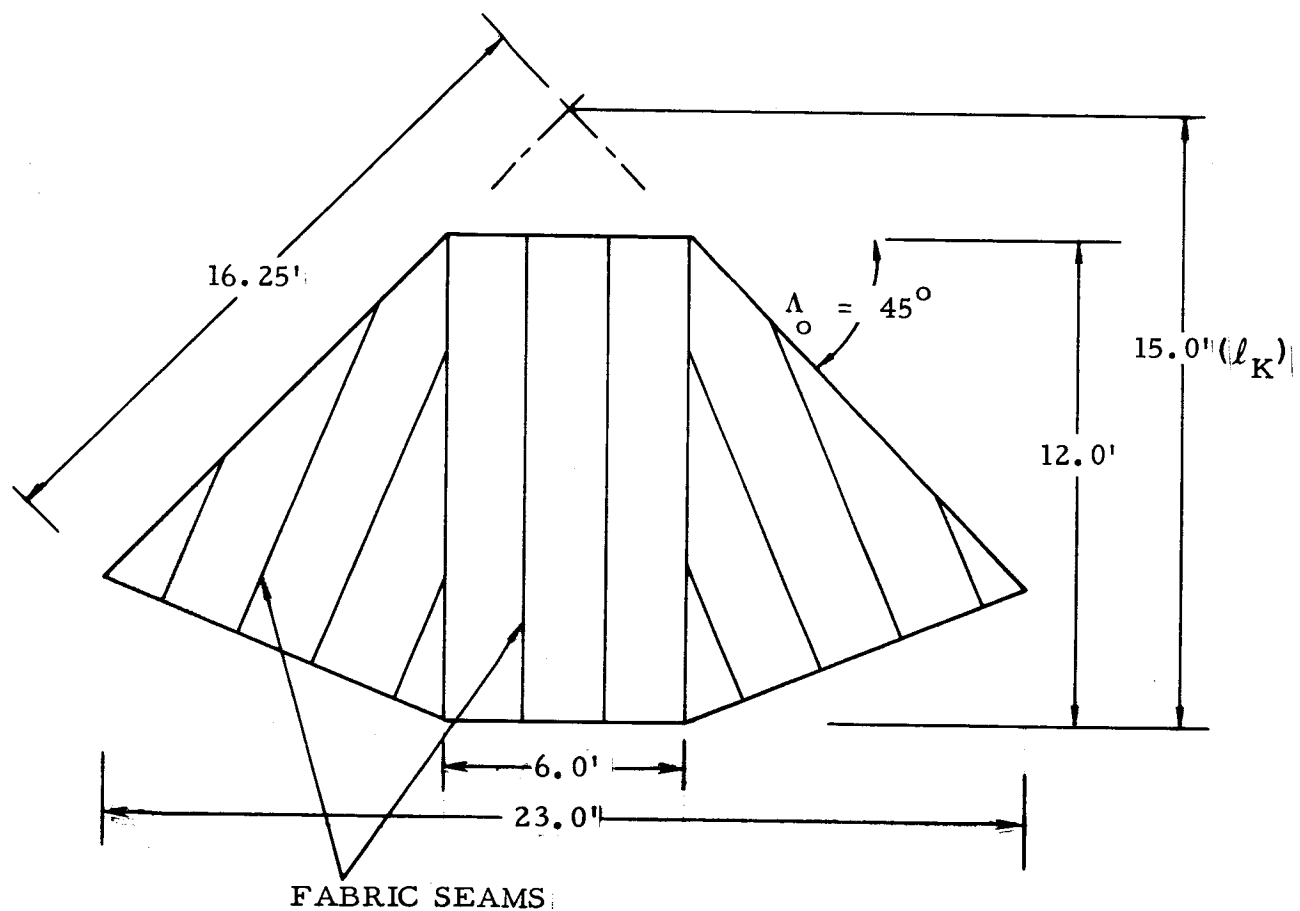


Figure 4. Twin Keel Wind Tunnel Model Basic Planform
and Models T-1 And T-2 Canopy Construction

Model T-3: This model was designed for reefing tests. It had the basic twin keel planform with a radial reinforcing network in the outboard sections of the wing. The wing fabric was oriented with seams normal to the trailing edges in both of the outboard sections and parallel to the trailing edge in the center section of the wing. The outboard sections of this model had semicircular reinforcing bands which served as reference lines from which all peripheral suspension lines could be rigged to the same length. These bands served as a reference for attachment of reefing rings.

This model had 42 suspension lines, including 6 trailing edge lines. Reefing rings were installed at the reference semi-circles, around the periphery of the wing and in double rows along the keels. "Daisy chain" loops were provided along the keels on the upper and lower surfaces of the wing. Provisions were made for shortening all suspension lines to the same length from the semi-circular reference lines and from the edges and keels of the wing. Figure 5 shows the wing planform and seam orientation of the T-3 model.

Materials

All model canopies were fabricated from a low porosity acrylic coated nylon sail cloth with the following characteristics:

Manufacturer's Designation	Lamport AF-120
Unit weight	1.52 oz/yd ²
Tensile strength, lb/in	50 (warp and fill)
Ultimate elongation	31% (warp), 51% (fill)
Tearing strength, lbs	3.7 (warp), 5.6 (fill)
Permeability,	<u>ft³/min/ft²</u>
p = 0.5 inch H ₂ O	0.85
p = 5.0 inches H ₂ O	4.9
p = 10.0 inches H ₂ O	8.0

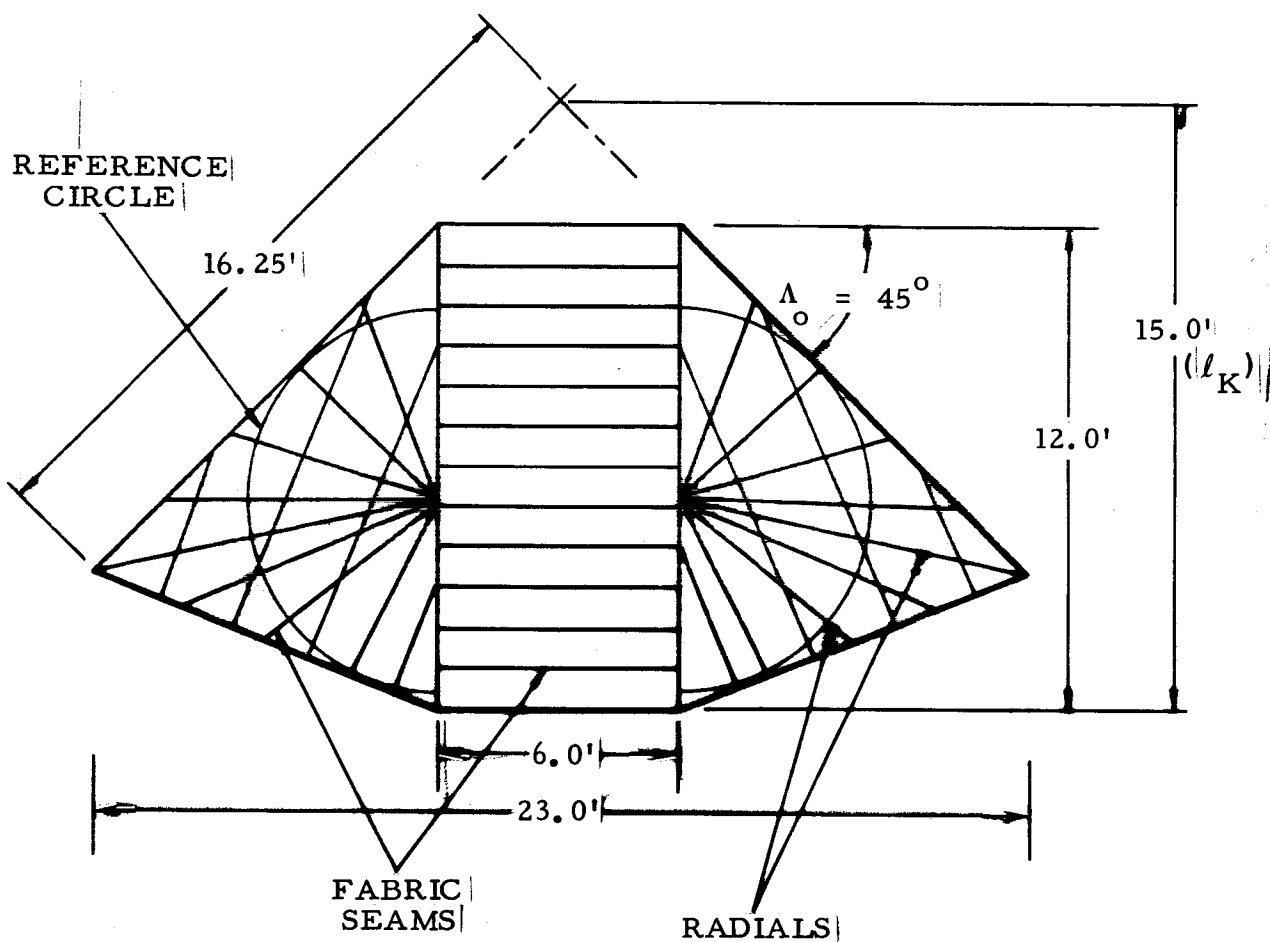


Figure 5. Twin Keel Model T-3 Planform and Canopy Construction

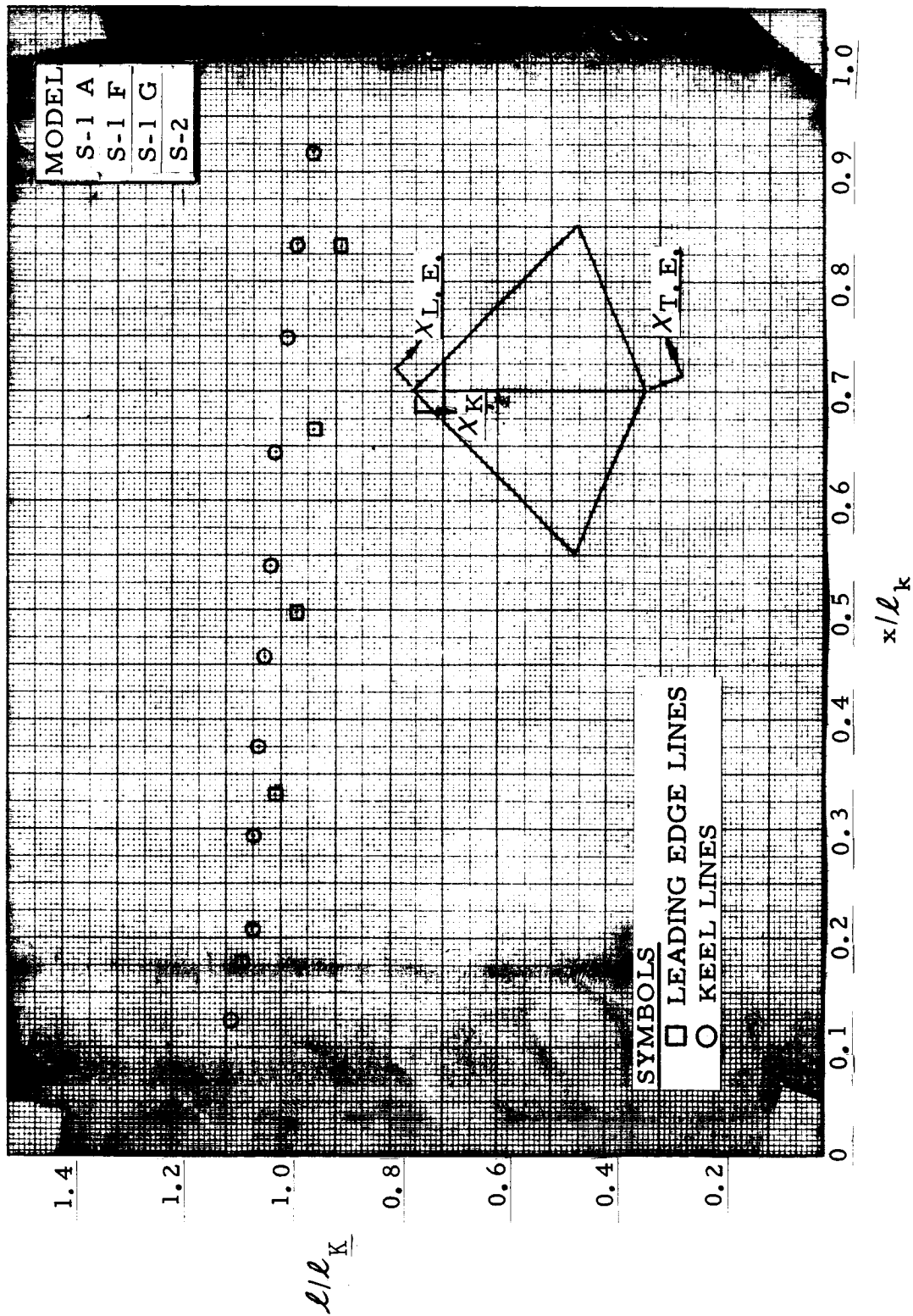


Figure 6. Single Keel Wind Tunnel Model Line Location and Length Ratios

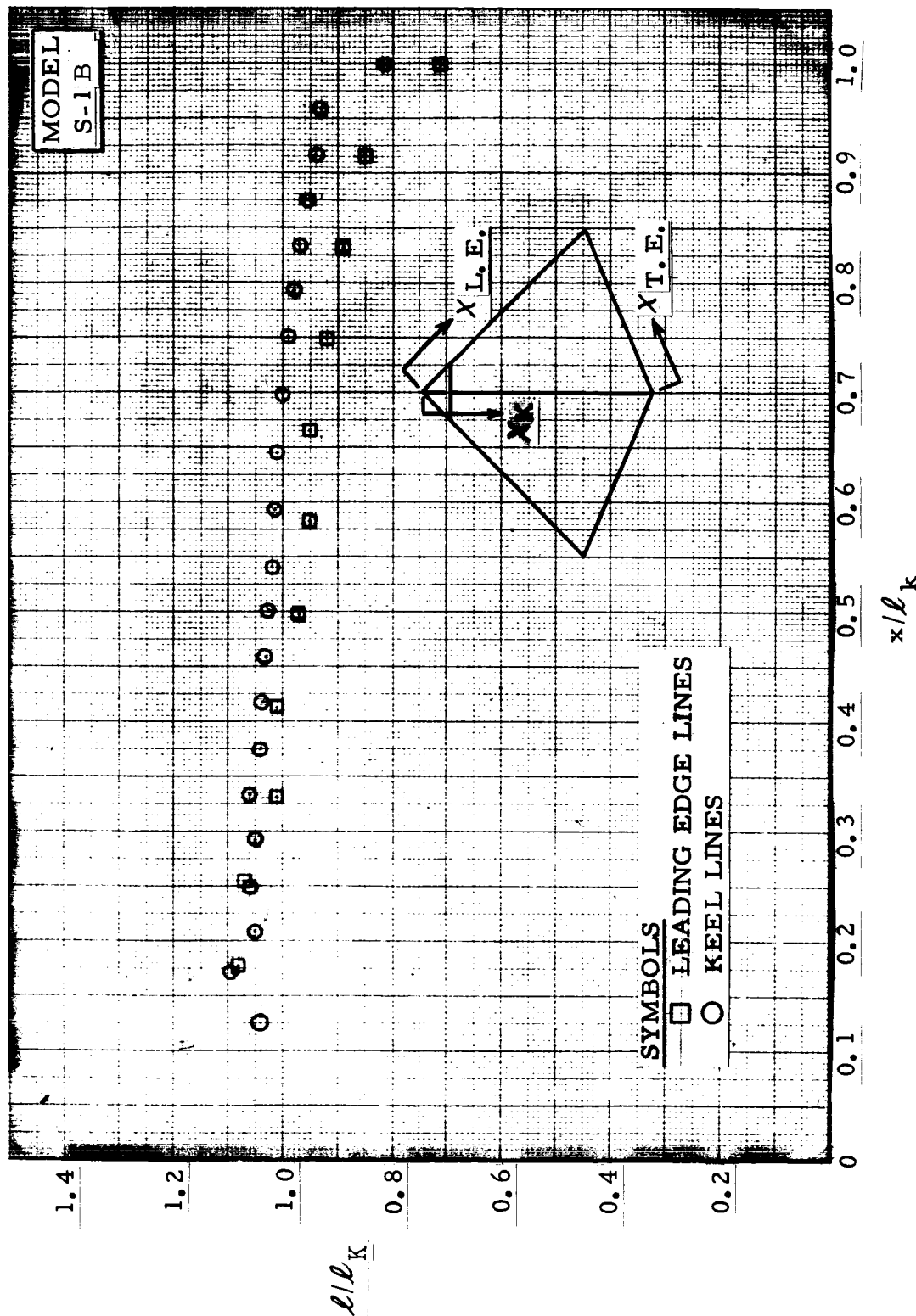


Figure 7. Single Keel Wind Tunnel Model Line Location and Length Ratios

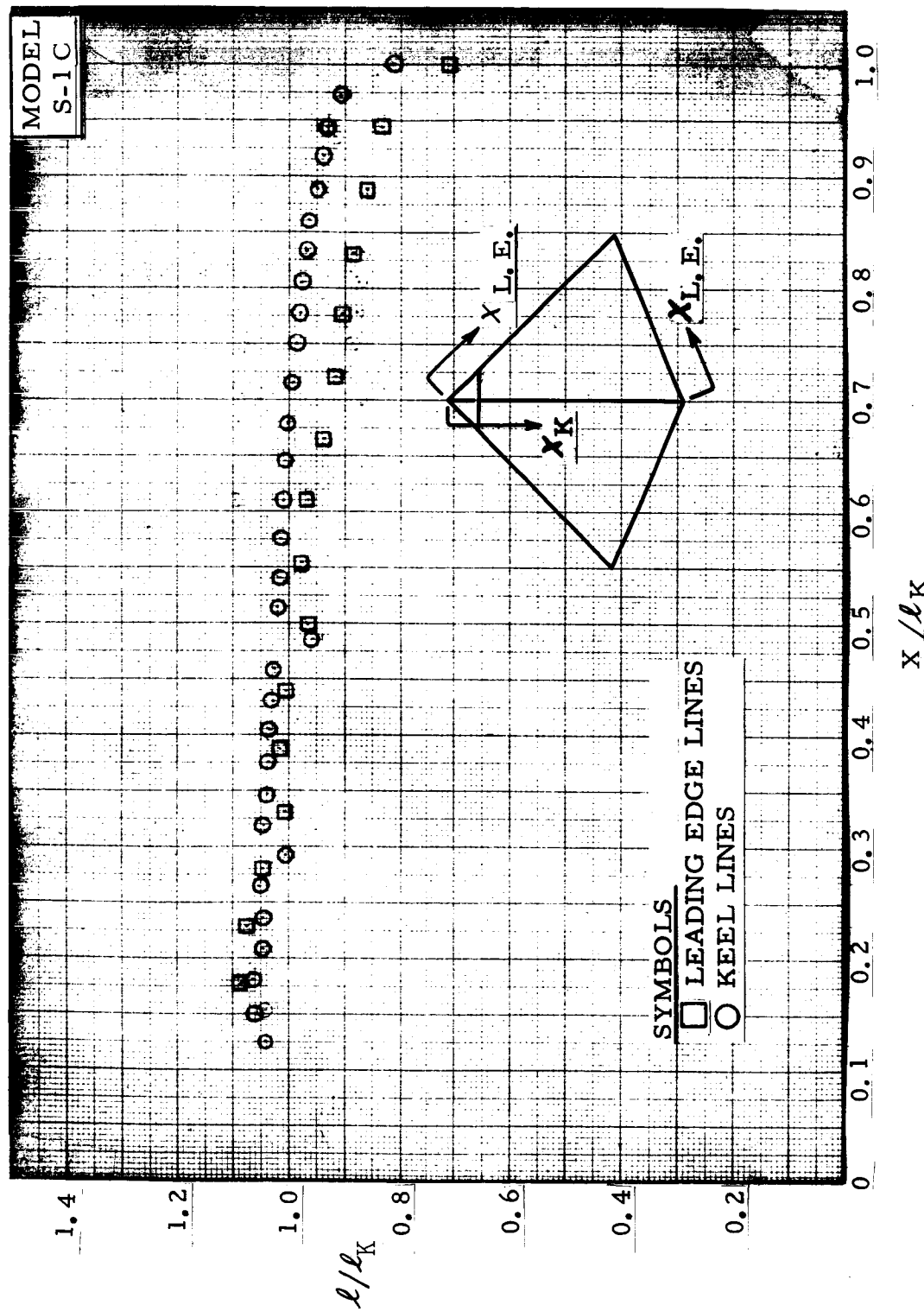


Figure 8. Single Keel Wind Tunnel Model Line Location and Length Ratios

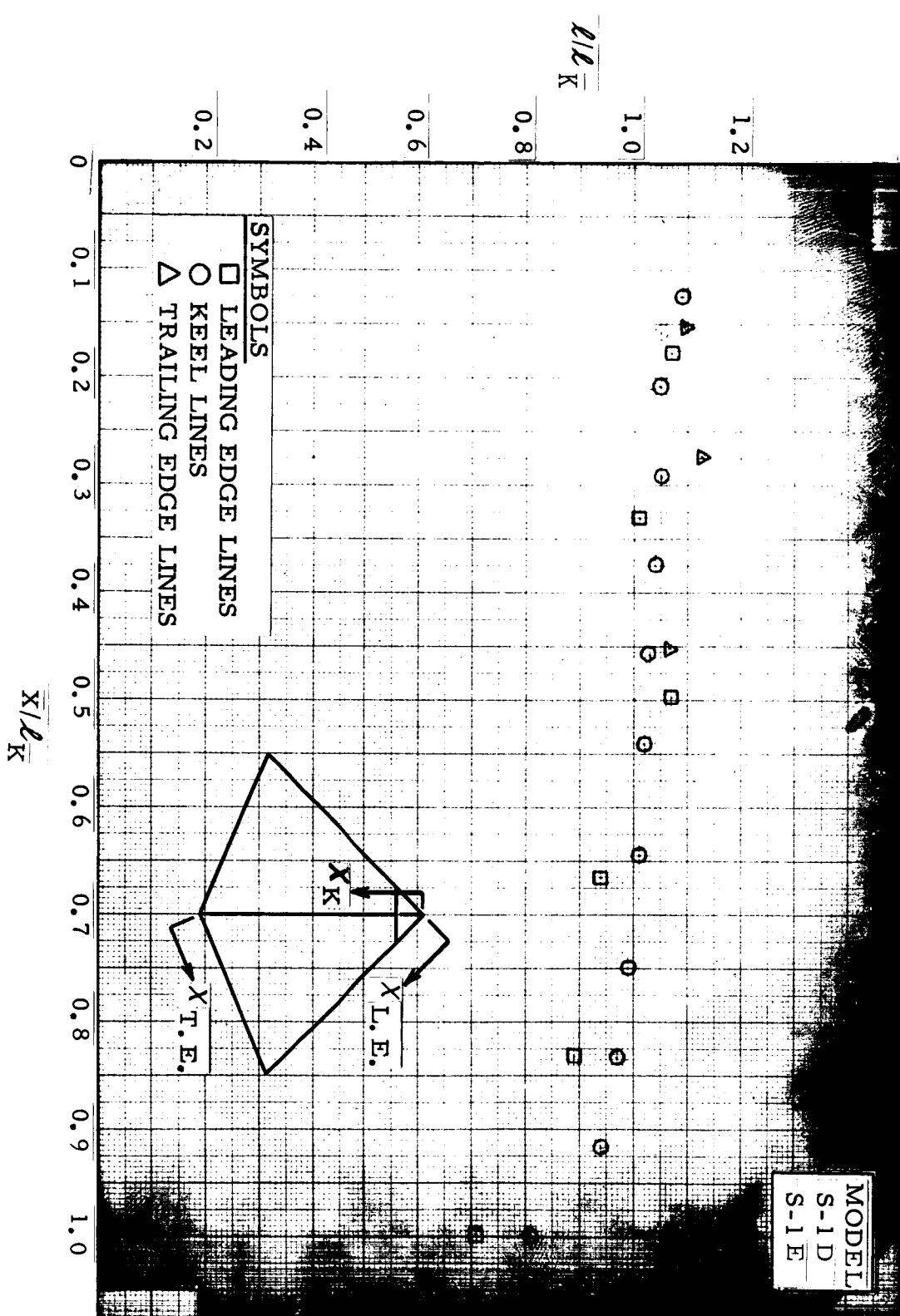


Figure 9. Single Keel Wind Tunnel Model Line Location and Length Ratios

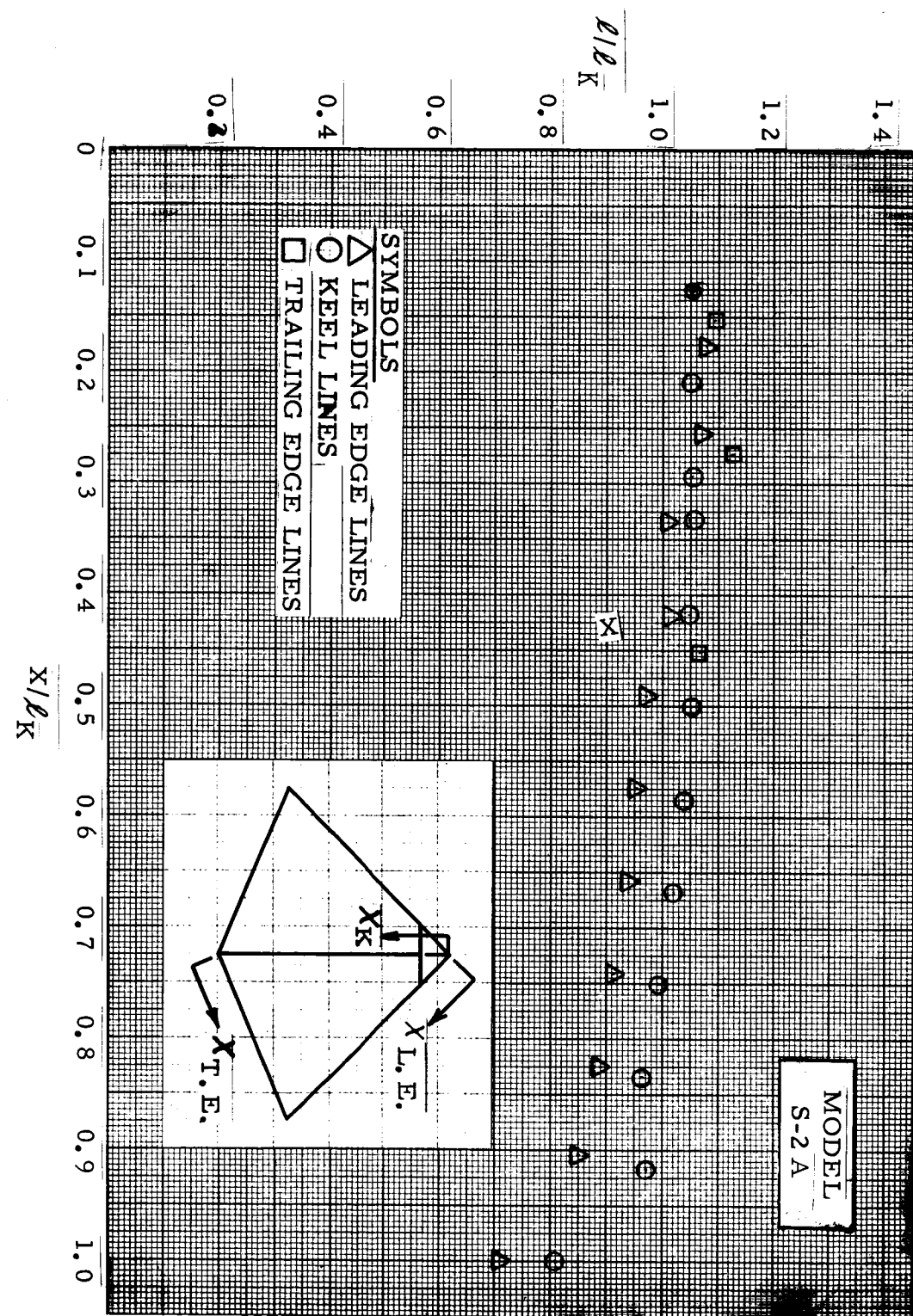


Figure 10. Single Keel Wind Tunnel Model Line Location and Length Ratios

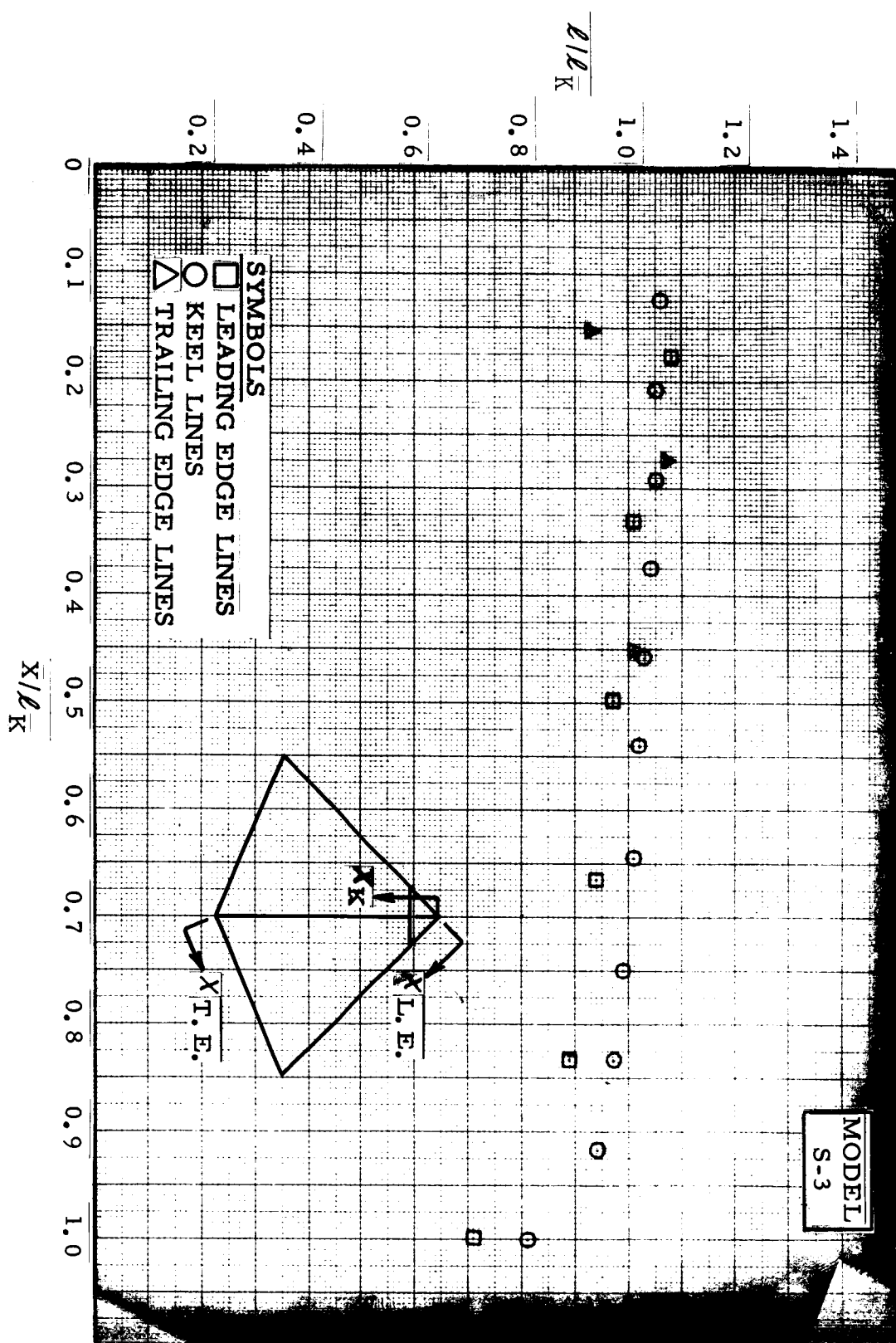


Figure 11. Single Keel Wind Tunnel Model Line Location and Length Ratios

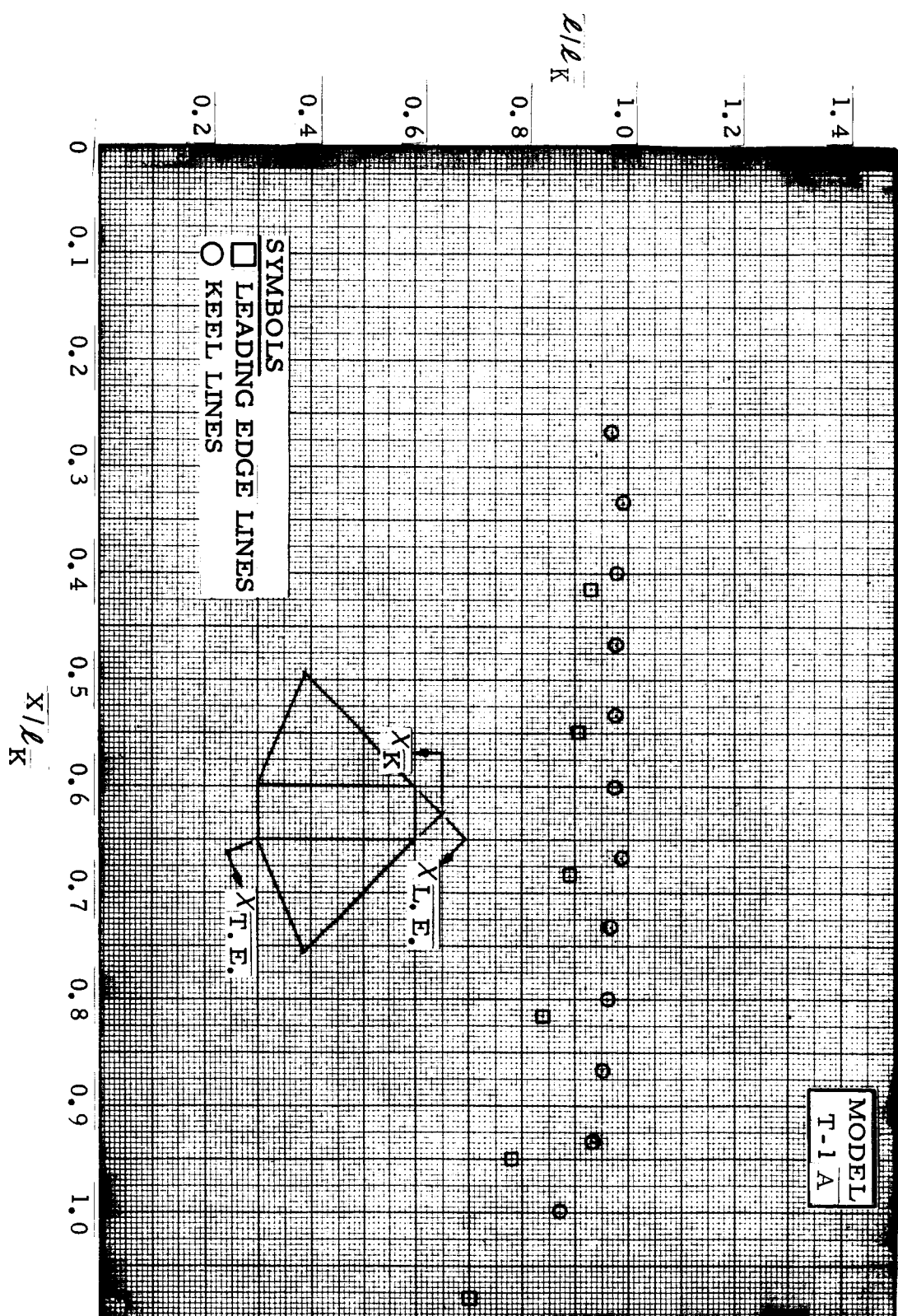


Figure 12. Twin Keel Wind Tunnel Model Line Location and Length Ratios

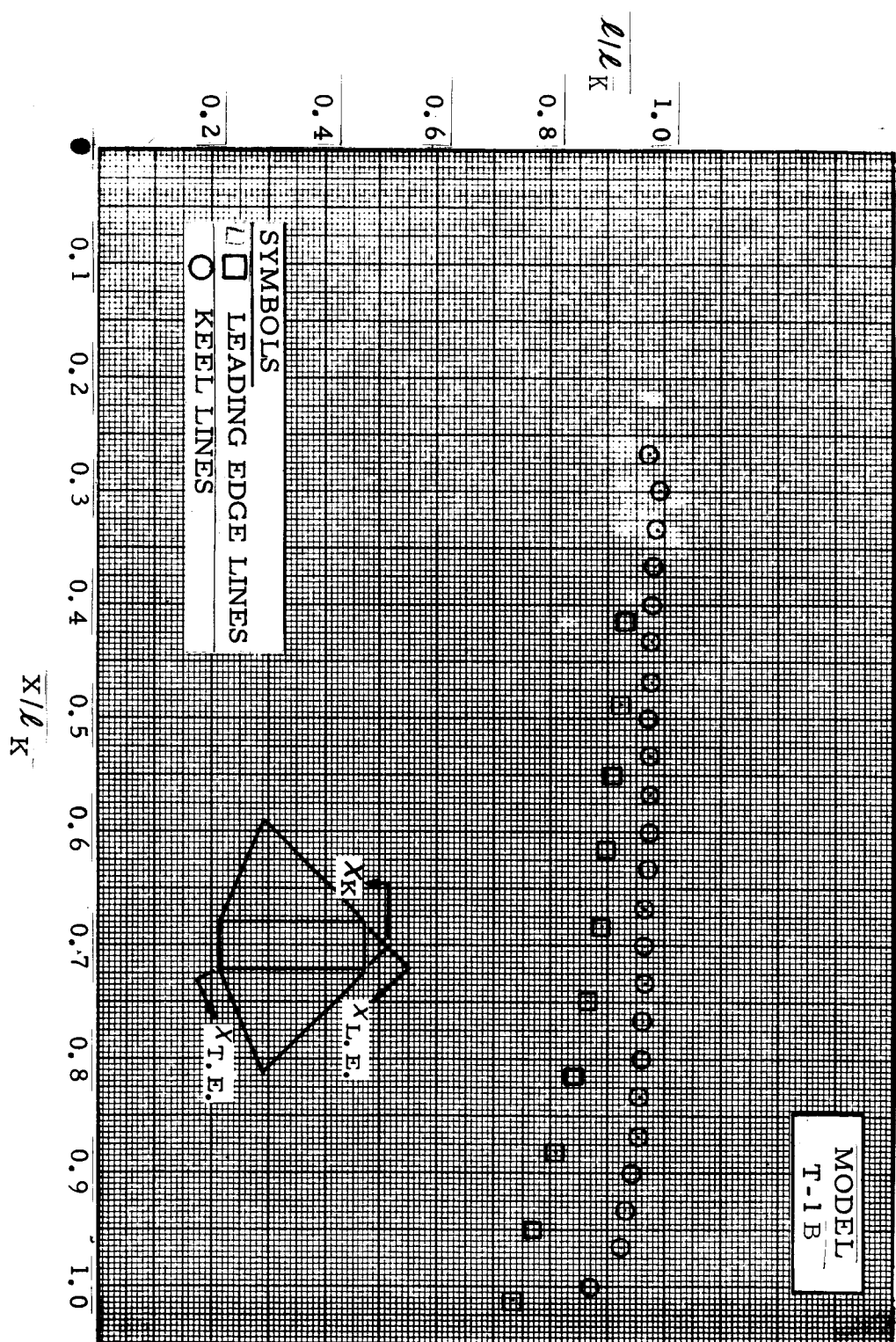


Figure 13. Twin Keel Wind Tunnel Model Line Location and Length Ratios

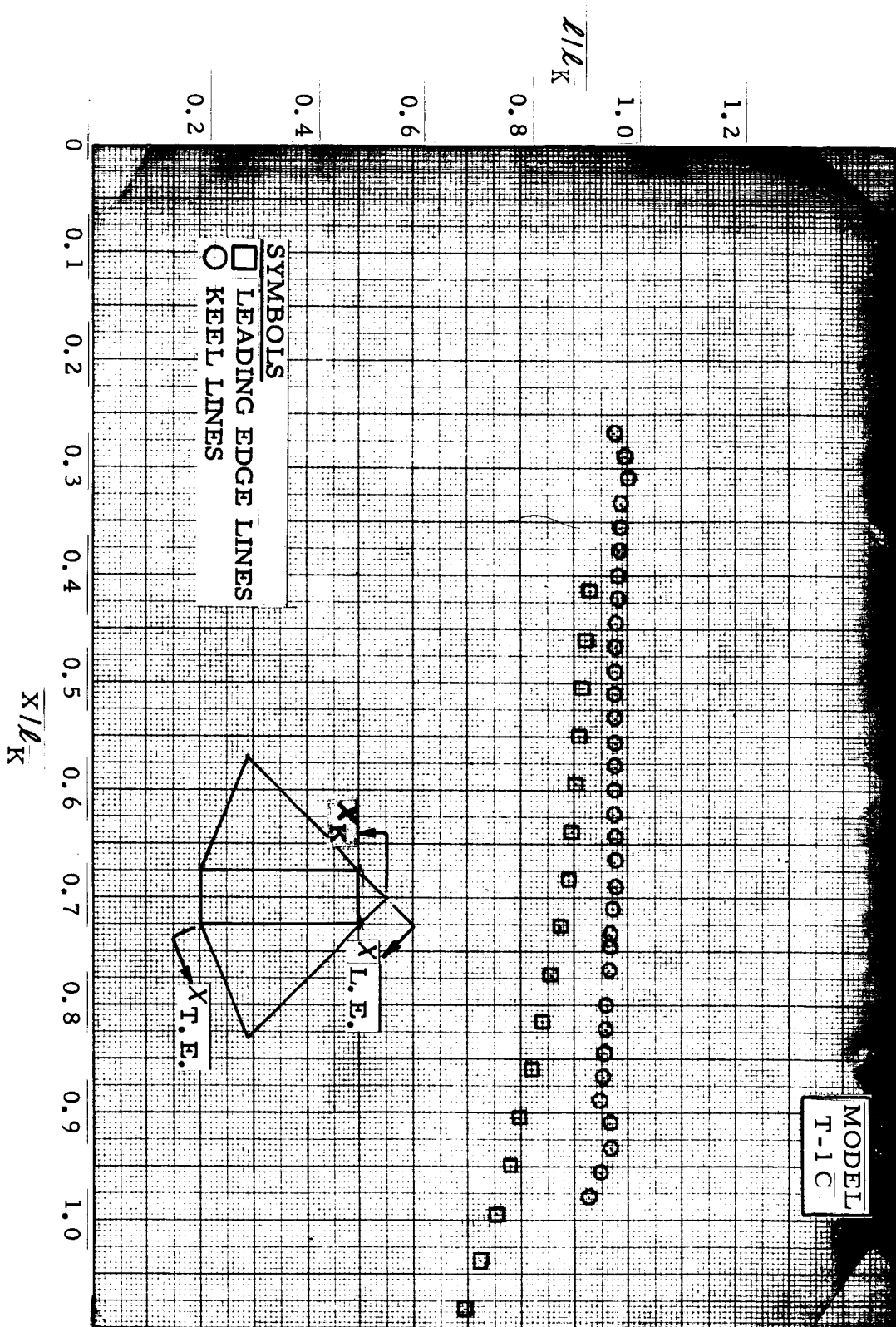


Figure 14. Twin Keel Wind Tunnel Model Line Location and Length Ratios

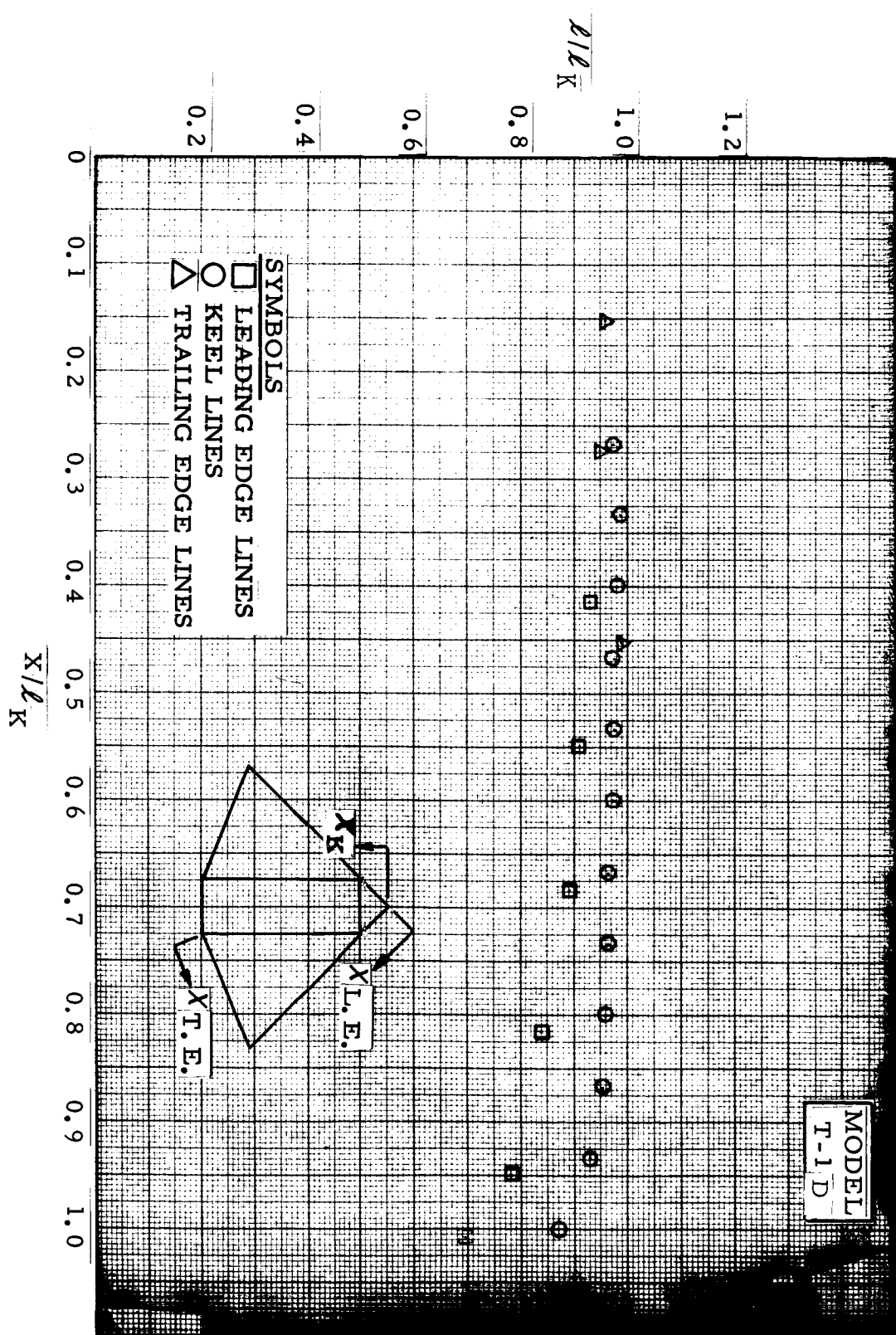


Figure 15. Twin Keel Wind Tunnel Model Line Location and Length Ratios

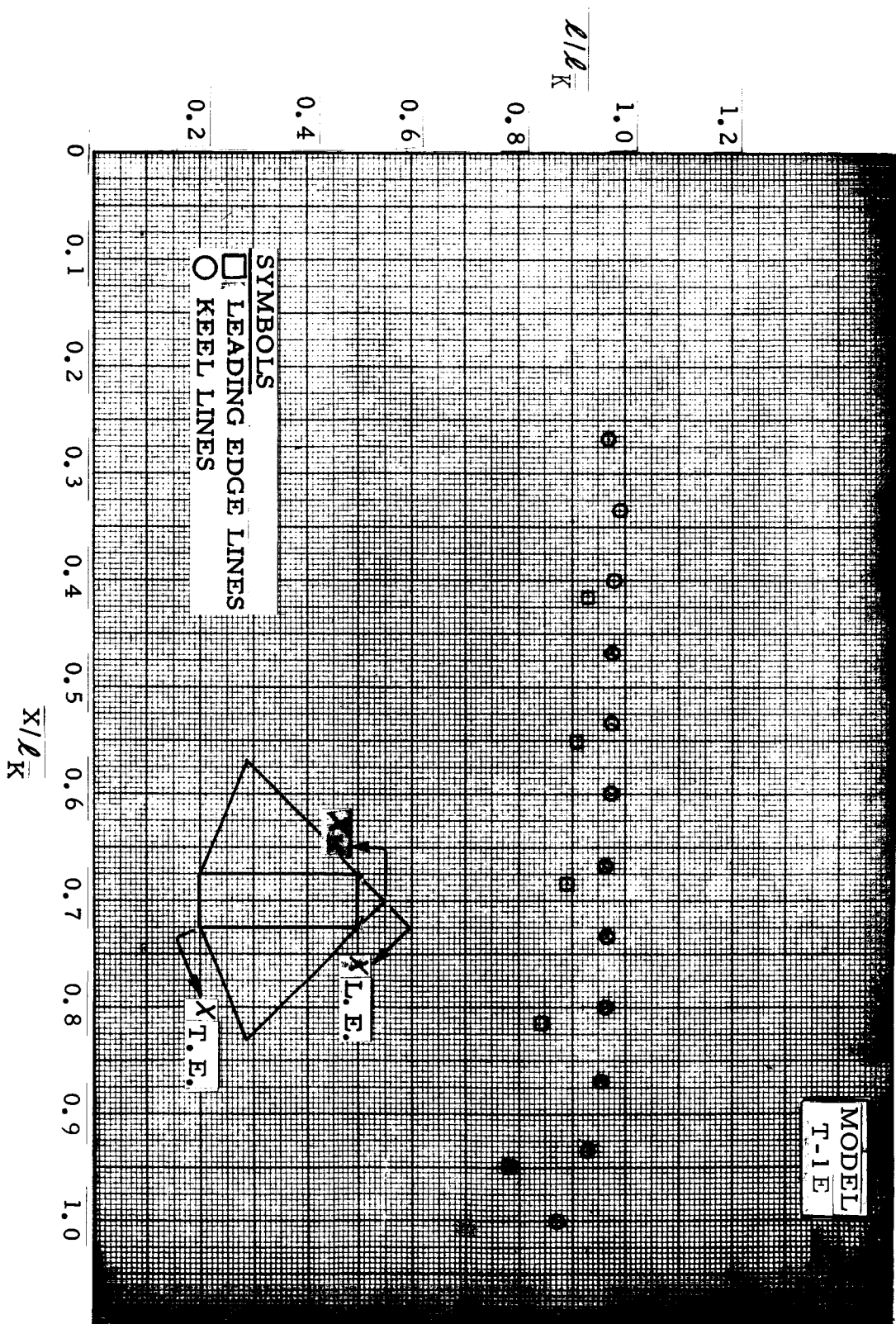


Figure 16. Twin Keel Wind Tunnel Model Line Location and Length Ratios

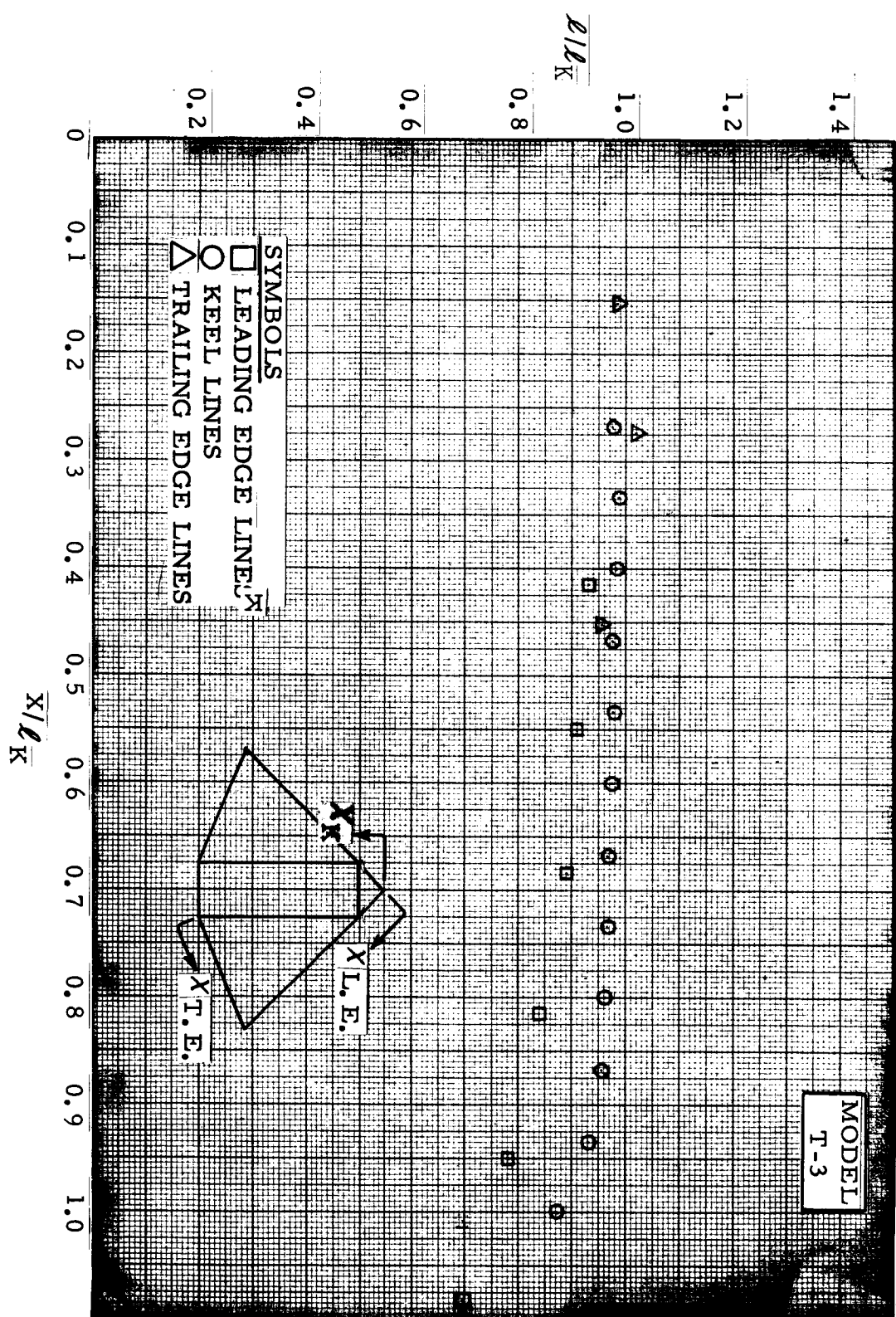


Figure 17. Twin Keel Wind Tunnel Model Line Location and Length Ratios

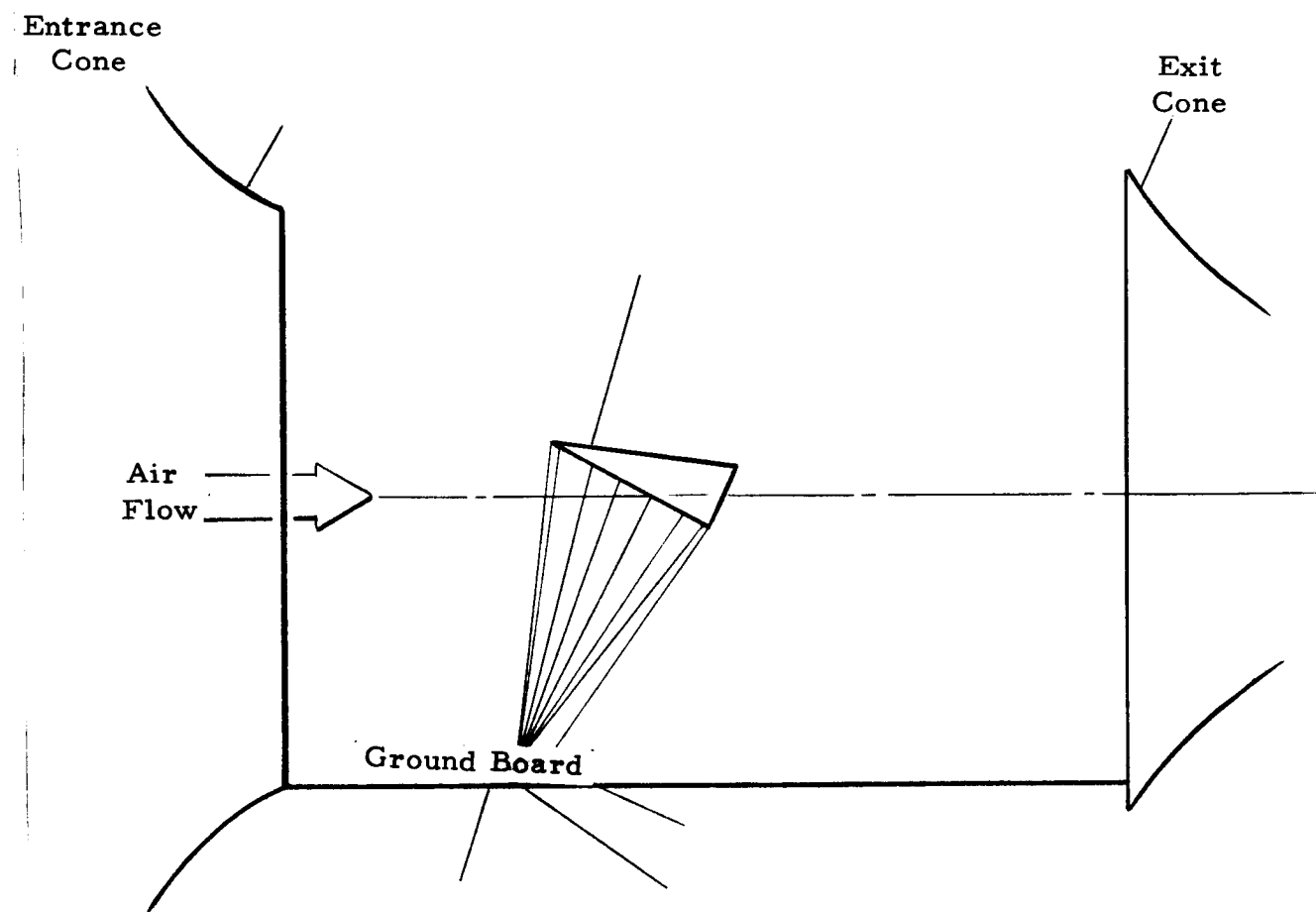


Figure 18. Tethered Gliding Flight Test Setup

Depending on the model, suspension lines were made of either 250 pound hot-stretched dacron cord, 500 pound hot-stretched dacron cord, or 1/32 inch (185 pound) steel cable. Table 3 identifies the suspension line material for each of the models tested.

Wind Tunnel Test Procedure

Both tether tests and deployment tests of the 15-foot (ℓ_K) parawing models were performed in the open throat section of the Langley full-scale 30 ft by 60 ft Wind Tunnel.

Pre-test checkout. - In preparation for wind tunnel testing, the models were first tether tested in the wind at Northrop Ventura. By this means, the rigging of each of the various configurations was checked and preliminary adjustments made.

Tethered flight test method. - The test set up for tethered tests is shown in Figure 18. The suspension lines of each model were attached to a "T" bar line attachment fixture shown in Figure 19. Adjustment of the lengths of the tip and aft keel lines was provided for by means of short lengths of chain attached to each of these lines. The fixed lines were attached to a common point at the base of the "T" bar. The adjustable aft keel line or lines were attached to the top center of the "T" and the tip lines to the ends for the arms of the "T". The spread attachment of the "T" bar was used to provide sufficient longitudinal and roll stability of the models in the wind tunnel. It should be noted that this method of attachment, although necessary for wind tunnel testing, does not correspond to the type of attachments normally used for free flight testing. The wind tunnel attachment system resulted in rear keel suspension line lengths approximately correct for a confluence point attachment system and tip suspension lines effectively $0.02 \ell_K$ longer than if the same length lines were used with a confluence point attachment system.

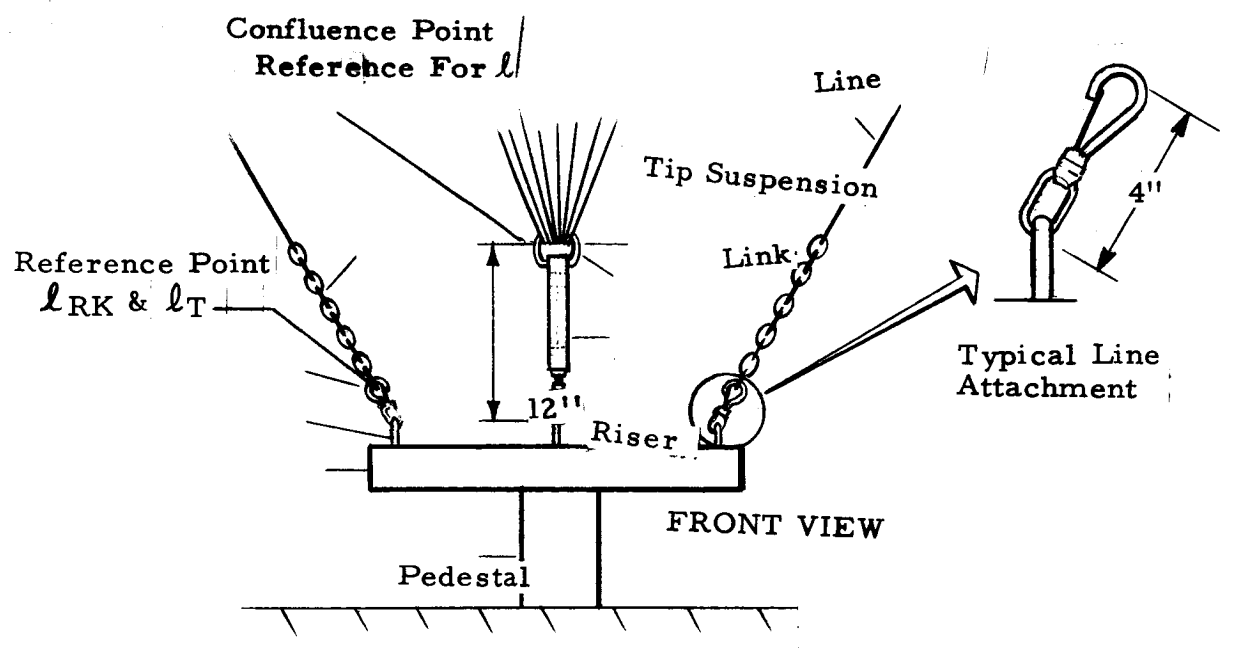
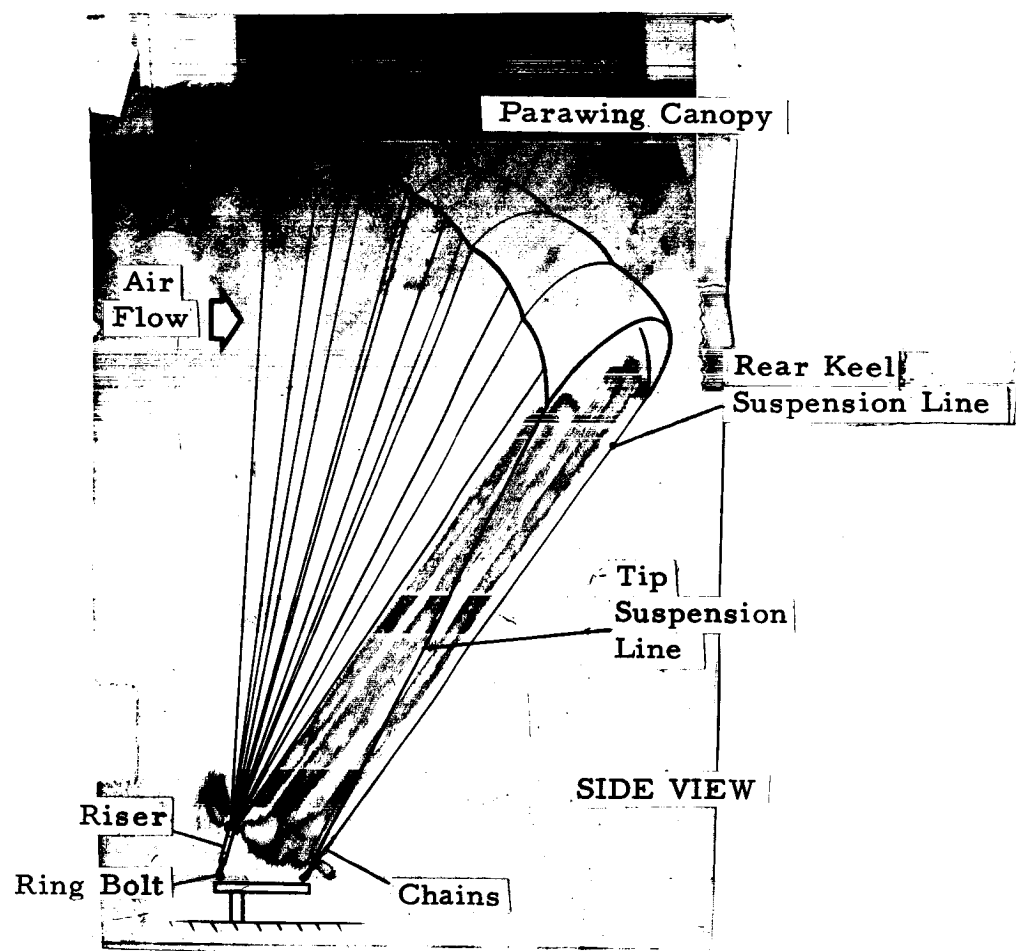


Figure 18.(Concluded) Tethered Gliding Flight Test Setup

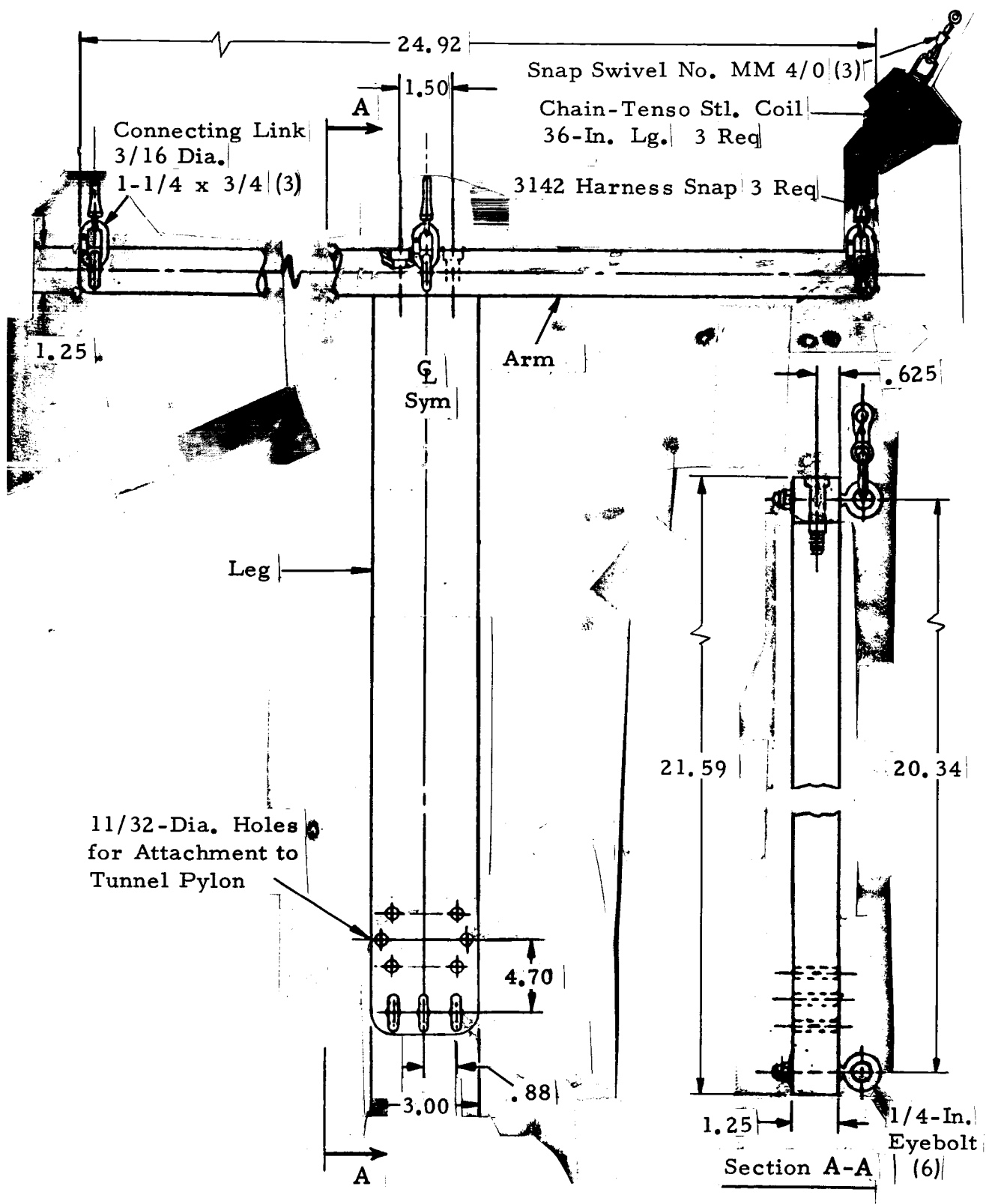


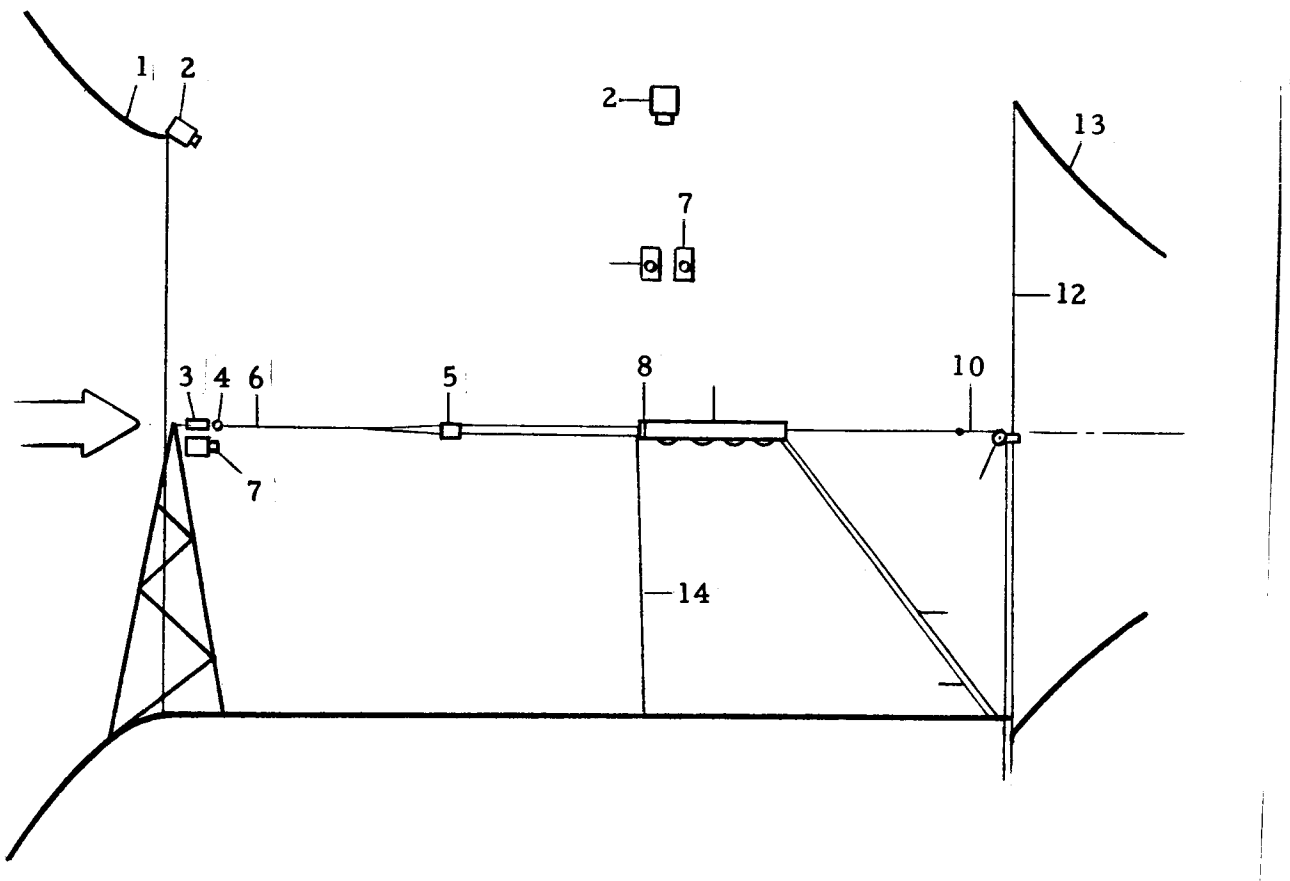
Figure 19. T-Bar Model Attachment Fixture

The "T" bar was rigidly mounted in the horizontal position on the wind tunnel balance pylon near the floor of the test section. This enabled the model to fly near the central axis of the airflow from the throat.

Most of the runs were made at a nominal dynamic pressure of 1 psf. During some of the runs the dynamic pressure was increased in steps to nominal values of 2, 3 and 4 psf. A typical run was performed with a fixed tip line length, while the length of the aft keel line was varied over the stable flight range bounded by leading edge collapse near L/D maximum at low angles of attack, and descent of the model to the floor due to the wing stalling at high angles of attack. When the lengths of the added trailing edge lines were varied, both tip and aft keel lines were held constant.

Deployment test method. - The wind tunnel set-up used in the deployment tests is shown in Figure 20. The model, packed in a deployment sleeve, was supported on the tunnel axis in the horizontal position with a webbing riser attached to a load link on the mounting pylon. The down-stream end of the deployment sleeve was supported by a stretched elastic cord with a tether line passing over a cable-mounted pulley in the center of the exit cone. The mouth of the deployment sleeve was held closed by a cord passing through an electrically initiated pyrotechnic line cutter. Upon firing of the cutter, the deployment sleeve was pulled away by contraction of the elastic cord, allowing the reefed parawing model to inflate.

For reefed stages following the initial reefed stage, the test procedure consisted of inflating the model in one of the reefed configurations. An electrically actuated reefing cutter was then fired to cut a reefing line and allow the wing to open into the next stage of the deployment sequence.



1	Entrance Cone	9	Deployment Sleeve
2	70mm Camera	10	Elastic Cord
3	Total Loadlink	11	Pulley
4	Riser Attachment Fitting	12	Steel Cable
5	Suspension Line Load Links	13	Exit Cone
6	Riser	14	Tether Line
7	16mm Camera	15	Electrical Lead To Cutter
8	Pyro Reefing Cutter	16	Safety Line

Figure 20. Deployment Test Setup

Air flow was established in the tunnel prior to parawing deployment to provide a dynamic pressure suitable for each reefed stage. Dynamic pressure limits were established to prevent peak opening loads from exceeding 850 pounds, since the load transducer used for total riser load had a full scale rating of 1000 pounds. Selected suspension lines, four on the leading edge and four on the keel of each model, were instrumented with tensile load transducers. For some of the runs, one or two reefing lines carried load transducers.

Before each run, zero readings and calibrations were recorded with all strain links unloaded. During the run, data recorders and cameras were started prior to wing deployment. The deployment sleeve line cutter was fired and a few seconds after the deployment transients leveled out, data recorders and cameras were shut down.

Summary of Wind Tunnel Gliding Performance Characteristics

Table 4 lists the maximum L/D measured for each of the configurations tested. As shown in Figures 6 to 11, the suspension line rigging for all single keel models was basically the same; this was also true for all of the twin keel models, as shown in Figures 12 to 17. The configuration variables during the testing of a given model were the lengths of the tip suspension lines and length of the aft keel suspension lines. Table 4 shows the effective tip line length (as a ratio of tip suspension line length to reference keel length) for which maximum L/D was obtained. It should be noted that the maximum L/D measured for the single keel models always occurred at approximately the same tip line length. This tip line length ($\ell_T/\ell_K = 0.723$) was the shortest length tested. This test series showed a definite increase of L/D with decreased tip line length. The series did not necessarily identify the tip line length yielding maximum L/D, since the trend in

TABLE 4.

Summary of Performance Data From
Wind Tunnel Tether Tests

Parawing (Keel) Planform	Model Number	Performance Summary	
		Tip Line Length (ℓ_T / ℓ_K)	Maximum L/D
Single	S-1A	.718	2.55
Single	S-1B	.721	2.50
Single	S-1C	.720	2.45
Single	S-1D	.718	2.45
Single	S-1E	.718	2.50
Single	S-1F	.718	2.45
Single	S-1G	.718	2.50
Single	S-2	.724	2.40
Single	S-2A	.718	2.35
Single	S-3	.736	2.40
Twin	T-1A	.648	2.80
Twin	T-1B	.659	2.75
Twin	T-1C	.637	2.80
Twin	T-1D	.637	3.15
Twin	T-1E	.603	3.40
Twin	T-2	(1)	(1)
Twin	T-3	.662	2.50

(1) This model not tether tested.

L/D was upward at the shortest length tested. The single keel data presented in Table 4 show the effect of structure on maximum L/D for a common tip line length.

The minimum tip line lengths for the twin keel models varied with the model configurations tested. With the T-1 series of models, maximum L/D increased as the tip line length was decreased. However, it should be noted that the same minimum tip line length was not tested for each model of the T-1 series of models. Therefore, a direct comparison (within the T-1 model series) of maximum L/D capability is not possible. The highest L/D measured with the twin keel models (3.40 for model T-1E) was obtained at a tip line setting considerably shorter than that rigged for any other of the T-1 models. The maximum L/D shown for Model T-3 was obtained at the minimum tip line length that resulted in stable flight. The minimum tip line length that could be used with the T-1 models was shorter than could be successfully flown on the T-3 model. This difference in performance was apparently caused by the structural differences between the T-1 series of models and the T-3 model.

In summary, it appears that canopy structure, number and diameter of suspension lines (within the range of diameters tested) did not have a significant effect on the maximum L/D capability of the single keel parawing models tested. For the twin keel models, structure did have an effect on maximum attainable L/D. Model T-3 could not be successfully flown with tip line lengths as short as was possible with the T-1 models. Therefore, its performance was limited. No effect on twin keel maximum L/D could be seen for variations in suspension line diameter.

Apparently the large number of suspension lines on model T-1C affected this model's performance. Model T-1B with 68 suspension lines showed a maximum L/D of 2.75 with $\ell_T/\ell_K = 0.664$,

while model T-1C with 100 suspension lines had a maximum L/D of 2.55 at the same ℓ_T/ℓ_K ratio. The maximum L/D performance of models T-1A and T-1B was nearly the same.

Figures 21 through 24 show photographs of models S-1G and S-2, and typical plots of aerodynamic performance data for these models. The data for these two models were selected for presentation to show the measured performance with the basic single keel design (model S-1G) compared to the performance of a model with different structure (model S-2). Model S-1G had the panel seams running normal to the trailing edge of the model, whereas model S-2 had these seams parallel to the trailing edge. The panel seams in model S-2 provide a natural load path from leading edge suspension lines to keel suspension lines. This type of structure, as compared to the model S-1G structure, was felt to be superior for carrying deployment loads from the canopy surface into the suspension lines. Figures 22 and 24 show that there was little difference in the performance of the two designs. Figures 25 and 26 show photographs and performance data for model T-1E. The data shown by Figure 26 are typical for the twin keel design and show the effect of tip line length variation on gliding performance. L/D performance was optimum for this model with a tip line length ratio of approximately 0.616.

General Discussion and Evaluation of the Reefed Configurations

This section gives a general discussion of the behavior of the reefed configurations tested in the LRC wind tunnel. The discussion is based primarily on visual observation of the tests and review of motion picture coverage of the tests. The material which follows is arranged to discuss in general the observed characteristics of the reefed configurations in terms of the previously discussed evaluation criteria. A general evaluation of the reefing sequences is shown in Tables 5 and 6.

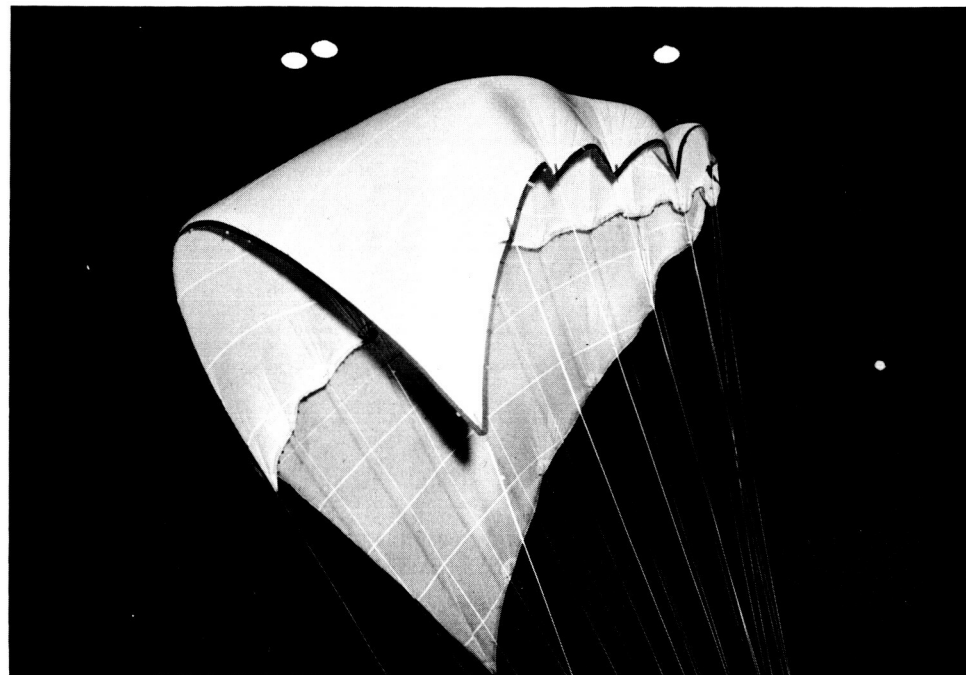
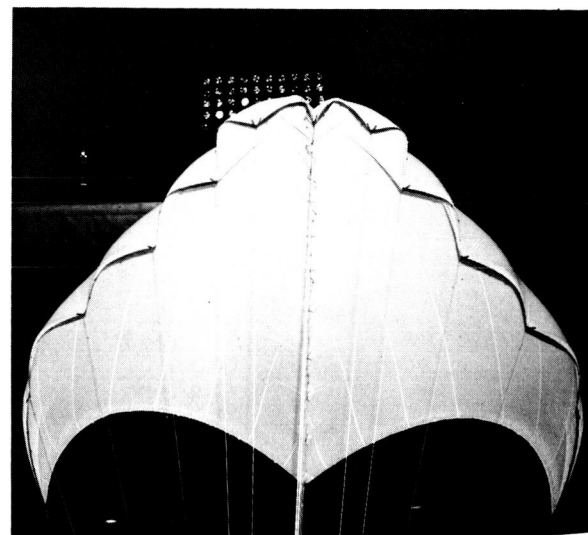
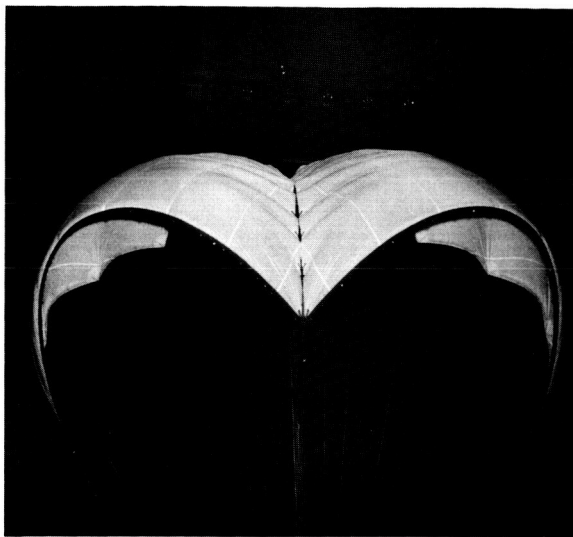


Figure 21. Single Keel Model S-1G Inflated in
LRC Full Scale Wind Tunnel

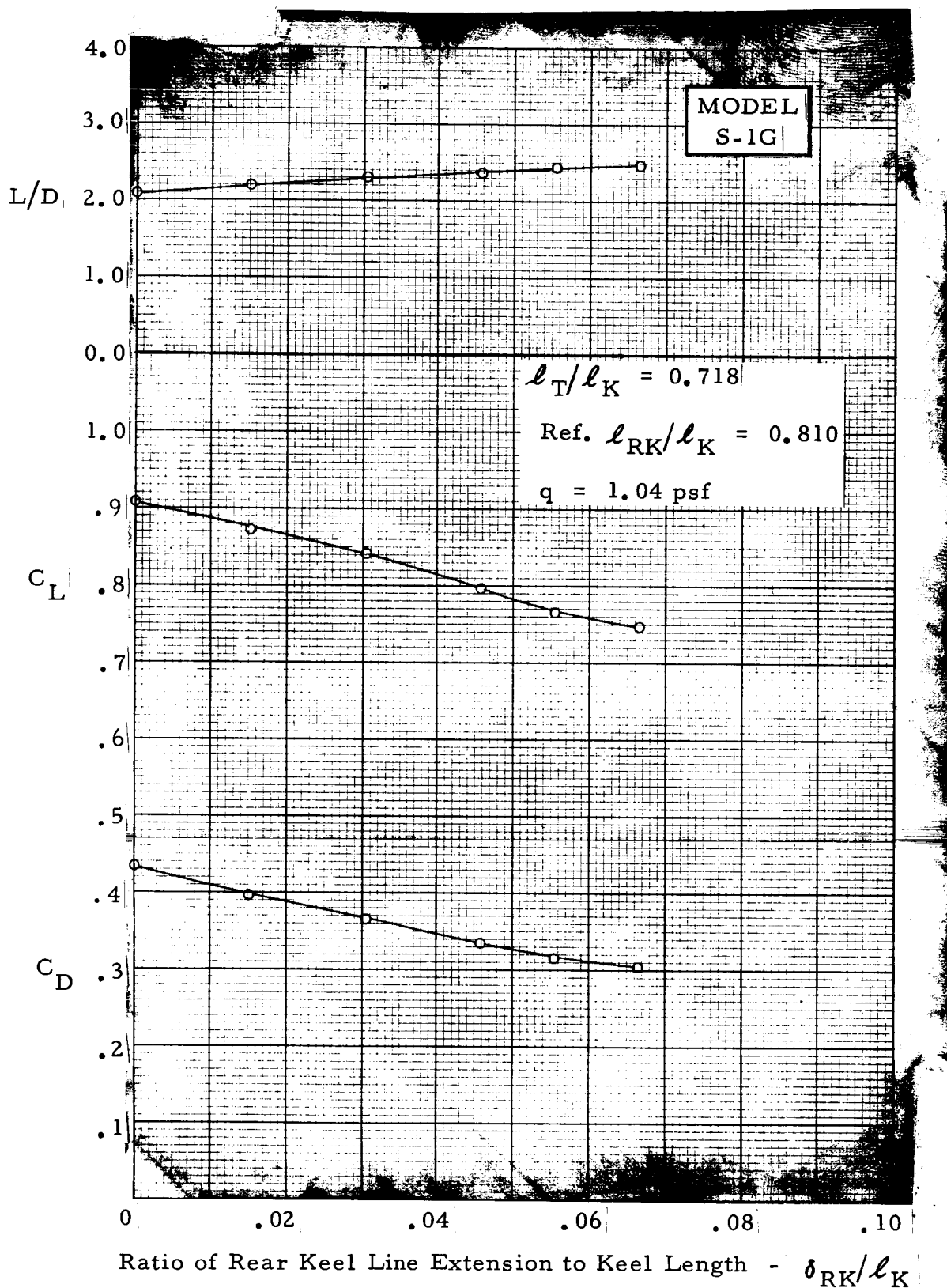


Figure 22. Single Keel Model S-1G Aerodynamic Performance

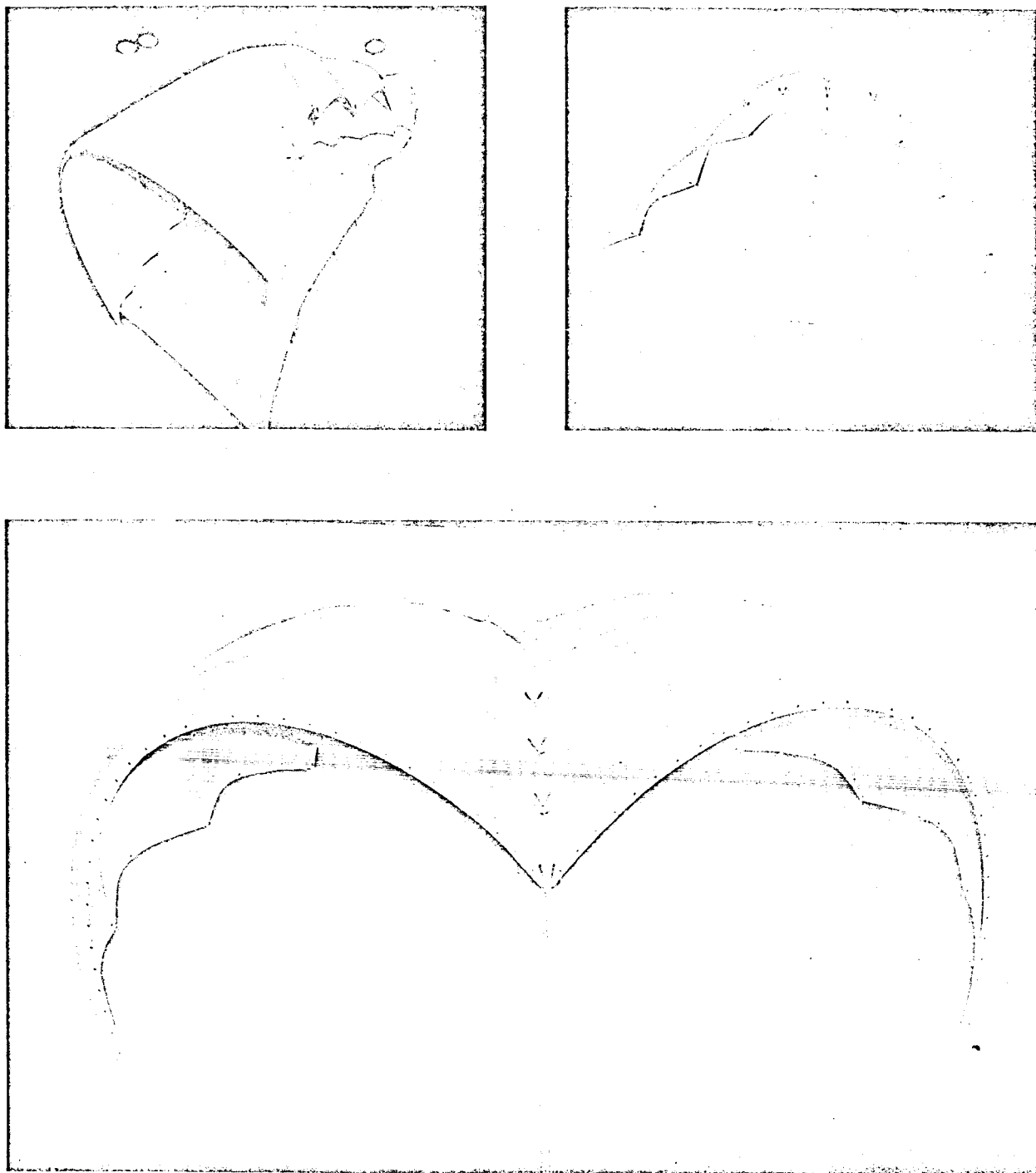


Figure 23. Single Keel Model S-2 Inflated in Langley full-scale tunnel

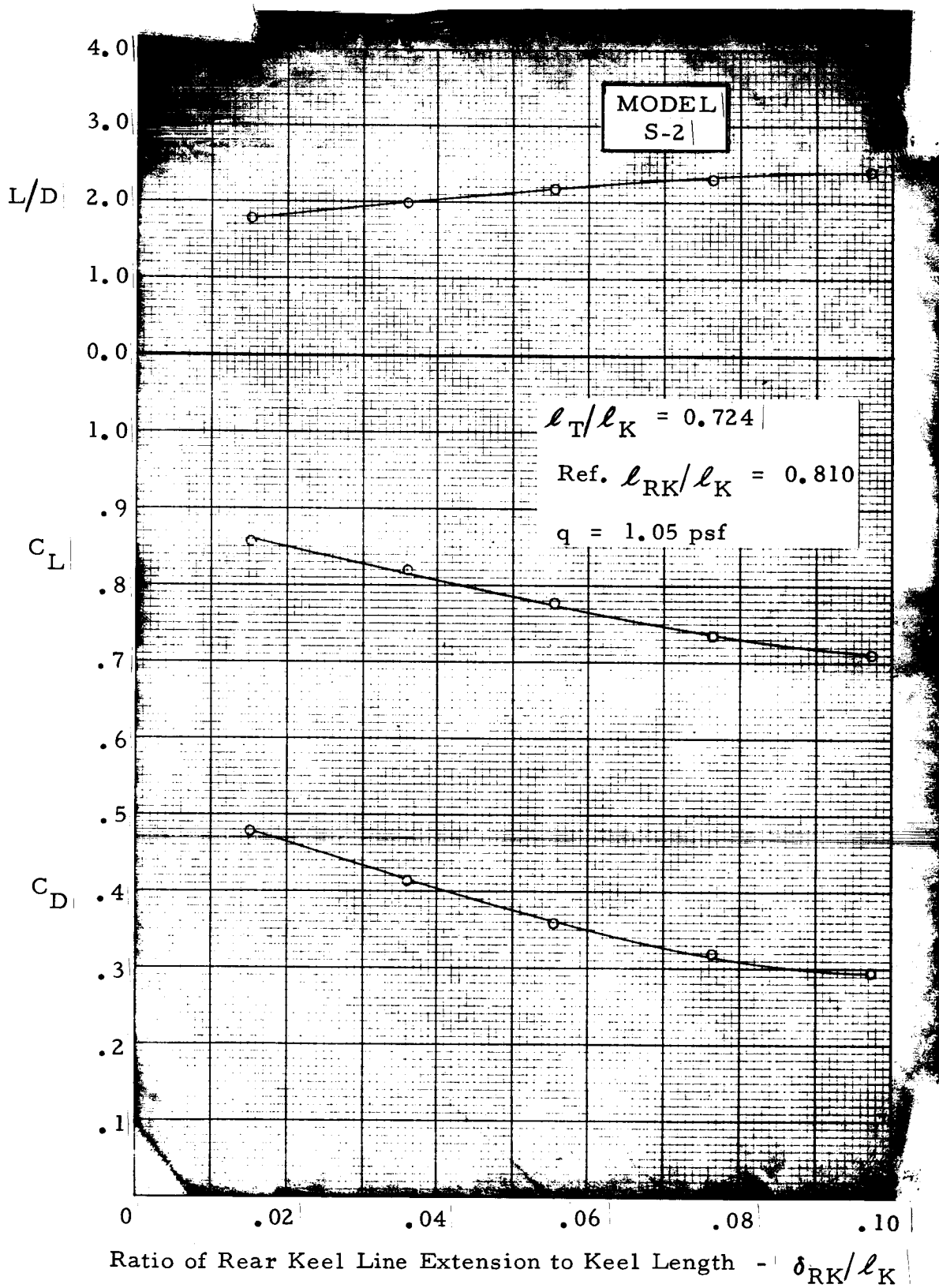


Figure 24. Single Keel Model S-2 Aerodynamic Performance

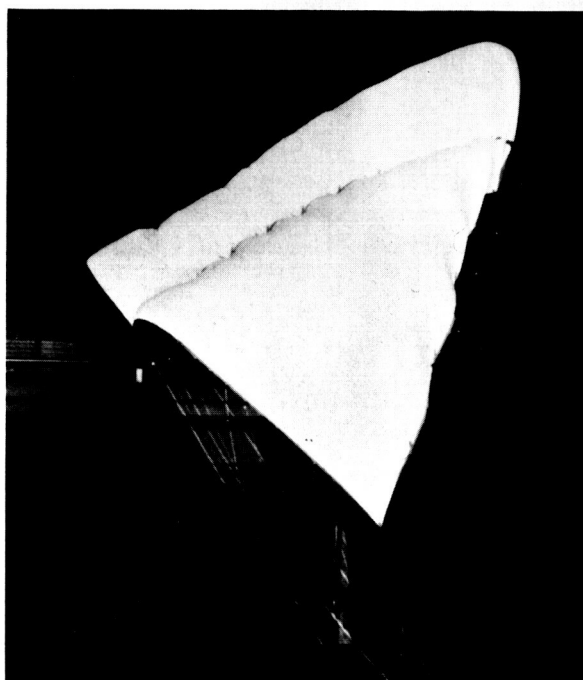
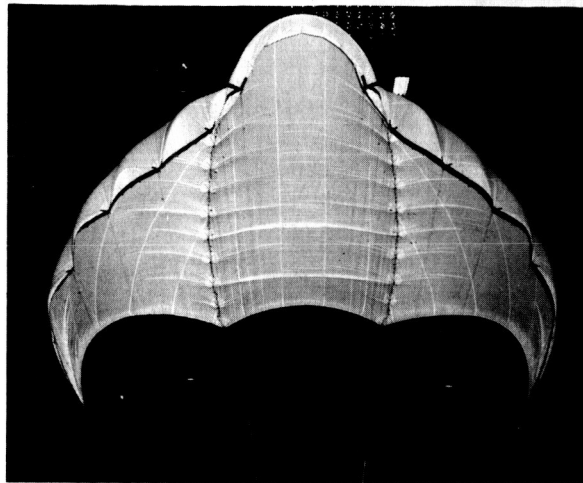


Figure 25. Twin Keel Model T-1E Inflated in
LRC Full Scale Wind Tunnel

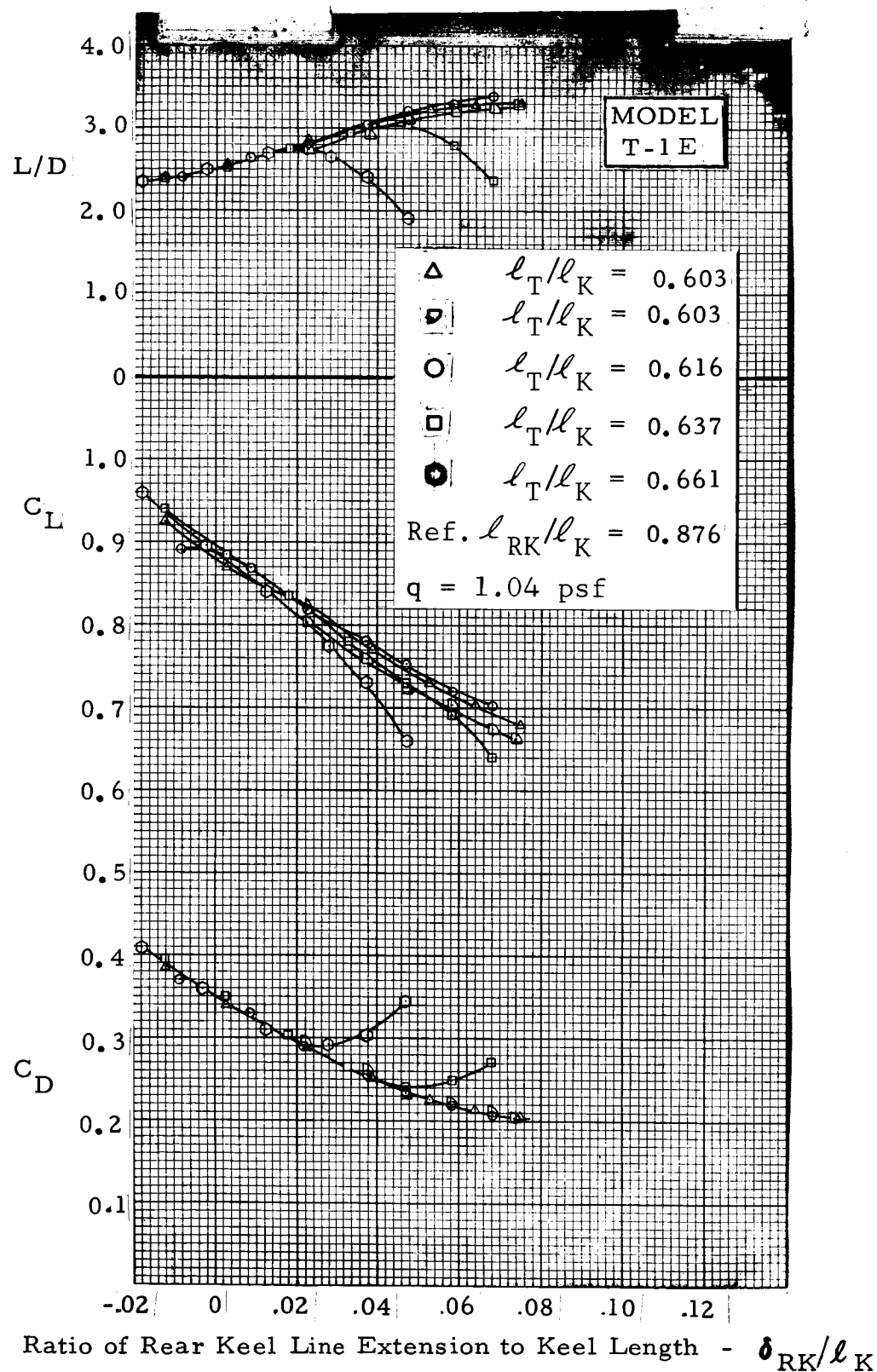


Figure 26. Twin Keel Model T-1E Aerodynamic Performance

These tables list the reefing sequences tested and present a qualitative evaluation of each sequence in terms of the evaluation criteria given earlier in the report.

Multi-step drag area capability. - All of the configurations tested had the capability of providing several stages of drag area during the deployment sequence. The configurations with laced or gathered trailing edges and reefing lines or daisy chains forming separate lobes from the major divisions of the wing surface appeared to have superior capability for drag area variation. Major divisions of the wing surface are defined as 1) the right and left halves of the single keel wing and, 2) the two portions of the wing outboard of the keels and the portion of the wing between the keels for the twin keel wing.

Reliable and repeatable inflation characteristics. - All of the configurations tested inflated to a characteristic balloon shape during first stage. While in this stage, the parawing functioned strictly as a drag device. There were no pronounced indications of significant side forces being produced by any of the first stage configurations.

The models which had the best inflation characteristics used reefing lines or daisy chains and equal length suspension lines to control the entire periphery and the keels of the wing. The configurations which did not have equal length suspension lines around the wing periphery did not force the plane of the inlet to be perpendicular to the airstream; this resulted in erratic inflation behavior. Aerodynamically reliable inflation occurred during all stages following stage one for the configurations tested.

Stable reefed aerodynamic characteristics. - All configurations inflated in a bulbous or balloon shape during the first reefed stage. There were differences, however, in the stability

(1) RELIABLE AND REPEATABLE INFLATION CHARACTERISTICS	(2) DEGRADATION OF GLIDING CAPABILITY	(3) AUTOMATIC DRAG AREA	(4) CAPABILITY OF MAXIMUM GLIDING	(5) CAPABILITY MATERIAL CONTROL SUSPENSION LINES	(6) SUSPENSION LINE AERODYNAMICS
(1) TRAILING EDGES LACED TOGETHER. REEFING LINES AROUND PERIPHERY OF WING. NO CONTROL OF SUSPENSION LINES.	DOUBTFUL	NONE	GOOD	VERY POOR	GOOD
(2) ALL PERIPHERAL SUSPENSION LINES SAME LENGTH. REEFING LINES AROUND PERIPHERY OF WING. NO CONTROL OF KEEL LINES.	GOOD	NONE	FAIR	POOR	GOOD
(3) ALL PERIPHERAL SUSPENSION LINES SAME LENGTH FROM CIRCLE LAID OUT ON WING SUR- FACE. REEFING LINES AROUND CIRCLE ON WING SURFACE. NO CONTROL OF KEEL LINES.	DOUBTFUL	NONE	FAIR	POOR	FAIR
(4) ALL SUSPENSION LINES SAME LENGTH. TRAILING EDGES LACED TOGETHER. REEFING LINES AROUND LEADING EDGES AND KEEL TO FORM TWO LOBES.	GOOD	NONE	VERY GOOD	GOOD	POOR
(5) ALL SUSPENSION LINES SAME LENGTH. REEFING LINES AROUND LEADING EDGES. KEEL AND TRAILING EDGES TO FORM TWO LOBES.	GOOD	NONE	GOOD	GOOD	FAIR
ALL SUSPENSION LINES SAME LENGTH. TRAILING EDGES GATHERED TOGETHER. REEFING LINES AROUND LEADING EDGES AND KEEL TO FORM TWO LOBES.	GOOD	NONE	VERY GOOD	GOOD	FAIR

Table 5. Qualitative Evaluation of Single Keel Parawing Reefing Systems

	DOUBTFUL	NONE	GOOD	POOR	FAIR	FAIR
(1) KEELS LACED TOGETHER. ALL SUSPENSION LINES SAME LENGTH TO CIRCLE LAID OUT ON WING SURFACE. REEFING LINES AROUND CIRCLE ON CANOPY SURFACE.	GOOD	NONE	GOOD	GOOD	POOR	<u>FAIR</u>
(2) TRAILING EDGES LACED TOGETHER. ALL SUSPENSION LINES SAME LENGTH. REEFING LINES AROUND LEADING EDGES AND KEELS TO FORM THREE LOBES.	GOOD	NONE	GOOD	GOOD	GOOD	<u>FAIR</u>
(3) TRAILING EDGES GATHERED TOGETHER. ALL SUSPENSION LINES SAME LENGTH. REEFING LINES AROUND LEADING EDGES AND KEELS TO FORM THREE LOBES.	GOOD	NONE	VERY GOOD	GOOD	GOOD	<u>FAIR</u>
(4) ALL SUSPENSION LINES SAME LENGTH. REEFING LINES AROUND LEADING EDGES, TRAILING EDGES AND KEELS TO FORM THREE LOBES.	GOOD	NONE	GOOD	GOOD	GOOD	<u>FAIR</u>

Table 6. Qualitative Evaluation of Twin Keel Parawing Reefing Systems

of the configurations tested. The configurations which had the trailing edges laced showed strong tendencies to spin. The laced trailing edges resulted in a reefed shape which had a relatively sharp edge protruding along the rear of the reefed canopy. This sharp edge acted as a vane which caused the model to spin. None of the other configurations had severe spinning or oscillating characteristics.

During stage two, there were indications that some of the configurations developed lift and, therefore, began to glide.

All stages of reefing following stage two resulted in configurations which had strong gliding characteristics. Although the test setup with the model flying horizontal made evaluation of the stability characteristics of the reefed stages difficult, the configurations with gathered trailing edges were in general more stable than the other tested configurations.

Control of canopy material and suspension line control during deployment. - All of the configurations showed some cloth flutter during the early inflation of the first reefed stage. The configurations which did not incorporate equal length suspension lines developed line tangles. During disreef into second stage some suspension lines were pulled through the entanglement. Relative motion of this type where lines are in contact with each other can lead to friction burn damage. The configurations which used a reference circle on the canopy surfaces to determine the length of the suspension lines during the reefing sequence also had a problem. It appeared that the canopy material outside the reference circle could be blown

into the canopy inlets and partially block them, with resulting erratic inflation behavior. It was apparent from the wind tunnel tests that all suspension lines had to be made the same length until the canopy was fully open.

Suspension line load distribution. - The line load distribution during the first reefed stage was most uniform for the reefed configurations which had the greatest number of lines rigged at equal length and least uniform for those configurations which had the flying line lengths. During later stages, the suspension line load distribution depended on the geometry of the reefed configuration. For instance, a twin keel parawing, second stage configuration which had both leading edges free, the center lobe reefed and the trailing edges gathered had high loads in the leading edge lines relative to the remainder of the suspension lines on the canopy. Representative line load data are given in a subsequent part of this report.

Degradation of gliding flight performance. - None of the configurations tested depended on modifications of the canopy planform or changes in the suspension line arrangement for proper functioning of the system. However, structural changes such as the addition of a radial tape network did affect gliding performance.

Selection of Reefing System for Further Testing

The results of the evaluation of the tested reefing systems presented in Tables 5 and 6 indicated that the most promising reefing systems for further testing were System 6 for the single keel parawing and System 3 for the twin keel parawing.

Detailed Description of the Selected Reefing Systems

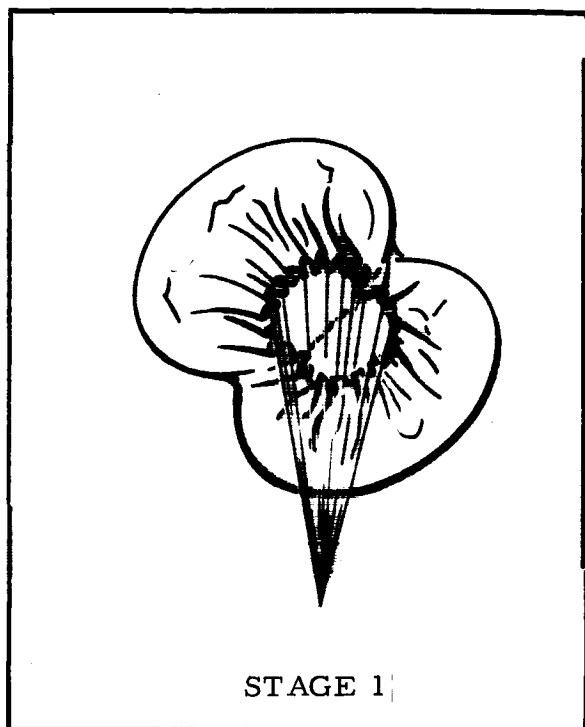
The reefing systems selected for the single keel and the twin keel parawing free flight deployment tests are described in this section. In addition, a discussion of the data obtained in the wind tunnel for these systems is presented.

Single keel reefing system. - Stage 1: Because of the problems induced by uneven suspension line lengths as previously discussed, all suspension lines were shortened in Stage 1 to the length of the shortest (tip) suspension line. Making all suspension lines the same length eliminated loose lines which could become entangled during the deployment process. It also prevented damage to the keel suspension lines from abrasion against the skirt reinforcing band of the wing.

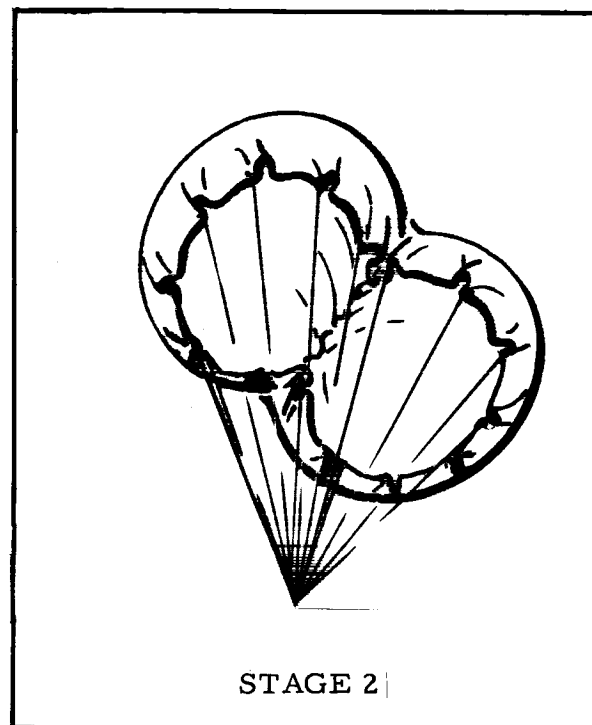
The canopy was reefed into two lobes by gathering the trailing edges and routing reefing lines around the leading edges, trailing edges and each side of the keel. Figure 27 shows a view of the canopy from below during Stage 1. As can be seen, two lobes are formed with the keel forming the partition between the lobes. For a range of reefing line ratios (ℓ_{RL}/ℓ_K) from approximately 0.15 to 0.25, the drag coefficient of the fully inflated reefed wing was relatively constant. This behavior is desirable, in that it allows the first stage filling time to be varied without reducing the first stage drag coefficient.

Stage 2: Stage 2 was the same as Stage 1, except that the length of the reefing lines was increased to give a higher drag coefficient. Figure 27 shows a view of the canopy from below during second stage.

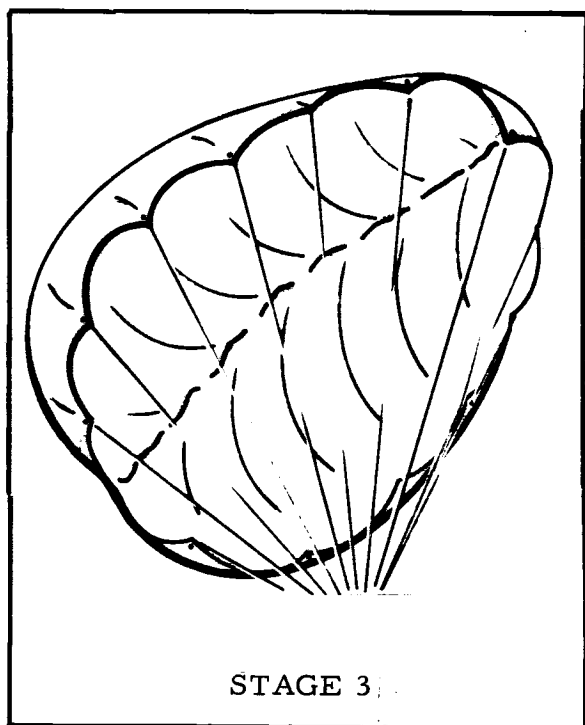
Stage 3: For Stage 3 the leading edge and keel reefing lines were severed, leaving the suspension lines all equal in length and the trailing edges still gathered. Figure 27 shows the appearance of the third stage from below. The gathering



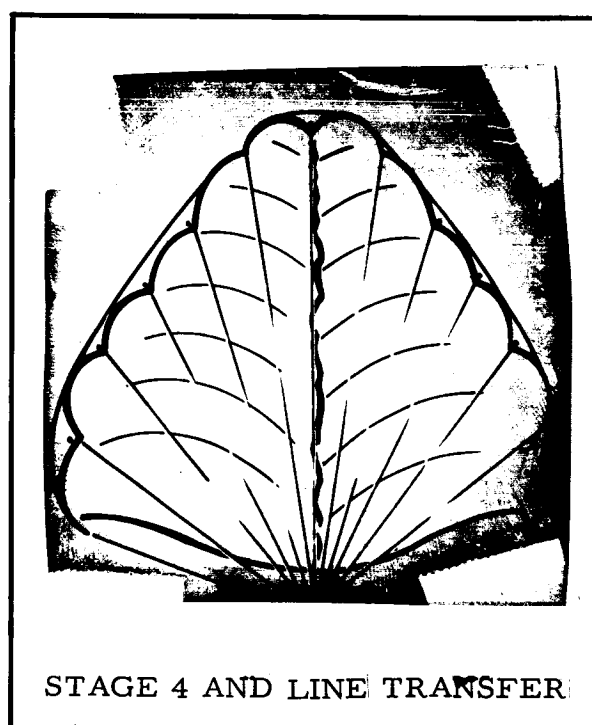
STAGE 1



STAGE 2



STAGE 3



STAGE 4 AND LINE TRANSFER

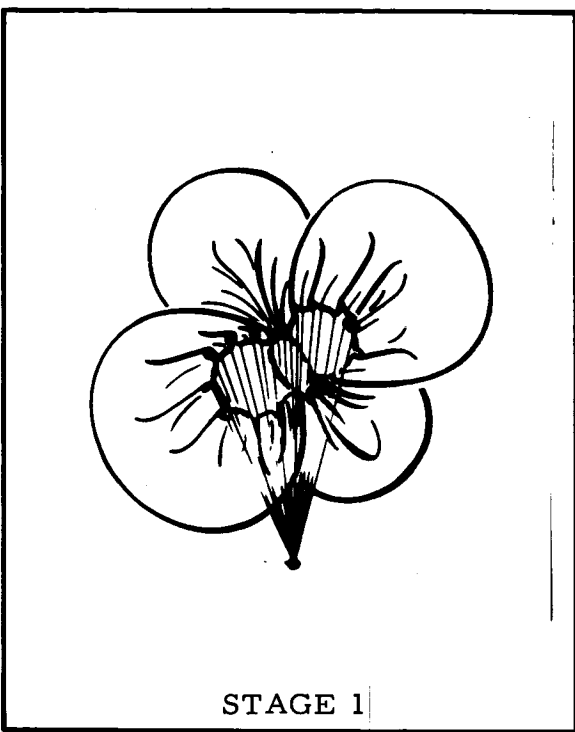
Figure 27. Planforms of Selected Single Keel Reefing System

of the trailing edges is evident, as shown by the rounded shape of the trailing edge portion of the canopy. The trailing edges were gathered by routing a line through reefing rings from wing tip to wing tip and then pulling the line tight. This reefing method brought each wing tip up next to the keel and gathered all of the trailing edge skirt band between the wing tips. In this stage, the wing makes the transition from a parachute-like ballistic drag device to a gliding wing. The glide direction during this stage was rearward.

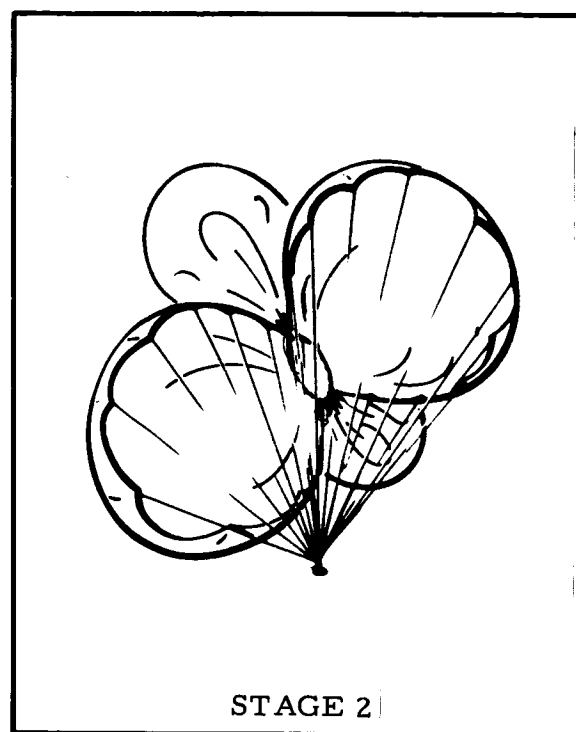
Stage 4: For Stage 4 the trailing edge gathering line was released and the wing allowed to inflate fully. The wing continued to glide rearward during this stage. Figure 27 shows a view of the canopy from below during fourth stage. In order to obtain stable canopy inflation and stable flight in this stage, trailing edge lines were necessary.

Stage 5: For Stage 5 the suspension lines which had been shortened were allowed to go to the correct lengths for gliding flight. Following the change in suspension line lengths, the wing underwent a transition to forward gliding flight. The trailing edge lines were lengthened sufficiently to become slack during the gliding phase.

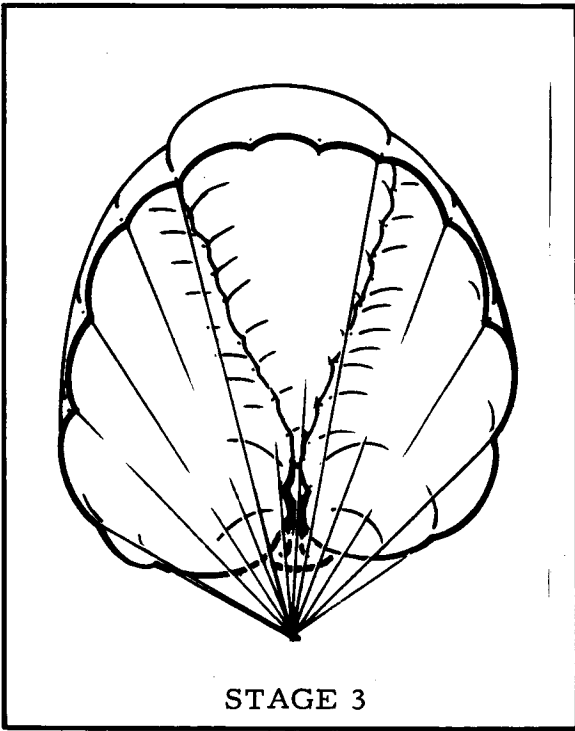
Twin keel reefing system. - For Stage 1, all suspension lines were shortened to the length of the shortest (tip) line. This was done for the same reason as previously discussed for the single keel reefing system. The wing surface was reefed into three lobes by use of a reefing line around the periphery of each section of the wing (i.e., the center and two side panels) and by gathering the trailing edges. This resulted in three separate inlets through which air entered for inflation. The inlets were separated from each other by the keels. Figure 28 shows a view of the canopy from below during Stage 1. The variation of drag coefficient with reefing line ratio was the



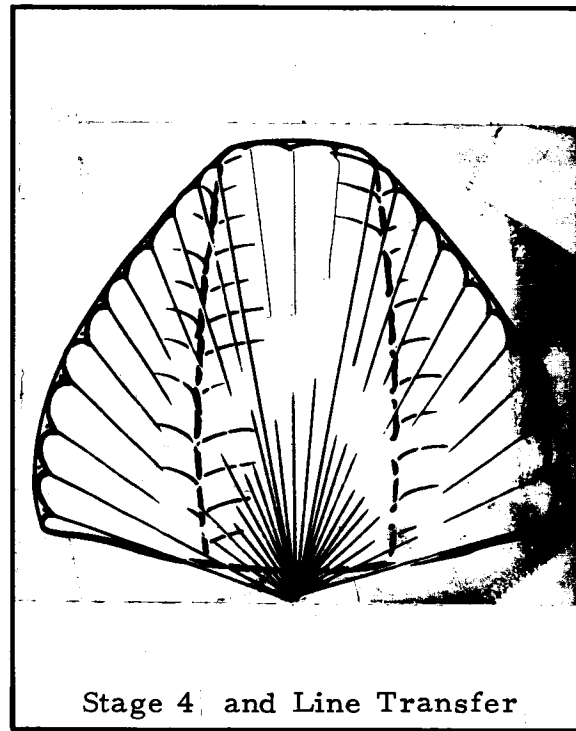
STAGE 1



STAGE 2



STAGE 3



Stage 4 and Line Transfer

Figure 28. Planforms of Selected Twin Keel Reefing System

same for both the twin and single keel wings. As previously stated in the discussion of the single keel reefing system, the relatively constant drag coefficient over a range of reefing line ratios allowed control of filling time, while still providing a stable inflated shape. This constant drag coefficient allowed control of the opening forces experienced during Stage 1, while providing sufficient drag area to give a relatively low terminal velocity for the first reefed stage.

Stage 2: For Stage 2 the reefing lines in the side panels of the wing were severed, allowing the leading edges of the side panels to inflate fully. The resulting inflated planform is as shown by Figure 28. This stage continued to act as a ballistic drag device similar to a parachute.

Stage 3: For Stage 3 the center section reefing line was severed. The wing planform in this stage is shown in Figure 28. The trailing edges remained gathered as described for the single keel reefing system. During this stage, the wing went into rearward gliding flight.

Stage 4: For Stage 4 the trailing edge gathering line was severed and the wing allowed to inflate fully. The wing underwent a transition to forward gliding flight in this stage.

Stage 5: The suspension lines were released to their gliding flight lengths, and the wing made a transition to high performance gliding flight.

Representative Data for the Selected Reefing Systems

Force coefficients during deployment stages. - Figures 29 and 30 show a series of typical wind tunnel force coefficient-time histories (C_D and C_R) during a single keel parawing inflation sequence. Figures 31 and 32 present similar data for a typical twin keel parawing wind tunnel inflation sequence.

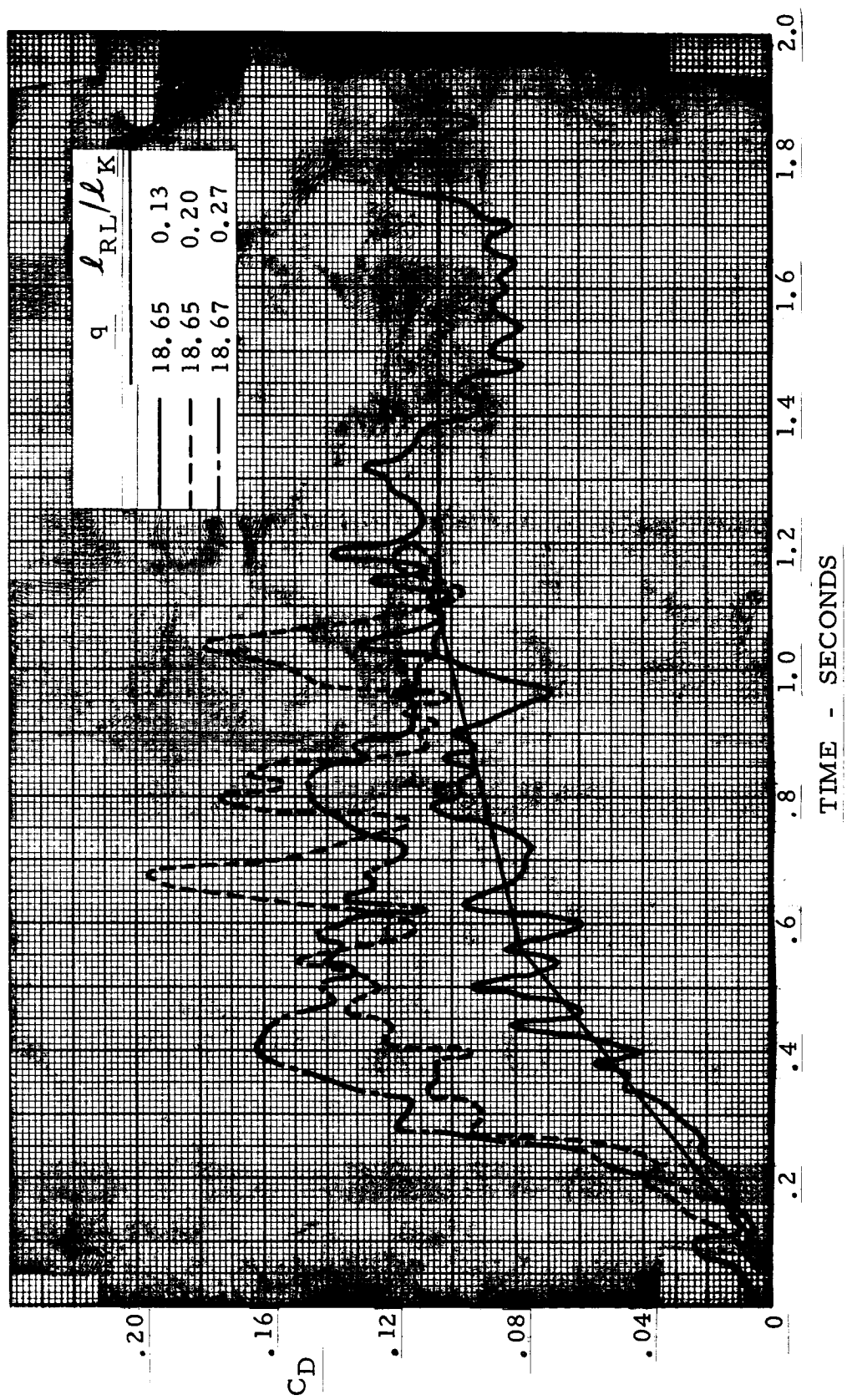


Figure 29. Typical Single Keel Parawing Wind Tunnel Model First Stage C_D Histories

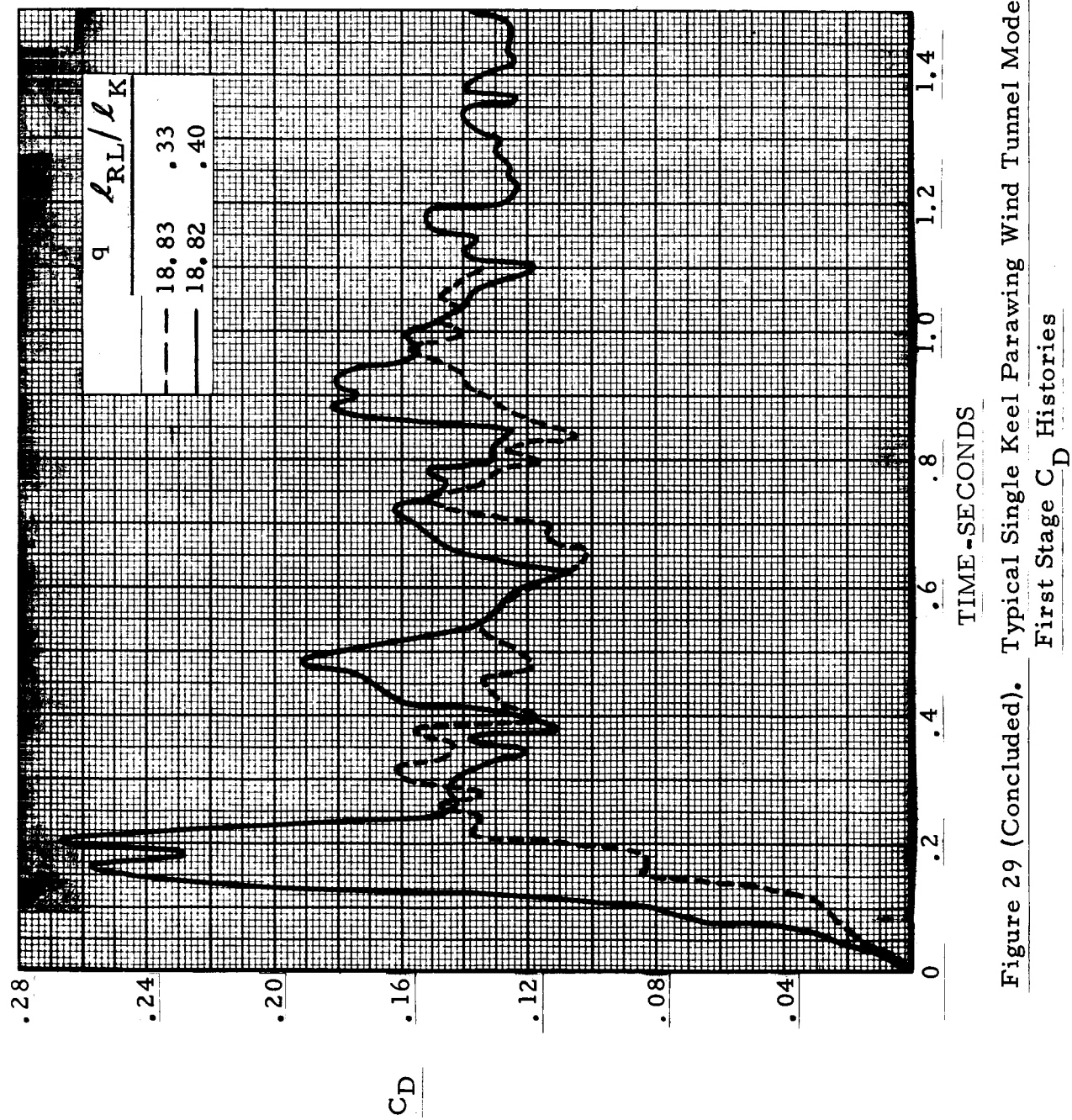


Figure 29 (Concluded). Typical Single Keel Parawing Wind Tunnel Model, First Stage C_D Histories

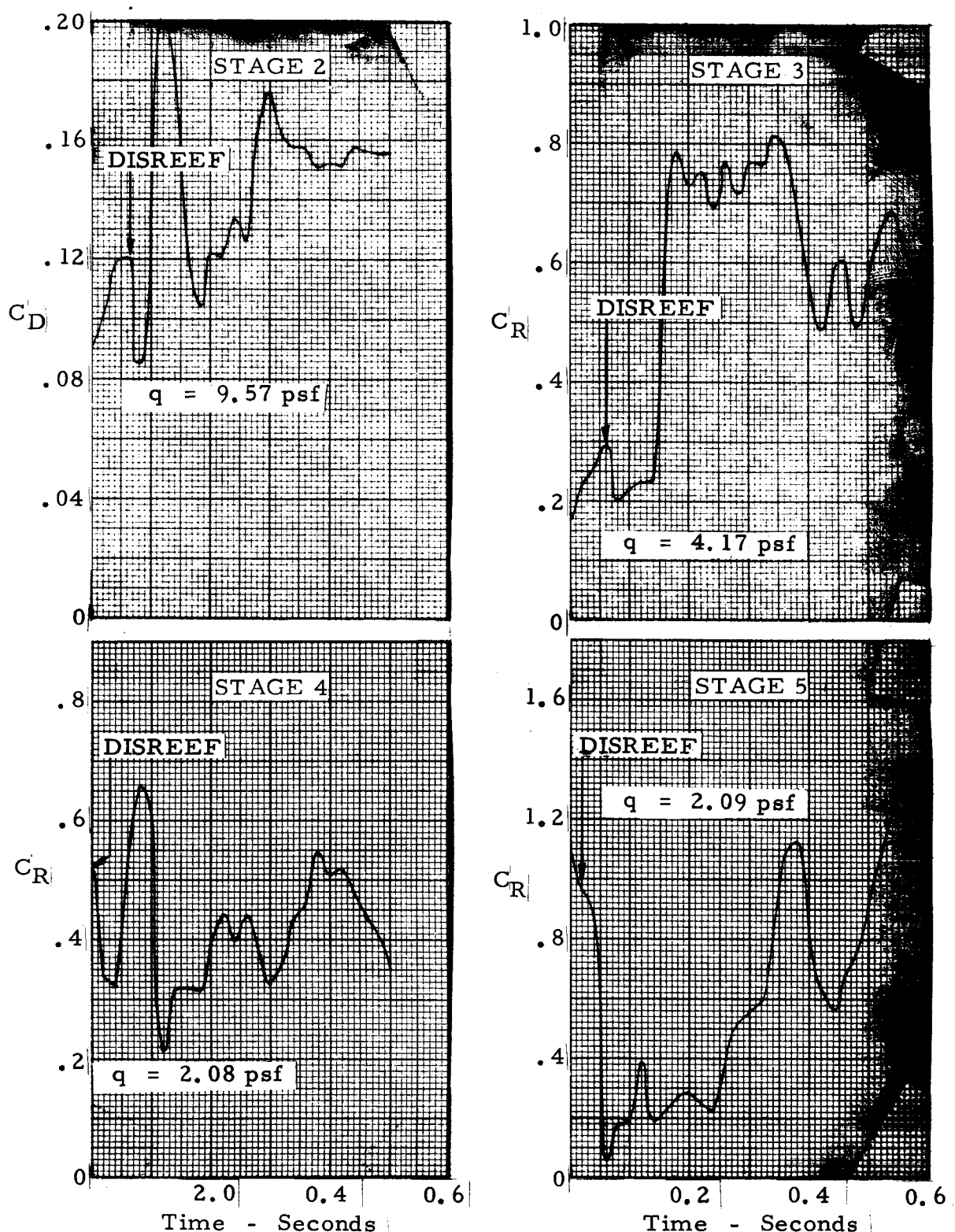
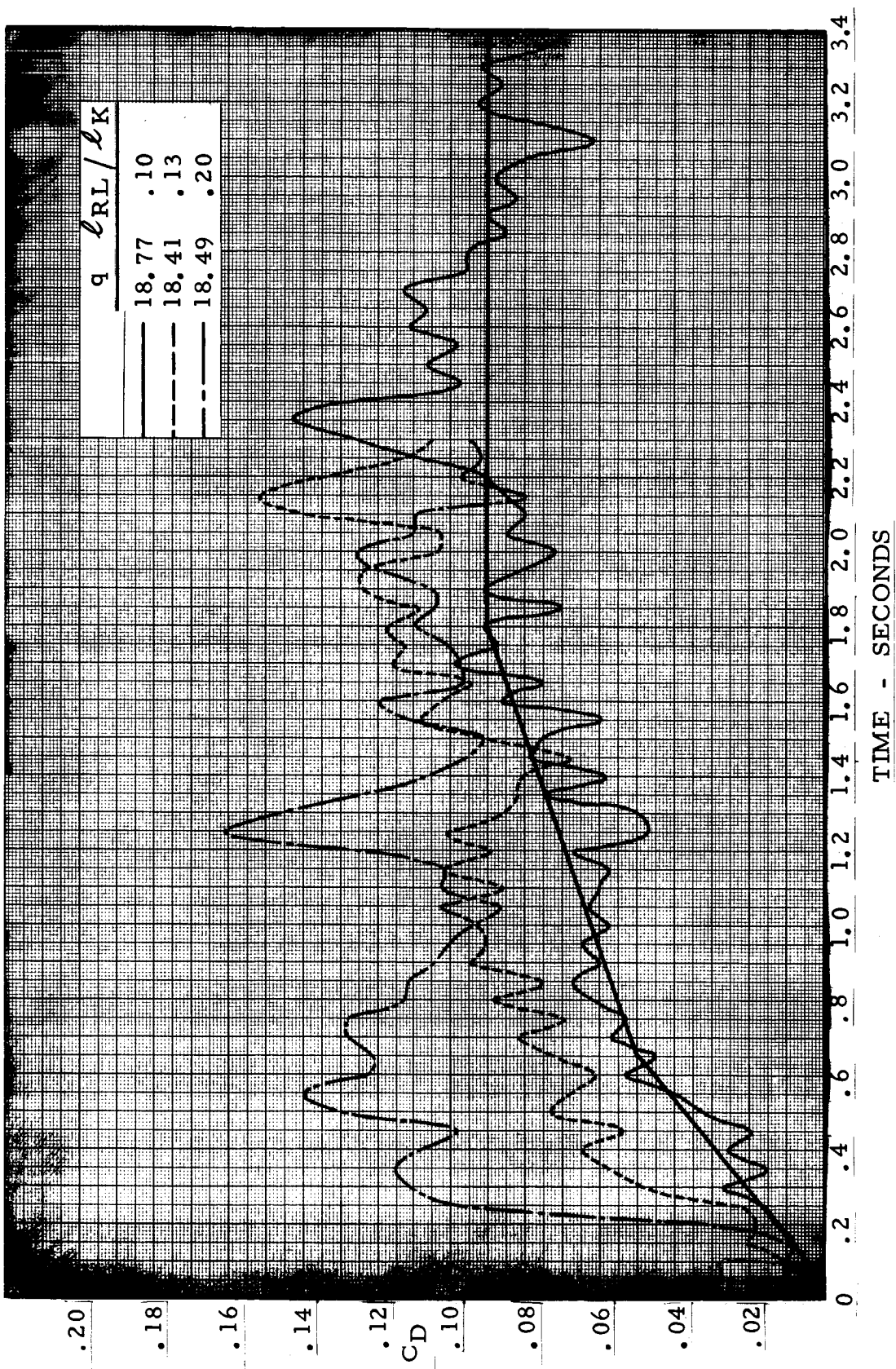


Figure 30. Typical Single Keel Parawing Wind Tunnel Model Disreef Sequence

Figure 31. Typical Twin Keel Parawing Wind Tunnel Model First Stage C_D Histories

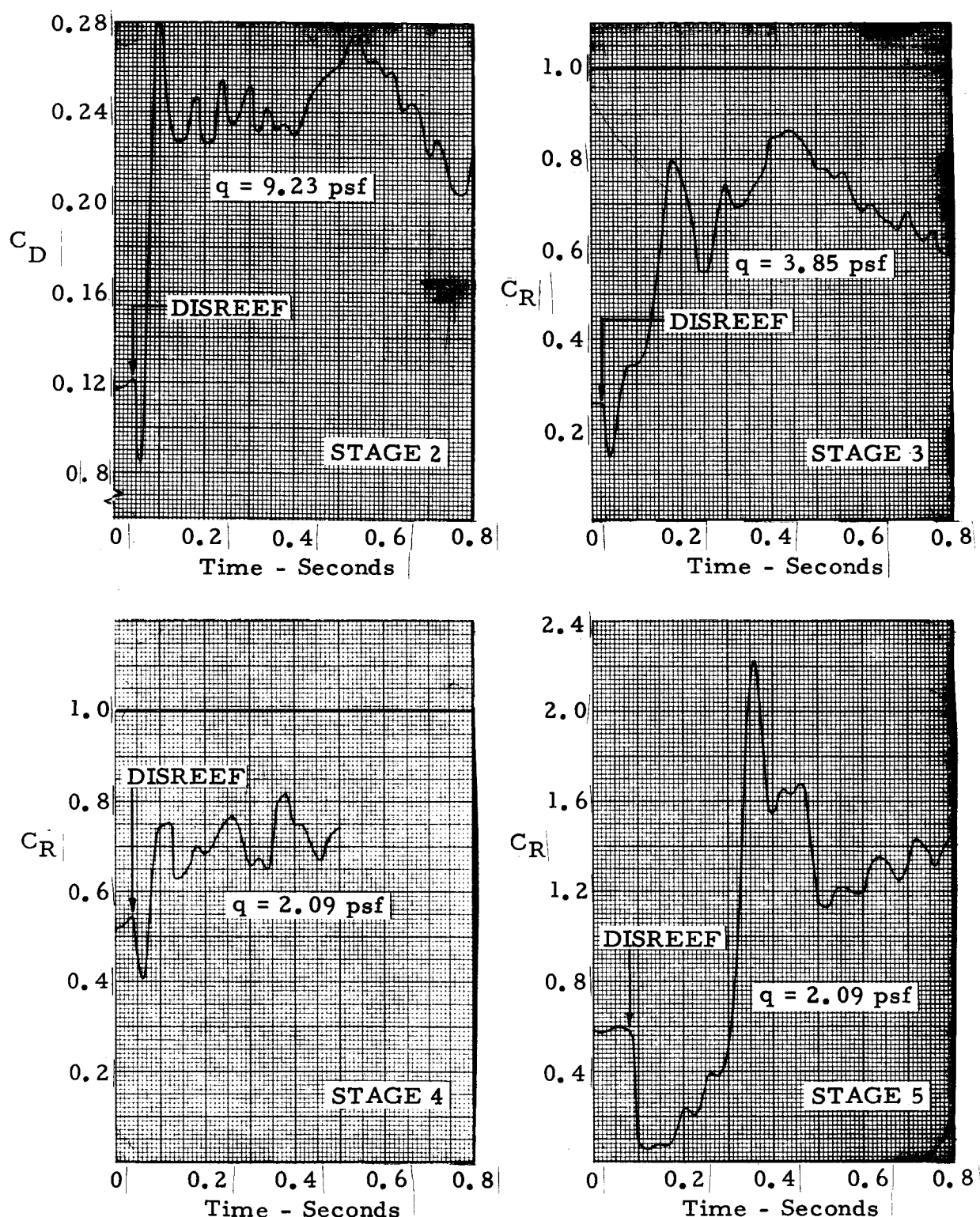


Figure 32 . Typical Twin Keel Parawing Wind Tunnel Model Disreef Sequence !

Figures 29 and 31 show the effect of reefing ratio on first stage inflation behavior. These figures are composites of drag area time histories for varying reefing line ratios for single and twin keel parawings. As would be expected, Figures 29 and 31 show that the filling time increases as the reefing line ratio is decreased. The shape of the drag coefficient curves shows a distinctive change in slope during the inflation process. This effect appears to be most pronounced for the low reefing ratio curves and is illustrated by the straight line approximations on Figures 29 and 31. As shown by these figures (29 and 31), the C_D versus time curve can be approximated by a two slope curve which has the steeper slope during the first part of the inflation process.

Figure 33 presents the first stage steady state and peak drag coefficients as a function of reefing line length ratio. The peak drag coefficients show a relatively large amount of scatter; however, in general the peak drag coefficient increased as reefing ratio increased. The steady state drag coefficients in Figure 33 were obtained by averaging the measurements over a relatively long period of time with the model fully inflated in the reefed state. For this reason, the data shown in Figure 33 may not agree exactly with the steady state drag coefficients over the short periods of time shown by Figures 29 and 31. The steady state drag coefficients for both twin and single keel parawings reefed in the first stage exhibited a relatively constant drag coefficient over the range of reefing line ratios from approximately 0.15 to 0.35. The reason for this behavior was that the inflated shape of the parawing during the first stage resembled a balloon. Changing the reefing ratio over the 0.15 to 0.35 range changed only the diameter of the canopy inlets and did not appreciably change the inflated diameter of the parawing. For reefing ratios less than 0.15, the diameter of the inlets was reduced to a

Symbol	Model Type	Reefing Configuration
○	Single Keel	(6)
△	Twin Keel	(3)
□	Single Keel	(5)
◊	Twin Keel	(4)

See Tables 5
and 6 for
description
of stage one
configuration

NOTE: Flagged data points are peak C_D values and unflagged points are steady-state C_D values.

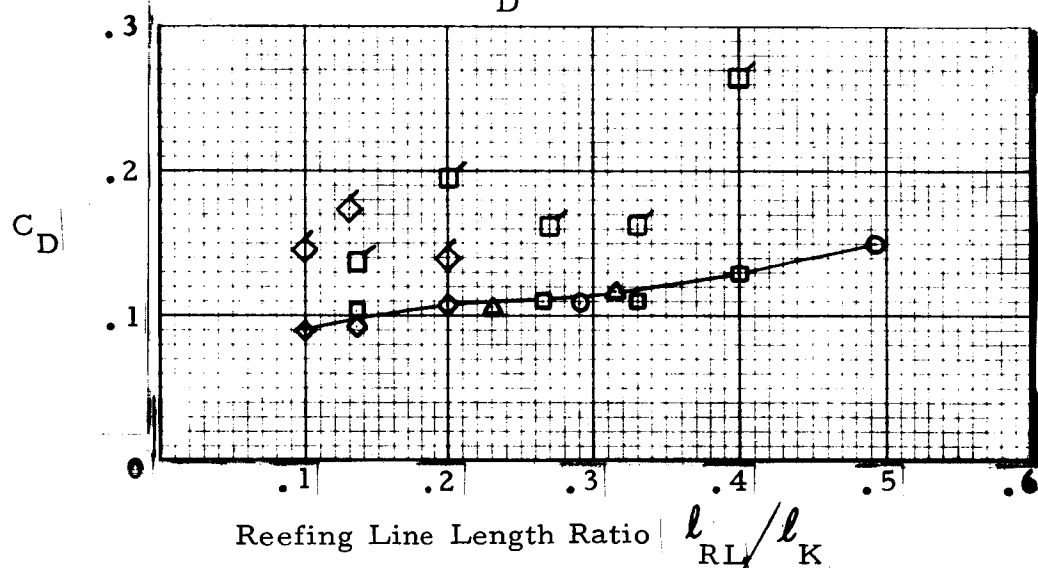


Figure 33. First Stage Reefed Drag Coefficient vs.
Reefing Line Length Ratio

point where there was sufficient pressure drop across the inlet to reduce the internal pressure in the canopy. The pressure reduction was induced by the restricted opening plus suspension line blockage of the inlet. With a reduced internal pressure, the inflated diameter of the reefed parawing was reduced.

First reefed stage filling time. - Figure 34 is a plot of filling time versus the inverse of the reefing ratio squared. By presenting filling time as a function of inverse reefing ratio squared, the effect of reefing ratio on filling time is shown as a function of inlet area ratio. With the balloon type of inflation obtained with the parawing during the first reefed stage, the volume of the fully inflated first stage was relatively constant for the range of reefing ratios for which data are given in Figure 34. Therefore, in the wind tunnel with a constant air stream velocity, filling time should be a linear function of only the reciprocal of the ratio $(\ell_{RL}/\ell_K)^2$. Figure 34 shows that this type of behavior was obtained. The data show that long filling times could be obtained while still maintaining reliable inflation. In order to meet the 3.0 g requirement for first stage, fill times in excess of 2.0 seconds would be necessary with the full scale system. Therefore, the wind tunnel test data showing long filling times with reliable inflation indicated that the selected reefing technique was feasible.

Disreef force coefficients. - Figures 30 and 32 show typical disreef sequences for the single keel and twin keel parawings, respectively. As mentioned previously, the second stage configurations showed only slight tendencies to glide. All stages following second stage had strong gliding characteristics. Therefore, it was necessary to restrain the model during testing of the latter stages of the sequence to confine the model to the test section. The force coefficient shown for stages

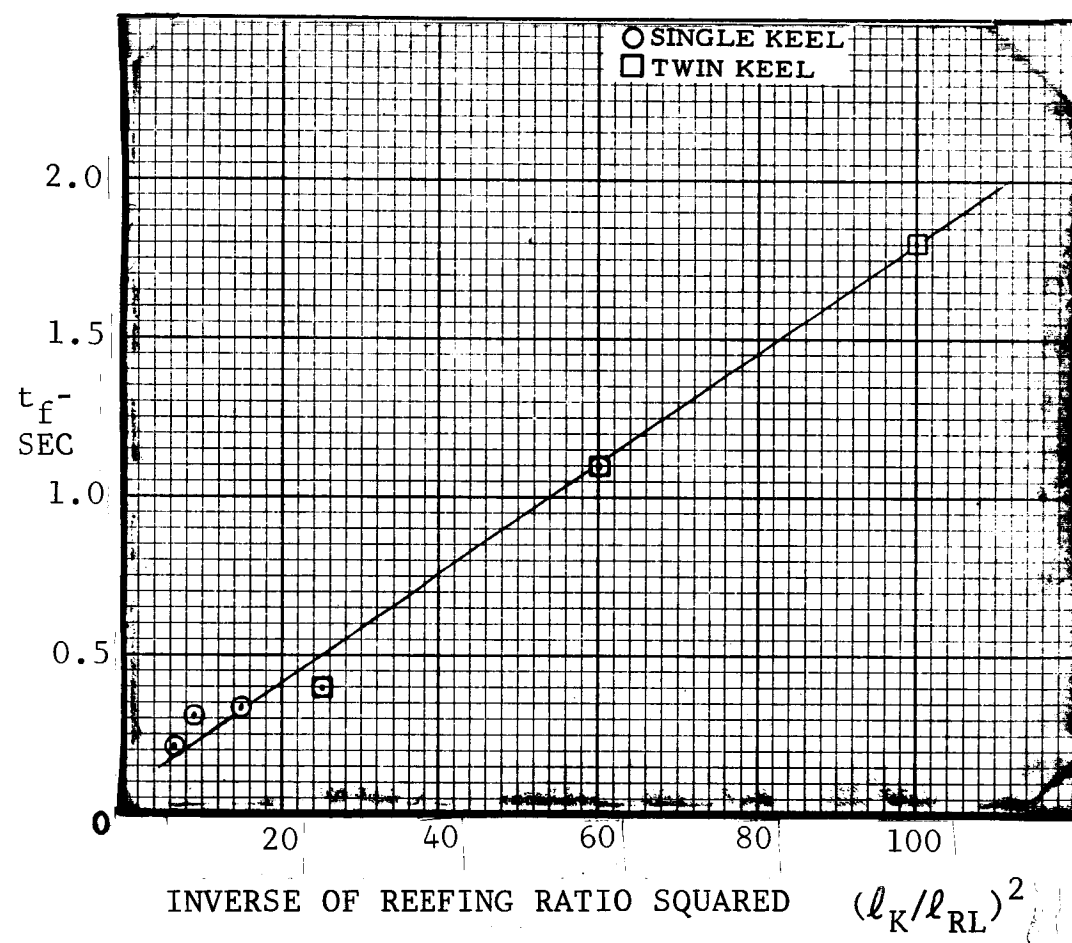


Figure 34. First Stage Filling Time vs. Inverse of Reefing Ratio Squared

three, four, and five is not a drag coefficient, but a resultant force coefficient. Possible effects of the tether lines on data presented in Figure 30 and 32 were not considered.

Suspension line loads. - Suspension line load data were obtained during the LRC wind tunnel test program. Tables 7 and 8 present these data as ratios of individual suspension line load to the peak total load measured for each reefing stage. The data shown are representative of the reefing sequence selected for further testing. Where reefing lines were used, the ratio of individual reefing line length to reference keel length is shown in a foot note below the tables.

The single keel line loads data were taken from tests of several different models. Data for the first three stages were obtained with models that did not have trailing edge lines; however, the absence of trailing edge lines should not seriously affect the load results. There are two exceptions: the loads measured in the tip lines and in the rear keel line. The loads in these lines are higher than they would have been if there had been trailing edge lines to help carry the load. The data for Stages 4 and 5 were obtained with models that had trailing edge lines.

The line load data for twin keel reefing were obtained during a single test sequence.

AMES WIND TUNNEL TEST PROGRAM

General

This section presents the results of a wind tunnel test program conducted at the Ames 40 ft by 80 ft tunnel. The models tested during this program were versions of the single and twin keel parawing designs developed at the Langley Research Center, Hampton, Virginia.

TABLE 7.

Single Keel Composite Line Load Distribution at Deployment

Line No.	Line Loca-tion	Reefing Stage				
		1(1)	2(2)	3	4	5
	X/ ℓ_K	1(1)	2(2)	3	4	5
L1	0.177	0.014	0.005	0.031	-	0.087
L3	0.500	0.043	0.019	0.113	0.084	0.090
L6	1.000	-	-	-	0.017	0.229
K1	0.125	0.012	0.005	0.044	0.028	0.055
K4	0.333	0.041	0.028	0.083	-	0.021
K7	0.583	0.043	0.061	0.029	0.090	-
K10	0.833	0.027	0.033	0.008	0.047	0.021
K12	1.000	-	-	-	-	0.020

(1) Reefing line ratio $\ell_{RL}/\ell_K = 0.284$. (2) $\ell_{RL}/\ell_K = 0.444$

TABLE 8.

Twin Keel Line Load Distribution at Deployment

Line No.	Line Loca-tion	Reefing Stage				
		1(1)	2(2)	3	4	5
	X/ ℓ_K	1(1)	2(2)	3	4	5
L2	0.549	0.026	0.098	0.063	0.023	0.034
L4	0.816	0.039	0.098	0.032	0.045	0.048
L6	1.083	0.047	0.039	0.041	0.040	0.059
LK1	0.267	0.017	0.000	0.043	0.048	0.031
LK3	0.400	0.069	0.062	0.047	0.039	0.029
LK6	0.600	0.036	0.028	0.034	0.019	0.036
L10	0.867	0.025	0.037	0.005	0.020	0.040
LK12	1.000	0.049	0.0096	0.057	0.041	0.097

(1) 3-lobes $\ell_{RL}/\ell_K = 0.234$ (2) $\ell_{RL}/\ell_K = 0.234$ (centered load)

NOTE: Line load distributions in Tables 7 and 8 are expressed as ratios of peak individual suspension line load to peak total load of the stage.

The principal objective of this wind tunnel test program was to determine the effects of canopy construction on the performance of the twin keel parawing. A secondary objective was to provide comparative wind tunnel data on models which had been used in free flight tests. These data could then be used in predicting free flight performance. In addition to the free flight models, one other model which had previously been tested in the Langley full-scale tunnel was also tested. This model was tested to provide a basis for comparing the test results obtained in the Langley wind tunnel with those obtained in the Ames wind tunnel.

Test Model Configurations

Figures 35 through 38 show the suspension line lengths and their attachment locations as ratios of suspension line length to keel length and line location to keel length. The lengths of the tip lines and rear keel lines are not shown in the figures, because these were varied during the test program.

The following are brief descriptions of the models:

1. 15-ft ℓ_K Single Keel Parawing (Model S-2A) - Basic parawing design with the exception that twelve keel lines were used instead of the eleven used on the original LRC parawing design. Also, eight trailing edge lines were installed on this model. Figure 35 shows the model construction, the suspension line lengths and the line attachment positions. The canopy seams were parallel to the wing trailing edges.
2. 24.0 ft ℓ_K Single Keel Parawing - Basic parawing design with the exception that twelve keel lines were used instead of eleven. As on the 15-ft parawing, eight trailing edge lines were also added.

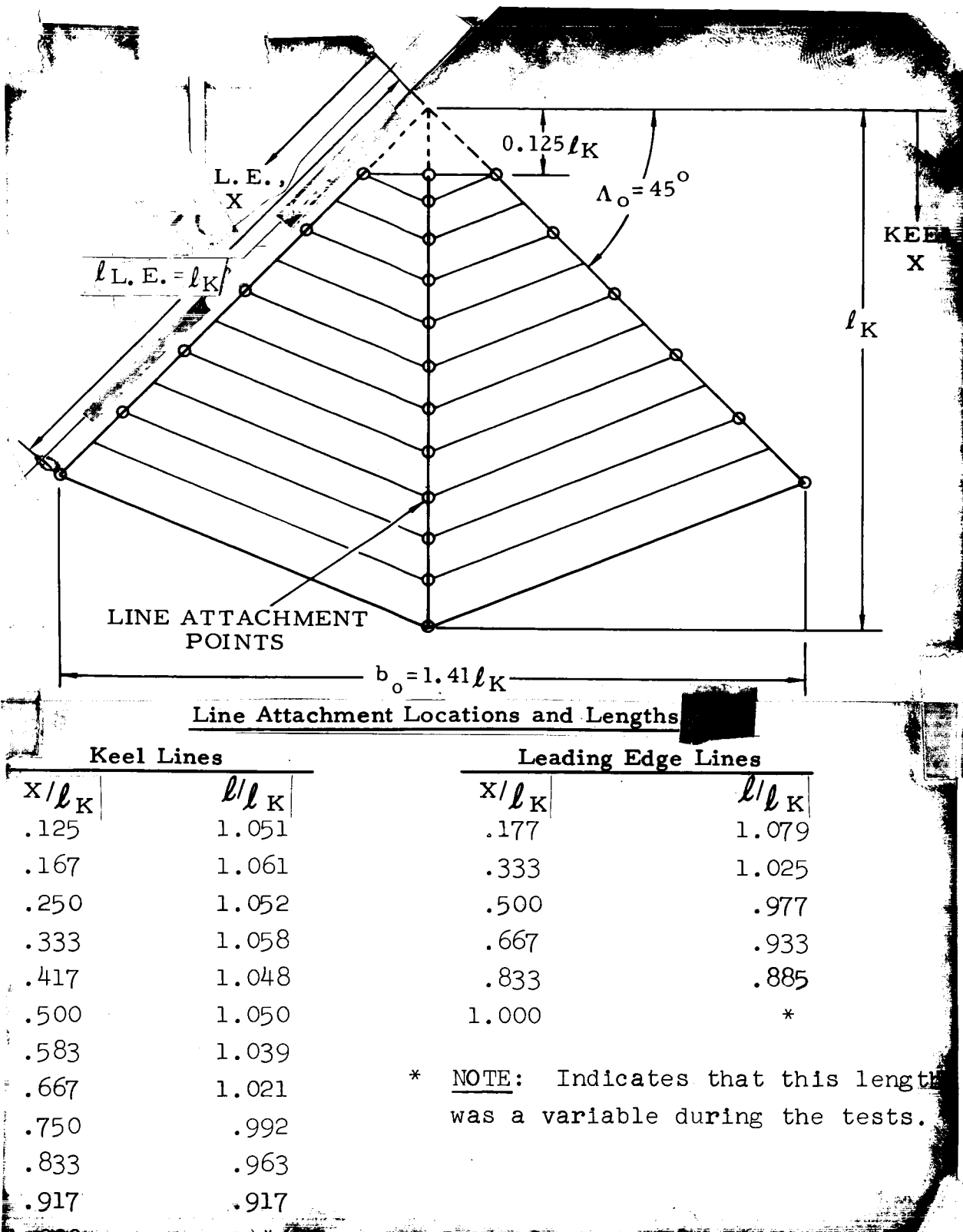
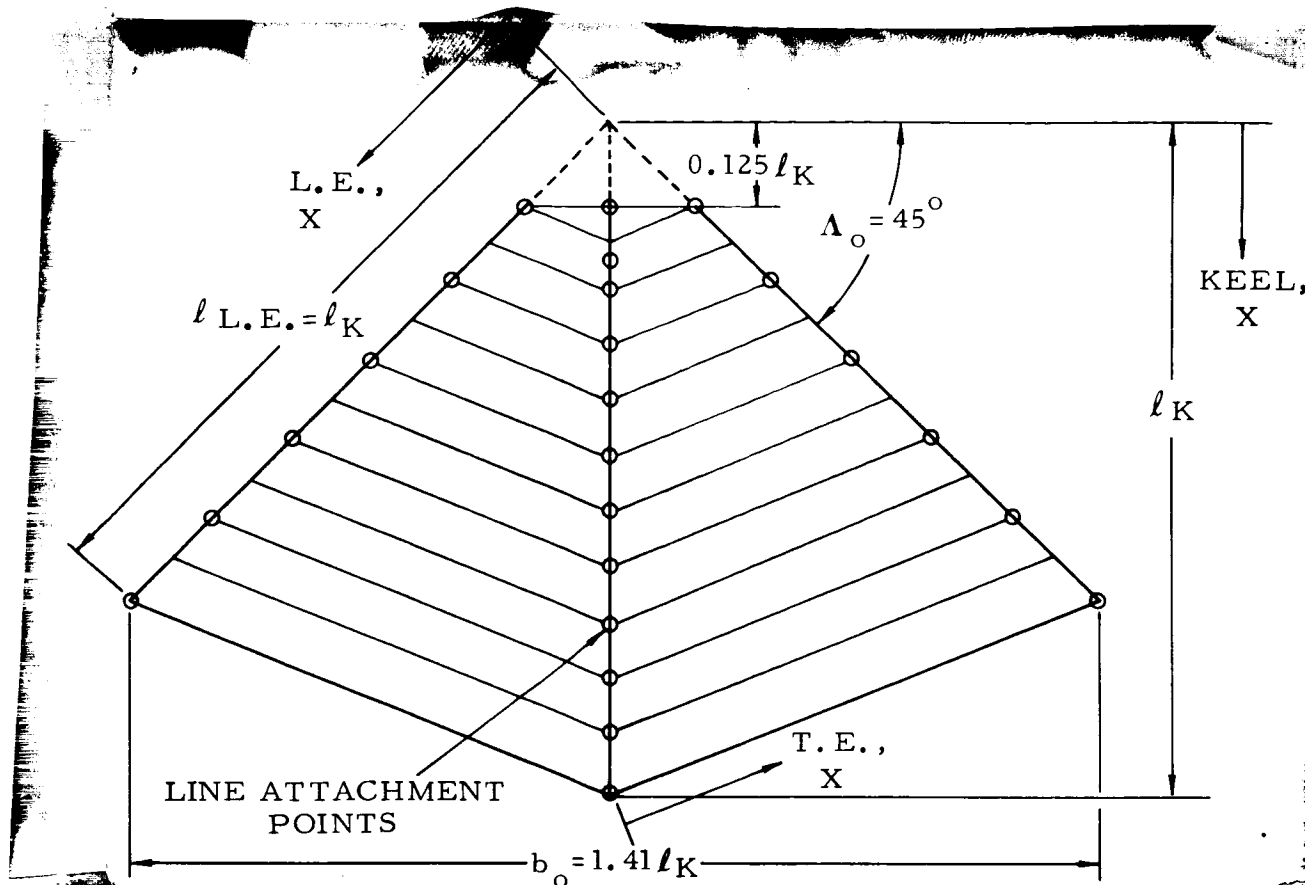


Figure 35. Flat Pattern Details of the 15-ft
 l_K Single Keel Parawing Model S-2A

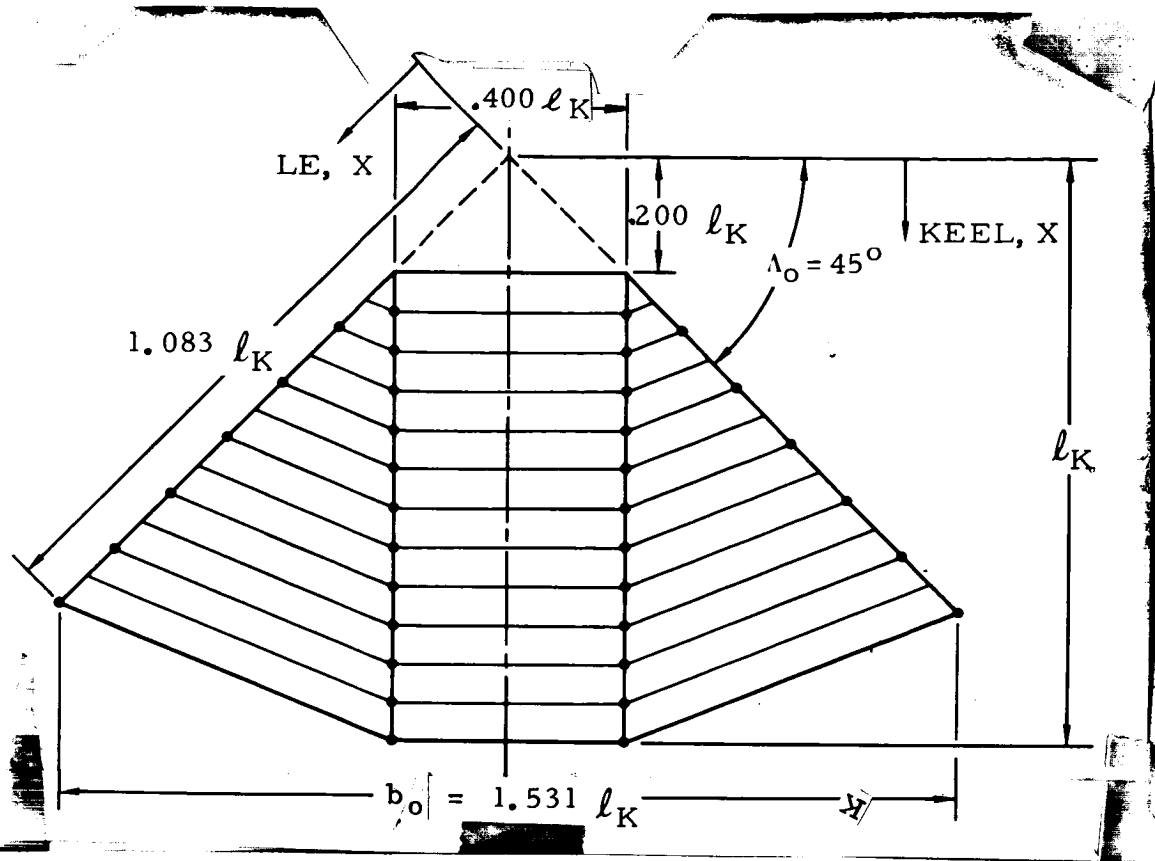


Line Attachment Locations and Lengths

Keel		Leading Edge		Trailing Edge	
x/l_K	ℓ/ℓ_K	x/l_K	ℓ/ℓ_K	x/l_K	ℓ/ℓ_K
.125	1.068	.177	1.074	.153	1.085
.209	1.058	.333	1.009	.306	1.124
.243	1.047	.500	.968	.459	1.066
.334	1.058	.667	.935	.612	.970
.417	1.048	.833	.883		
.500	1.043	1.000	*		
.583	1.032				
.667	1.018				
.750	.989				
.833	.970				
.916	.951				
1.000	*				

* NOTE: Indicates that this length was variable during the tests.

Figure 36. | Flat Pattern Details of the 24-ft
 ℓ_K Single Keel Parawing Model



Line Attachment Locations and Lengths

Keel		Leading Edge	
x/l_K	ℓ/l_K	x/l_K	ℓ/l_K
.267	.969	.416	.923
.333	.986	.549	.904
.400	.979	.683	.887
.467	.971	.816	.839
.533	.970	.949	.759
.600	.968	1.083	*
.667	.966		
.733	.965	*NOTE: Indicates that this length was variable during the tests	
.800	.954		
.867	.944		
.933	.925		
1.000	*		

*NOTE: Indicates that this length
was variable during the tests

Figure 37. Flat Pattern Details of 22.7-ft l_K Twin Keel Parawing Model Without Ripstop Tapes

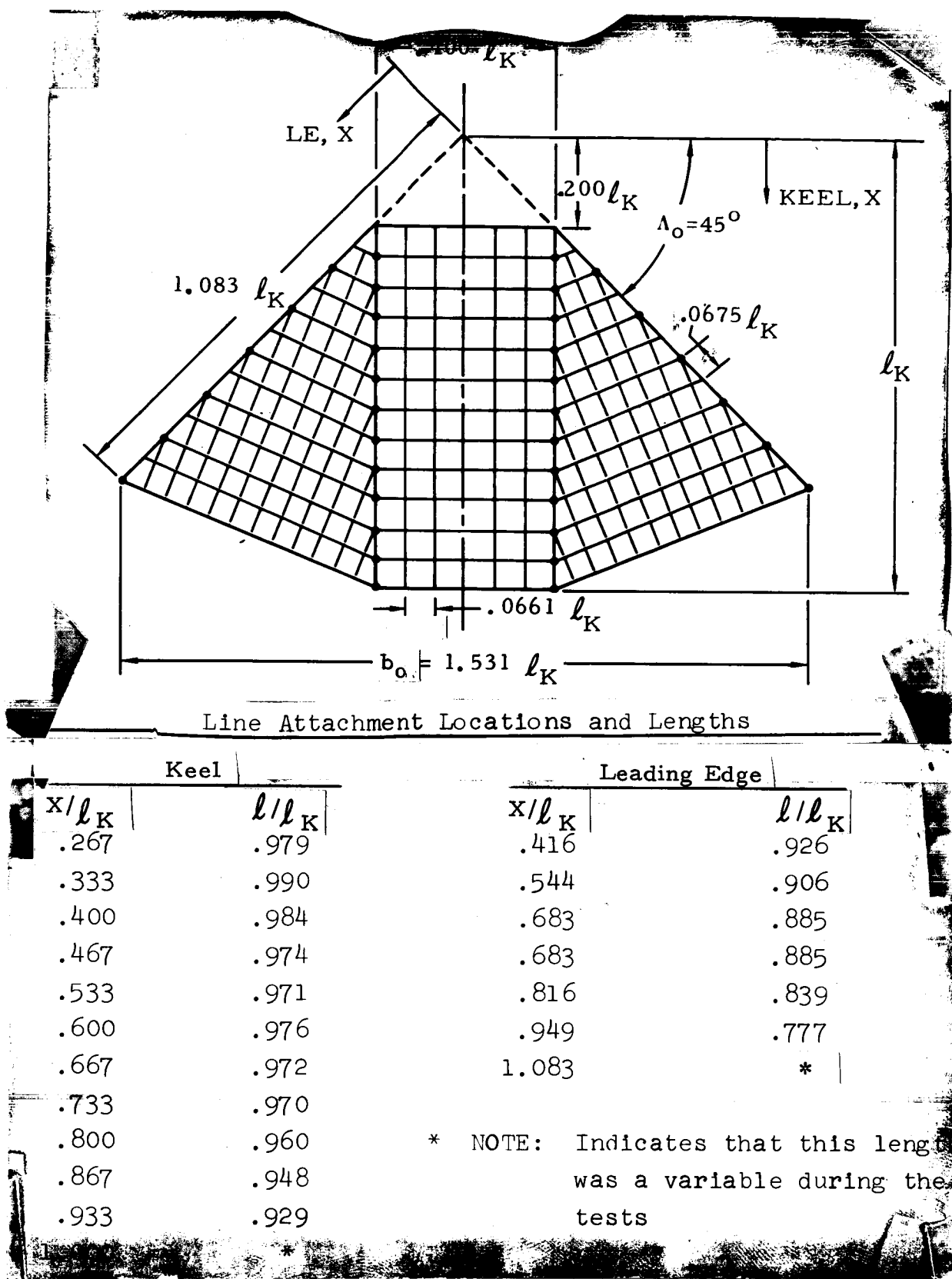


Figure 38. Flat Pattern Details of 22.7-ft l_K Twin Keel Parawing Model With Ripstop Tapes^K

The canopy seams were parallel to the wing trailing edges. Figure 36 shows a sketch of the model construction, along with the suspension line lengths and attachment locations.

3. 22.7-ft ℓ_K Twin Keel Parawing - Basic twin keel parawing design with the exception that the canopy seams were parallel to the wing trailing edges for each section of the wing. Figure 37 shows the model construction, along with the individual suspension line lengths and their attachment locations.
4. 22.7 ft ℓ_K Twin Keel Parawing with Ripstop Tapes - Basic twin keel parawing design with the exception that the canopy seams were parallel to the wing trailing edges for each section of the wing. Ripstop tapes were also added parallel to the keels in the center section of the wing and perpendicular to the trailing edges in the outboard sections of the wing. Figure 38 provides a sketch of the model planform and identifies the individual suspension line lengths and line attachment locations.

Ames Wind Tunnel Test Procedures

Procedures for the tests conducted in the Ames wind tunnel were basically the same as those previously described for the tethered flight performance tests conducted in the Langley full-scale tunnel. The test setup for the Ames wind tunnel tests was the same as for the Langley full-scale tunnel tests, ~~except for~~ the attachment point geometry on the T-bar. The dimensions of the T-bar for the 400 square foot wing area model tests were 1.6 times those used for the Langley full-scale tether tests. The 15 ft ℓ_K model tested at the Ames wind tunnel used the same

attachment geometry as was used during the Langley full-scale tunnel tether tests.

Summary of Test Results

During the Ames tests, four parawing models were tested over a range of dynamic pressures, tip line lengths and rear keel line lengths. Table 9 is a partial summary of the results of this test program. The data in this table show the maximum L/D measured on the four wings for each tip line length tested. The values shown for the rear keel line lengths are those which provided the maximum L/D for the indicated tip line length. All of the data shown were obtained at a nominal dynamic pressure of 1.0 psf.

Figures 39 through 42 are plots of the data obtained during the Ames tests. Figure 43 shows a comparison of the test results obtained with wing Model S-2A in the Ames and Langley wind tunnels. Making allowances for the scatter in the Ames data, the results from the two test series show that the L/D performance of the 15-ft ℓ_K single keel parawing as measured in the Ames wind tunnel was consistent with the performance measured in the Langley wind tunnel.

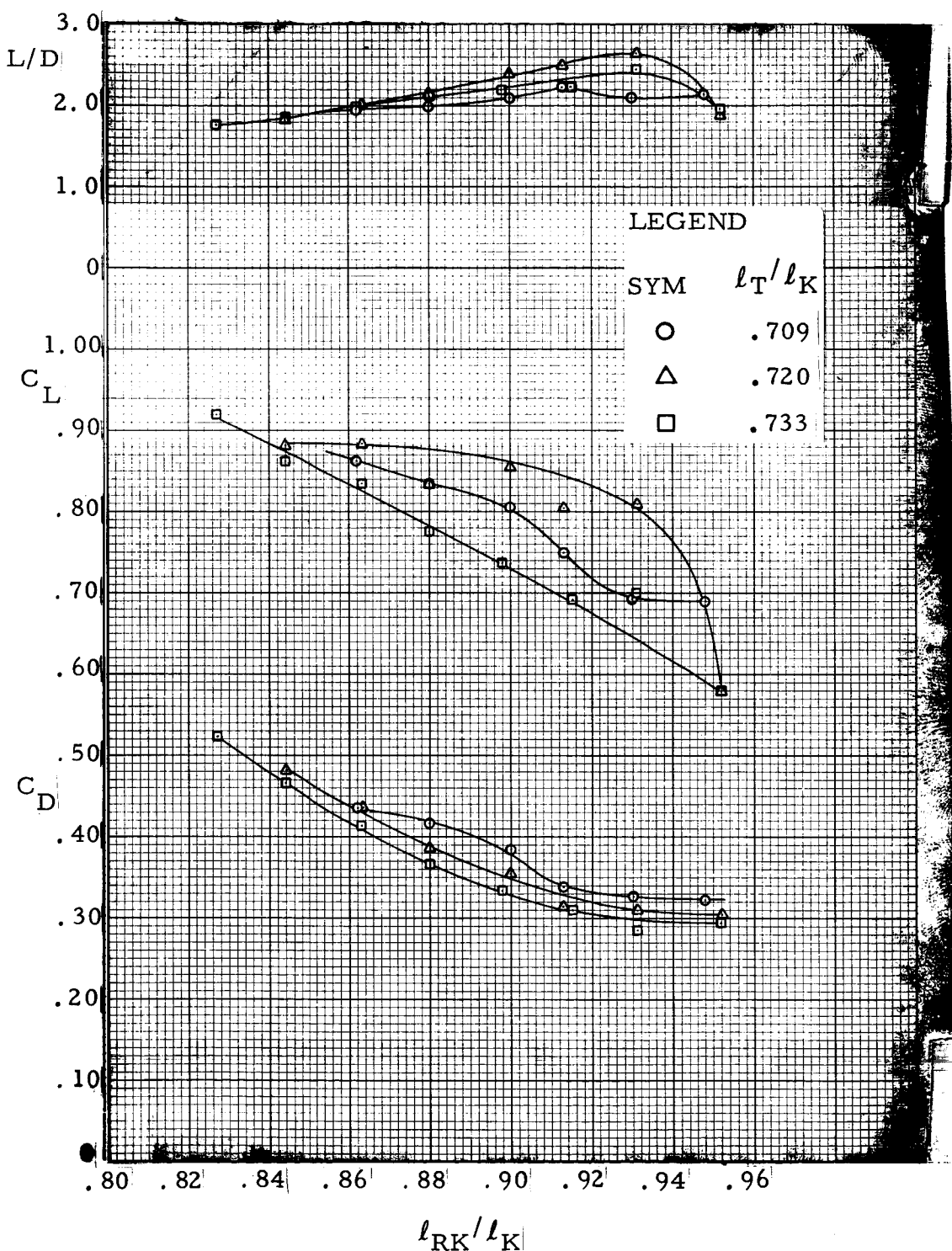
Figure 44 provides a comparison of the performance of the twin keel model with different types of canopy structure. As shown by Figure 44 (assuming no change in performance between a 15-ft and a 22.7-ft twin keel parawing) maximum L/D performance is reduced by 6 percent on parawings with the canopy seams oriented parallel to the trailing edge, when compared to parawings with the canopy seams oriented perpendicular to the trailing edges.

The effect of the ripstop tapes is shown by a comparison of Figures 41 and 42. The effect of adding these tapes was a reduction in maximum L/D of approximately 10 percent. The

TABLE 9.

Summary of Gliding Performance Measured During Ames Wind Tunnel Tests.

Model	ℓ_T/ℓ_K	ℓ_{RK}/ℓ_K	L/D Max
15-ft Single Keel (Model S-2A)	.709	.913	2.24
15-ft Single Keel (Model S-2A)	.720	.931	2.65
15-ft Single Keel (Model S-2A)	.733	.931	2.47
24-ft Single Keel	.670	.897	2.58
24-ft Single Keel	.688	.872	2.71
24-ft Single Keel	.706	.872	2.55
22.7-ft Twin Keel	.590	.917	3.20
22.7-ft Twin Keel	.606	.905	2.98
22.7-ft Twin Keel	.629	.904	2.62
22.7-ft Twin Keel with tapes	.569	.892	2.91
22.7-ft Twin Keel with tapes	.588	.917	2.92
22.7-ft Twin Keel with tapes	.607	.892	2.84
22.7-ft Twin Keel with tapes	.626	.892	2.50

Figure 39. Performance Data for 15-ft l_K Single Keel Parawing (Model S-2A)

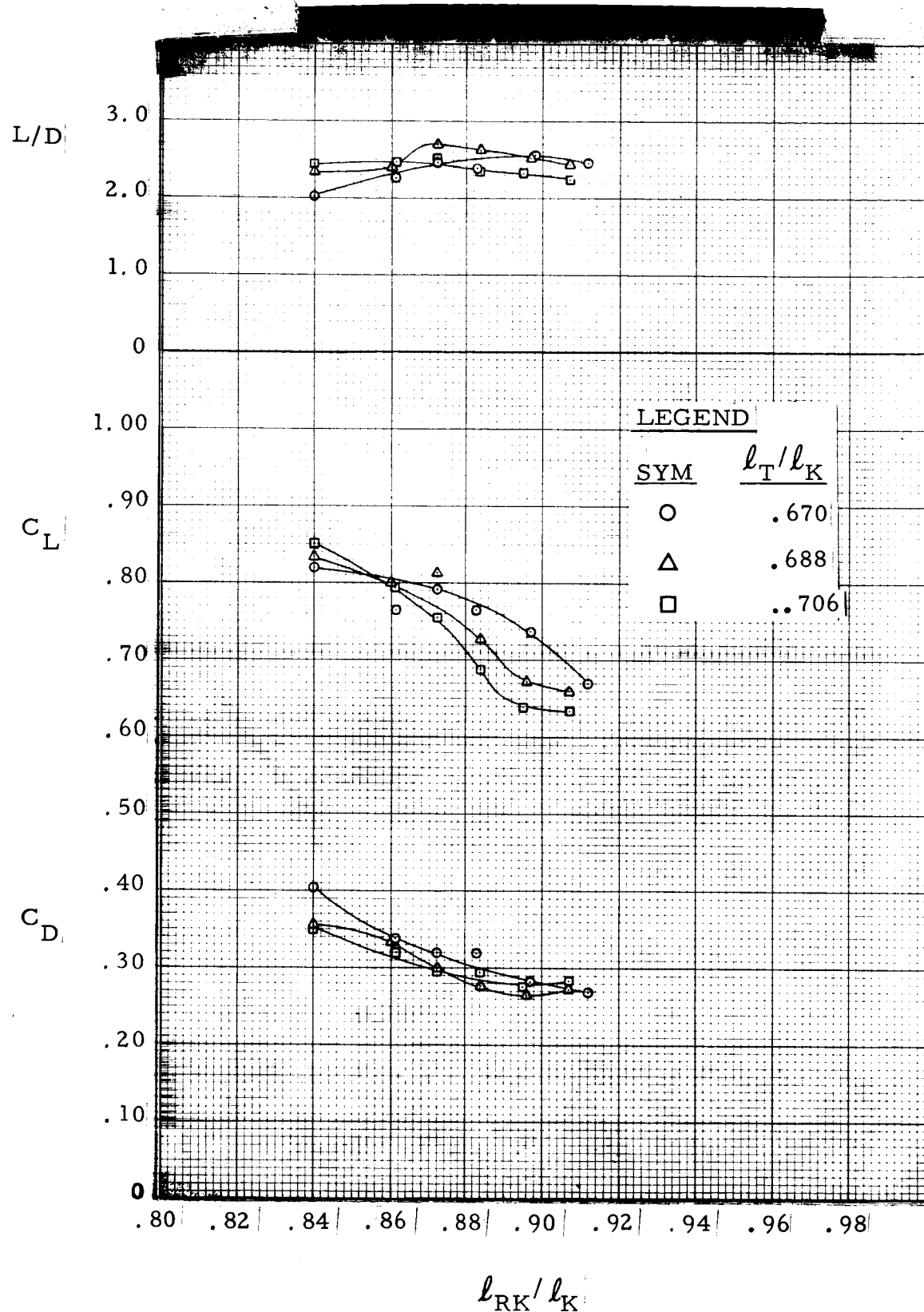


Figure 40. Performance Data for 24-ft ℓ_K Single Keel Parawing

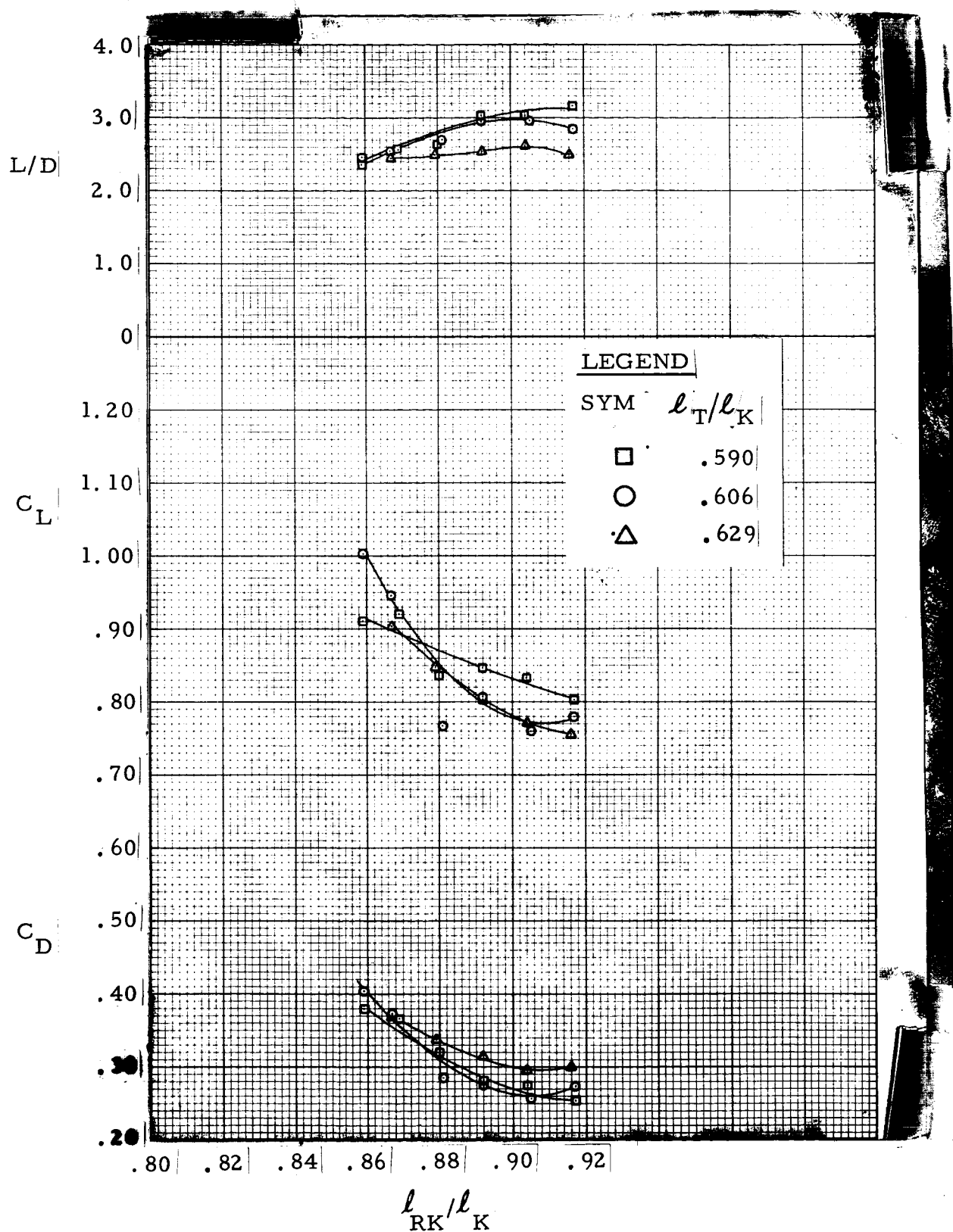


Figure 41. Performance Data for 22.7-ft ℓ_K Twin Keel Parawing

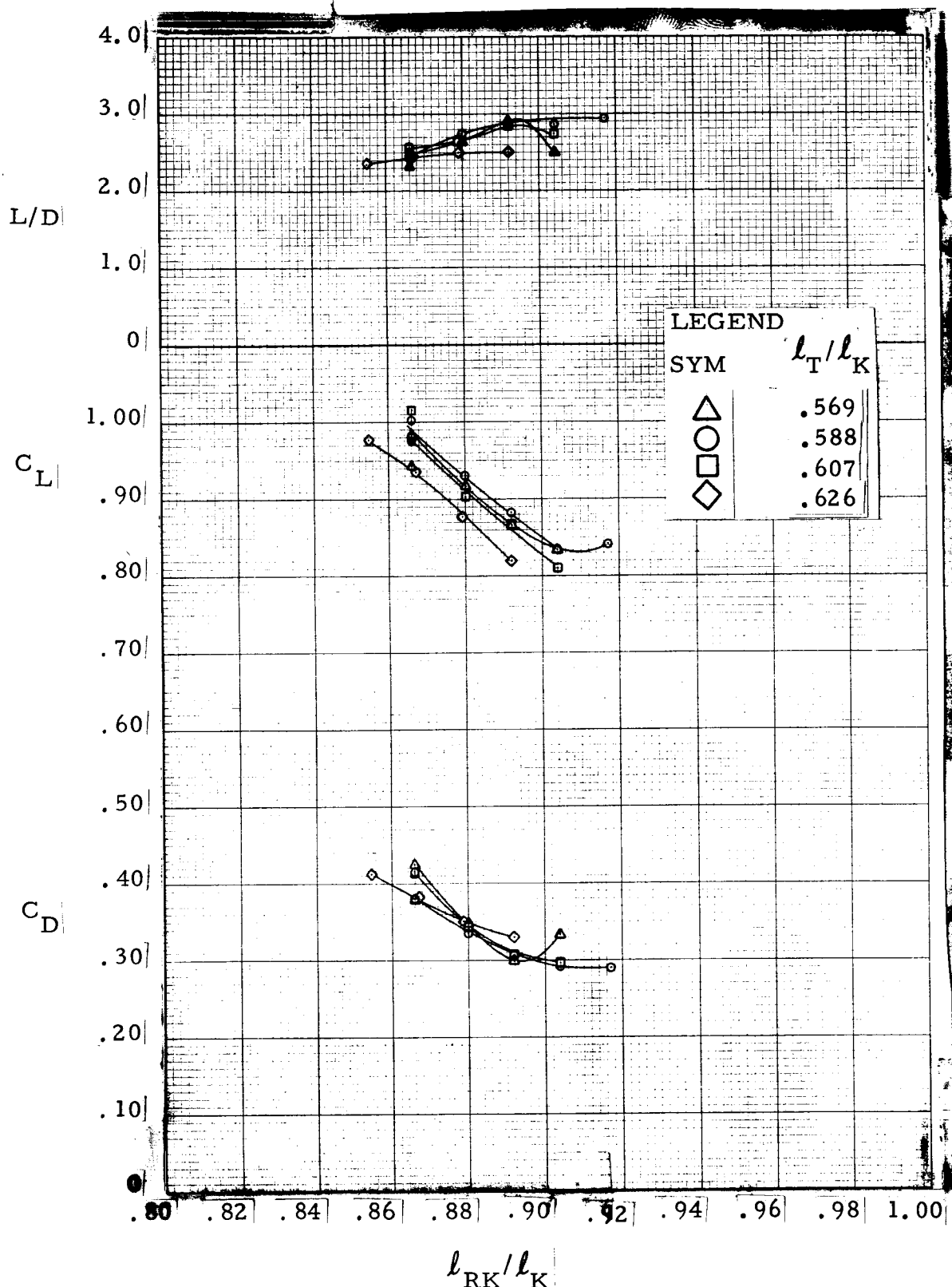


Figure 42. Performance Data for 22.7-ft l Keel Parawing With Ripstop Tapes

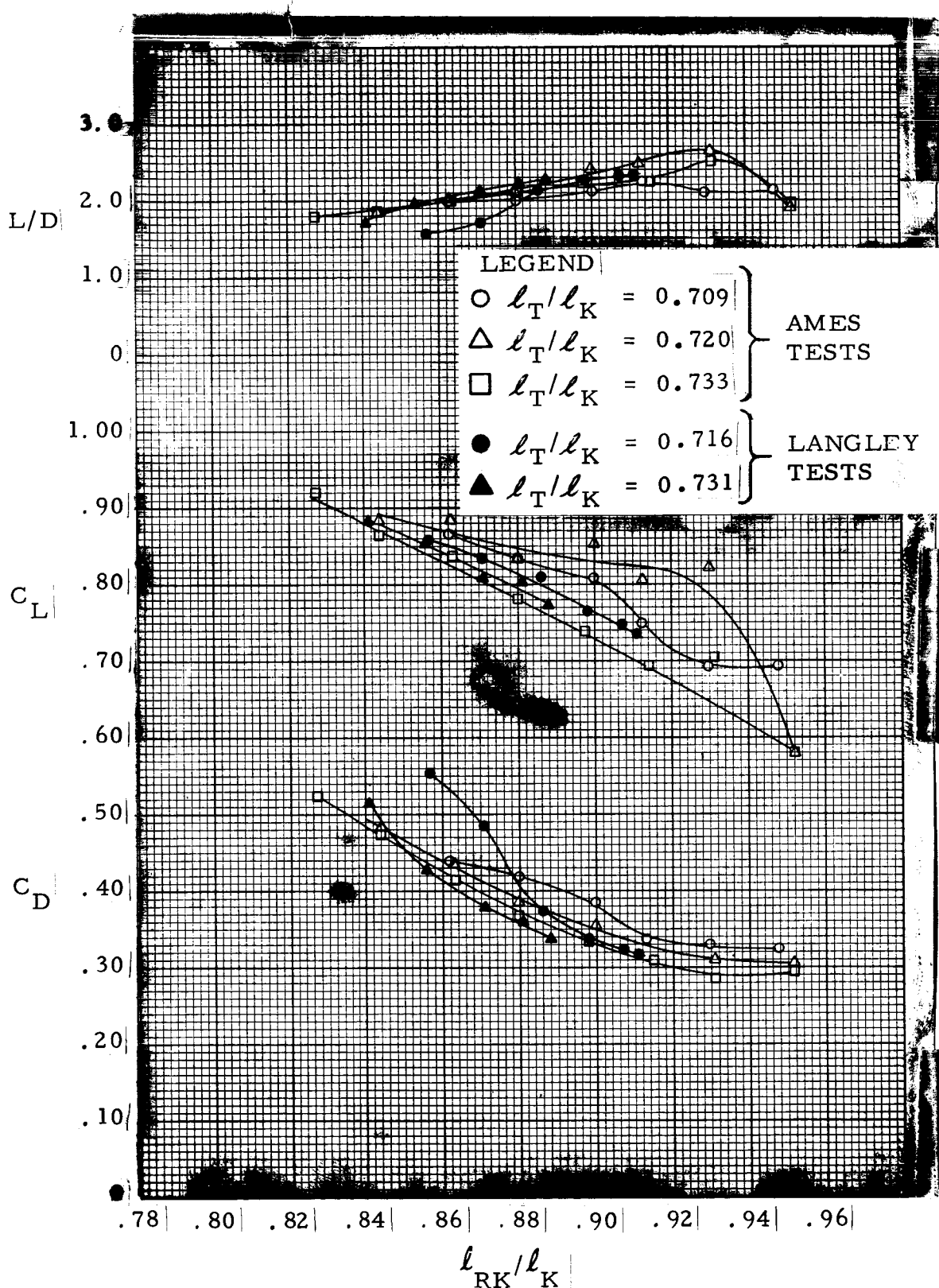


Figure 43. Comparison of Data for a 15-ft ℓ_K Single Keel Parawing Tested in the Ames and Langley Full Scale Wind Tunnels (Model S-2A).

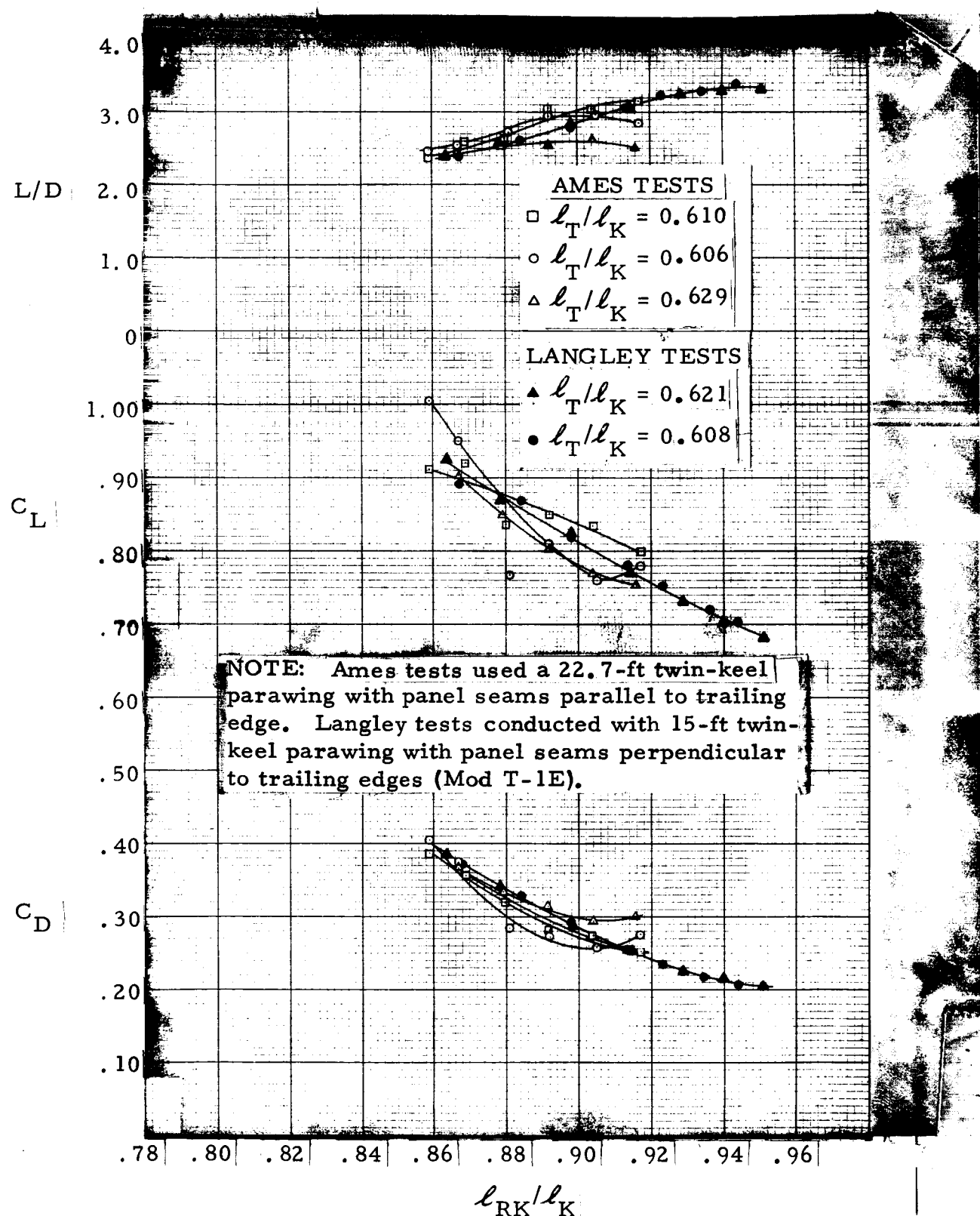


Figure 44. Comparison of Test Data for Two Twin Keel Parawings With Different Methods of Construction

reduction in L/D is believed to have been caused by distortions in the nose area of the wing induced by the addition of the tapes after the canopy had been built.

GENERAL DISCUSSION OF TETHERED FLIGHT CHARACTERISTICS OBSERVED DURING WIND TUNNEL TESTS

Investigations were made during the two wind tunnel test programs of the effects on tethered flight performance of the number of suspension lines, suspension line diameter, canopy structure, canopy size, dynamic pressure, rear keel suspension line length and tip suspension line length. The following paragraphs discuss the effects of these variables on performance and, where possible, explain the various trends.

Single Keel Parawing

Figure 40 shows the effects of rear keel line length and tip line length on L/D. It can be seen that L/D generally increased as the rear keel line length was increased. The limit of this relationship is that point at which the nose of the wing collapses and folds under. The nose collapse was apparently caused by the stagnation point in the nose area of the model moving from the lower surface to the upper surface of the wing. A fold is normally formed in the wing surface on single keel parawings between the second leading edge line and the second keel line. This fold appeared to be necessary to give the proper formation of the nose of the wing for best L/D performance. This fold, which is normal to the keel and extends below the surface of the wing, is believed to stabilize the position of the stagnation point on the lower surface of the wing. The other limit on rear keel line length occurs when retraction of this line causes the wing to stall.

Inspection of Figure 40 shows that L/D is also a function of tip line length. Indeed, L/D may be a function of the length of every suspension line on the wing. However, during the test program, only the lengths of the rear keel lines and the tip lines were varied. As shown by Figure 40, maximum L/D occurs at approximately the same rear keel line length ratio (ℓ_{RK}/ℓ_K), regardless of the tip line lengths. Figure 45 is a typical plot of the variation of L/D with tip line length ratio (ℓ_T/ℓ_K) for a constant value of (ℓ_{RK}/ℓ_K). A maximum L/D position occurs about midway through the range of tip line lengths tested.

During the Langley wind tunnel tests, the number and diameter of the suspension lines were varied. The same canopy was used in order to isolate changes in performance to those due only to the effects of variations in suspension lines. These tests showed that the number of suspension lines along the keel, except in the area forward of and just aft of the previously mentioned transverse fold, did not appreciably affect gliding flight performance. However, additional suspension lines along the forward two-thirds of the wing leading edge did produce an effect on maximum attainable L/D. A local arching of the wing leading edge in this area of the wing is evidently necessary to maintain the proper inflated shape. To obtain acceptable performance with the models having additional leading edge lines, it was found necessary to lengthen the additional lines to the point where they were slack during test. If for structural reasons, additional leading edge lines are required, provisions should be made to have these lines slack during gliding flight. In this way, the added lines would not influence the leading edge shape of the wing over the forward two-thirds of its length.

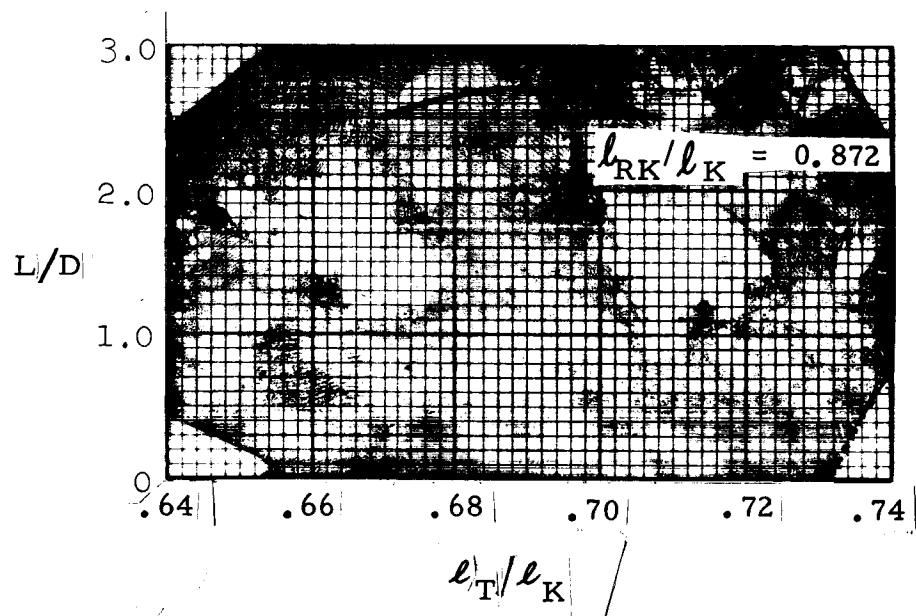


Figure 45. L/D vs. Tip Line Length Ratio for 24 FT ℓ_K Single Keel Model

Sym	Model	ℓ_{RK}/ℓ_K	ℓ_T/ℓ_K
○	15 ft SK	.952	.721
□	24 ft SK	.897	.688

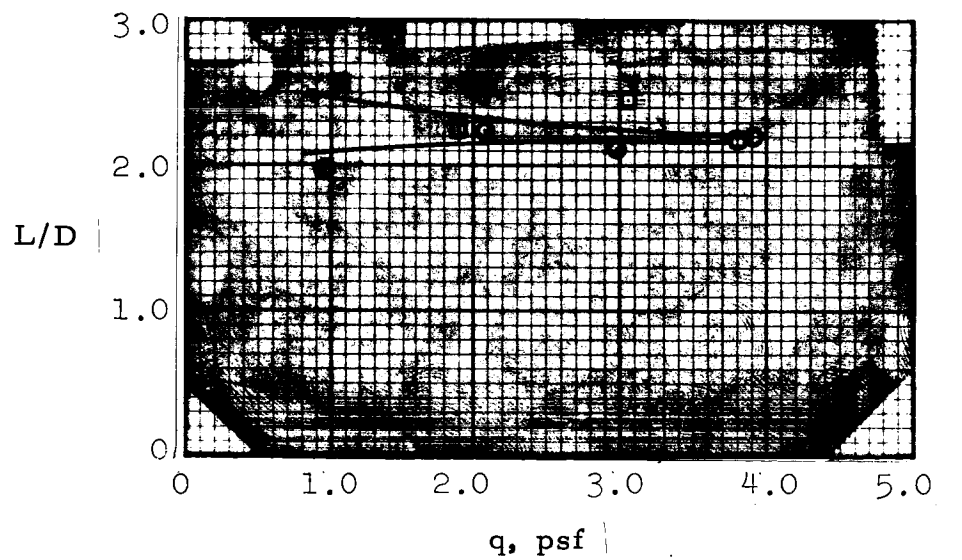


Figure 46. L/D vs. Dynamic Pressure for Two Typical Single Keel Models

The effect of suspension line diameter on gliding performance was so small that appreciable differences in performance could not be detected for the range of suspension line diameters tested.

Two other effects on maximum attainable L/D noted during the test programs were those of canopy structure and dynamic pressure. These two effects are apparently related, in that the inflated shape of the wing is a function of the elastic properties of the wing structure and the aerodynamic loading. Data obtained during the Langley wind tunnel program showed relatively small variations in maximum attainable L/D with changes in canopy structure. The types of structures tested had (1) canopies with seams perpendicular to the trailing edge, (2) canopies with seams parallel to the trailing edge, and (3) canopies with radial networks of reinforcing tapes. Also, as shown by Figure 46, changes in the dynamic pressure had little effect on the performance of either the 24-ft ℓ_K model or the 15-ft ℓ_K model.

Twin Keel Parawing

As with the single keel design, L/D for the twin keel parawing generally increased as the rear keel line length was increased. The maximum and minimum values which could be obtained in the wind tunnel were governed by minimum and maximum angles of attack at which the wings would fly.

Figure 41 shows that as in the case of the single keel models, maximum L/D for the twin keel parawings occurred at approximately the same rear keel line setting, independent of tip line position.

A plot of L/D as a function of tip line length for a typical twin keel model is shown in Figure 47. This figure shows that

L/D increased with decreasing tip line length within the range of tip line lengths tested.

With the models used during the Langley wind tunnel tests, the minimum angle of attack was limited by nose collapse and maximum angle of attack was limited by aerodynamic stall of the wing. With the twin keel models tested at Ames, the rigging used on the models did not allow the wing to go to a low enough angle of attack to collapse the nose. For these tests, slackening of the rear keel lines was the limiting factor on minimum angle of attack. Maximum angle of attack, and concomitant minimum L/D was limited by aerodynamic stalling of the wing.

Placement of lines in the nose area of the twin keel models was found to be less critical to L/D performance than in the case of the single keel models. Also, increasing the number of suspension lines along the leading edge of the twin keel models did not cause a significant change in gliding performance. In tests with the increased numbers of leading edge lines, it was unnecessary to vary the lengths of the added intermediate lines to form the local arching found to be necessary for proper inflation of the single keel models. In general, the twin keel models appeared to be less critical with respect to individual line lengths than were the single keel models tested.

The differences in behavior between the twin keel models tested in the Langley tunnel and those tested in the Ames tunnel were probably due to structural differences in the two sets of models. The models tested at Langley had the seams in the center section of the wing oriented perpendicular to the trailing edge, while the twin keel models tested in the Ames tunnel had the seam reinforcements parallel to the trailing edge. Figure 44 shows that the Langley models with seams perpendicular to the

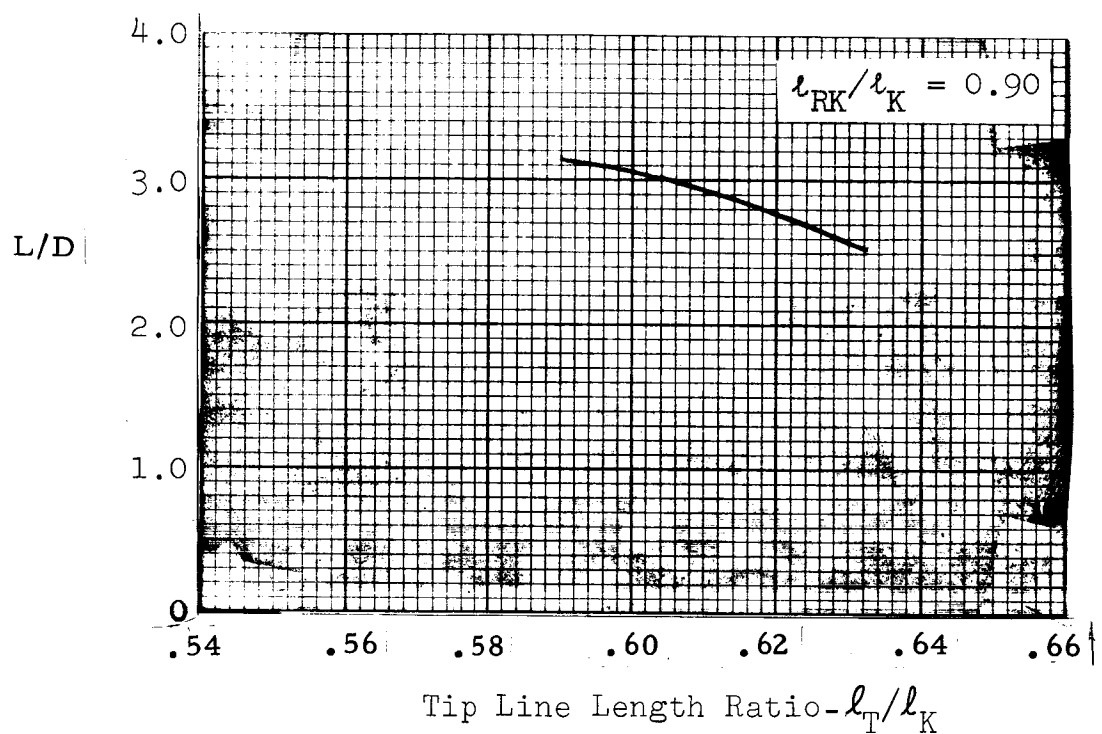


Figure 47. L/D vs. Tip Line Length Ratio for Typical Twin Keel Model

trailing edge were able to attain a lower angle of attack and a higher L/D than the Ames models with seams parallel to the trailing edge.

Dynamic pressure had an effect on the L/D performance of the twin keel models in the Ames tunnel. Figure 48 shows an appreciable drop in L/D when dynamic pressure was increased above 2.0. The decrease in performance was caused by both a decrease in lift coefficient and an increase in drag coefficient. Unlike the single keel parawing design, the twin keel parawing surface was highly loaded over the forward center section of the canopy. Apparently, the higher loading in this area of the wing with increased dynamic pressure is enough to induce distortions in the wing surface. These distortions could cause unfavorable changes in the flow over the wing.

As with the single keel models, changing the diameter of suspension lines on the twin keel parawings did not have a discernible effect on L/D performance for the range of line diameters tested.

APPROACH USED FOR DYNAMIC SCALING

The primary objective of the small scale test programs was to determine the deployment sequences and gliding flight configurations to be tested during the intermediate scale test program. In order to interpret the results of small model tests and relate these results to intermediate scale test conditions, a method of scaling was needed. The rationale used was one of dynamic similitude as presented in References 6 and 7. The two dynamic processes of concern were: 1) deployment, and 2) turning maneuvers during gliding free flight. In the case of the deployment process, the desired scale parameter was linear acceleration. For gliding free flight, the scale parameter was turn rate.

Sym	Model	ℓ_{RK}/ℓ_K	ℓ_T/ℓ_K
◇	22.7 ft TK (without tapes)	.914	.590
△	22.7 ft TK (with tapes)	.892	.607

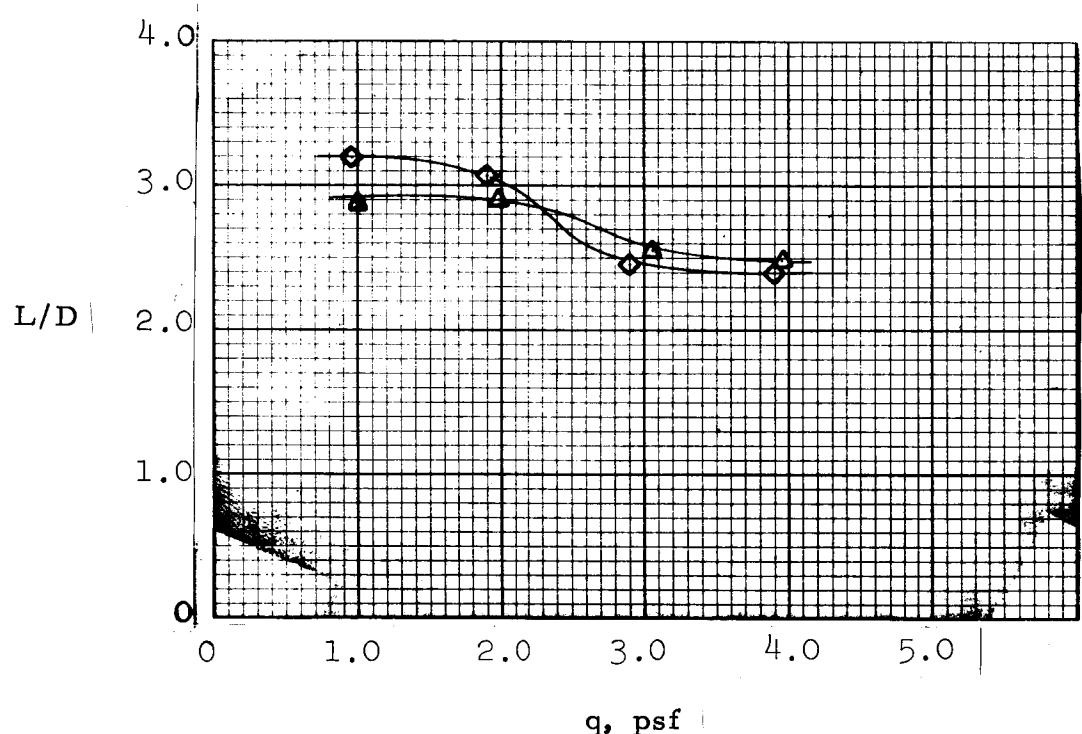


Figure 48. L/D vs. Dynamic Pressure

For the case of constant g , Barton, in Reference 7 expresses the scaling relationships in terms of two ratios: $R_d = d_m/d_f$ and $R = \rho_m/\rho_f$. Here, d and ρ denote diameter and air density and subscripts m and f refer to model and full scale.

In this report, area ratio is used instead of diameter ratio, and the notation is changed slightly as follows:

$$R_S = S_1/S_0$$

$$R = \rho_1/\rho_0$$

Here, S and ρ denote wing area and air density; subscripts l and 0 refer to the model and reference flight systems (or conditions), respectively.

The required conditions for dynamic scaling are that the Froude number ratio and vehicle mass ratio are both equal to 1.0. With these constraints, the scaling relationships shown in Table 10 were derived.

To determine small scale parawing test conditions, scaled to a reference intermediate scale parawing test point, the following procedure was used; the wing areas of the small and the intermediate scale models were fixed at 400 and 4000 square feet, respectively. The wing area ratio was, therefore, $R_S = 0.1$. For deployment tests, the three parameters that could be varied were test weight, deployment altitude (i.e., air density), and velocity (i.e., dynamic pressure) at the start of the deployment process. If a deployment altitude is selected, then the weight and velocity are determined from the following relationships:

$$W_1 = R_\rho (R_S)^{3/2} W_0,$$

based on the relation $R_M = R_\rho (R_S)^{3/2}$ given in Table 10. Here W_1 and W_0 denote the test parawing system weight and reference parawing system weight, respectively.

Also, we have

$$q_1 = R_p (R_S)^{1/2} q_0,$$

based on the relationship, $R_q = R_p R_S^{1/2}$ given in Table 10. Here q_1 and q_0 denote the test dynamic pressure and the reference dynamic pressure, respectively.

For example, if it is desired to conduct a test with $S_1 = 400 \text{ sq ft}$ wing at $h_1 = 10,000 \text{ ft}$ to scale a test with the conditions that $S_0 = 4,000 \text{ sq ft}$, $w_0 = 5000 \text{ lbs}$, $h_0 = 18,000 \text{ ft}$, and $q_0 = 100 \text{ psf}$, then the test weight and deployment q for the test are determined as follows:

$$\begin{aligned} w_1 &= \left(\frac{\rho_{10,000 \text{ ft}}}{\rho_{18,000 \text{ ft}}} \right) \times \left(\frac{400 \text{ sq ft}}{4000 \text{ sq ft}} \right)^{3/2} \times (5000 \text{ lbs}) \\ &= 204.9 \text{ lb} \end{aligned}$$

and

$$\begin{aligned} q_1 &= \left(\frac{\rho_{10,000 \text{ ft}}}{\rho_{18,000 \text{ ft}}} \right) \times \left(\frac{400 \text{ sq ft}}{4000 \text{ sq ft}} \right)^{1/2} \times (100 \text{ psf}) \\ &= 41.0 \text{ psf} \end{aligned}$$

With these test conditions, the accelerations experienced by the 400 sq ft parawing during the deployment process should be equal to those experienced by the 4000 sq ft parawing, within the limits of the assumptions on which the scaling relationships are based.

A complete discussion of scaling theory is beyond the scope of this report, and the reader is referred to References 6 and 7 for more complete discussions of scaling as applied to parachute and parawing-type opening processes.

Table 10. Dynamic Similitude Relationships

	RATIO DEFINITIONS	RATIO DEFINITIONS
<u>CLASS, M</u>		
FORCE, F	$R_F = F_1/F_0$	$R_F = R_\rho R_S^{3/2}$
LENGTH, L	$R_L = L_1/L_0$	$R_L = R_S^{1/2}$
TIME, t	$R_t = t_1/t_0$	$R_t = R_S^{1/4}$
TEMPERATURE, T	$R_T = T_1/T_0$	$R_T = R_T$
<u>FLIGHT SYSTEM VARIABLES</u>		
WEIGHT, W	$R_W = W_1/W_0$	$R_W = R_\rho R_S^{3/2}$
AREA, S	$R_S = S_1/S_0$	$R_S = R_S^{3/2}$
VOLUME, V	$R_V = V_1/V_0$	$R_V = R_S$
SPECIFIC WEIGHT, γ	$R_\gamma = \gamma_1/\gamma_0$	$R_\gamma = R_\rho$
CANOPY LOADING, W/S	$R_{W/S} = (W/S)_1/(W/S)_0$	$R_{W/S} = R_\rho R_S^{1/2}$
MOMENT OF INERTIA, I	$R_I = I_1/I_0$	$R_I = R_\rho R_S^{5/2}$
LINE UNIT WEIGHT, W/L	$R_{W/L} = (W/L)_1/(W/L)_0$	$R_{W/L} = R_\rho R_S^{1/2}$
MATERIAL SOUND SPEED, C	$R_C = C_1/C_0$	$R_C = 1$
<u>ENVIRONMENT VARIABLES</u>		
ACCELERATION OF GRAVITY, g	$R_g = g_1/g_0$	$R_g = 1$
AIR DENSITY, ρ	$R_\rho = \rho_1/\rho_0$	$R_\rho = R_\rho$
AIR PRESSURE, P	$R_P = P_1/P_0$	$R_P = R_\rho R_T$
SOUND SPEED, a	$R_a = a_1/a_0$	$R_a = R_T^{1/2}$
VISCOSEITY, η	$R_\eta = \eta_1/\eta_0$	$R_\eta = R_T$
<u>DYNAMICS VARIABLES</u>		
ATTITUDE ANGLE, θ (OR ψ, ϕ)	$R_\theta = \theta_1/\theta_0$	$R_\theta = 1$
STRODYNAMIC ANGLE, α (OR β)	$R_\alpha = \alpha_1/\alpha_0$	$R_\alpha = 1$
PRESSURE COEFFICIENT, C_p	$R_{C_p} = C_{p1}/C_{p0}$	$R_{C_p} = 1$
FORCE COEFFICIENT, C_x (OR C_y, C_z)	$R_{C_x} = C_{x1}/C_{x0}$	$R_{C_x} = 1$
MOMENT COEFFICIENT, C_f (OR C_m, C_n)	$R_{C_f} = C_{f1}/C_{f0}$	$R_{C_f} = 1$
VELOCITY, v	$R_v = v_1/v_0$	$R_v = R_S^{1/4}$
ACCELERATION, v.	$R_{v'} = \dot{v}_1/\dot{v}_0$	$R_{v'} = 1$
ANGULAR VELOCITY, ω	$R_\omega = \omega_1/\omega_0$	$R_\omega = R_S^{-1/2}$
ANGULAR ACCELERATION, $\dot{\omega}$	$R_{\dot{\omega}} = \dot{\omega}_1/\dot{\omega}_0$	$R_{\dot{\omega}} = R_S^{-1/2}$
ANGLE OF PRESSURE, q	$R_q = q_1/q_0$	$R_q = R_S^{1/2}$
<u>DIMENSIONS</u>		
MASS RATIO, $\mu = M/M_0$	$R_\mu = \mu_1/\mu_0$	$R_\mu = 1$
NUMBER, $FN = v/\sqrt{gL}$	$R_{FN} = FN_1/FN_0$	$R_{FN} = 1$

FREE FLIGHT GLIDING PERFORMANCE TESTS

A series of free flight tests was conducted with various wing loadings at El Mirage Dry Lake (near Edwards AFB, California). The objectives were:

1. Evaluation of free flight L/D performance.
2. Evaluation of flight stability.
3. Evaluation of turn rate performance.
4. Evaluation of L/D modulation.

In order to accomplish these objectives, three types of tests were conducted. These were:

1. Flights to verify that models were trimmed to fly relatively straight.
2. Flights to measure the effects of wing loading and rear keel line length on L/D performance.
3. Flights to measure turn rate as a function of tip line length and wing loading.

For the trim verification tests, an uninstrumented and uncontrolled test vehicle was utilized. For the L/D performance and turn rate performance tests, a radio controlled, instrumented test vehicle was employed. These vehicles are described in Appendix A, along with the instrumentation used.

TEST MODELS

Four models of the parawing, each having a wing area of 400 sq ft, were tested during the free flight tests. Two versions of both the single and the twin keel parawing types were flown. The only difference between the two versions of each type of wing was the number of suspension lines along the leading edges of the models. Models with additional

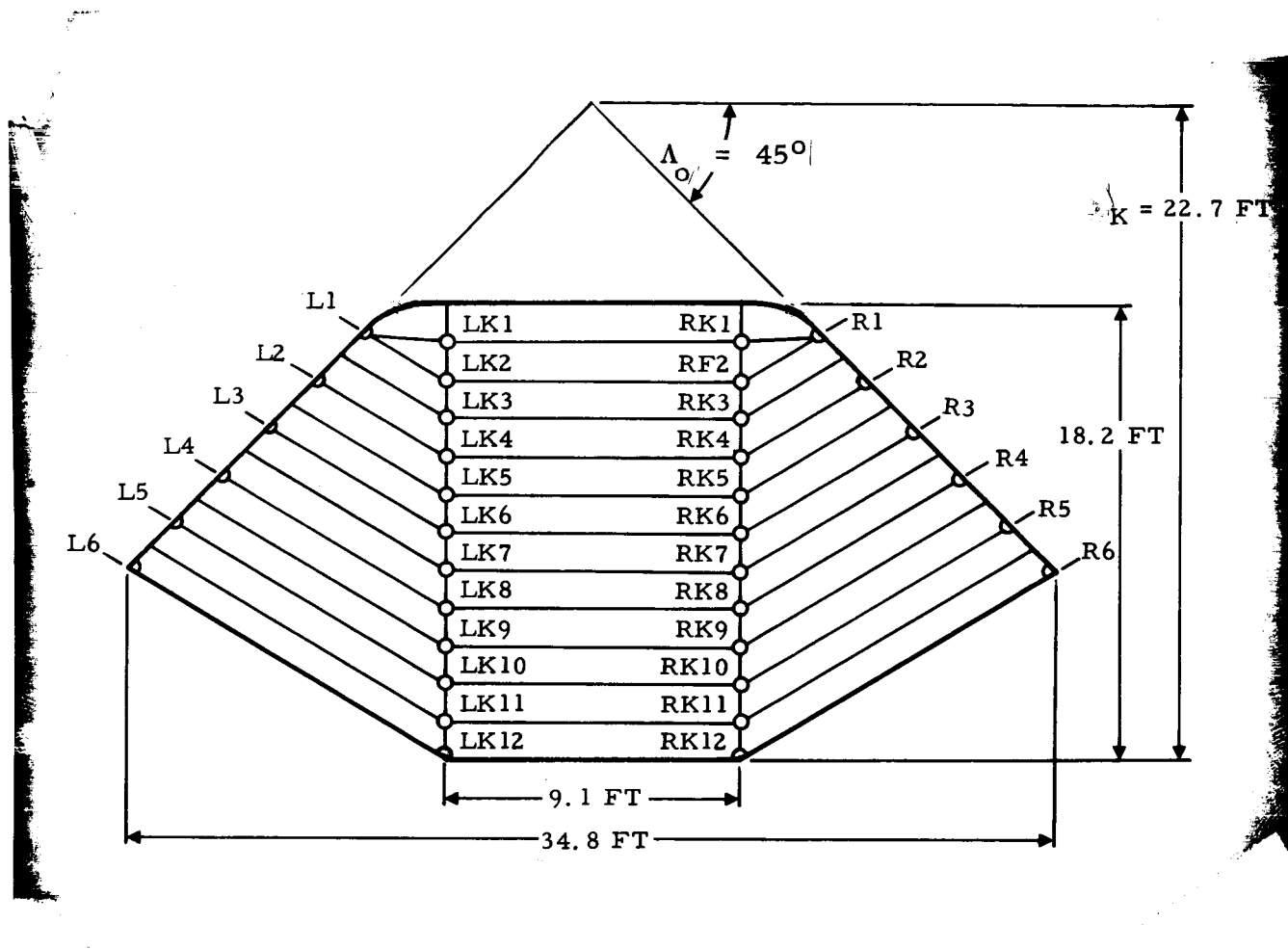
leading edge lines were included to determine if the drag of the added lines would have a discernible effect on gliding performance. The addition of these lines was prompted by the possibility that for the larger parawings, additional suspension lines might be required for structural reasons.

Description of Twin Keel Parawings

The twin keel small scale parawings had canopies constructed of 2.25 oz/sq yd low permeability nylon parachute cloth and had dacron suspension lines. Two similar configurations were tested at the El Mirage test site. The models differed in that one was constructed with 36 suspension lines and the other with 44. The overall dimensions of these two canopies are shown in Figures 49 and 50. Seam construction is illustrated in Figure 51. The two wing-tip lines and the two aft keel lines (the four controlling lines) were 1400 pound cord; all other suspension lines were 1000 pound cord. All lines were attached to the canopy with spliced end loops formed through attachment loops stitched to the canopy. Attachment loop constructions are shown in Figures 52 and 53. The lower ends of the lines were attached in groups to metal links, as shown in Figure 54. Table 11 lists suspension line lengths for these models.

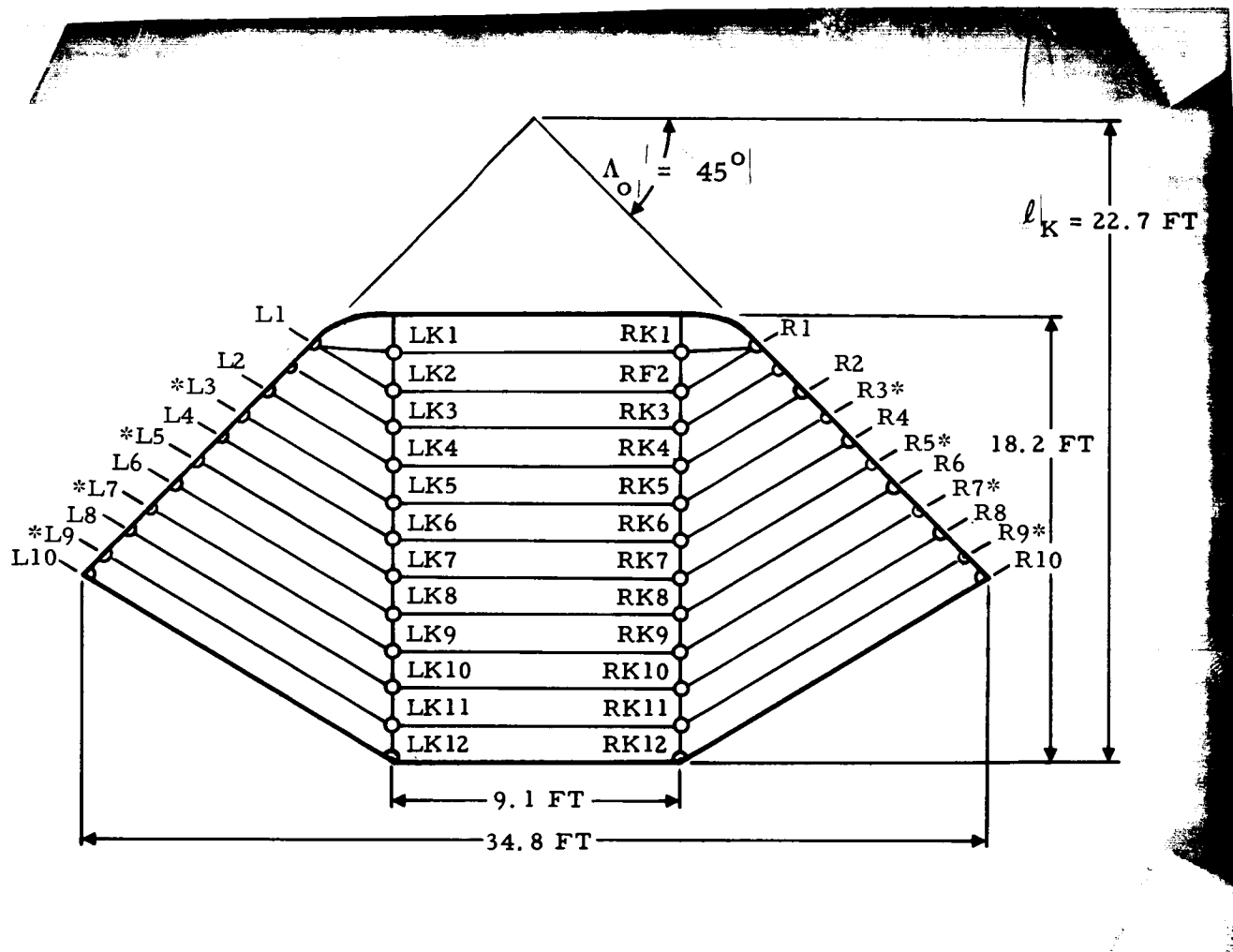
Description of Single Keel Parawings

The single keel small scale parawing had canopies constructed from 2.25 oz/sq yd low porosity nylon cloth and had dacron suspension lines. Two similar configurations were tested at the El Mirage test site. The models differed in that one configuration was constructed with 32 suspension lines and the other with 40.



NOTE: See Table 11 for suspension line lengths and locations.

Figure 49. Twin Keel Parawing, 36 Line Version



*INTERMEDIATE LINES ADDED TO 36 LINE VERSION

NOTE: See Table 11 for suspension line lengths and locations.

Figure 50. Twin Keel Parawing, 44 Line Version

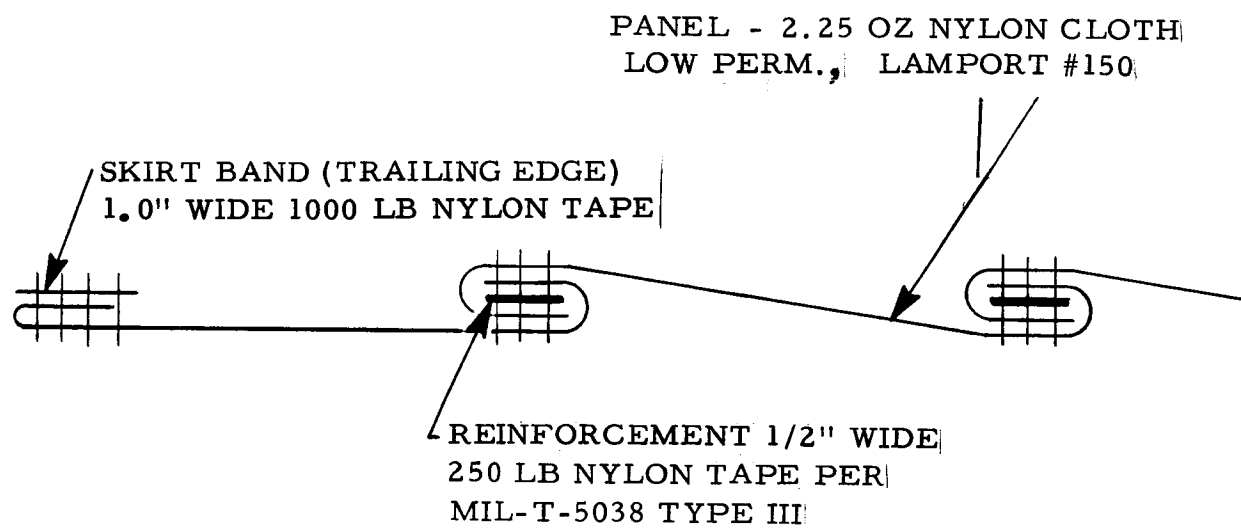


Figure 51. Canopy Seam Construction

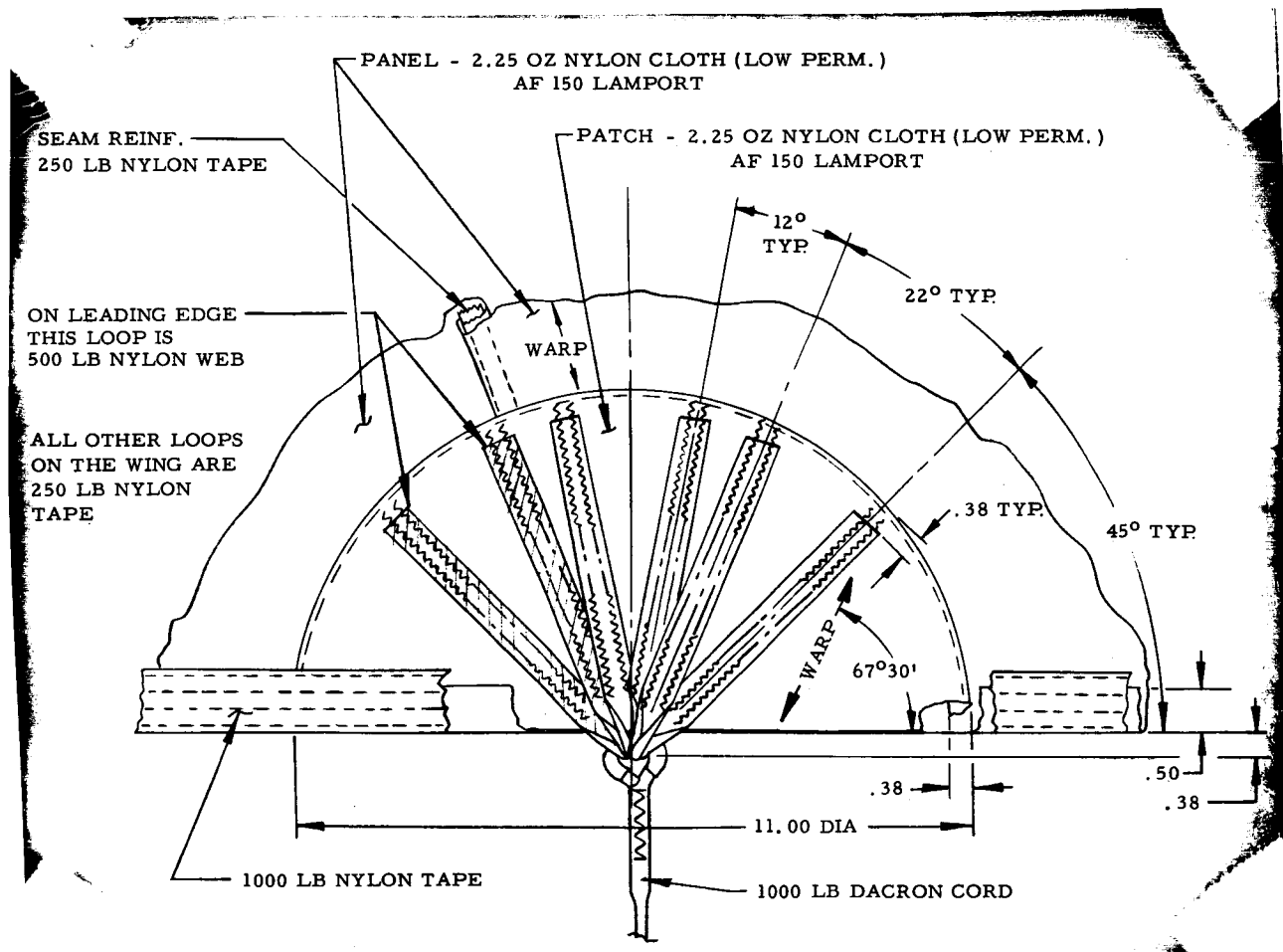


Figure 52. Suspension Line Attachment - Leading Edge, Trailing Edge, and Keel

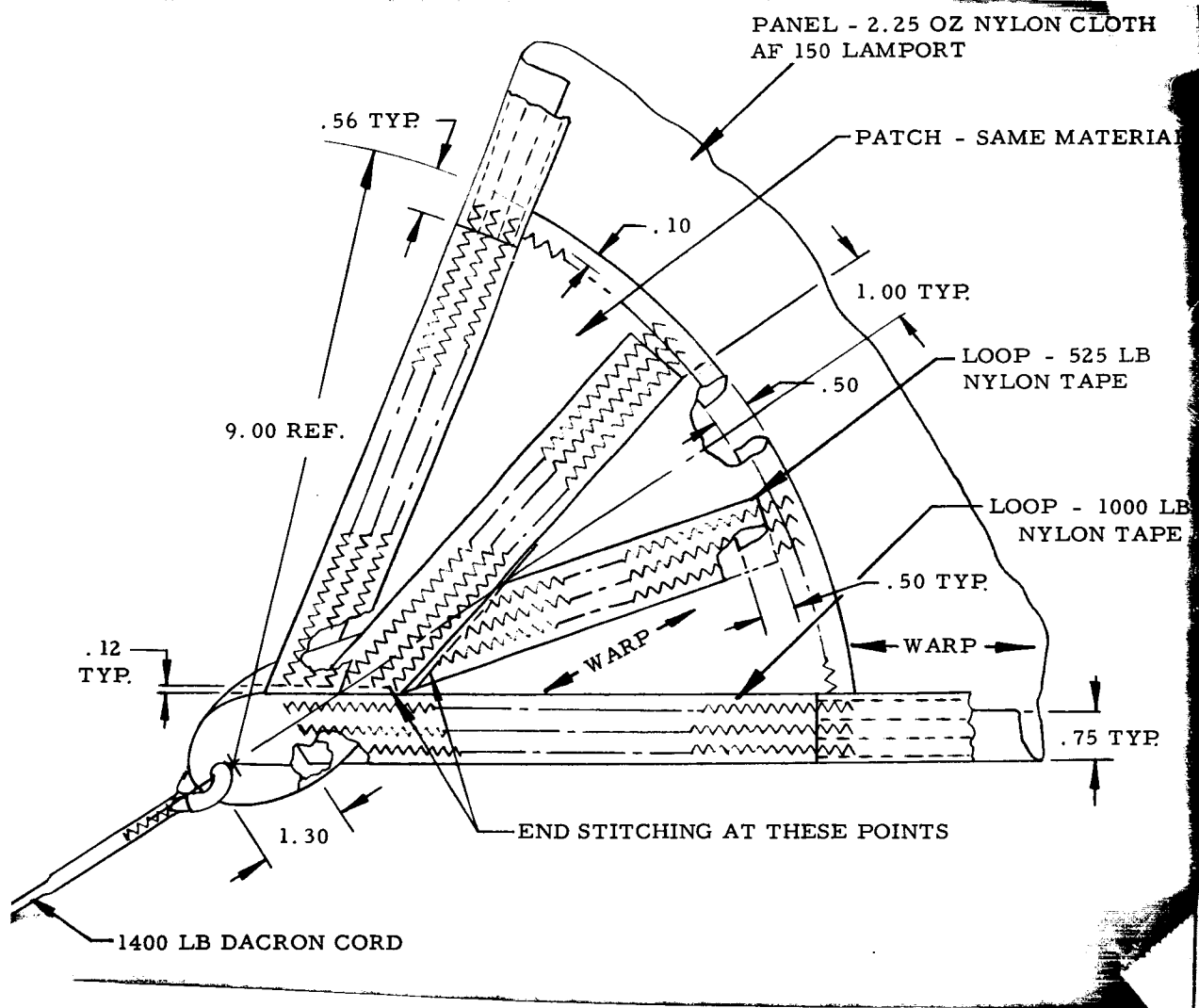


Figure 53. Suspension Line Attachment - Tip

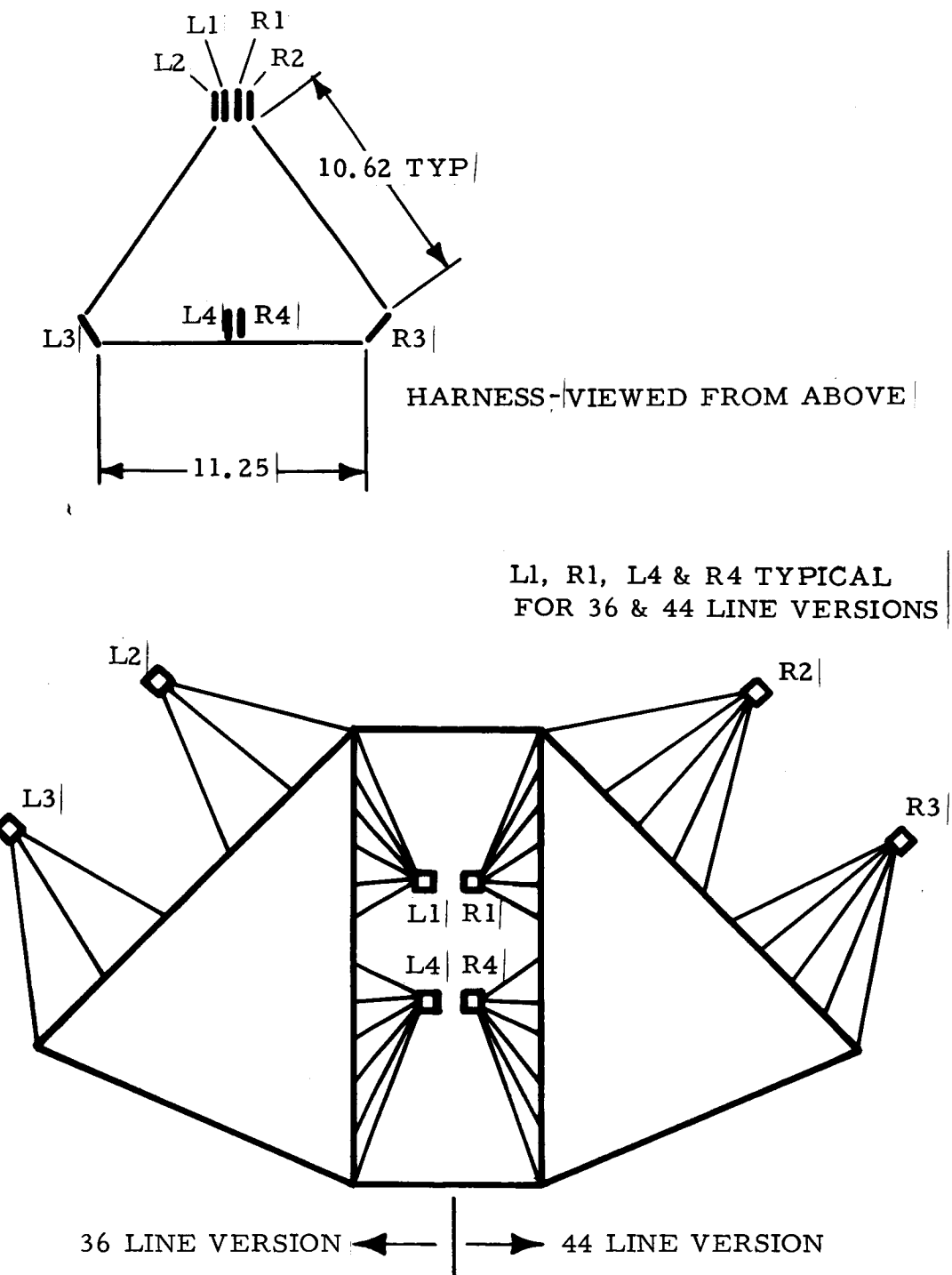


Figure 54. Twin Keel Suspension Line Arrangement

TABLE 11

Suspension Line Lengths and Locations for
Wings Flown in Gliding Performance Tests

Single Keel Model				Twin Keel Model							
32 Line			40 Line			36 Line			44 Line		
Line No.	Line Location X/ ℓ_K	Line Length (Inches)	Line No.	Line Location X/ ℓ_K	Line Length (Inches)	Line No.	Line Location X/ ℓ_K	Line Length (Inches)	Line No.	Line Location X/ ℓ_K	Line Length (Inches)
L1	.177	309.75	L1	.177	310.75	L1	.416	251.50	L1	.416	252.00
L2	.333	291.00	L2	.333	290.50	L2	.549	246.25	L2	.549	246.25
L3	.500	279.75	L3	.417	290.75	L3	.683	241.10	L3	.616	244.00
L4	.667	269.25	L4	.500	278.20	L4	.816	228.75	L4	.683	240.50
L5	.833	254.20	L5	.584	272.50	L5	.949	207.50	L5	.750	234.75
L6	1.000	215.25	L6	.667	269.75	L6	1.083	170.75	L6	.816	228.00
R1	.177	309.00	L7	.750	261.00	LK1	.267	264.00	L7	.883	219.50
R2	.333	290.25	L8	.833	255.10	LK2	.333	268.50	L8	.949	211.75
R3	.500	278.00	L9	.917	243.10	LK3	.400	266.50	L9	1.016	199.25
R4	.667	269.50	L10	1.000	215.00	LK4	.467	264.75	L10	1.083	169.00
R5	.833	254.60	R1	.177	311.75	LK5	.533	264.50	R1	.416	252.50
R6	1.000	216.25	R2	.333	290.50	LK6	.600	264.75	R2	.549	247.10
K1	.125	307.60	R3	.417	290.10	LK7	.667	263.60	R3	.616	244.25
K2	.209	304.75	R4	.500	277.75	LK8	.733	263.25	R4	.683	241.50
K3	.293	301.50	R5	.584	272.50	LK9	.800	260.25	R5	.750	234.75
K4	.334	304.75	R6	.667	269.50	LK10	.867	257.25	R6	.816	229.10
K5	.417	301.70	R7	.750	261.60	LK11	.933	252.50	R7	.883	219.50
K6	.500	300.50	R8	.833	253.75	LK12	1.000	249.50	R8	.949	211.50
K7	.583	297.20	R9	.917	243.25	RK1	.267	264.10	R9	1.016	200.10
K8	.667	293.10	R10	1.000	207.30	RK2	.333	268.75	R10	1.083	174.50
K9	.750	284.75	K1	.125	307.10	RK3	.400	267.10	LK1	.267	266.20
K10	.833	279.25	K2	.204	305.00	RK4	.467	264.10	LK2	.333	268.50
K11	.916	273.75	K3	.293	392.00	RK5	.533	264.10	LK3	.400	267.50
K12	1.000	266.75	K4	.334	304.10	RK6	.600	252.75	LK4	.467	265.00
LT1	.153	313.25	K5	.417	302.25	RK7	.667	263.00	LK5	.533	264.00
LT2	.306	323.50	K6	.500	300.75	RK8	.733	262.50	LK6	.600	265.50
LT3	.459	307.75	K7	.583	298.00	RK9	.800	259.75	LK7	.667	264.50
LT4	.612	279.25	K8	.667	292.75	RK10	.867	257.10	LK8	.733	264.00
RT1	.153	311.75	K9	.750	284.50	RK11	.933	251.50	LK9	.800	261.50
RT2	.306	324.00	K10	.833	278.20	RK12	1.000	249.00	LK10	.867	258.50
RT3	.459	306.50	K11	.916	273.50	R1	.416	251.25	LK11	.933	253.25
RT4	.612	279.75	K12	1.000	249.25	R2	.549	246.20	LK12	1.000	248.50
			LT1	.153	312.00	R3	.683	240.25	RK1	.267	265.10
			LT2	.306	324.50	R4	.816	228.50	RK2	.333	269.75
			LT3	.459	307.75	R5	.949	206.50	RK3	.400	268.50
			LT4	.612	258.50	R6	1.083	166.50	RK4	.467	265.50
			RT1	.153	312.25				RK5	.533	265.10
			RT2	.306	322.10				RK6	.600	266.00
			RT3	.459	307.10				RK7	.667	265.00
			RT4	.612	258.50				RK8	.733	264.50
									RK9	.800	261.50
									RK10	.867	257.70
									RK11	.933	253.00
									RK12	1.000	249.25

The overall dimensions of these two canopies are shown in Figures 55 and 56. Seam construction is illustrated in Figure 51. All but three suspension lines were 1,000 pound cord; the two wing-tip lines and the aft keel line (the three controlling lines) were made from 1,400 pound cord. All lines were attached to the canopy with spliced end loops formed through attachment loops stitched to the canopy. Attachment loop construction is shown in Figures 52 and 53. The lower ends of the lines were attached in groups to metal links, as shown in Figure 57. Table 11 lists the constructed suspension line lengths for the single keel models flown.

Parawing Materials

The major structural materials used in the fabrication of the four parawings tested at the El Mirage test site are described in Table 12. Materials were the same (except for quantities) for all four wings.

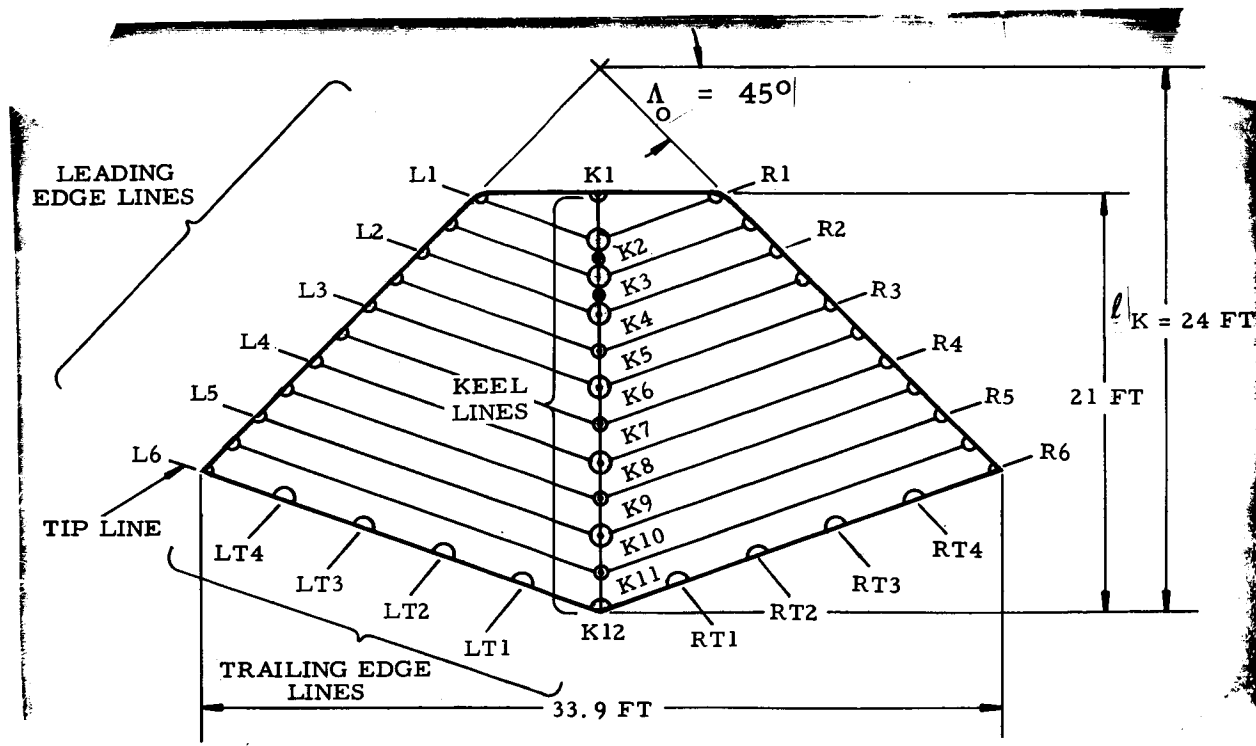
Harness and System Rigging

The harness used in all El Mirage tests was made from nylon webbing. The load-bearing members were constructed of a double layer of 3,600 pound webbing and a single layer of 8,700 pound webbing. The harness rigging method is shown in Figure 58. Suspension line link attachment arrangements are shown in Figures 54 and 57 for the twin and single keel models, respectively.

TEST PROCEDURES FOR FREE FLIGHT GLIDING PERFORMANCE TESTS

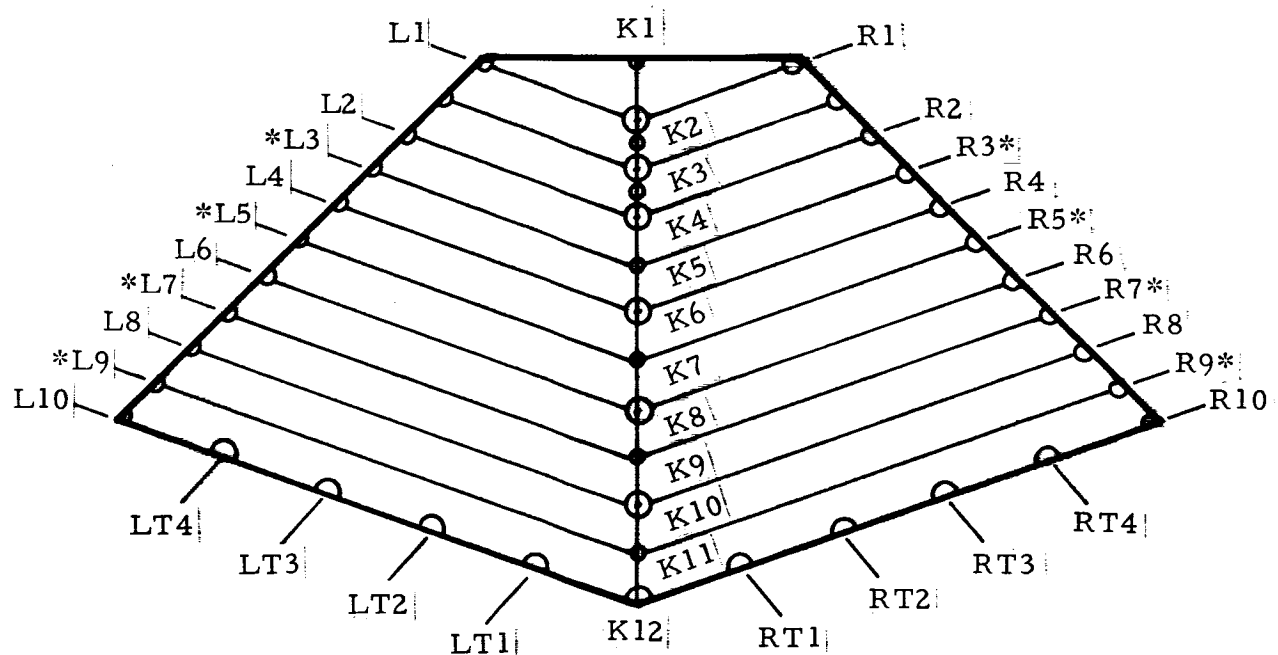
General

The drop test procedure was the same for the three types of tests conducted. All flight tests were initiated by dropping



NOTE: See Table 11 for suspension line lengths and locations.

Figure 55. Single-Keel Parawing 32-Line Version (8 Trailing Edge Lines)



*Intermediate lines added to 32-line version.

Dimensions for this model same as 32-line version (Figure 55).

NOTE: See Table 11 for suspension line lengths and locations.

Figure 56. Single Keel Parawing 40-Line Version (8 Trailing Edge Lines)

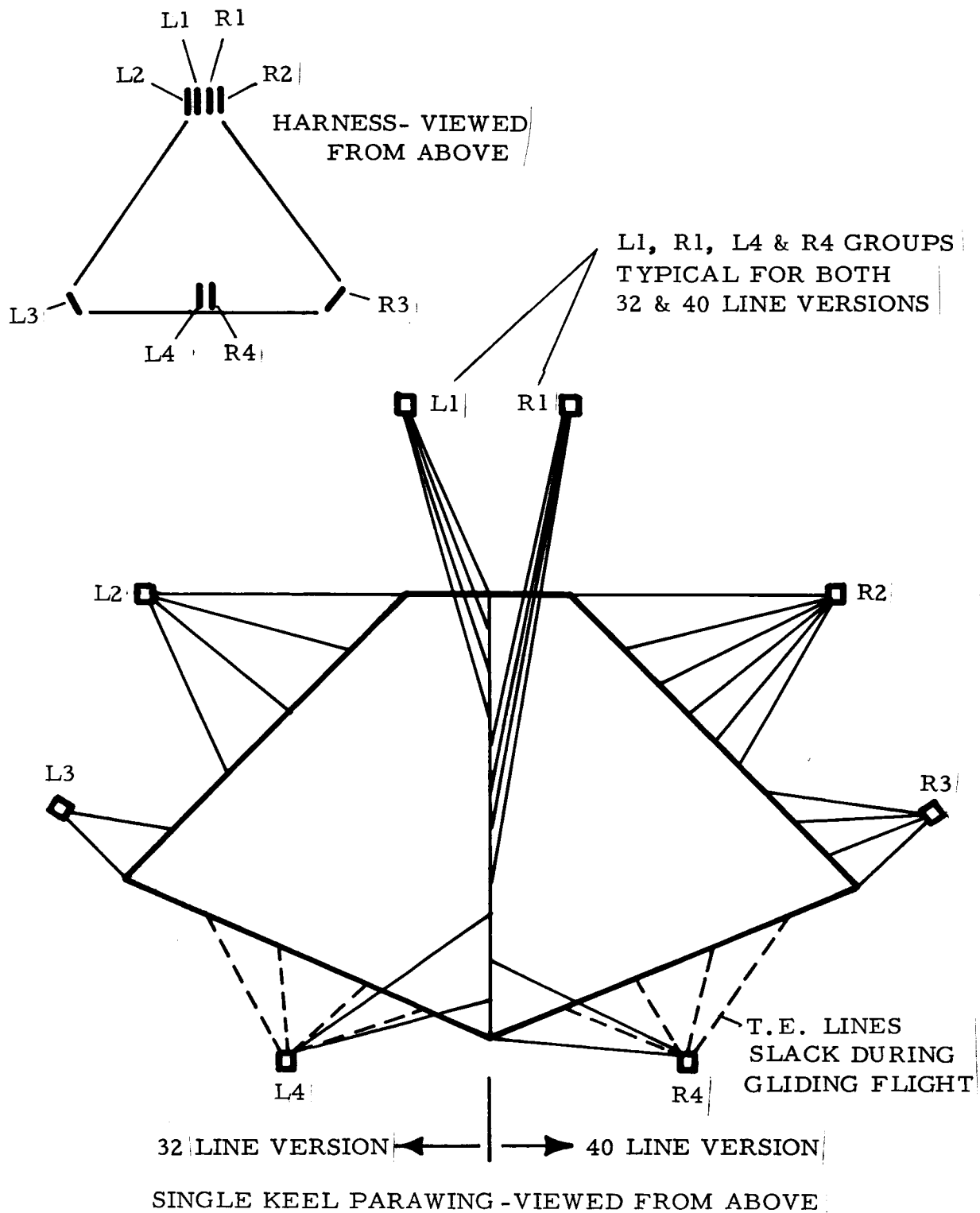


Figure 57. Single Keel Suspension Line Arrangement

Table 12. Parawing Materials

MEMBER	MATERIAL	SPECIFICATION
CANOPY PANELS	2.25 - ounce nylon cloth	MPDS 5-25.201 Type III A
SUSPENSION LINES	1000-lb dacron cord	MPDS 5-25.601 Type I
	1400-lb dacron cord	MPDS 5-25.601 Type III
SEAM REINFORCING	250-lb nylon tape	MIL-T-5038 Type III
SKIRT BANDS	100-lb nylon tape	MIL-T-5038 Type IV
	525-lb nylon tape	MIL-T-6134 Type I
SUSPENSION LINE ATTACH BECKETS	250-lb nylon tape	MIL-T-5038 Type III
	500-lb nylon webbing	MIL-T-4088 Type I
	525-lb nylon tape	MIL-T-6134 Type I
	1000-lb nylon tape	MIL-T-5038 Type IV
THREAD	Size E and FF nylon	V-T-295 Type I Class 1

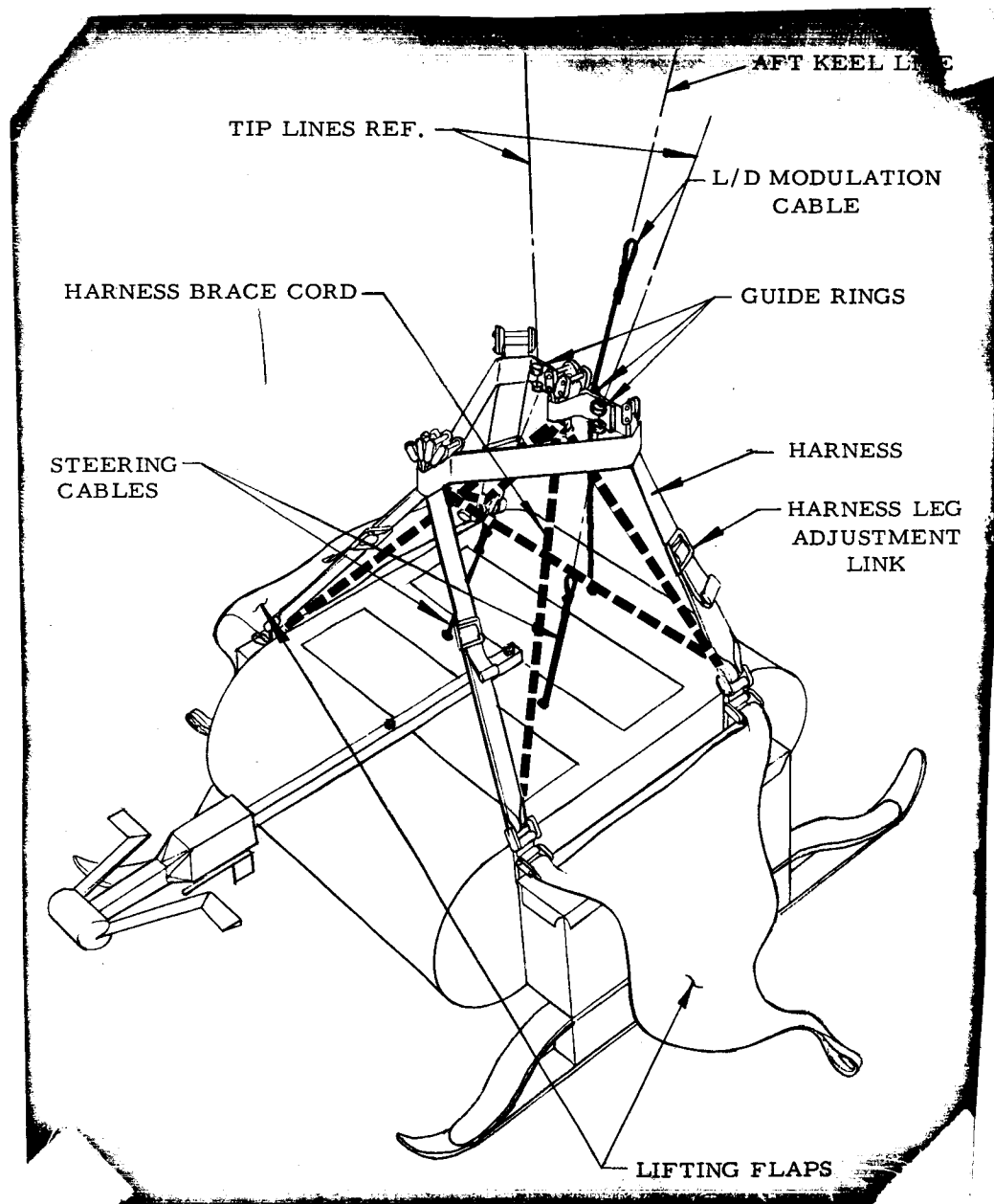


Figure 58. Wing/Test Vehicle Harness Rigging

the test vehicle from a helicopter. Each wing to be tested was packed and stowed on the upper deck of the test vehicle. At release from the helicopter, a static line lifted the pack off of the test vehicle deck and deployed the parawing which was allowed to inflate directly without reefing. Figure 59 is a pictorial representation of a typical launch/deployment sequence.

Trim Verification Tests

The weight vehicle used for the trim verification tests had no instrumentation nor control provisions. Visual observation of the tests was used to evaluate, qualitatively, flight stability of the wings. Turn rates were timed with a stopwatch. Based on these observations, corrections to the rigging were made and the wings retested. This procedure was repeated until properly inflated canopies with acceptably low turn rates were obtained.

Flight Performance and L/D Modulation Tests

For these tests, control of rear keel suspension line(s) and tip suspension line lengths was available. With these controls, it was possible to control flight direction and to modulate L/D. The instrumentation carried for these flights consisted of an L/D indicator and position indication for the control cables.

The first step in the flight test procedure was to permit the parawing/test vehicle system to damp out deployment induced transients and establish a flight path without control inputs. The system was then brought to the desired heading and the rear keel line was adjusted to the desired length. The system was allowed to fly for a period of 15 to 20 seconds with no additional control inputs. Necessary corrections to flight path direction were then made and the system allowed to return to straight flight.

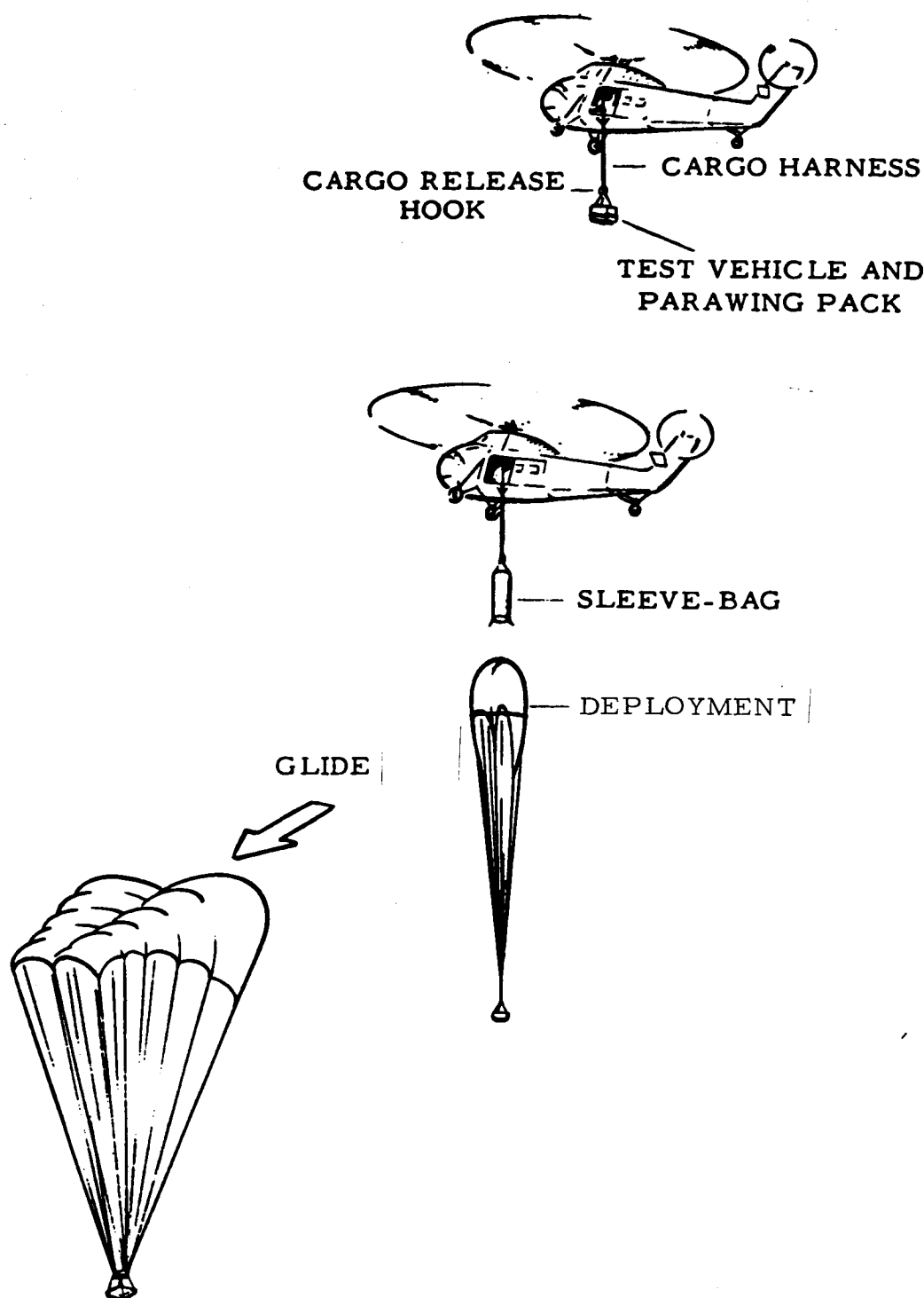


Figure 59. Helicopter Drop Sequence of Events

Another rear keel line position was then set and the system again allowed to fly without control inputs for another 15 to 20 seconds time interval. This procedure was repeated until the desired number of rear keel line lengths had been tested. The usual range of rear keel line settings was the full \pm 15 inch range of available control. In some cases, the range of extension or retraction of the rear keel line was restricted by nose collapse or stalling of the wing.

Turn Rate Tests

For the turn rate tests, the rear keel line length and tip suspension line lengths were controllable. The instrumentation for these flights consisted of a directional gyro and position readout of the tip control lines.

The first step of the flight test procedure was to permit the parawing/test vehicle system to damp out deployment induced transients and establish a steady flight path, prior to applying any control input. The system was then brought to the desired flight path heading and the rear keel line set to a predetermined length. After the system had stabilized following these initial control inputs, a predetermined right turn command was given. This command was then held until the system had achieved a constant turn rate for at least 5 to 10 seconds. The tip control line was then reset to neutral and the system allowed to stabilize in straight flight. This sequence was repeated for alternating left and right turn inputs of increasing tip control line retraction, until the full turn command available from the test vehicle had been utilized. The range of turn control available was \pm 8 inches from neutral for both the left and right turn control cables. The functioning of the turn control system is discussed in Appendix A.

SUMMARY OF SMALL SCALE FREE FLIGHT TESTS

Table 13 lists the small scale free flight performance tests conducted. Twenty-six tests were planned, of which ten were to be uninstrumented trim verification tests and sixteen were to be used to obtain L/D and turn rate data. Actually, a total of thirty-seven tests were conducted. Sixteen tests were used to check out and adjust the parawing model rigging, ten were used to obtain L/D data, and eleven were used to measure turn rates. The increased number of stability evaluation tests was necessary to determine riggings which gave the necessary flight stability to allow the wings to be tested with the controllable, instrumented test vehicle. During the test program, additional test weights were deemed desirable in order to obtain a more complete set of test data. Therefore, additional tests were conducted to obtain a wider range of weight conditions. The goal, though not completely achieved, was to fly three different wing loadings on both of the single keel models and three wing loadings on both of the twin keel models.

TEST RESULTS

This section of the report presents the data obtained in gliding performance tests, together with a discussion of the data.

L/D Performance Test Results

Figures 60 through 63 present the test results obtained during the free flight L/D performance tests. These figures show plots of L/D versus rear keel line deflection. The control deflection is presented as a ratio of rear keel incremental line length change to the reference keel length. The length of the tip lines is also shown on the figures as a ratio of line length to reference keel length. Each figure shows the data obtained for all of the L/D performance tests conducted with

**Table 13. Small Scale Parawing
Free Flight Test Program.**

Test No.	Test Vehicle	Vehicle	Weight Pounds	Parawing	Descent	Type	Test	Test Conductor's Comments
3S	W/B(a)	159.4	21.2		180.6	Stability		Appeared to be stalled, left turn to landing
3T	W/B	159.4	22.1		181.5	Stability		Nose pushed in, needed to shorten rear keel line
1S	W/B	159.4	19.1		178.5	Stability		Turned to right approximately 30 degrees per sec
1T	W/B	159.4	20.6		180.0	Stability		Flight looked good, turned to left at approx. 14 deg
3TR1(c)	W/B	159.4	22.1		181.5	Stability		Marginal nose shape, post flight inspection revealed length errors
3SR1	W/B	159.4	21.2		180.6	Stability		Approximately 45 deg per sec left turn rate, canopy shape looked good
2S	W/B	582.9	19.1		602.0	Stability		Did not establish stable glide, impacted in tight right turn
2T	W/B	582.9	20.6		603.5	Stability		Very high rate of turn to right, was rigged with 10 in differential tip
4T	W/B	582.9	22.1		605.0	Stability		Turn rate of approximately 70 deg per sec to the right
3SR2	W/B	159.4	21.2		180.6	Stability		Good flight, slow turn to the right
1TR1	W/B	159.4	20.6		180.0	Stability		Good flight, turn rate of approximately 19 deg per sec
1TR2	W/B	159.4	20.6		180.0	Stability		Excellent flight, approximately 270 degrees total turn during descent
1SR1	W/B	159.4	19.1		178.5	Stability		Started flying straight, then dropped off into left turn
3TR2	W/B	159.4	22.1		181.5	Stability		Canopy shape looked good, right turn of approximately 22 degrees per second
8S	Cont. (b)	199.3	21.2		220.5	Turn		Flight OK, would not hold hands off straight flight path
1SR2	W/B	159.4	19.1		178.5	Stability		Nose tucked under, flight condition was stable
8SR1	Cont.	199.3	21.2		220.5	L/D		L/D indicator not operational during first part of flight
3TR3	W/B	159.4	22.1		181.5	Stability		Poor directional stability
9S	Cont.	199.3	21.2		220.5	Turn		Good test, one turn to left during descent
6T	Cont.	199.3	20.6		219.9	L/D		Slow response to control inputs, difficult to hold heading
								Good flight, stalled at maximum rear line retraction, smooth recovery from stall
7T	Cont.	199.3	20.6		219.9	Turn		Good flight
6TR1	Cont.	226.7	20.6		247.3	L/D		Good flight, excellent turn control, very stable
9T	Cont.	226.7	22.1		248.8	Turn		Differential tip control, excellent turn response
8T	Cont.	226.7	22.1		248.8	L/D		Excellent flight, everything looked good
6S	Cont.	226.7	19.1		245.8	L/D		Good flight, would drop off into a turn at longer keel line settings
7S	Cont.	226.7	19.1		245.8	Turn		Good control response
11S	Cont.	341.2	19.1		360.3	Turn		Excellent turn response and control, held heading well
11T	Cont.	341.2	20.6		361.8	Turn		Good turn response
6TR2-T	Cont.	242.0	20.6		262.6	L/D		Test to get effect of tip line length, rigging error negated test results
10T	Cont.	341.2	20.6		361.8	L/D		Good test
10S	Cont.	341.2	19.1		360.3	L/D		Had tendency to wander around directionally
12S	Cont.	341.2	21.2		362.4	L/D		Touchy to control, test range from nose collapse to wing stall
12T	Cont.	341.2	22.1		363.3	L/D		Differential tip control test
16T	Cont.	479.1	22.1		501.2	Turn		Very touchy to control, extremely fast turn rates
17S	Cont.	471.6	21.2		492.8	Turn		Good flight, difficult to control, fast response
15S	Cont.	471.6	19.1		490.7	Turn		Very high bank angle in turns
15T	Cont.	471.6	20.6		492.2	Turn		Stalled during high rate right turn, good flight

(a) W/B indicates weight bucket test vehicle
(b) Cont. indicates controllable test vehicle
(c) R indicates repeat test

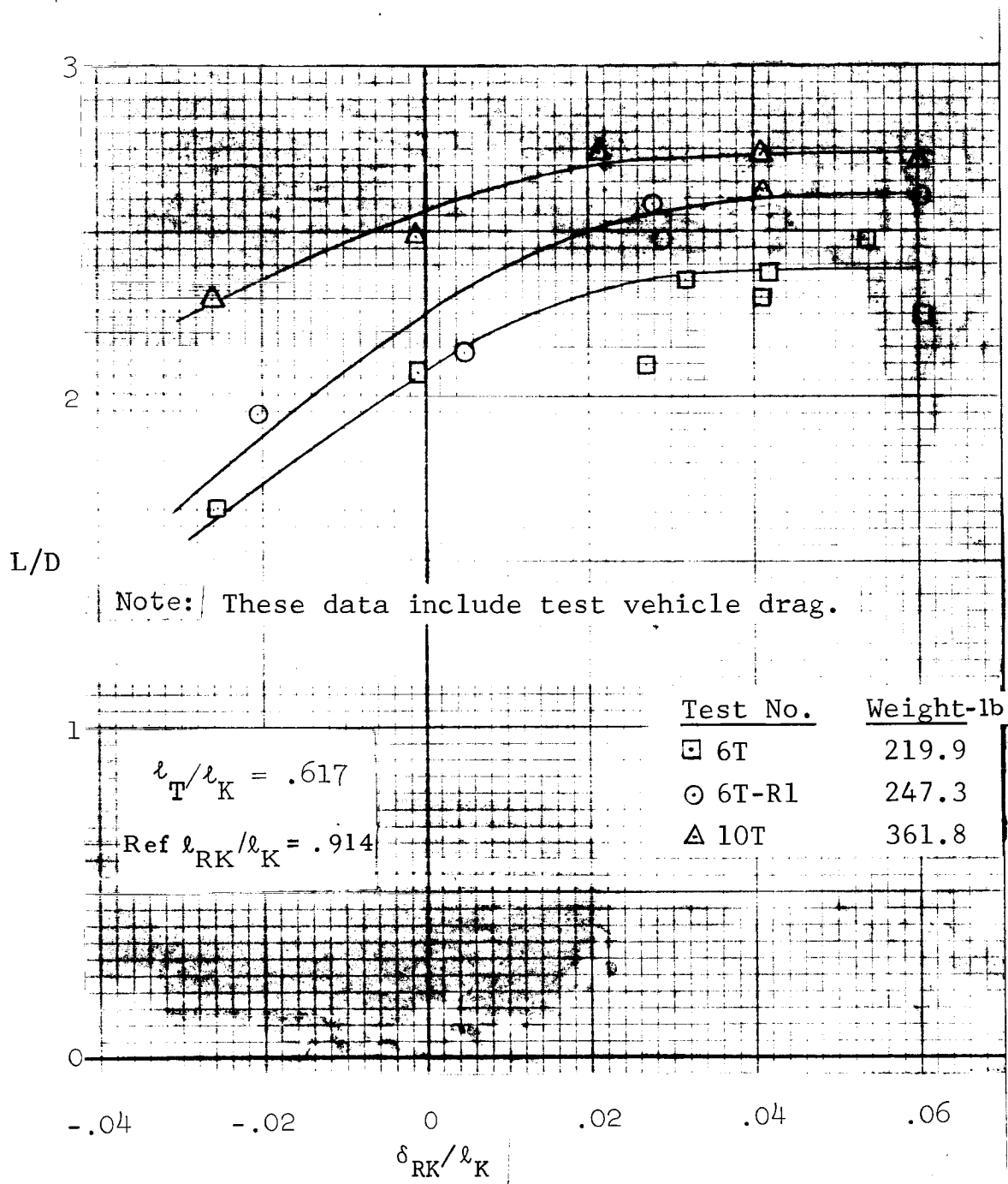


Figure 60. L/D versus Rear Keel Line Control Deflection for 36-Line Twin Keel Model

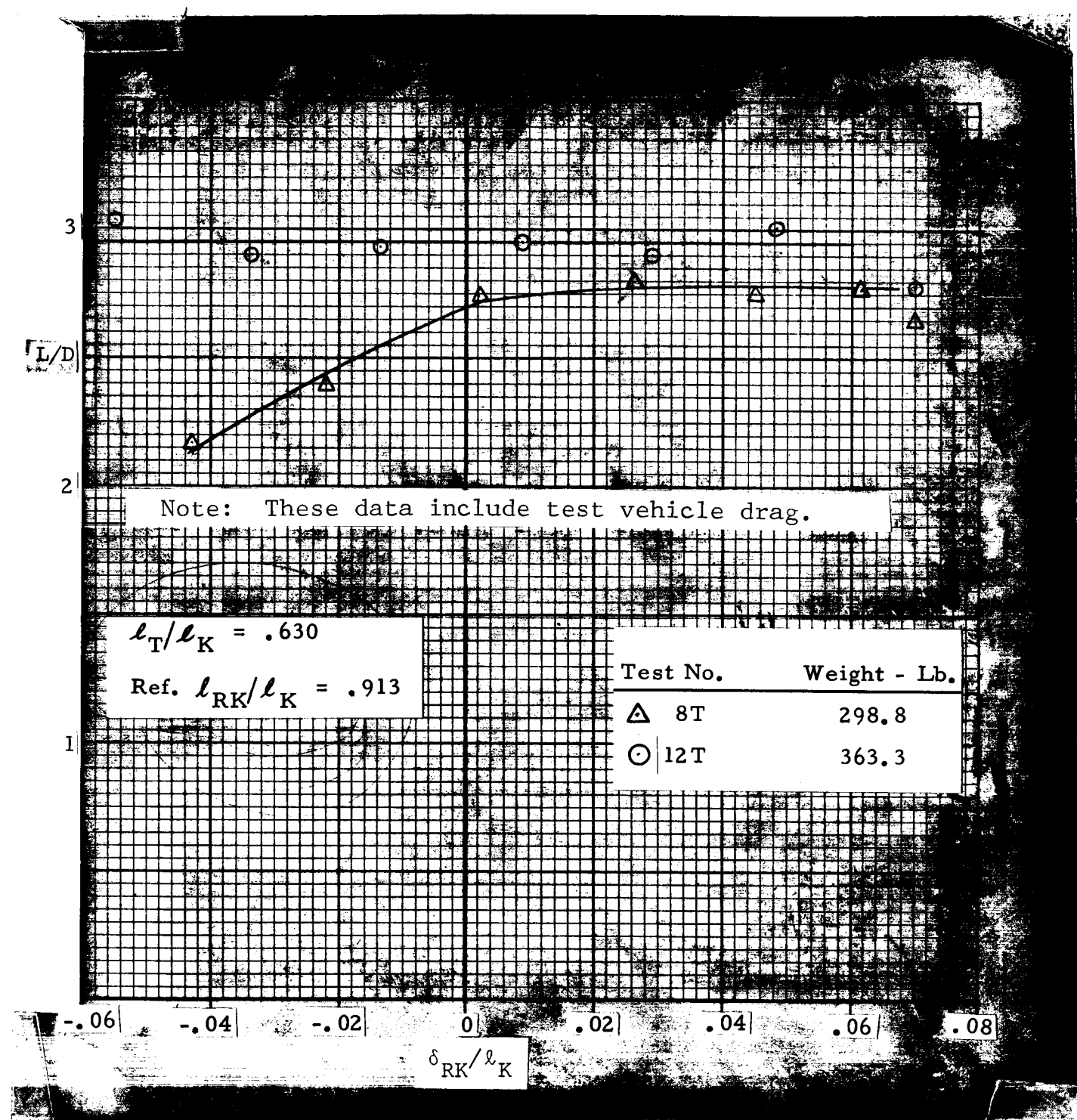


Figure 61. L/D versus Rear Keel Line Control Deflection for 44-Line Twin Keel Model

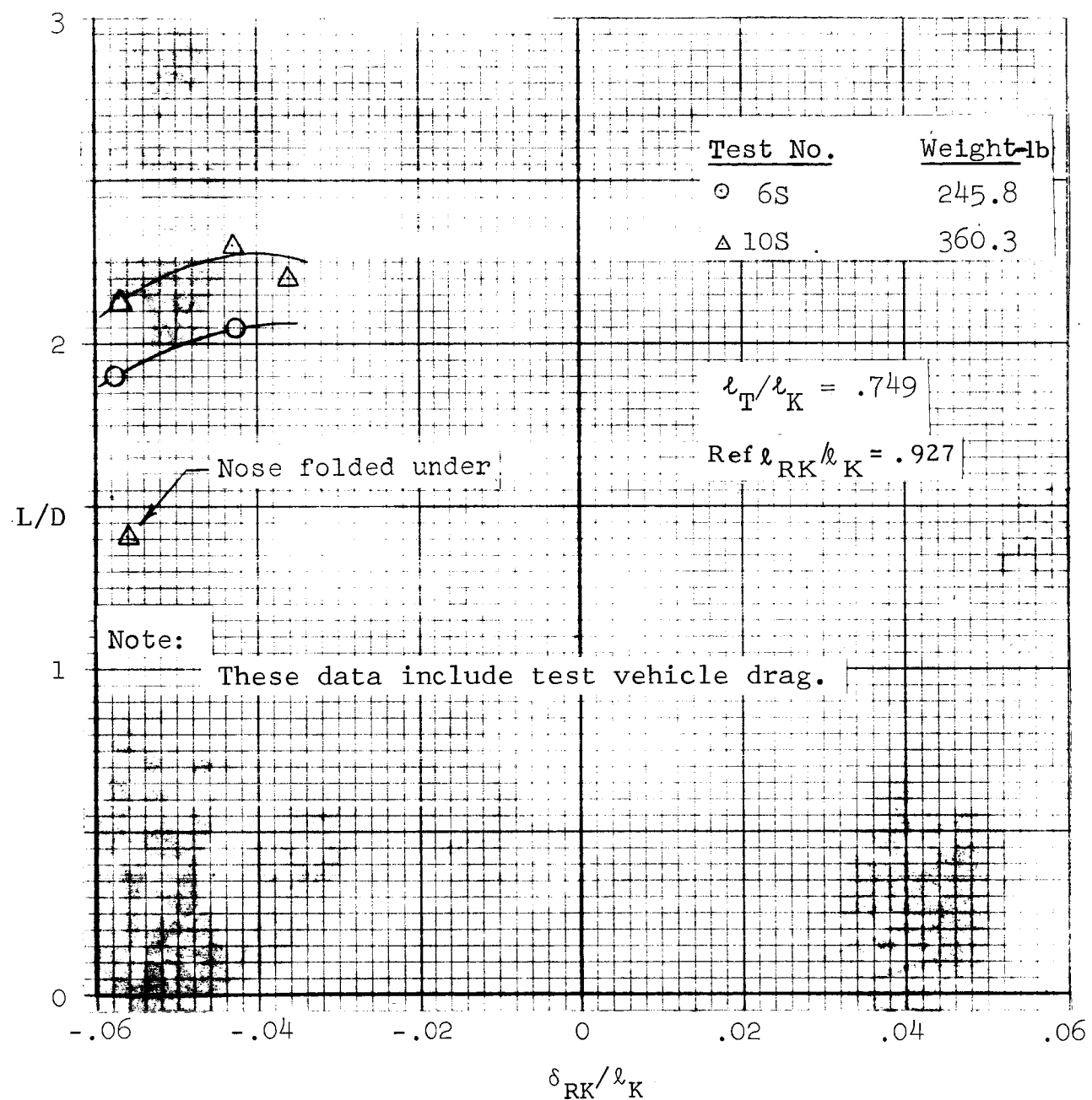


Figure 62. L/D versus Rear Keel Line Control Deflection for 32-Line Single Keel Model

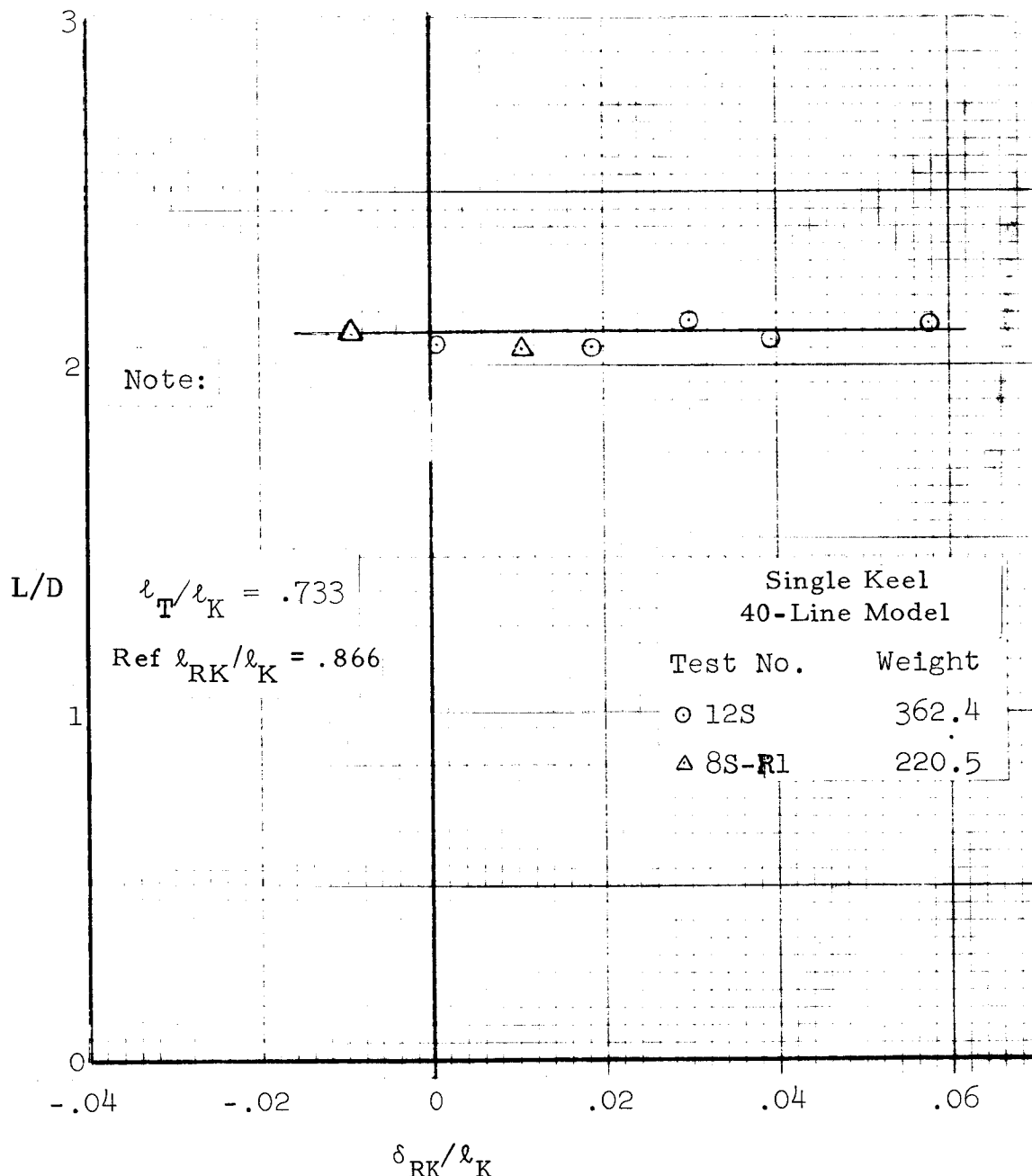


Figure 63. L/D versus Rear Keel Line Control Deflection for 40-Line Single Keel Model

a given model. Table 14 is a summary of the performance tests and lists type of model, test number, test weight, wing loading, and maximum and minimum L/D obtained with each model. It should be noted that in most cases, the minimum L/D listed does not represent the maximum rear keel line retraction attempted for that particular test flight. To determine the maximum allowable retraction of the rear keel line would have required going to the stall condition during each flight. This was not considered desirable, although in some flights, the wing was put into a stalled condition and recovered from the stall.

Discussion of Free Flight L/D Performance Test Results

Twin keel models. - Figures 60 and 61 show L/D performance test results obtained with the twin keel parawing. These figures show that L/D was a function of both wing loading and rear keel line length. The general trend of L/D with increased wing loading was such that an increase in wing loading resulted in a higher value of L/D for a given value of rear keel line length. Another trend shown in Figures 60 and 61 is a decrease in L/D with decreased keel line length at a constant wing loading. In general, it was found that the minimum value of L/D that could be obtained with any model was approximately 0.5 less than the maximum value obtained with that model. The one exception to this trend was Test 12T in which no modulation in L/D was obtained. Although there is no evidence to explain this behavior, it is believed that the rear keel control lines were improperly rigged in this test, with the result that the rear keel suspension lines were effectively slack for the range of control available. In light of the modulation of L/D shown by the other four L/D performance tests with the twin keel models, it is unlikely that the aerodynamic behavior of the model should change for this one test flight to the extent that no modulation of L/D was possible.

TABLE 14.
SUMMARY OF GLIDING FLIGHT DATA

<u>MODEL</u>	<u>TEST NO.</u>	<u>DESCENT WEIGHT</u>	<u>W/S</u>	<u>MAX L/D</u>	<u>MIN L/D</u> (Obtained during test)
36 Line (TK)	6T	219.9	.55	2.37	1.65
	6T-R1	247.3	.62	2.60	1.95
	10T	361.8	.90	2.73	2.30
44 Line (TK)	8T	248.8	.62	2.75	2.15
	12T	363.3	.91	2.97	2.90
32 Line (SK)	6S	245.8	.61	2.05	1.90
	10S	360.3	.90	2.30	2.13 (1)
40 Line (SK)	8S-R1	220.5	.55	2.10	2.05
	12S	362.4	.91	2.10	2.05

NOTES: These data include test vehicle drag.

(1) A minimum L/D of 1.40 was measured during a period of nose collapse.

Figure 64 shows maximum L/D versus wing loading for both the thirty-six line and the forty-four line twin keel models. This figure illustrates the increase in maximum L/D obtained as wing loading was increased. The rate of change of L/D with wing loading is about the same for the two models, and in general, the 44-line model obtained higher L/D values than the 36-line model. For example, at a wing loading of approximately 0.9 psf, the maximum L/D was 2.97 for the 44-line model and 2.73 for the 36-line model. In addition to the difference in number of suspension lines, the two twin keel models differed in the average length of their tip lines. The ratio of tip suspension line length to keel length was 0.617 for the 36-line model and 0.630 for the 44-line model.

Single keel models. - Figures 62 and 63 show the L/D performance test results for the single keel models. The results of four test flights are shown, two each with the 32-line and 40-line single keel models. The 32-line model showed the same trend in L/D as shown by the twin keel models with changes in wing loading and rear keel line (i.e., increasing wind loading increased L/D and retracting the rear keel control line reduced L/D). The 40-line single keel model as rigged showed no appreciable change in L/D as wing loading and rear keel line length were changed. Although no modulation was obtained during flight Number 12S, both the nose collapse and stall conditions were induced, showing that the rear keel control was functioning properly.

In addition to the small range of modulation shown by Figure 62, this figure also shows a data point which gives an indication of the performance of the single keel wing with the nose collapsed. It should be noted that for the 32-line single keel model, the reference rear keel line length was longer than for the 40-line model. For this reason, all of the 32-line model data are in the -0.04 to -0.06 range of line length change ratio.

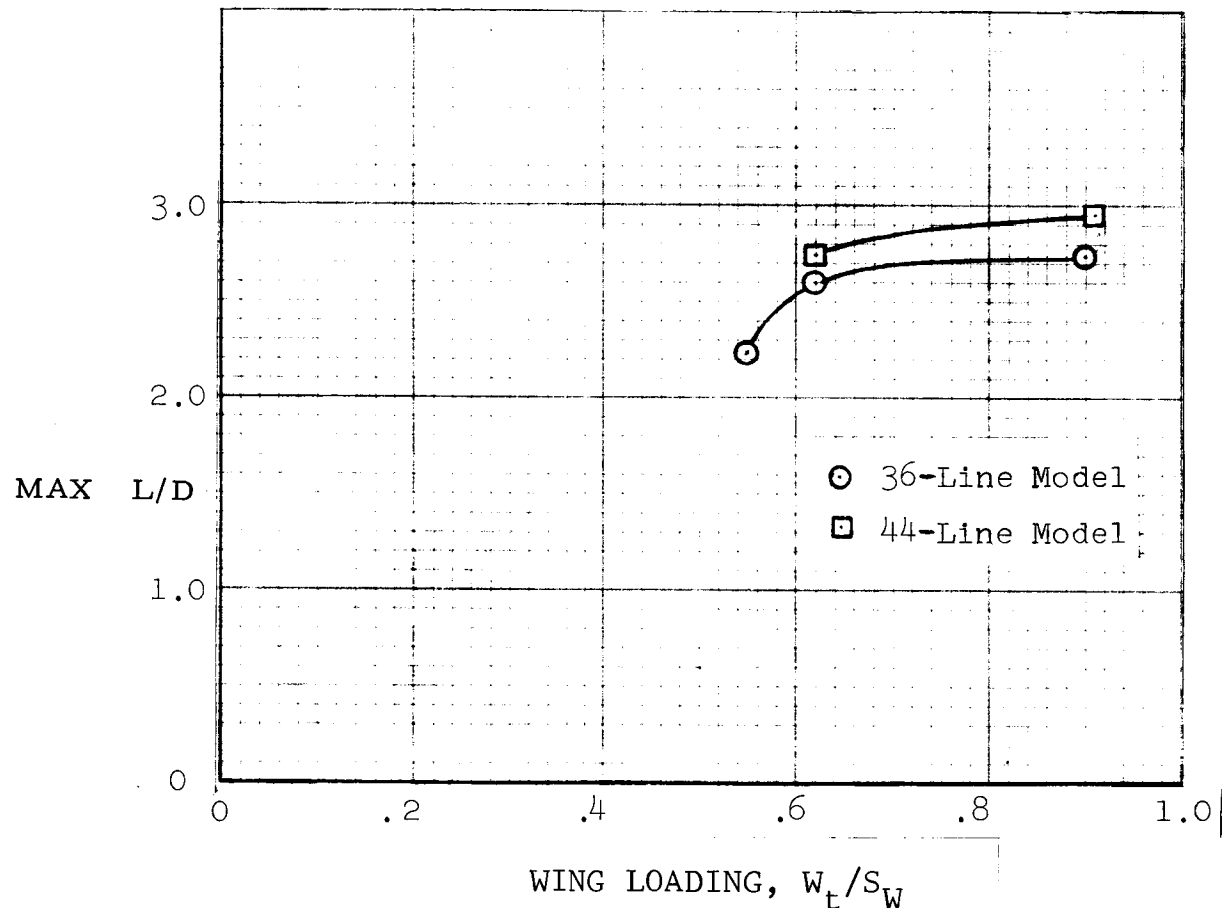


Figure 64. Maximum L/D vs. Wing Loading for the Twin Keel Models

Free Flight Turn Rate Tests

Figures 65 through 68 present the results of the free flight turn rate tests. These data are presented as plots of turn rate (in degrees per second) as a function of the change of the tip control line length (as a ratio of control line travel to reference keel length). The same four models used for the L/D performance tests were used for the turn rate tests. For the single keel model tests, all turn rate data were obtained with the single tip control method. With this method, turns were accomplished by pulling down on the tip suspension line on the side of the wing in the direction of the turn. The tip on the opposite side of the wing remained fixed at its rigged length.

Two methods of turn control were tested for the twin keel models. These were the single tip and the differential tip methods of control. The single tip control method was as previously described above for the single keel model tests. Differential tip control was accomplished by pulling down on the tip suspension lines on the side of the wing in the direction of the turn and at the same time extending by an equal amount the opposite tip suspension line. The single tip method of control was used for the 36-line twin keel model, and the differential tip method was used with the 44-line twin keel model. For the single tip control data, δ_T/l_K represents the ratio of the control line travel to the reference keel length. The control line travel in this case is the distance moved by the tip being actuated for turn control. Positive numbers indicate a right turn input and negative numbers indicate a left turn input.

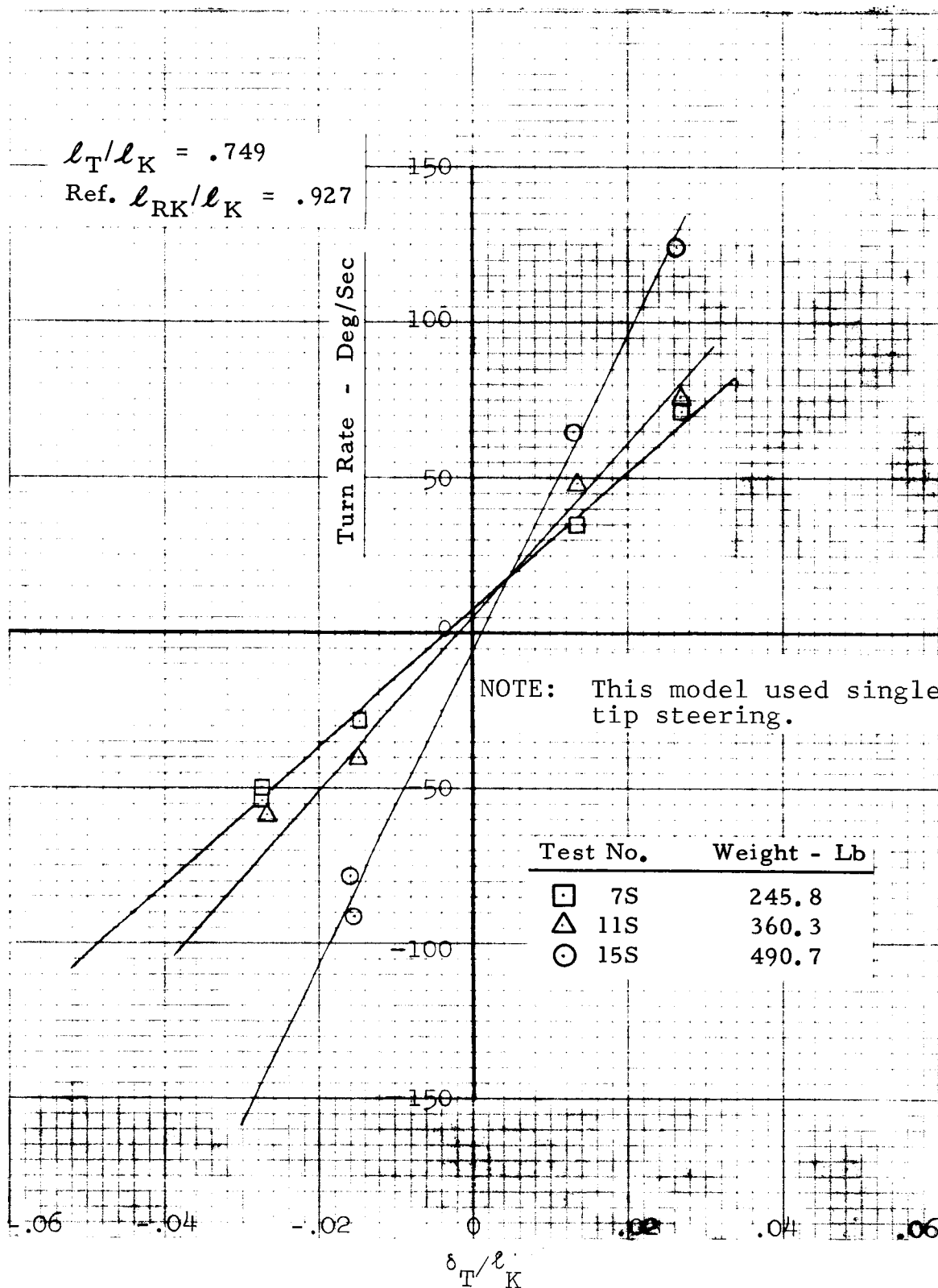


Figure 65. Turn Rate versus Tip Control Line Deflection for Single Keel, 32-Line Model

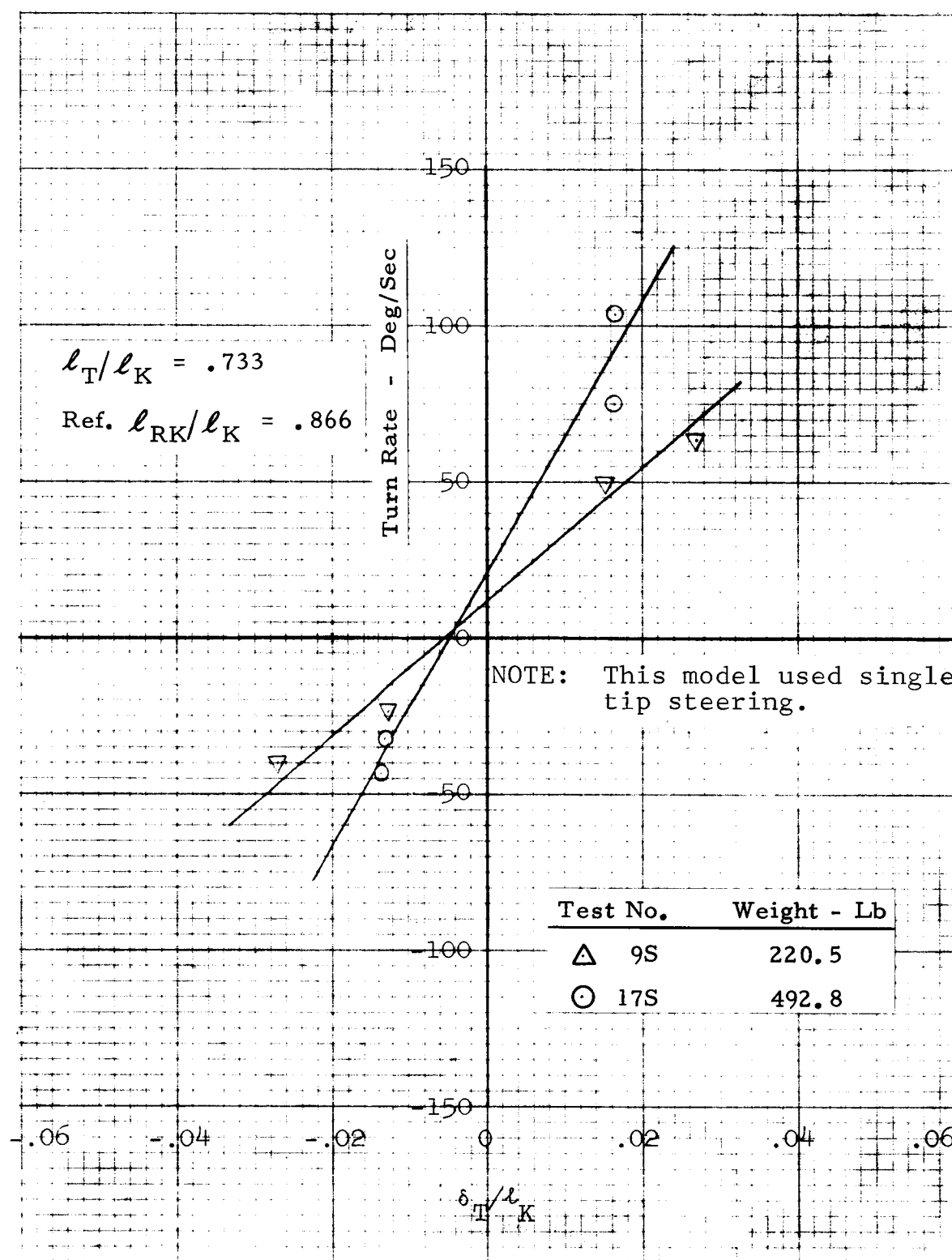


Figure 66. Turn Rate versus Tip Control Line Deflection for Single Keel, 40-Line Model

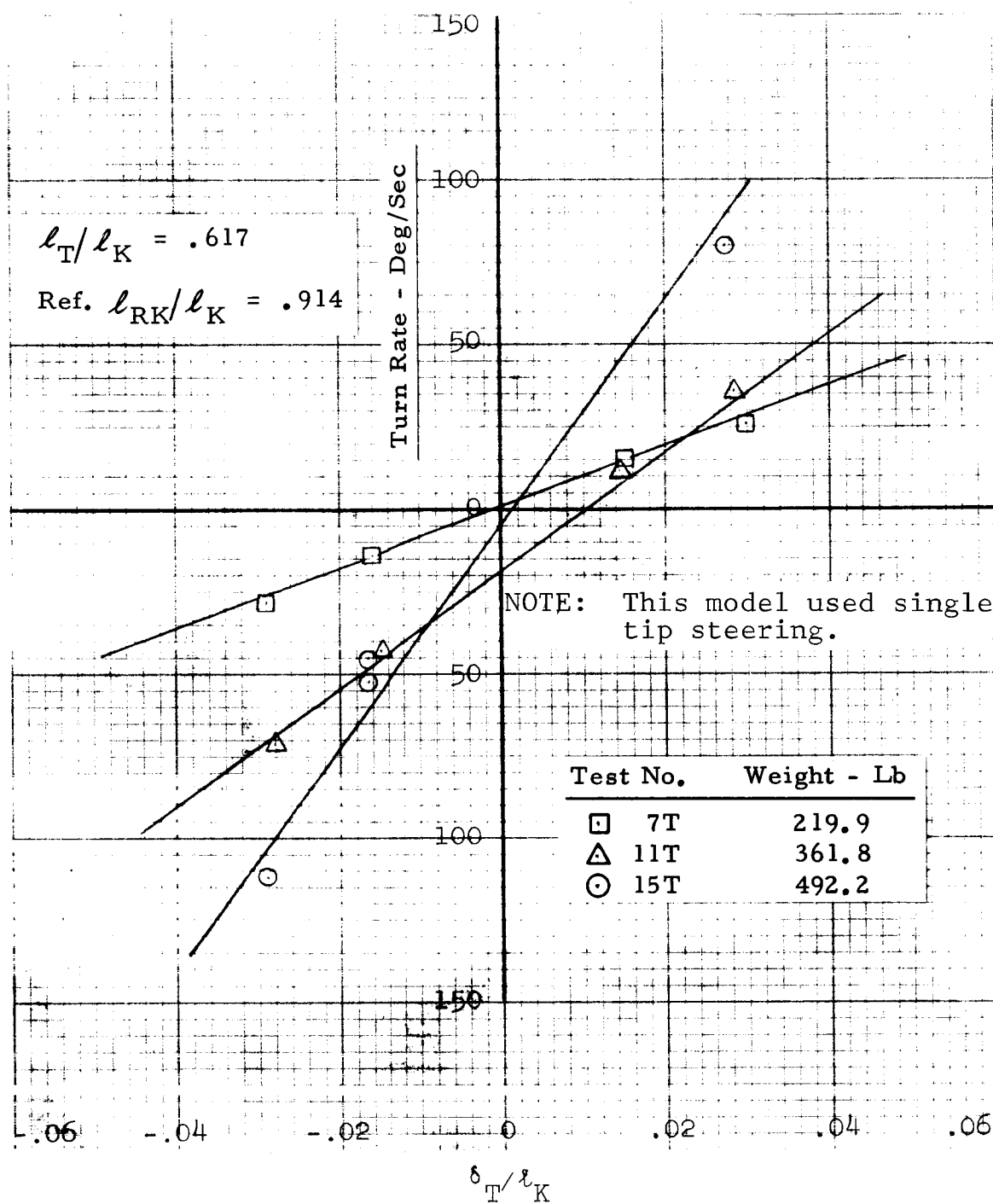


Figure 67. Turn Rate versus Tip Control Line Deflection for Twin Keel, 36-Line Model

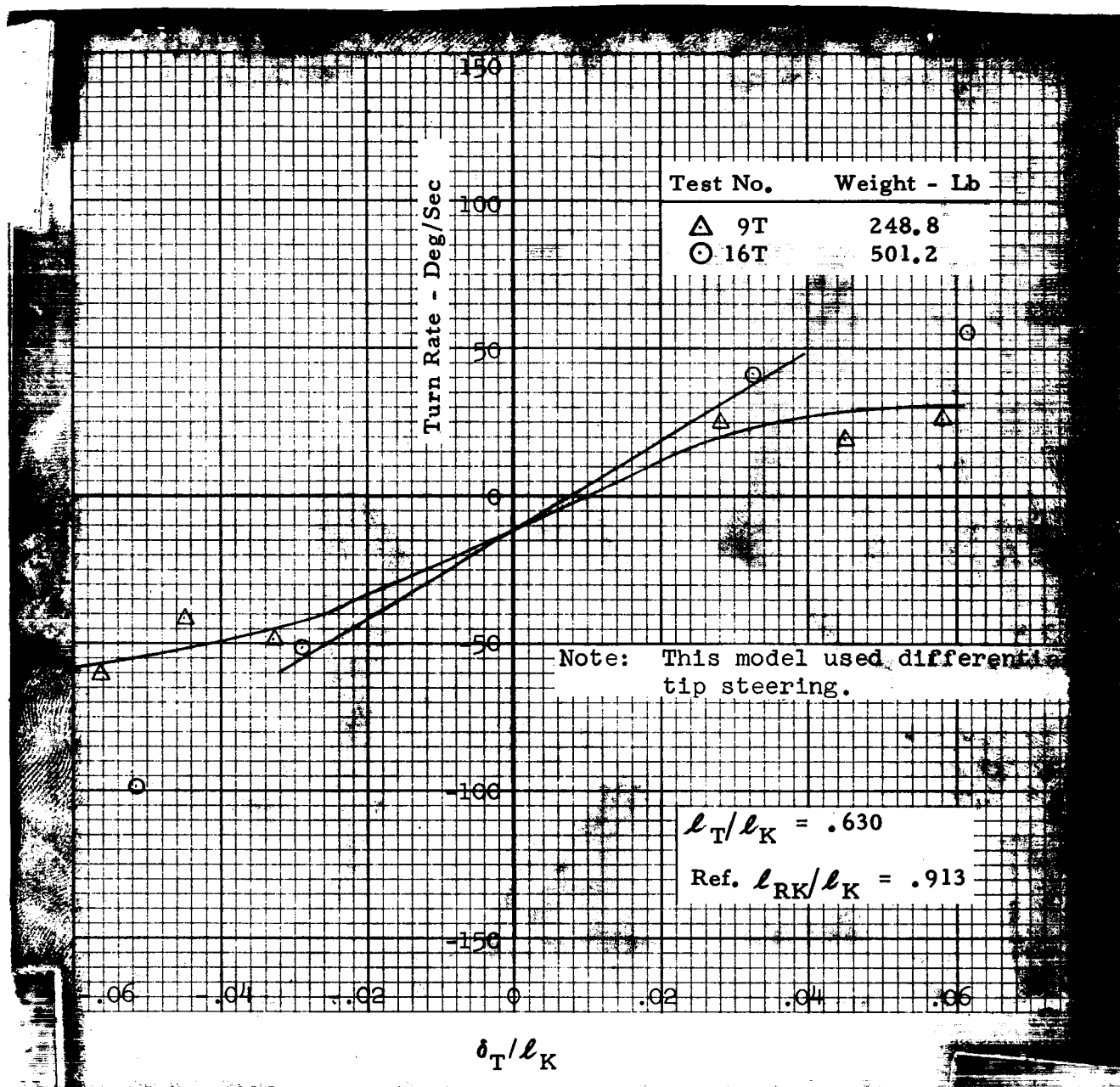


Figure 68. Turn Rate versus Tip Control Line Deflection for Twin Keel, 44-Line Model

For the differential tip turn control data, δ_T/l_K represents the ratio of the sum of the control line extension on one side and the control line retraction on the opposite side of the model, to the reference keel length. As with the single keel model data, positive numbers represent right turn inputs and negative numbers indicate left turn inputs.

Discussion of Free Flight Turn Rate Test Data

The slopes of the curves plotted on Figures 65 through 68 represent the control response of the wings tested. The greater the slope of the curve, the higher the turn rate for a given control input. Inspection of Figures 65 through 68 shows that some of the curves do not pass through the zero point on both axes. This type of behavior can be ascribed either to the wing being built with a turn bias, or the control lines rigged asymmetrically. Neither of these errors affects the slopes of the curves, which are the data of importance obtained during these tests.

The data obtained from the single tip control tests (Figure 65, 66 and 67) indicate that with this method of turn control, turn rate is a linear function of control line movement over the range of wing loadings and control line movement tested.

Figure 69 presents a plot of the slopes of turn rate versus control input as a function of system flight weight. These data show that the single keel models were more responsive than the twin keel models to turn control inputs. The data from the differential tip control tests (Figure 68) are not presented on this figure, since the turn rate data obtained during these tests were non-linear functions of control input.

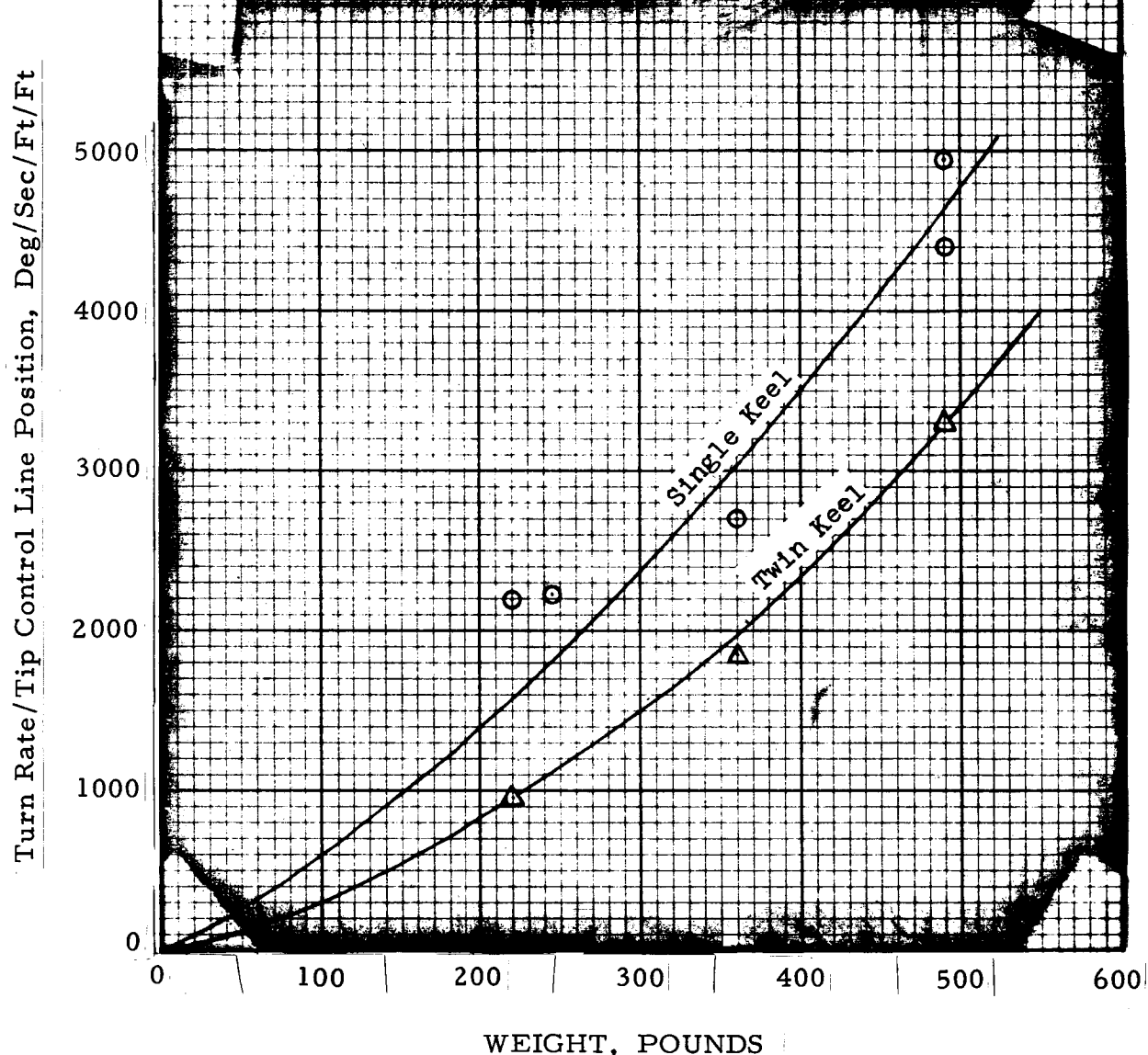


Figure 69. Slope of Turn Rate vs. Tip Control Line Deflection as a Function of Test Weight

The probable cause of the non-linearity of the turn rate response with differential turn control inputs appears to be loss of lift on the side of the wing on which the tip was extended. Other tests had shown that excessive tip suspension line lengths resulted in distorted leading edges and leading edge collapse with resultant loss of lift. Either of these conditions could be induced by extension of a tip suspension line as a turn input and result in loss of lift on the side of the wing being extended. Reducing the lift on the side of the wing towards the outside of the turn would have the effect of producing a rolling moment opposed to the turn. Also, an adverse yawing moment could be generated by leading edge distortion on one side of the wing.

Discussion of Flight Handling Qualities

The comments contained within this section are based on the impressions of the flight controller during the test flights. They are qualitative opinions, and reflect the experience gained by the flight controller during the thirty-seven tests conducted.

The directional stability of the single keel models, as rigged for these tests, appeared to be approximately neutral. The model could be set initially on a straight flight path. If left alone, the wing would fly straight for a few seconds, and then fall off into a turn. However, the twin keel models were relatively easy to fly compared to the single keel models. Their directional stability properties were such that the models would hold a heading for long periods of time without control inputs. For this reason, more data points on L/D performance were obtained during flights with the twin keel models than with the single keel models. To obtain steady state L/D performance data, it was necessary for the model to be in stable

straight flight. Because the single keel models required frequent turn control inputs, the amount of time available for obtaining L/D data with these models was severely limited.

Comparison of Performance in Free Flight and Wind Tunnel Tethered Flight

Two models were common to both the wind tunnel test program and the free flight test program. These were the 36-line, 22.7 ft keel length, twin keel model and the 32-line, 24 ft keel length, single keel model. Figures 70 and 71 are plots of wind tunnel and free flight L/D performance. Figure 70 shows comparable data from the Ames Wind Tunnel tests. The free flight data shown on this figure are adjusted for drag of the test vehicle and should, therefore, be comparable with the wind tunnel data. The wind tunnel data shown are for an ℓ_T/ℓ_K ratio of 0.706. This value was the highest ratio tested in the Ames tunnel for this model. The free flight tests were conducted with a tip line to keel ratio of 0.749. Therefore, the two sets of data are not exactly compatible; however, some conclusions can be drawn from these data. The rear keel line length to keel length ratio at which maximum L/D occurred is different for the wind tunnel data as compared to the free flight data. The probable cause of the offset between the two sets of data was the difference in the way the model was mounted in the wind tunnel, compared to the way it was attached to the test vehicle in the free flight tests.

Figure 70 shows lower values of L/D obtained in the free flight tests than in the wind tunnel tests with the single keel model. This difference in performance may not be significant in light of the wind tunnel data shown in Figure 45. Figure 45 shows that there was a trend of decreasing L/D with increasing tip line length for values of ℓ_T/ℓ_K in excess of 0.710.

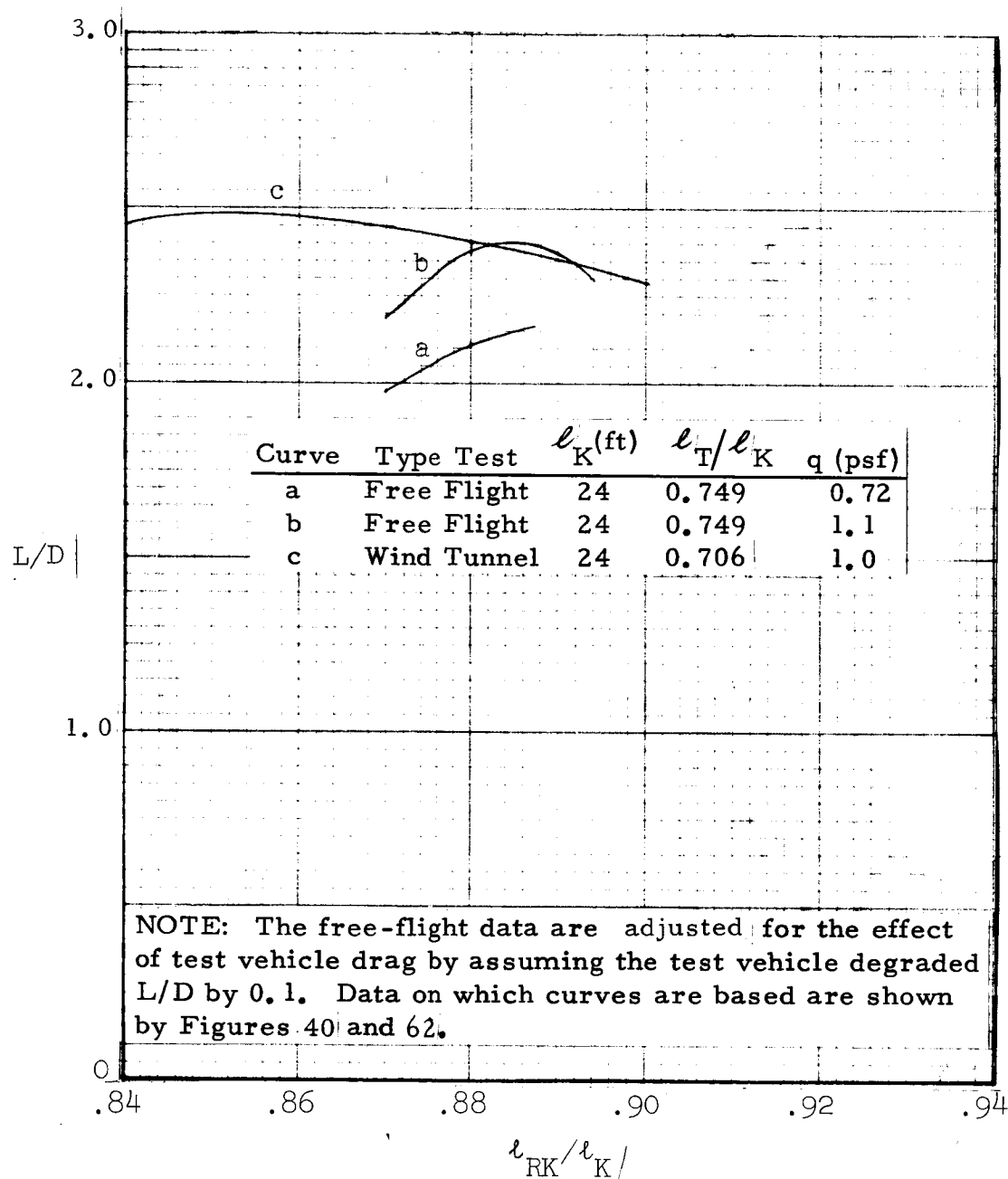


Figure 70. Comparison of Free-Flight and Wind Tunnel Gliding Performance for 32-Line Single Keel Parawing

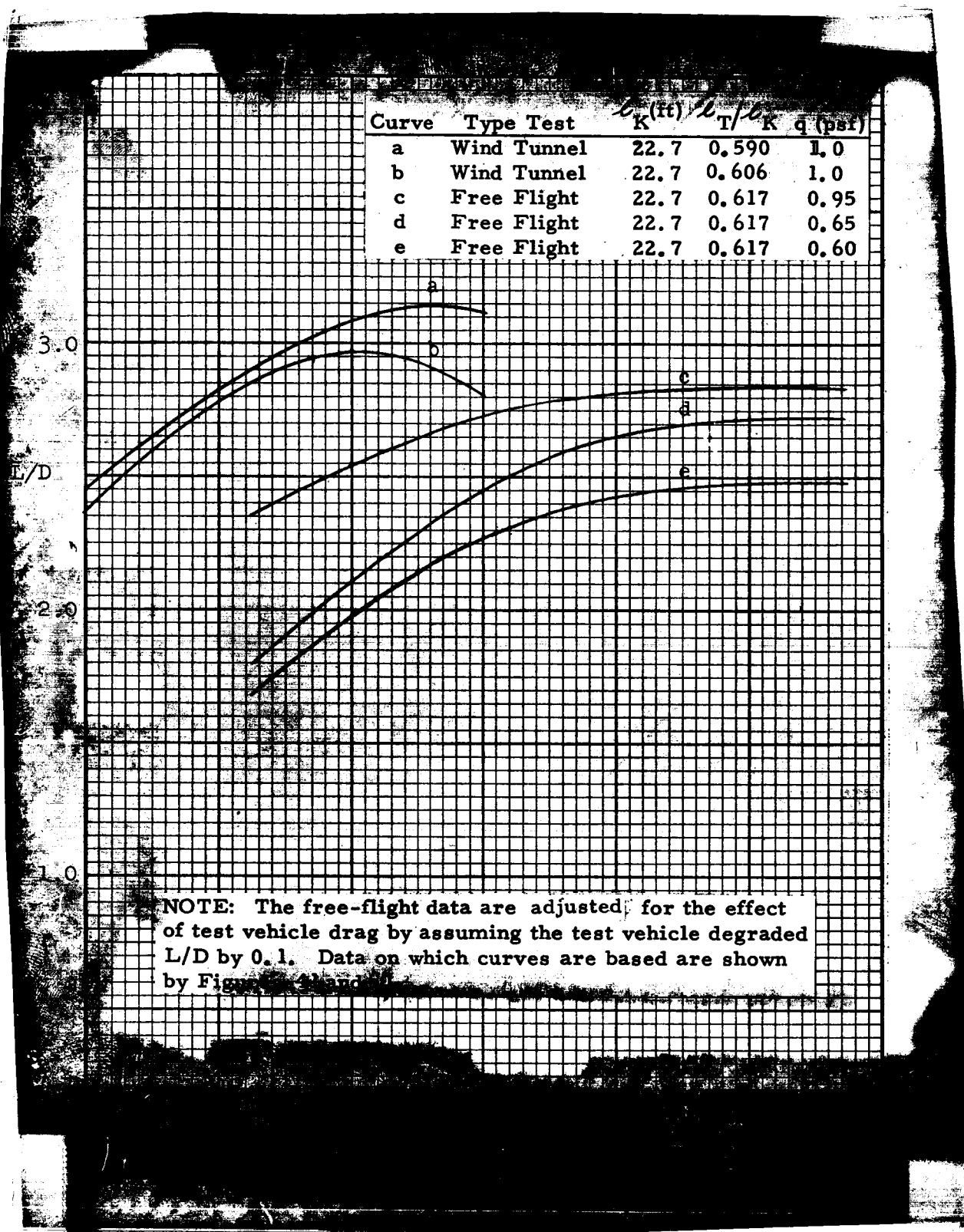


Figure 71. Comparison of Free-Flight and Wind Tunnel Gliding Performance for 36-Line Twin Keel Parawing.

The wind tunnel data show very limited L/D modulation resulting from rear keel line retraction, and the same limited capability is shown by the free flight data. Wind tunnel data were obtained at rear keel line ratios in excess of those which produce maximum L/D. In free flight, comparable data could not be obtained because air turbulence disturbed the nose area of the wing, causing it to fold inward.

Figure 71 shows the comparable wind tunnel and free flight twin keel data. For the model shown, wind tunnel data are available at tip line ratios which bracket the tip line ratio used for the free flight tests. Figure 71 indicates an offset between the rear keel line length ratio for which maximum L/D occurred in the wind tunnel test versus free flight test data, similar to the offset noted with the single keel parawing. Also, the wind tunnel data and free flight data differ in maximum L/D, with the wind tunnel data showing appreciably higher maximum L/D values. The offset in rear keel line length ratio for maximum L/D was probably due to the differences in the way the model was mounted in the wind tunnel, compared to the way it was rigged for the free flight tests.

It is difficult to determine the cause of the differences between free flight and wind tunnel data relative to the effect of wing loading on maximum L/D. The data available are not sufficiently complete to establish the cause of this variance. For example, increasing dynamic pressure (wing loading) caused L/D to increase during the free flight tests. The same model when tested in the wind tunnel at still higher dynamic pressure resulted in a decrease in L/D performance, as shown in Figure 48.

FREE FLIGHT DEPLOYMENT TESTS

This section of the report presents a discussion of the planning, the test equipment, and the test results for a series of free flight deployment tests conducted with 400 sq ft wing area parawing models. These tests were conducted at the DOD Joint Parachute Test Facility Range, NAF, El Centro, California, in the period of April through August 1968.

The objectives of these tests were as follows:

1. Evaluate the functioning of reefing systems, including determination of opening force factors, effective drag areas, and aerodynamic stability for the various reefing stages.
2. Determine suspension line load distributions and obtain reefing line load information.
3. Obtain design data for larger parawing systems by conducting scaled deployment tests.
4. Evaluate the capability of the 400 sq ft wings to withstand deployment at specified limit altitudes, dynamic pressures, and system descent weights.
5. Develop techniques for packing and rigging of larger parawing models.

Three types of tests were conducted to meet these objectives:

1. Functional verification tests at minimum attainable weight and deployment dynamic pressure to check the mechanical functioning of the reefing systems.

2. Tests under conditions that were directly related to scaling laws to a specific set of test conditions for a larger wing. (The larger wing reference size was in all cases 4000 sq ft.)
3. Tests to prove the capability of the parawing models to withstand dynamic pressure of 100 psf, an altitude of 18,000 feet, and a descent weight of 500 pounds.

The overriding concern during this test program was to develop a reefing system with stable aerodynamic characteristics during each stage of the opening process, which could be applied to parawings having wing areas as large as 10,000 to 12,000 sq ft.

PLANNED AND ACTUAL DEPLOYMENT TESTS

The deployment tests were made to obtain data which would define the inflation, deceleration, and deployment-to-glide transition characteristics of both single and twin keel parawings. Table 15 presents the test program that was conducted.

TEST PROCEDURE

A programmer parachute was used to bring the test vehicle to a proper dynamic pressure and near-vertical flight path angle prior to deployment of the parawing test model. A typical test began with deployment of the programmer parachute by static line upon launch from the drop aircraft. After a predetermined time interval required to achieve the desired test conditions, an on-board electronic sequencer actuated pyrotechnic devices which disconnected the programmer parachute. The disconnected programmer parachute in turn deployed the parawing test specimen. Figure 72 illustrates a typical test sequence.

TABLE 15
Small Scale Parawing Deployment Tests

Test Order	NV Test Number	Wing S/N	DEPLOYMENT CONDITIONS		
			Weight* (lbs.)	Alt (ft)	q (psf)
1	102T	3	254.2	2,800	39.75
2	104T	2	254.2	2,707	54.7
3	104S	2	252.8	3,066	53.9
4	102S	3	257.2	3,174	38.5
5	103T	1	254.0	3,101	50.1
6	103S	1	247.5	2,400	50.4
7	101T	2	218.5	12,832	41.3
8	101S	2	210.0	13,200	39.6
9	100T	1	220.6	10,883	40.6
10	106T	2	502.4	18,600	74.1
11	100S	1	210.8	12,880	41.6
12	105T	1	255.8	3,380	51.1
13	106S	2	500.3	18,541	79.7
14	105S	1	255.9	3,204	47.9
15	107T	3	498.7	19,336	95.3
16	107S	3	493.9	19,390	87.8

*Descent weight

NORTHROP VENTURA

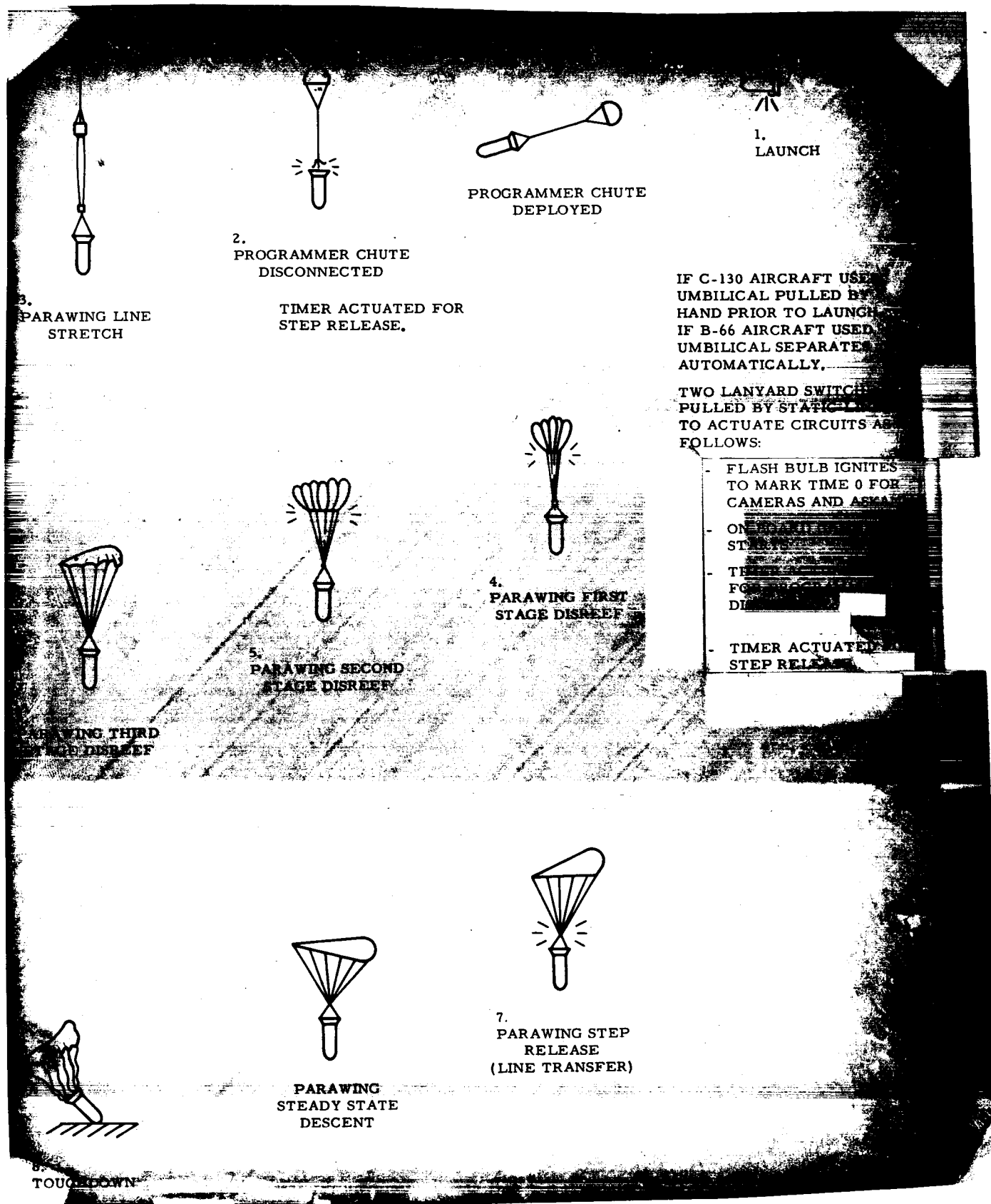


Figure 72. Sequence of Parawing Test Events

TEST MODELS

The canopy structure for the models used during the deployment tests was essentially the same as the free flight performance test models (see Figures 49 and 55). Reefing rings were added, along with provisions for the installation of reefing cutters, reefing lines, and means to equalize suspension line lengths. The twin keel models used for the first three deployment tests had 36 suspension lines along the leading edges and keels. All tests of the twin keel parawing after the first three tests used models which were modified by the addition of six suspension lines, three on the trailing edge of each outer lobe. The single keel parawing models were similar to the 32-suspension line model flown during the flight performance tests, with the exception of added provisions for reefing the canopy and equalizing the suspension lines during the deployment phase of the flight.

Table 16 lists the suspension line lengths for each model used during the test program.

PARAWING REEFING SYSTEMS

During the test program, several different reefing systems were tested. The first deployment test of each of the single keel and the twin keel designs was made with the reefing system selected from the data obtained from the LRC wind tunnel program. These systems are described in detail in the wind tunnel section of this report. As the test program progressed, changes in each of the reefing systems were, for various reasons, found to be necessary. The following paragraphs describe the various configurations tested, followed by a section devoted to a discussion of the reasons for the various changes.

TABLE 16.
Deployment Test Preflight Suspension Line Lengths
SINGLE KEEL

Line No	Test Number							
	100S	101S	102S	103S	104S	105S	106S	107S
L1	309.5	312.0	312.5	310.5	309.75	312.5	310.5	312.0
L2	291.0	292.0	292.5	290.5	292.0	297.0	292.0	297.0
L3	279.0	280.0	280.25	279.3	280.0	284.4	279.5	284.4
L4	272.0	271.5	272.0	270.4	271.0	264.0	270.3	264.4
L5	256.5	256.5	257.0	255.8	257.0	250.2	256.7	250.2
L6	214.0	215.0	204.0	214.0	215.25	225.0	215.0	225.0
LT1	314.5	314.0	314.5	314.5	314.5	314.0	314.0	314.0
LT2	324.5	326.0	325.5	325.0	326.75	329.0	325.5	329.0
LT3	308.0	309.25	308.5	307.5	309.5	318.0	309.0	318.0
LT4	259.5	267.0	260.5	259.0	262.25	270.0	262.0	270.0
K1	308.0	309.5	309.0	308.3	310.5	300.0	305.3	300.0
K2	304.5	306.5	306.0	305.0	307.3	306.6	302.4	306.6
K3	301.5	302.0	303.5	302.0	303.0	309.6	302.4	309.6
K4	305.0	307.5	305.2	304.3	308.5	303.6	300.4	303.6
K5	301.0	303.0	303.75	302.5	303.75	296.4	298.1	296.4
K6	302.0	302.0	303.0	310.5	302.0	294.0	296.4	294.0
K7	299.5	300.0	301.25	299.5	300.0	294.0	292.3	294.0
K8	295.0	295.0	296.0	293.5	295.5	294.0	289.2	294.0
K9	285.5	289.0	286.5	284.5	286.25	294.0	285.5	294.0
K10	278.0	280.0	280.25	278.5	280.75	289.7	279.7	289.7
K11	274.0	274.5	276.0	274.8	275.0	268.0	272.0	268.0
K12	262.0	257.0	257.0	257.0	247.0	240.0	261.0	240.0
R1	311.0	312.0	312.25	311.3	309.25	312.0	310.2	312.0
R2	291.0	295.25	292.0	291.3	292.0	297.0	292.0	297.0
R3	279.4	279.5	280.25	279.3	280.0	284.4	279.2	284.4
R4	270.5	271.0	272.0	270.5	271.0	264.0	271.0	264.4
R5	257.0	257.0	257.0	256.3	257.25	250.2	257.0	250.2
R6	214.0	215.0	204.0	214.0	215.25	225.2	215.0	225.0
RT1	314.5	315.0	314.0	314.3	314.0	314.0	313.5	314.0
RT2	325.25	326.5	325.0	325.0	326.0	329.0	325.5	329.0
RT3	308.5	309.0	309.0	307.5	308.5	318.0	308.2	318.0
RT4	260.0	260.0	260.5	259.5	259.75	270.0	259.0	270.0

NOTE: Dimensions are in inches.

TABLE 16. (Concluded)
Deployment Test Preflight Suspension Line Lengths
TWIN KEEL

Line No	Test Number							
	100T	101T	102T	103T	104T	105T	106T	107T
L1	247.9	251.5	256.0	253.8	253.5	259.9	251.5	253.9
L2	242.4	246.3	246.75	248.0	246.25	254.4	246.25	248.4
L3	237.0	241.3	244.75	242.8	252.5	249.0	241.25	243.0
L4	224.7	229.0	229.0	230.5	229.0	236.7	229.0	230.7
L5	201.5	210.3	213.5	212.5	212.5	218.9	210.25	206.5
L6	171.5	171.5	171.0	154.0	171.0	172.0	171.5	171.5
LT1	287.0	293.0	--	294.0	--	285.0	293.0	293.0
LT2	287.0	293.0	--	293.0	--	286.0	293.0	293.0
LT3	250.0	256.5	--	256.0	--	248.75	256.5	256.0
LK1	260.2	263.3	266.75	266.2	266.0	272.2	263.25	266.2
LK2	264.3	265.5	265.25	269.8	265.5	276.3	265.5	270.2
LK3	262.9	264.3	264.0	268.0	264.25	274.9	264.25	268.9
LK4	260.2	261.8	261.75	265.0	261.75	272.2	261.75	266.2
LK5	260.2	262.0	262.0	264.8	262.0	272.2	262.0	266.2
LK6	260.2	261.8	262.0	264.8	261.75	272.2	261.75	266.2
LK7	258.5	259.0	261.75	263.3	262.5	269.5	259.0	263.5
LK8	257.5	259.3	258.75	263.0	259.25	269.5	254.25	263.5
LK9	256.1	257.5	258.0	262.3	257.5	268.1	257.5	262.1
LK10	253.3	254.8	254.25	259.5	254.75	265.3	254.75	259.3
LK11	247.9	249.0	248.75	254.3	249.0	259.9	240.0	253.9
LK12	248.0	250.0	264.25	260.8	260.75	259.9	250.0	253.9
RK1	260.2	263.3	264.0	266.0	263.25	272.2	263.25	266.2
RK2	264.3	265.0	266.0	270.0	265.0	276.5	265.0	270.3
RK3	262.9	263.5	263.75	268.5	263.5	274.9	263.5	268.9
RK4	260.2	261.5	261.0	266.5	261.5	272.2	261.5	266.2
RK5	260.2	261.8	261.5	266.0	261.75	272.2	261.75	266.2
RK6	260.2	261.5	261.5	266.0	261.5	272.2	261.5	266.2
RK7	258.5	259.0	259.0	263.5	259.0	269.5	259.0	263.5
RK8	257.5	259.3	258.5	264.0	259.25	269.5	259.25	263.5
RK9	256.1	258.0	257.5	262.0	258.0	268.1	258.0	262.1
RK10	253.3	254.5	254.75	259.5	254.5	265.3	254.5	259.3
RK11	247.9	248.8	249.25	253.3	248.75	259.9	248.75	253.4
RK12	248.0	250.0	260.0	261.0	259.25	259.9	250.0	253.9
R1	247.9	251.5	255.5	254.5	215.5	259.9	251.5	253.9
R2	242.4	246.3	246.5	248.0	246.25	254.4	246.25	248.4
R3	237.0	241.3	241.0	243.0	241.25	249.0	241.25	243.0
R4	224.7	228.5	227.5	230.0	228.5	236.7	228.5	230.7
R5	201.5	210.3	211.0	212.3	210.25	218.9	210.25	206.5
R6	171.5	171.5	171.0	154.5	171.0	172.0	171.5	171.5
RT1	287.0	293.0	--	293.5	--	285.5	293.0	293.0
RT2	287.0	293.0	--	293.0	--	285.5	293.0	293.0
RT3	250.0	256/5	--	256.0	--	284.75	256.5	256.0

NOTE: Dimensions are in inches

Single Keel Reefing System, Version I

In stage one, all suspension lines were rigged to a length equal to the length of the tip suspension lines. The trailing edges were gathered, and a two-stage reefing line was routed around each side of the wing. The reefing lines ran along the keel and the leading edges to form two separate lobes.

Figure 73 shows the layout of the reefing lines with the wing reefed for the first stage. The disreef sequence was as follows:

1. First stage reefing line cut to allow inflation to the limits of the second stage reefing lines.
2. Second stage reefing lines cut to free leading edges and keel.
3. Trailing edge gathering line cut to allow full inflation of the canopy.
4. Suspension lines released to flying configuration lengths.

Single Keel Reefing System, Version II

In stage one all suspension lines were rigged to a length equal to the length of the tip suspension lines. The trailing edges were gathered, the keel was gathered, and reefing lines were run along each leading edge to form two separate lobes.

Figure 74 shows the layout of the reefing lines with wing reefed for first stage. The disreef sequence was as follows:

1. First stage reefing lines cut to free leading edges of the wing. Keel and trailing edges remained constrained.
2. Second stage reefing lines cut to free the keel.

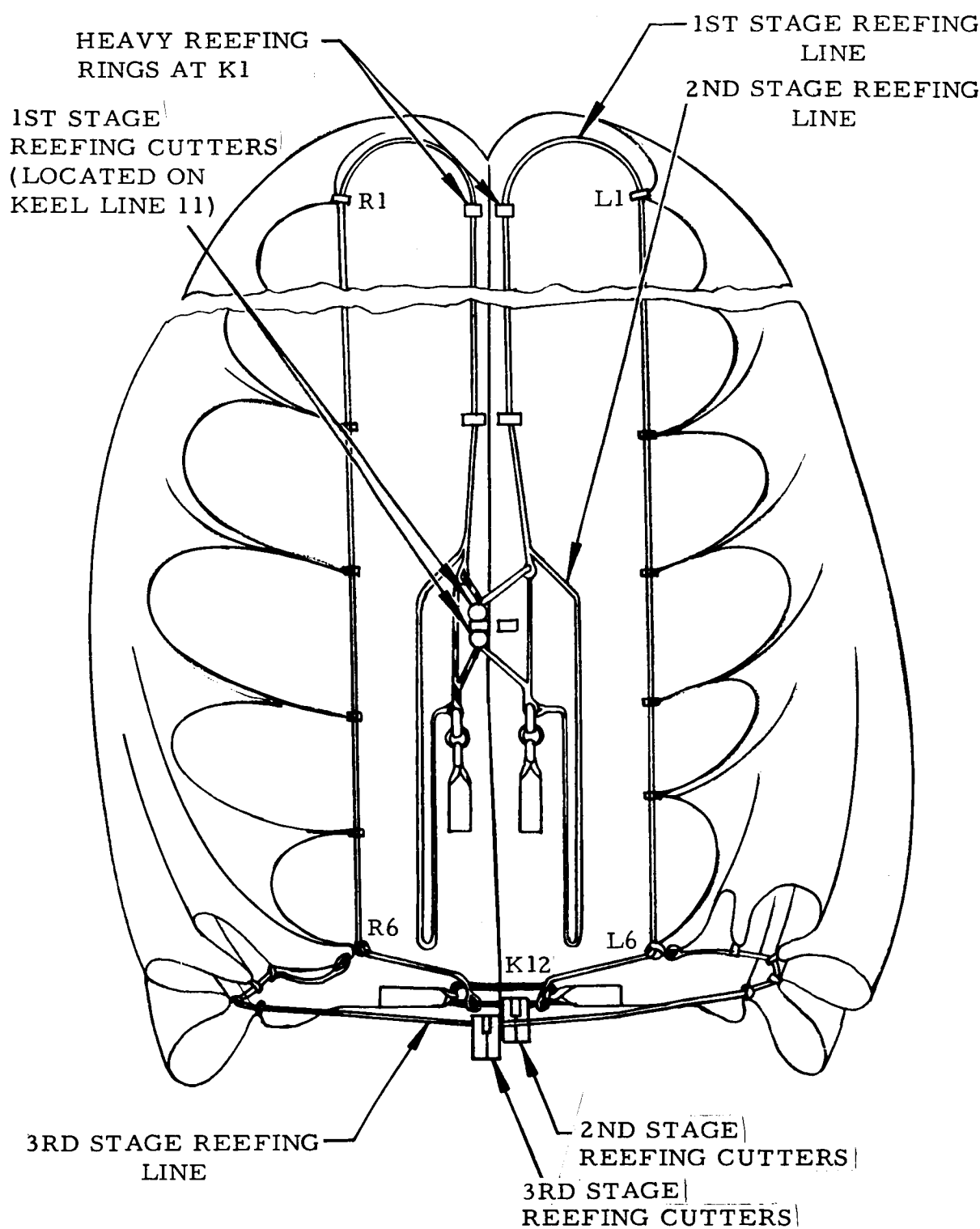


Figure 73. Schematic of Single Keel Reefing Version I

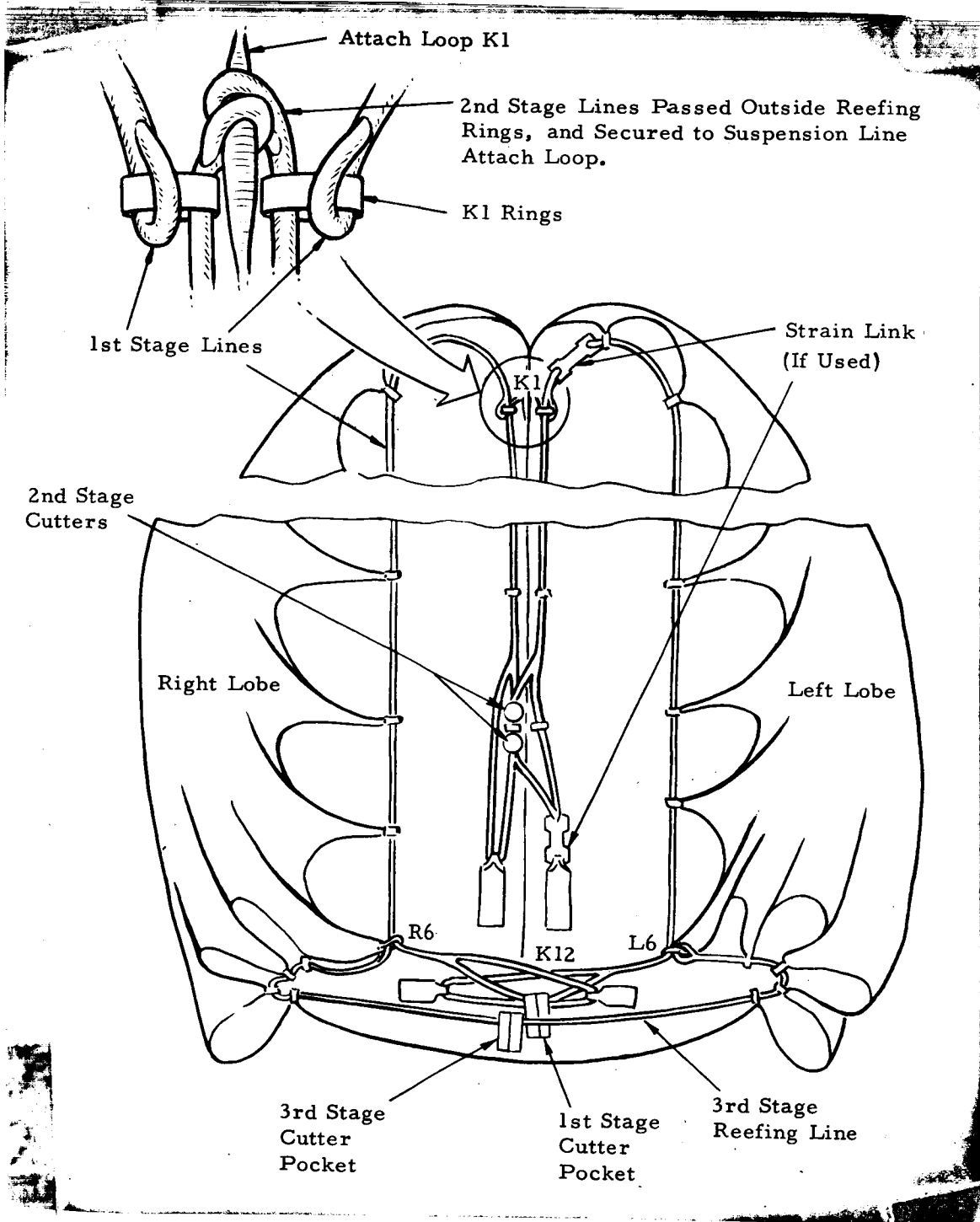


Figure 74. Schematic of Single Keel Reefing Version II

3. Trailing edge gathering line cut to allow full inflation of the canopy.
4. Suspension lines released to flying configuration lengths.

Single Keel Reefing System, Version III

In stage one all suspension lines were rigged to a length equal to the length of the tip suspension lines. The left and right lobes were reefed separately. The trailing edges were gathered. The keel and leading edge from the front end of the keel to the second leading edge suspension line on each side were gathered. Reefing lines were run from the second leading edge line through the reefing ring at the tip suspension line on each side of the canopy and terminated at the aft keel suspension line. Figure 75 shows the layout of the reefing lines with the wing reefed for first stage. The disreef sequence was as follows:

1. First stage reefing lines cut to allow leading edges from the second suspension line to the tip to inflate on each side. The leading edges from the front end of the keel to the second suspension line on each side, the keel and the trailing edges remained constrained.
2. Second stage reefing lines cut to completely release leading edges and keel.
3. Trailing edge gathering line released to allow full inflation of the canopy.
4. Suspension lines released to flying configuration lengths.

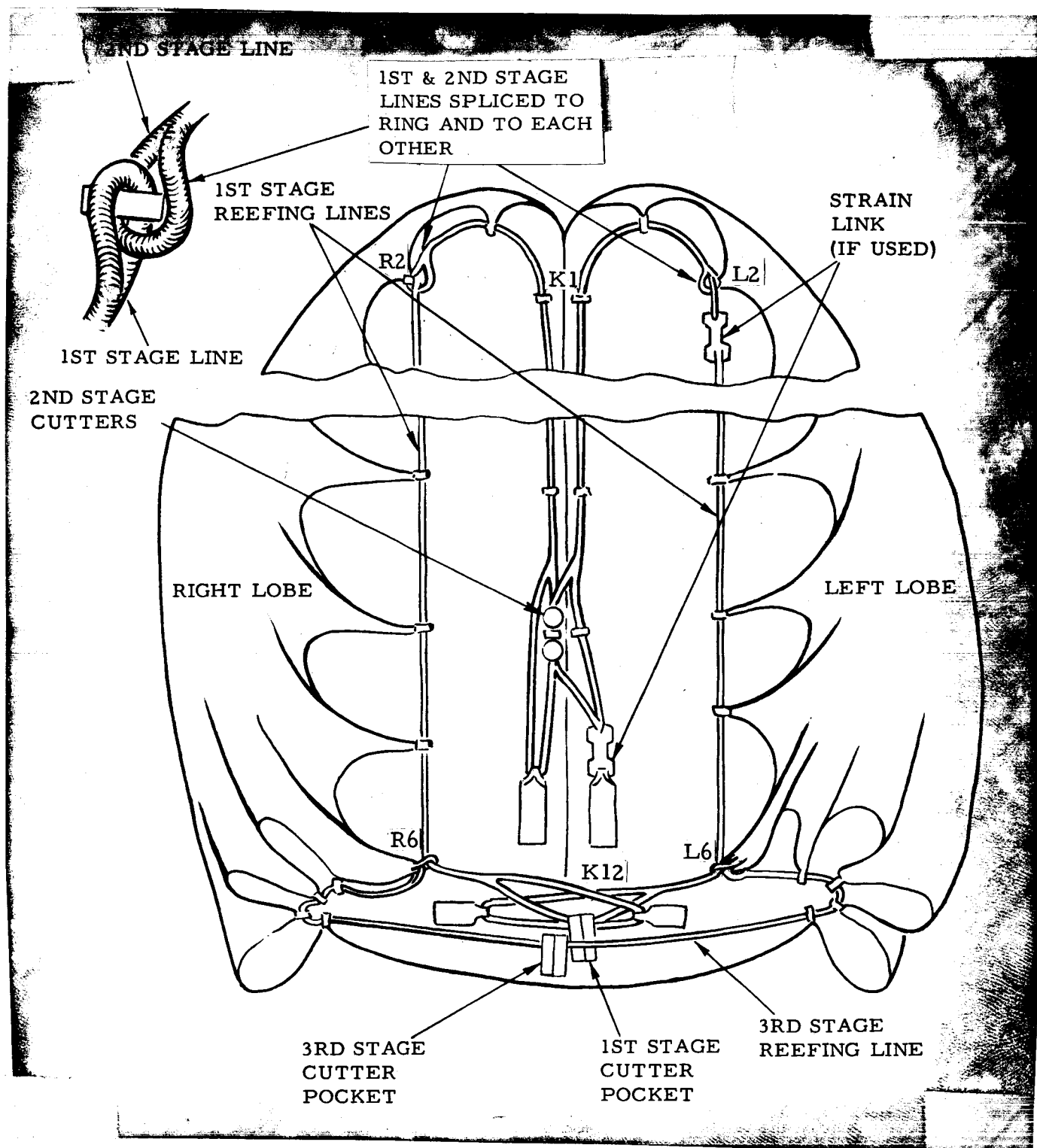


Figure 75. Schematic of Single Keel Reefing Version III

Twin Keel Reefing System, Version I

In stage one, all suspension lines were rigged to a length equal to the length of the tip suspension lines. The trailing edges were gathered, and three reefing lines were routed around the leading edges and keels to form three separate lobes. Figure 76 shows the layout of the reefing lines for Stage one. The disreef sequence was as follows:

1. First stage reefing lines cut to completely free the leading edges of the two outboard lobes.
2. The second stage reefing line cut to free the center lobe leading edge and keels.
3. Trailing edge gathering line cut to allow canopy to completely inflate.
4. Suspension lines released to flying configuration lengths.

Twin Keel Reefing System, Version II

In stage one, reefing was the same as used in reefing Version I. The difference between reefing Versions I and II was in the disreef sequence. The disreef sequence for reefing Version II was as follows:

1. First stage reefing lines cut to free the leading edges of the two outboard lobes. The keel and trailing edges remained constrained.
2. The second stage reefing line was cut to free the center lobe leading edge and the keels.
3. Suspension lines released to flying configuration lengths.
4. Trailing edge gathering line cut to allow canopy to completely inflate.

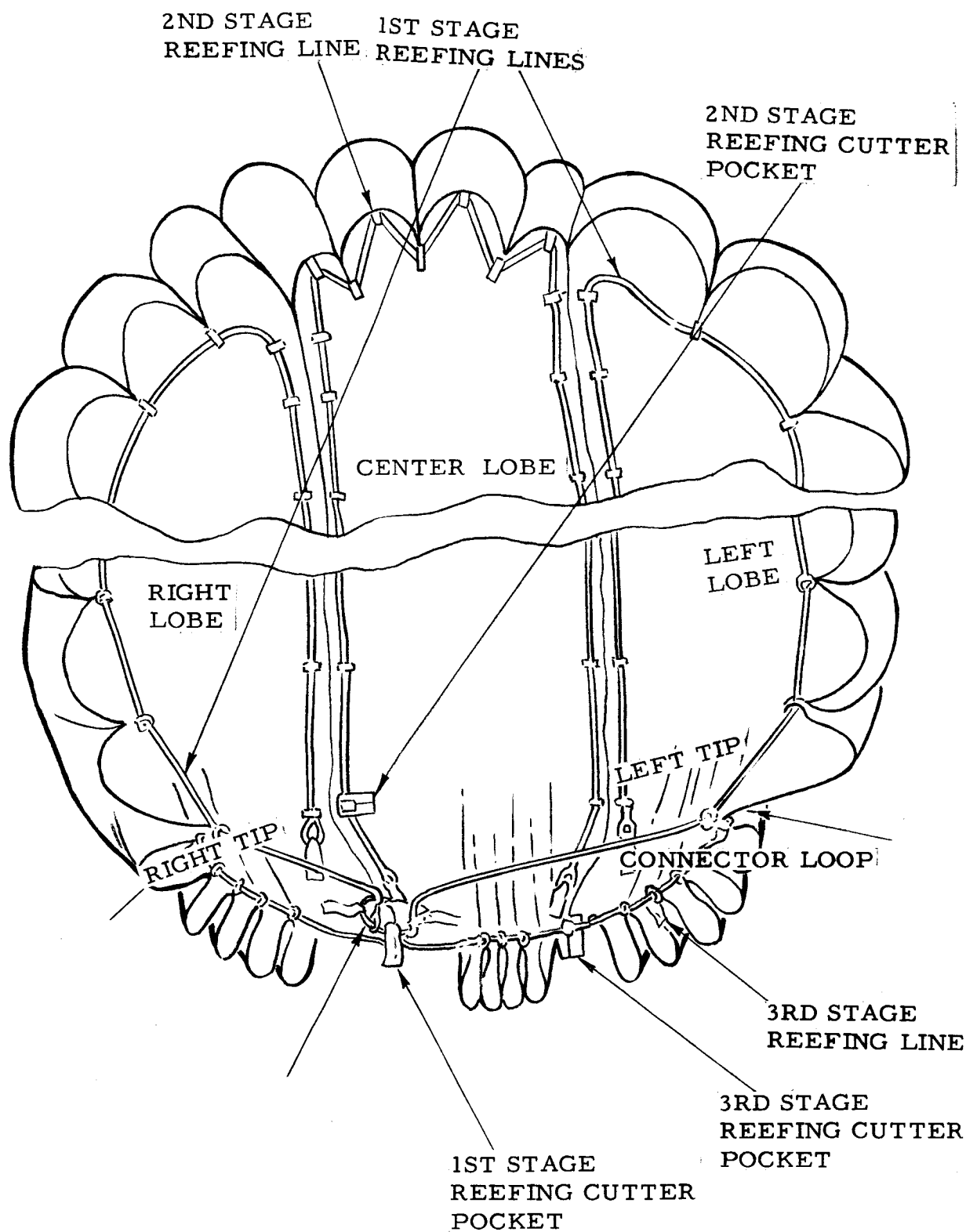


Figure 76. Twin Keel Reefing Line Arrangement

VARIATIONS IN REEFING SYSTEMS USED DURING DEPLOYMENT TESTS

The following paragraphs discuss the changes made to the reefing systems during the test program and the reasons for the changes. The reefing systems discussed are described in the preceding section of this report. Conditions for the tests discussed are given in Tables 17 and 18.

Single Keel Parawing Deployment Tests

The first two deployment tests with the single keel parawing were a verification test at El Mirage Dry Lake and Test No. 104S at El Centro. The reefing method used for these tests was single keel reefing Version I. During both of these tests, a mechanical problem was encountered in deploying the stowed portion of the second stage reefing lines. Subsequent bench tests showed that the first stage reefing line was being inadvertently locked in place by the bunching of reefing rings along the keel. This prevented reefing line payout when the reefing line cutters fired. To solve this problem, reefing Version II was devised.

Tests 102S and 103S were conducted with reefing Version II. This reefing method gave satisfactory operation, except that the second and third stage opening loads were not balanced. The second stage loads were higher than desired, and the third stage loads were lower than the maximum allowable. Therefore, reefing Version III was adopted and employed in Tests 101S and 100S. Although this reefing method was marginally successful in reducing the second stage loads, there was an unacceptable increase in third stage loads. Also, reefing Version III produced a longitudinal pitch oscillation during the second stage. With this method of reefing, the two lobes formed during Stage 2 could inflate unsymmetrically. This in turn induced a spin and attendant problems in the transition to Stage 3 of the reefing

Table 17. Single Keel Deployment Tests

Sequence No.	Test No.	Line Stretch Deployment Conditions				Model Config.	Objective	Reeling System	Comments on Test
		q (psf)	Alt (ft)	W (lbs)	PInd.	Act.			
1	E1 Mirage						Basic Plus TE Lines	System verification	1st Version
2	104S	50.8	53.9	3,000	3,066	254	252.8	Basic Plus TE Lines	Scale W = 5,000 lbs S = 4,000 sq ft h = 18,000 ft q = 100 psf
3	102S	36	38.5	3,000	3,174	254	257.2	Basic Plus TE Lines	Scale W = 5,000 lbs S = 4,000 sq ft h = 18,000 ft q = 70 psf
4	103S	50.8	50.4	3,000	2,900	254	247.5	Basic Plus TE Lines	Scale W = 5,000 lbs S = 4,000 sq ft h = 18,000 ft q = 100 psf
5	101S	38.0	39.6	12,500	13,200	190	210.0	Basic Plus TE Lines	Scale W = 5,000 lbs S = 4,000 sq ft h = 18,000 ft q = 100 psf
6	100S	38.0	41.63	12,500	12,880	190	210.8	Basic Plus TE Lines	Scale W = 5,000 lbs S = 4,000 sq ft h = 18,000 ft q = 70 psf
7	106S	70	79.7	18,000	18,541	500	500.3	Basic Plus TE Lines	Verify deployment capability for W = 500 lbs S = 400 sq ft h = 18,000 ft q = 100 psf
8	105S	50.8	47.9	3,000	3,204	254	255.9	Basic Plus TE Lines	Scale W = 5,000 lbs S = 4,000 sq ft h = 18,000 ft q = 100 psf
9	107S	100	87.8	18,000	19,390	500	493.9	Basic Plus TE Lines	Verify deployment capability for W = 500 lbs S = 400 sq ft h = 18,000 ft q = 100 psf

Table 18. Twin Keel Deployment Tests

Sequence No.	Test No.	Line Stretch Deployment Conditions						Model Config.	Objective	Reeling System	Comments on Test
		PInd.	q [psf]	Alt (ft)	W (lbs)	PInd.	Act.				
1	E1 Mirage							Basic	System Check Out	1st Version	All stages except line transfer functioned properly. Line transfer retention loops were improperly rigged causing only partial release of lines.
2	102T	36	39.75	3,000	2,800	254	254.2	Basic	Scale W = 5,000 lbs S = 4,000 sq ft h = 18,000 ft q = 70 psf	2nd Version	Stages 1, 2, & 3 functioned properly. Stage 4 and Stage 5 occurred so close together that it was not possible to evaluate functioning of stage four. Stable glide with left turn of approximately 11 deg/sec.
3	104T	50.8	59.7	3,000	2,707	254	254.2	Basic	Scale W = 5,000 lbs S = 4,000 sq ft h = 18,000 ft q = 100 psf	2nd Version	Stages 1, 2, and 3 functioned properly. Stage 4 inflation was unstable. Suspension line L1 did not release at line transfer because of tight retention loop. No valid gliding data.
4	103T	50.8	50.1	3,000	3,101	254	254.0	Basic Plus TE Lines	Scale W = 5,000 lbs S = 4,000 sq ft h = 18,000 ft q = 100 psf	1st Version	All stages functioned properly. Wing stalled during gliding flight because of tip lines being rigged 17 inches too short.
5	101T	38	41.3	12,500	12,832	190	218.5	Basic Plus TE Lines	Scale W = 5,000 lbs S = 4,000 sq ft h = 18,000 ft q = 100 psf	1st Version	All stages functioned properly. Wing glided with turn rate of approximately 6 deg/sec
6	100T	38	40.6	12,500	10,883	190	220.6	Basic Plus TE Lines	Scale W = 5,000 lbs S = 4,000 sq ft h = 18,000 ft q = 100 psf	1st Version	All stages occurred as planned. Oscillation of instrumentation mass induced high peaks in first stage total load. Wing glided with turn rate of approximately 10 deg/sec.
7	106T	70	74.12	18,000	18,600	500	502.4	Basic Plus TE Lines	Verify deployment capability for W = 500 lbs S = 400 sq ft h = 18,000 ft q = 70 psf	1st Version	All stages occurred as planned. Wing glided with turn rate of approximately 7 deg/sec.
8	105T	50.8	51.1	3,000	3,380	254	255.8	Basic Plus TE Lines	Scale W = 5,000 lbs S = 4,000 sq ft h = 18,000 ft q = 100 psf	1st Version	All stages occurred as planned. Wing glided with turn rate at approximately 2.5 deg/sec. All lines but tips extended 6 inches
9	107T	100	95.3	18,000	19,493	500	498.7	Basic Plus TE Lines	Verify deployment capability for W = 500 lbs S = 400 sq ft h = 18,000 ft q = 100 psf	1st Version	Line transfer on one side failed to occur because of broken wires on release mechanism

sequence. Therefore, this reefing version was abandoned, and Version II was used for the remainder of the single keel deployment tests.

Twin Keel Parawing Deployment Tests

The first twin keel deployment test was conducted at the El Mirage Dry Lake test site to verify proper functioning of the reefing system. For this test, twin keel reefing Version I was used. During this test, two anomalies were noted. The first was an aerodynamic stability problem. During fourth stage, the wing attempted to glide forward at an angle of attack that caused the nose to collapse. It appeared that canopy inversion or at best, extremely unstable canopy inflation would occur using this fourth stage configuration. The second anomaly was due to a misriggering of the line transfer mechanism which prevented suspension line transfer on one side of the wing. Inflation behavior and functioning of the reefing system was satisfactory for the first three stages of reefing.

Because of the instability during Stage 4 with reefing Version I, reefing Version II was used for subsequent Tests 102T and 104T. Reefing Version II was identical to reefing Version I, except that the times of activation for Stage 4 and line transfer were interchanged. The intent was to achieve stability during the fourth stage of the reefing sequence. During Test 102T, Stage 4 and line transfer occurred so close together that the stability during Stage 4 could not be evaluated.

During Test 104T using reefing Version II, staging occurred at the planned time intervals; however, this reefing configuration was unstable during the fourth stage. To solve this

problem, reefing Version I was reinstated with the addition of trailing edge lines on the outer lobes to stabilize canopy inflation during Stage 4. This reefing method was used successfully for all the remaining twin keel deployment tests.

DISCUSSION OF FLIGHT DEPLOYMENT TEST RESULTS

General Discussion of Parawing Behavior During the Reefing Sequence

In general, the free flight deployment tests provided qualitative results that agreed with the information that had been obtained during the wind tunnel deployment tests. As discussed earlier in the report, it was necessary to change the single keel parawing second stage reefing system and to add trailing edge suspension lines to the twin keel parawing. These, however, were not changes in the basic system delineated by the wind tunnel tests.

The change in single keel reefing was a change in the mechanics of obtaining the second stage reefed configuration and not a change in concept. Trailing edge lines were required on the twin keel parawing, because the wing attempted to glide at such a low angle of attack in the fourth stage that its leading edges collapsed. The trailing edge lines act to hold down the trailing edges of the side lobes. Also, they force the side lobes to both increase their drag and to fly at an increased angle of attack. The need for trailing edge lines on the twin keel parawing was not recognized during the wind tunnel tests, inasmuch as tether lines were used to confine the model to the tunnel test section. These lines restricted vertical and lateral movements of the models, and, therefore, masked the instability of the twin keel in the fourth stage when deployed without trailing edge lines.

Other than the difference described, flight behavior of the reefed parawing stages was the same as previously identified in the section on the Langley wind tunnel tests.

An interesting phenomenon occurred during Tests 106T, 107T, 106S and 107S. For these tests, an unstable condition developed during the first reefed stage. After the parawing was fully inflated in the first reefed stage, the test bomb went into a flat spin around the flight path axis. This motion developed from a small oscillation to a high rate of spin. The spin damped out when the first stage disreefed and second stage inflation occurred. This unstable condition may have been caused by the large mass of the line transfer cutters and suspension line load links which were located approximately one-third the distance from the test vehicle to the parawing. The mass appeared to be driven by small oscillations of the parawing and, in turn, coupled with the test vehicle to develop the spinning motion. This particular type of instability seemed to be peculiar to the five-hundred pound system tests, although relatively severe test vehicle oscillations were noted during Tests 100T and 100S conducted at 220 and 210 lbs, respectively. The oscillations during Tests 100T and 100S occurred during the first stage inflation process and damped out before first stage disreef. This oscillation phenomenon induced high peaks in the measured loads and invalidated the first stage peak opening force data for these two tests.

Bunching of the reefing rings and the canopy skirt band material physically limited the minimum reefing line length which could be used. Consequently, the lowest reefing ratio that could be tested was 0.116 for the single keel parawing and 0.153 for the twin keel parawing.

Opening Loads

Tables 17 and 18 list the flight deployment tests conducted. These tables also provide a summary of test conditions with remarks about test events.

Three types of tests were conducted during the deployment test program. These were:

1. Verification tests of the functioning of the reefing systems.
2. Scaling tests relating flight dynamics and deployment loads.
3. Verification tests to demonstrate the ability of the parawing structure to withstand deployment throughout the deployment envelope.

In order to gain a good understanding of relationships between small and large-scale models, the scaling tests were aimed at simulating test conditions for a 4000 square foot wing area with a total system weight of 5000 pounds. The primary objective of the structural tests was to verify the ability to deploy a 400 square foot parawing with a 500 pound system weight in the deployment envelope of 3000 feet to 18,000 feet at dynamic pressures from 30 to 100 psf.

Figures 77 and 78 show force and dynamic pressure histories for a typical single keel parawing deployment test and a typical twin keel parawing deployment test. These two tests, 105S and 105T were conducted with test conditions scaled to the previously listed intermediate scale test conditions.

A major objective of the scaling tests was to develop a reefing system which would limit peak accelerations during the opening sequence to 3.0 g's or less. Table 19 gives the peak loads measured during these deployment tests. The test

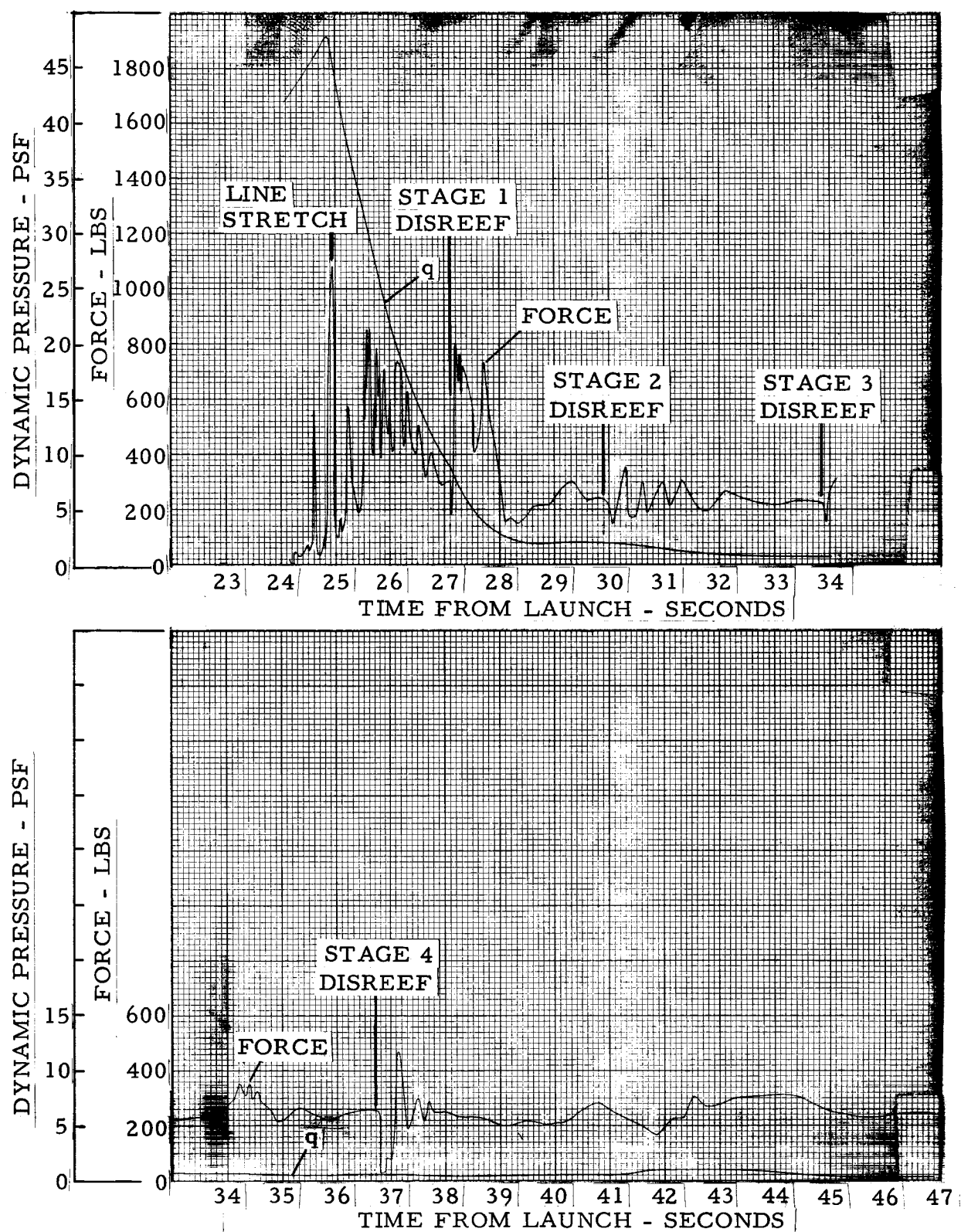


Figure 77. Force and Dynamic Pressure Histories for a Typical Single Keel Parawing Deployment Sequence (Test 105S)

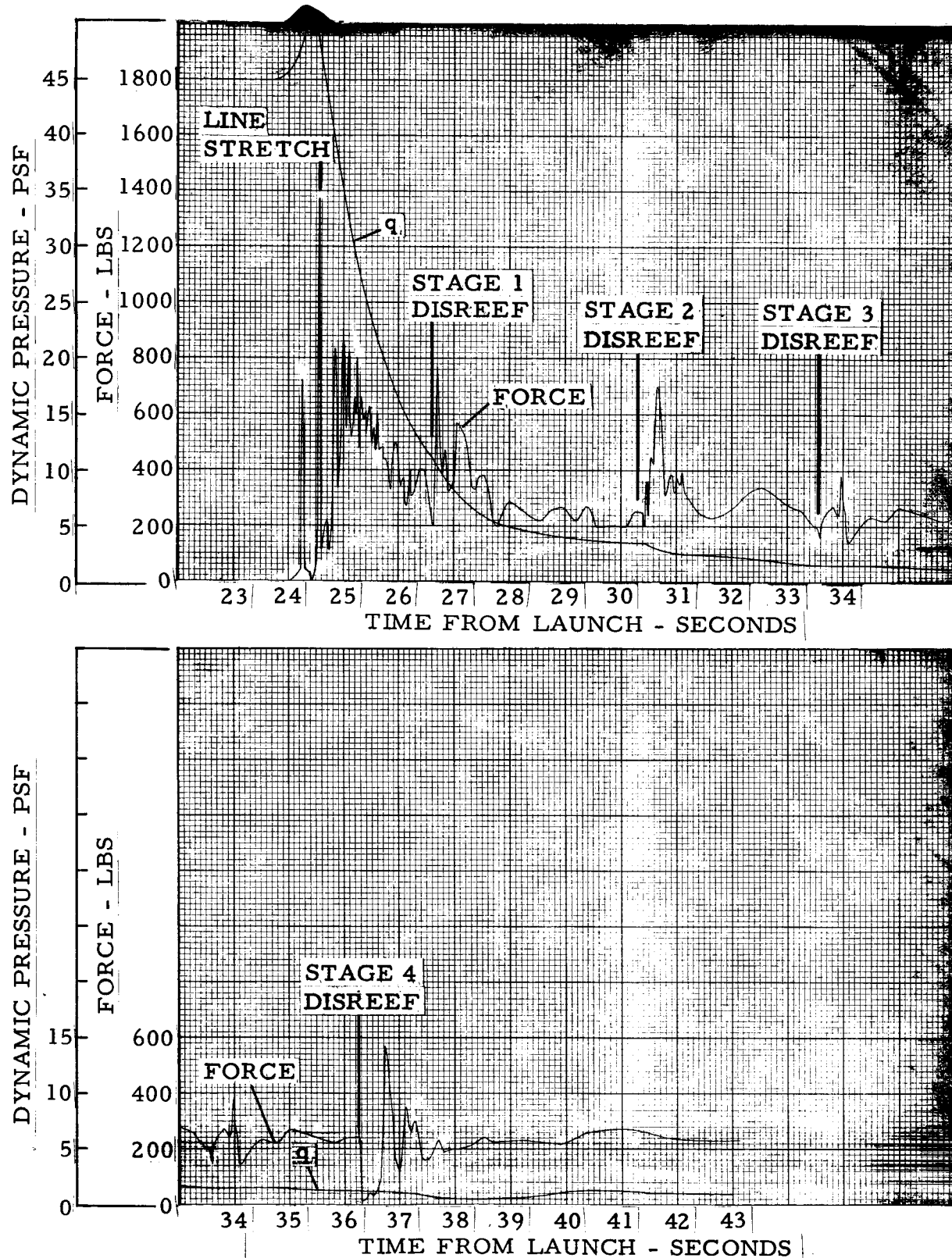


Figure 78. Force and Dynamic Pressure Histories for a Typical Twin Keel Parawing Deployment Sequence (Test 105T)

Table 19. Summary of Small Scale Deployment Data

T	q ₁₀	q ₁ (1)	G ₁ (C _D ^S _W) ₁	q ₂	G ₂ (C _D ^S _W) ₂	q ₃	G ₃ (C _D ^S _W) ₃	q ₄	G ₄	
105	120	39.6	NG	43	6.7	3.5	60	3.2	290	1.2
116	41.6	4.0	34	6.8	3.2	62	3.1	3.9	220	0.7
156	38.5	3.9	NA	5.9	3.5	NA	1.8	2.2	NA	0.5
141	50.4	5.8	40	7.5	3.7	119	2.3	2.6	200	1.0
201	53.9	4.3	41	-	-	NA	6.7	5.0	277	0.7
120	47.9	4.02	42	9.0	3.6	125	2.0	1.6	240	0.8
116	79.7	5.8	41	13.0	NG	119	4.5	1.81	230	2.6
116	87.8	4.9	38	17.0	3.4	120	4.2	1.9	250	2.0
age				40		61 (2) 121 (3)	244			
167	40.6	NG	30	7.3	3.6	70	2.9	2.6	220	1.9
156	41.3	4.2	35	7.1	3.6	50	4.4	3.2	120	2.0
219	39.7	4.4	42	6.6	2.3	62	4.1	2.3	170	1.3
167	50.1	3.9	35	11.4	3.4	65	4.0	3.3	110	1.5
219	59.7	6.8	50	6.5	3.0	88	4.3	3.0	135	1.1
241	51.1	4.04	NA	10.6	3.4	NA	3.6	3.1	-	1.4
153	74.1	3.6	40	15.3	3.4	72	7.5	3.1	170	3.5
153	95.3	5.3	45	13.7	2.9	70	7.9	3.1	130	4.3
age				40		68				
									151	

1) Subscripts denote deployment stages.

2) Applies for tests 100S and 101S.

3) Applies for tests other than 100S and 101S.

NG Indicates data not valid.

NA Indicates data not available.

parameters and test data shown in this table are as follows:

G = Peak deceleration ratio during each stage,
relative to earth gravity

$C_D S_W$ = Steady state drag area during a given stage in
square feet

q = Dynamic pressure at the start of the inflation
of a given stage, i.e., line stretch for stage one
and disreef of the previous stage for all sub-
sequent stages.

$C_D S_W$ for parawing reefing stages four and five are not shown.

The system glided during these stages; therefore, $C_D S_W$ during
the gliding mode is not a relevant parameter with respect to
the opening process.

A load factor (C_K) was used to correlate the loads data.
This factor is defined as:

$$C_K = \frac{G W_t}{C_D S_W q} \quad (1)$$

C_K relates the actual measured opening force to a reference
drag area of the parawing, the mass of the system, the velocity
of the system at the start of the reefing stage under consideration,
and the density of the air through which the system is moving.

C_K is the ratio of the actual peak force during an opening process
to the force that would have been generated, had there been no
velocity decay during the opening process and had the force been
equal only to the product of drag area and dynamic pressure.

C_K is a convenient parameter for comparing results of tests in
which there are only small variations between nominal and actual
test conditions. Reference 8 by Waters discusses C_K and gives
one approach to its use in computing opening loads.

The data necessary to compute C_K are given in Table 19. The
load factors computed from these data tabulated in Table 20.

Table 20. Summary of Load Factor Data |

Test No.	1st Stage Reefing Ratio	Reefing Version	Load Factor - C _K				
			Stage 1	Stage 2	Stage 3	Stage 4	Stage 5
100S	.120	3rd	-	1.80	-	.75*	3.03*
101S	.116	3rd	.50	1.62	1.08	1.27*	1.35*
102S	.156	2nd	.65	1.25*	1.26*	1.80*	2.44*
103S	.141	2nd	.71	1.01*	1.16*	.93*	-
104S	.201	1st	.50	-	.79	1.26*	2.27*
105S	.120	2nd	.54	.85*	.85*	1.27*	2.13*
106S	.116	2nd	.91	-	.84	.90	-
107S	.116	2nd	.69	.82	.92	.87	2.1
Average (1)				1.04	1.09	1.21	2.24
100T	.167	1st	-	1.57*	1.28*	.74*	2.39*
101T	.156	1st	.55	1.61*	1.04*	.40*	2.42*
102T	.219	2nd	.70	1.30*	1.10*	-	-
103T	.167	1st	.49	1.11*	1.39*	.97*	3.81*
104T	.219	2nd	.73	1.73*	1.18*	-	-
105T	.141	1st	.51	1.21*	1.46*	.73*	1.28*
106T	.153	1st	.61	1.64	1.38	.75	2.01
107T	.153	1st	.69	1.55	1.30	.49	-
Average (1)				1.42	1.24	.71	2.48

(1) Averages based on scale tests identified by *.

Inherent limitations in ASKANIA phototheodolite measurements of space position, velocity, and acceleration during periods of rapid velocity change make computation of steady state drag areas difficult. Therefore, in the calculation of C_K for stages one, two, and three, average values of C_{DSW} , based on the results of all applicable tests, were used. The balloon-like inflation of the first stage provided a drag area for the first stage that was relatively independent of the reefing ratio used. The drag area of the second and third stages was dependent only on the geometry of the reefed parawing.

The average drag area during the first stage was 40 sq ft, both for the twin keel and the single keel parawings. Based on a 400 square foot wing area, a drag coefficient, C_D , of 0.10 was used. For stages four and five, a value of C_{RSW} of 400 square feet and a resultant force coefficient, C_R , of 1.0 were assumed. For these stages, C_K was computed by the equation:

$$C_K = \frac{G W_t}{C_R S_W q}$$

Figure 79 shows a plot of the load factors obtained during stage one of the scaled tests. Load factor is plotted as a function of first stage reefing ratio for both the twin and the single keel scaled deployment tests.

As shown in Figure 79, C_K tends to decrease as the reefing ratio was reduced. The only datum point widely at variance with the general trend is the value obtained from Test 104S. This test differed from the other tests in that the flight path angle was not vertical at the start of the inflation process. Also, there is some question as to the accuracy of the ASKANIA data obtained from this test.

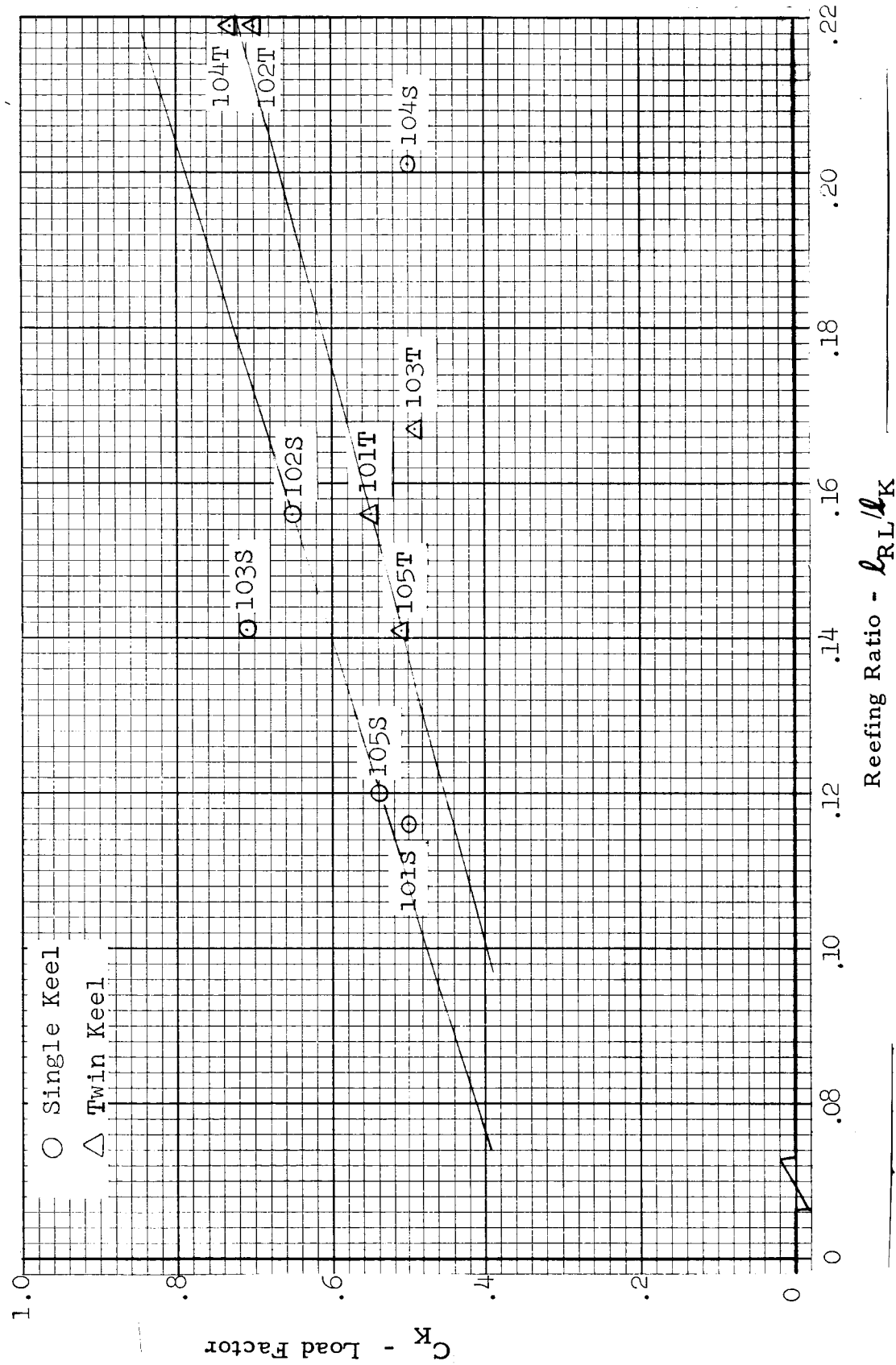


Figure 79. First Stage Load Factor (C_K) vs Reefing Ratio

During first stage the steady state drag coefficient remained constant over the range of reefing ratios tested. Therefore the decrease in C_K , as reefing ratio decreased, could be attributed to an increase in filling time.

Table 21 lists the first stage filling times obtained during the deployment tests. Both the times to maximum projected diameter and to peak first stage load are shown. The data from two groups of tests allow identification of the effects of a single variable. The 103, 104, 105 groups of single and twin keel tests were made at approximately the same dynamic pressure, altitude and wing loading, with reefing ratio as the variable. In the 106 and 107 groups of single and twin keel tests, reefing ratio, altitude and wing loading were held constant, and dynamic pressure at parawing line stretch was varied.

Figure 80 presents plots of filling time versus the reciprocal of the reefing ratio squared for the 103, 104 and 105 group of single and twin keel parawing deployment tests. Filling times were obtained from motion picture film analysis. The filling times are based on the judgement of the data analyst who judges when maximum projected diameter occurs. Because the fully inflated condition is usually not clearly defined and judgement is required to interpret when it occurs, the accuracy with which inflation times can be determined from photographic coverage is limited. Figure 80 shows that filling time was a linear function of the inverse of the reefing ratio squared. This was the same type of behavior exhibited by the filling times measured during the wind tunnel deployment tests.

Figure 81 presents a plot of first stage opening load versus filling time, with opening load represented by the load factor, C_K . The expected relationship for similar test conditions is one in which C_K decreases with increasing filling time.

TABLE 21. Summary of First Stage Filling Time

<u>Test No.</u>	ℓ_{RL}/ℓ_K	$(\ell_{RL}/\ell_K)^2$	C_K	t_f Sec	t_{p1} Sec
100S	.120	69	(1)	1.25	(1)
101S	.116	74	.50	1.09	.45
102S (3)	.150	44	.65	1.20	.56
103S	.141	50	.71	1.06	.57
104S	.201	25	.50	0.60	.48
105S	.120	69	.54	1.72	.49
106S	.116	74	.91	1.20	.43
107S (3)	.116	74	.69	(2)	.75
100T	.167	36	(1)	(2)	(1)
101T	.156	41	.55	1.37	.59
102T (3)	.219	21	.70	0.57	.26
103T	.167	36	.49	0.87	.72
104T	.219	21	.73	0.43	.40
105T	.141	50	.51	1.14	.45
106T	.153	43	.61	0.92	.47
107T (3)	.153	43	.69	0.69	.38

- (1) Data invalid, because of large peaks in load data induced by test vehicle oscillation.
- (2) Motion picture data not readable.
- (3) Nylon suspension line models.

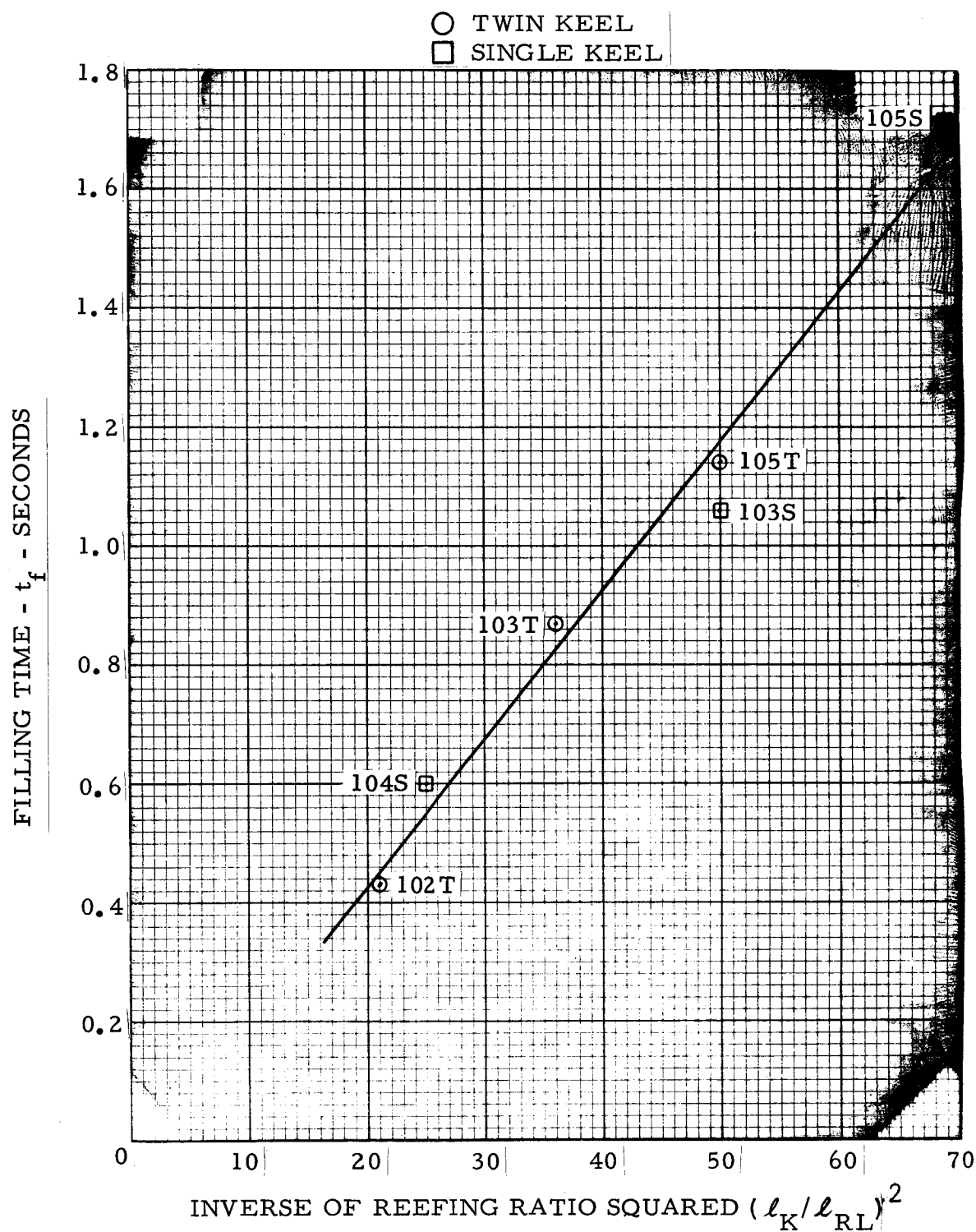


Figure 80. First Stage Filling Time vs. Inverse of Reefing Ratio Squared.

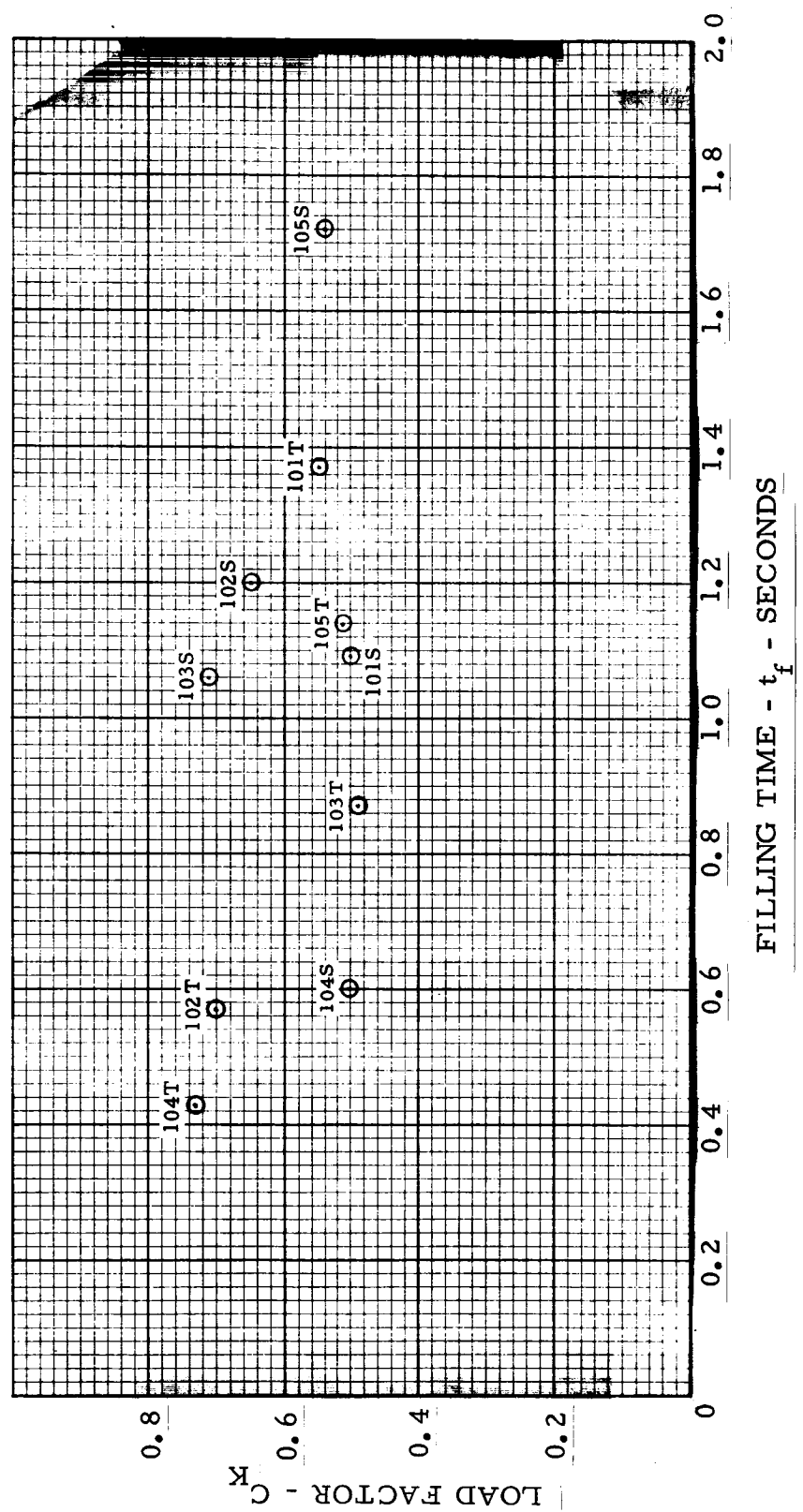


Figure 81. First Stage Load Factor (C_K) vs. Filling Time

Figure 81 confirms the expected trend. These data show considerable scatter which may be due to the randomness in the opening process or inaccuracies in the data acquisition process. As discussed previously, the determination of both C_K and filling time are subject to errors inherent in the data reduction methods. Combining the two sets of data, each of which have a large amount of scatter, accentuates the effect of scatter in the presentation.

Figure 82 shows the first stage filling time versus velocity at line stretch for twin keel Tests 106T and 107T and single keel Test 106S. The data indicate a decrease in filling time with an increase in velocity at line stretch.

Unlike stage one, comparable data is available from a number of tests for the inflation stages following stage one. This is because the reefing in the later stages was not changed from test to test. The twin keel parawing test in particular resulted in a repeatable set of data for stages two through five. In Table 20, the average C_K values shown are based on the data from the reefing system that appeared to perform best. This reefing system is identified as Number (3) in Table 6 and is described in the preceding section on reefing configurations. Table 20 shows the range of scatter in load factors for the later reefing stages. For example, the second stage data for the twin keel parawing shows an average C_K value of 1.42 for scale tests with maximum and minimum values of 1.73 and 1.11, respectively. This range is indicative of the repeatability of the twin keel second stage inflation process during the scale tests. Stage five shows large variations between the maximum and minimum load factors (C_K). To a great extent this variation is due to the inability of the ASKANIA phototheodolite system to accurately determine fourth stage end point dynamic pressure.

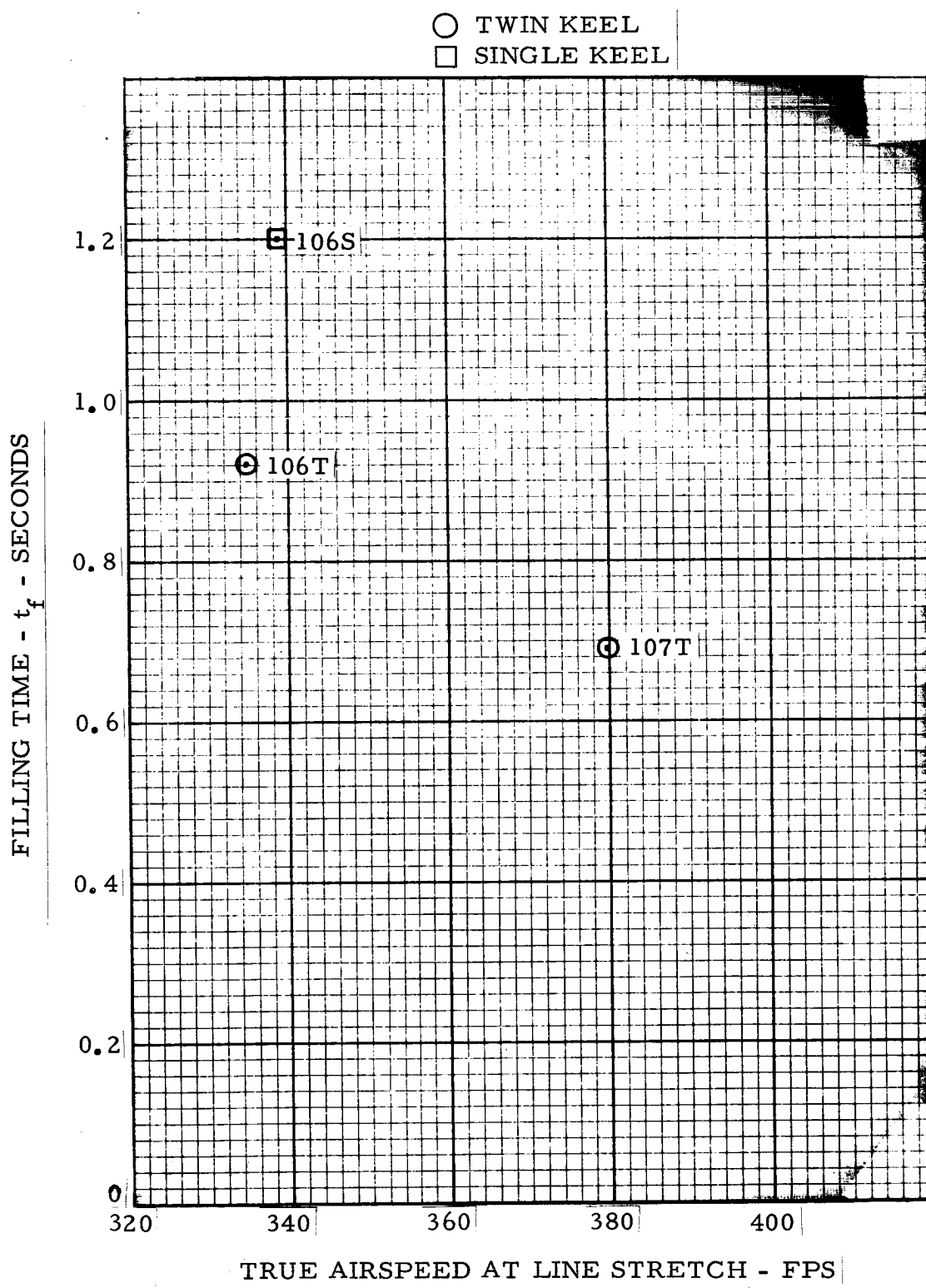


Figure 82. Filling Time vs. Line Stretch Velocity

This problem exists for all stages but causes a greater percentage error in the later stages where the velocity is lower.

Influence of Nylon and Dacron Suspension Lines on Deployment - Inflation Loads. - The models used for Tests 102T, 107T, 102S, and 107S had nylon suspension lines while the models used for all other deployment tests had dacron suspension lines. Because nylon has a lower spring constant than dacron, the deployment loads with nylon suspension line models could be possibly lower than the deployment loads with dacron suspension line models and equivalent test conditions. Table 20 shows no consistent pattern of lower loads for the nylon suspension line tests. The models had very high strength suspension lines relative to the loads applied to them. None of the lines stretched significantly; therefore, no effects on deployment loads were noted with either the dacron or nylon line models.

Parawing Geometry During the Opening Sequence

Figures 83 and 84 are sketches of the deployment sequence taken from on-board camera films. They show the projected plan-forms of the twin and single keel parawings during a typical disreefing sequence. The dimensions shown are in terms of ratio of the actual dimension to the reference keel length, ℓ_K .

Figures 85 and 86 present the projected-area time-histories during first stage inflation for typical twin and single keel deployment tests. The data are presented as ratios of the projected area at a given time to first stage fully inflated projected area. The area data are plotted against time in the form of a ratio of actual time for a given area to the time at which full inflation occurred for the stage.

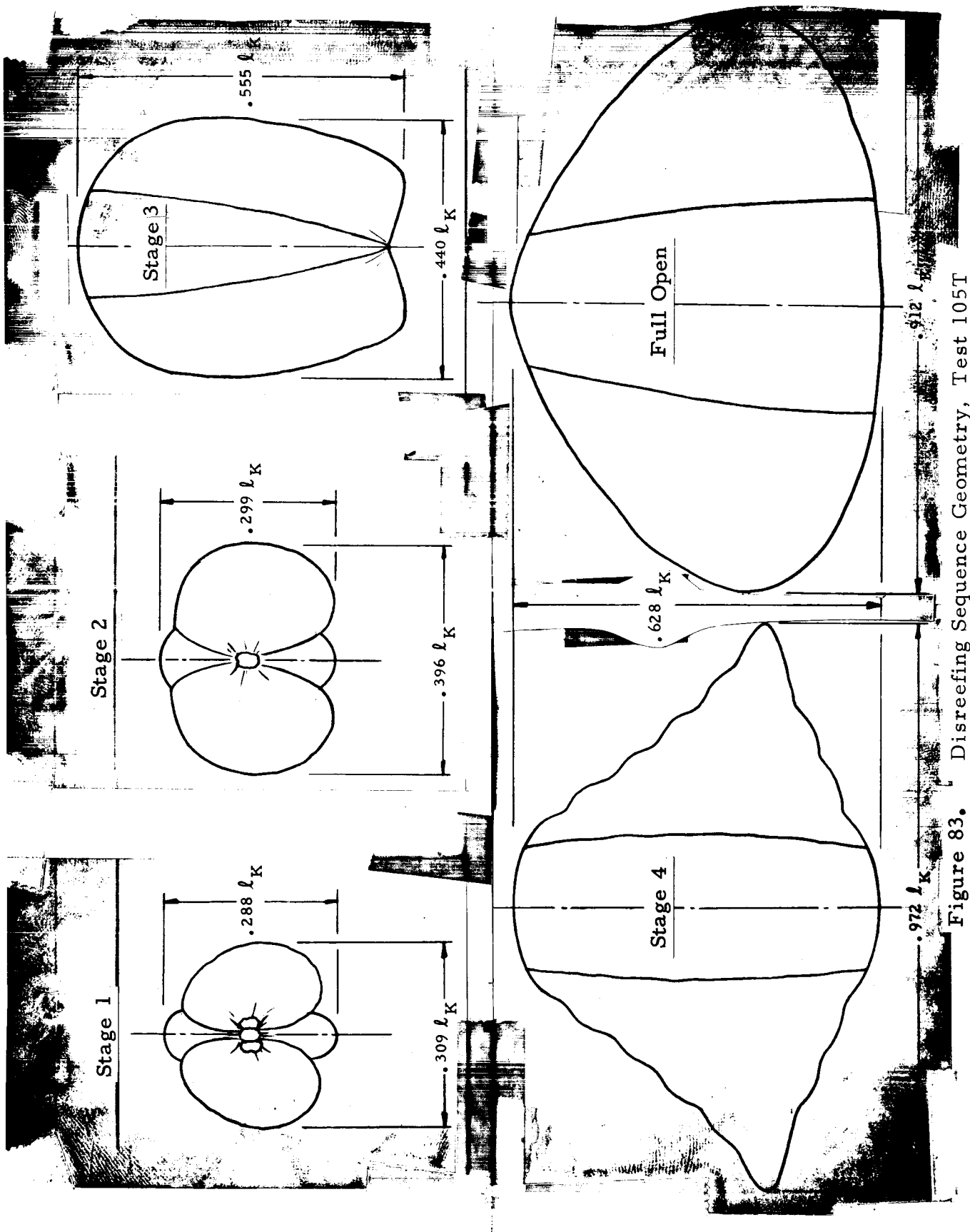


Figure 83. Disreefing Sequence Geometry, Test 105T

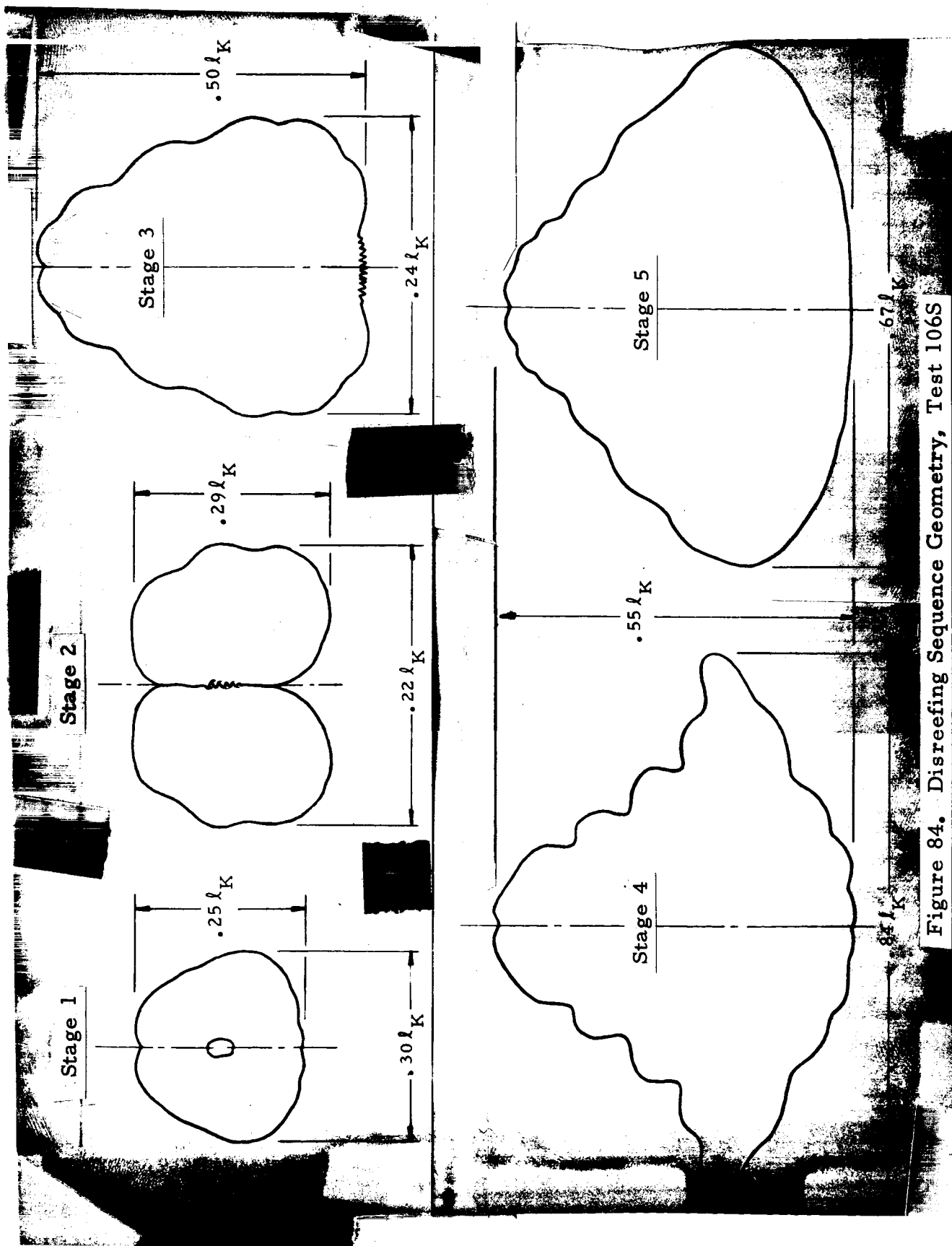


Figure 84. Disreefing Sequence Geometry, Test 106S

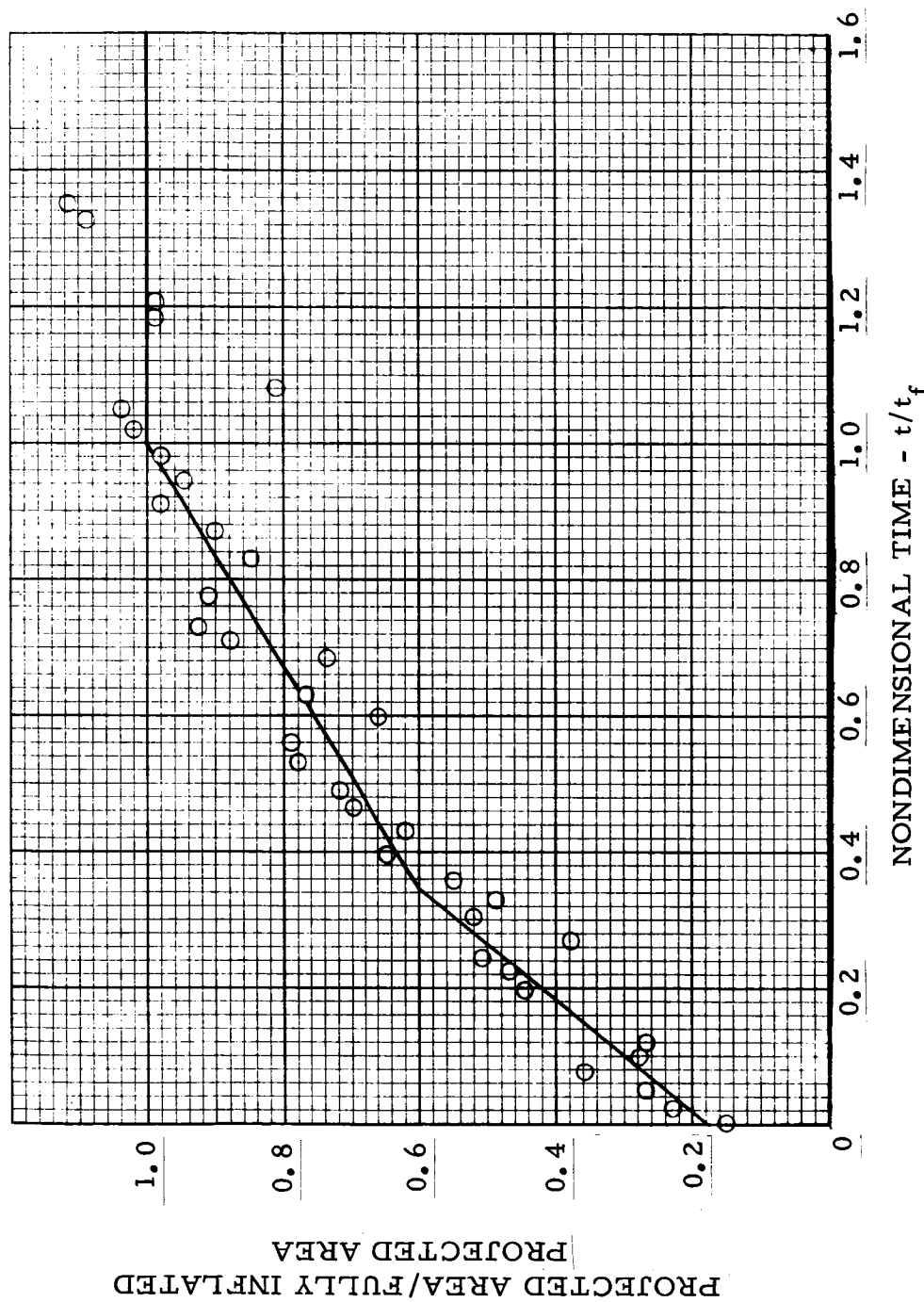


Figure 85. Drag-Area Ratio in First Reeved Stage vs. Time for Test 105 T

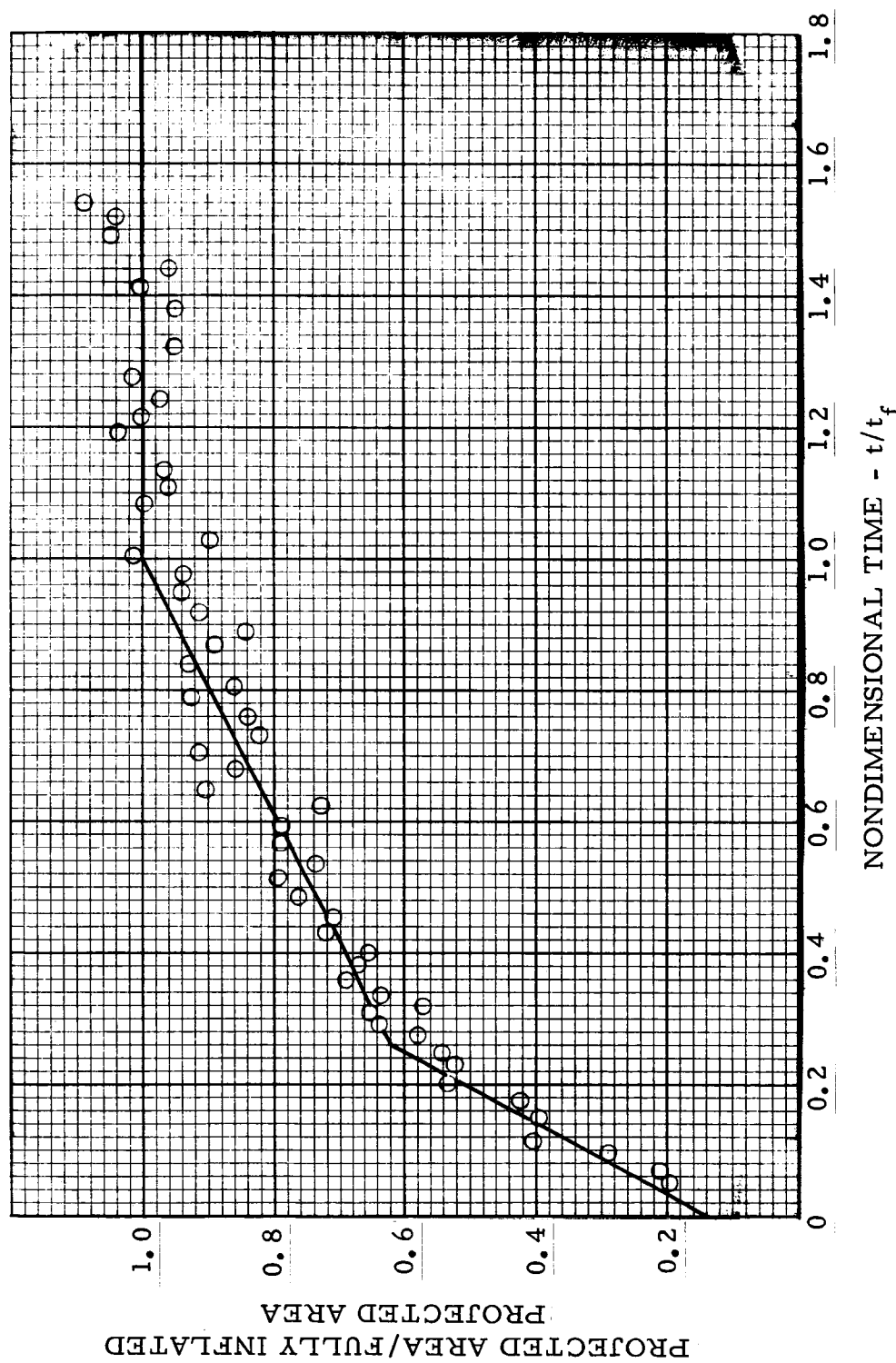


Figure 86. Drag-Area Ratio in First Reefed Stage vs. Time for Test 106 S

These data were obtained from measurements made with the on-board motion pictures. The scatter shown by the data is due both to actual fluctuations in the canopy projected area and inaccuracies in the measurement of the area. The data from both the single keel parawing and twin keel parawing indicate that the area-time history of the first stage inflation process can be simulated by two straight line segments. This is the same type of behavior that was shown during the Langley wind tunnel tests. The wind tunnel and the free flight data both showed that the change in slope occurs at an area ratio of approximately 0.6. However, the agreement between the wind tunnel data and free flight data is not as good with respect to the time at which the slope change occurs. The time to the slope change appears to be shorter for the free flight tests compared to the wind tunnel tests.

Predicted Loads for Hypothetical 5000 Pound System

With known drag areas and load factors for all stages of the opening process, peak accelerations for each stage of the opening process can be computed by assuming a percentage of terminal dynamic pressure reached in each stage. The equation used for these calculations is:

$$G_i = \frac{K_{i-1} (C_D S_W)_i C_{Ki}}{(C_D S_W)_{i+1}} \quad (2)$$

where

G_i = peak acceleration in Stage i

K_{i-1} = ratio of the dynamic pressure at the end of stage $i-1$ to the steady state dynamic pressure for stage $i-1$
 $(C_D S)_i$ = steady state drag area of stage i
 $(C_D S)_{i-1}$ = steady state drag area of stage preceding stage i
 C_K_i = load factor for stage i

A C_K of 0.38 corresponds to a 3 g first stage opening load for any set of conditions scaleable from the reference conditions of a payload weight, W_t , of 5000 lb, a wing area, S_W , of 4000 sq ft, a dynamic pressure, q , of 100 psf, and a test altitude, h , of 18,000 ft.

Figure 81 shows that this value was not attained during the test program. As discussed previously, the bunching of reefing rings and canopy skirt band material imposed a physical limit on the minimum reefing ratios that could be tested. Thus, for the lowest reefing ratios tested, a C_K value of approximately 0.5 was measured for both the twin and single keel parawings. Extrapolations of the data in Figure 79 indicate that the desired value of C_K equal to 0.38 would be achieved with reefing ratios of 0.070 for the single keel parawing and 0.094 for the twin keel parawing.

Table 22 lists predicted peak accelerations for stages two through five during a deployment of a 4000 sq ft parawing at 18,000 ft altitude with a dynamic pressure of 100 psf and a total system weight of 5000 lbs. As shown by this table, the twin keel model should meet the 3.0 g requirement for stages two through five, with the single keel model exceeding 3.0 g's in stage two.

Table 22. Intermediate Scale Opening Loads Predictions
Based on Small Scale Test Data

Single Keel ($W_t = 5000$ lbs, $S_W = 4000$ sq ft, $h = 18,000$ ft,
 $q = 100$ psf)

Stage	1	2	3	4	5
Average C_K	-	1.04	1.09	1.21	2.24
Average $C_D S_W$	40	120	244	400	400
Peak Acceleration	-	3.27	2.33	2.07	2.36

Twin Keel ($W_t = 5000$ lbs, $S_W = 4000$ sq ft, $h = 18,000$ ft,
 $q = 100$ psf)

Stage	1	2	3	4	5
Average C_K	-	1.42	1.24	.71	2.48
Average $C_D S_W$	40	68	151	400	400
Peak Acceleration	-	2.53	2.89	1.98	2.61

Note: A value of $K_i = 1.05$ was used for Stages 2, 3, 4, and 5.

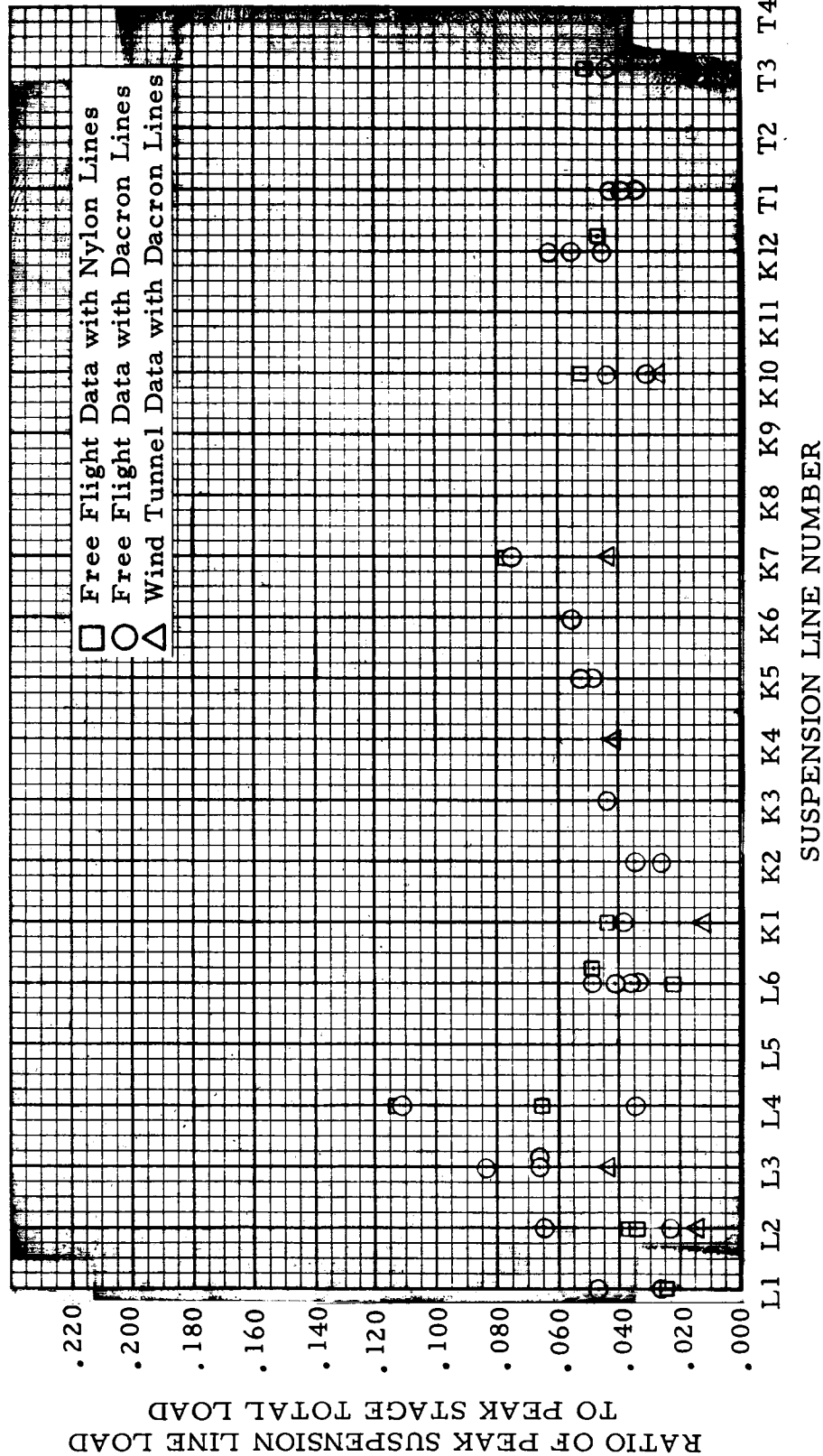
Suspension Line Loads

Figures 87 through 96 present the suspension line load data for the single keel and twin keel parawing tests. The data are presented as ratios of peak force in the suspension line to the maximum total opening force for each stage. The data shown are representative for reefing Version II for the single keel parawing and reefing Version I with trailing edge lines for the twin keel parawing.

As discussed previously, some of the models had dacron suspension lines while others had nylon suspension lines. Figures 87 through 96 differentiate between the data obtained for models with the different suspension line materials. The data in these figures show that there was no apparent difference in the measured suspension line load ratios because of suspension line material.

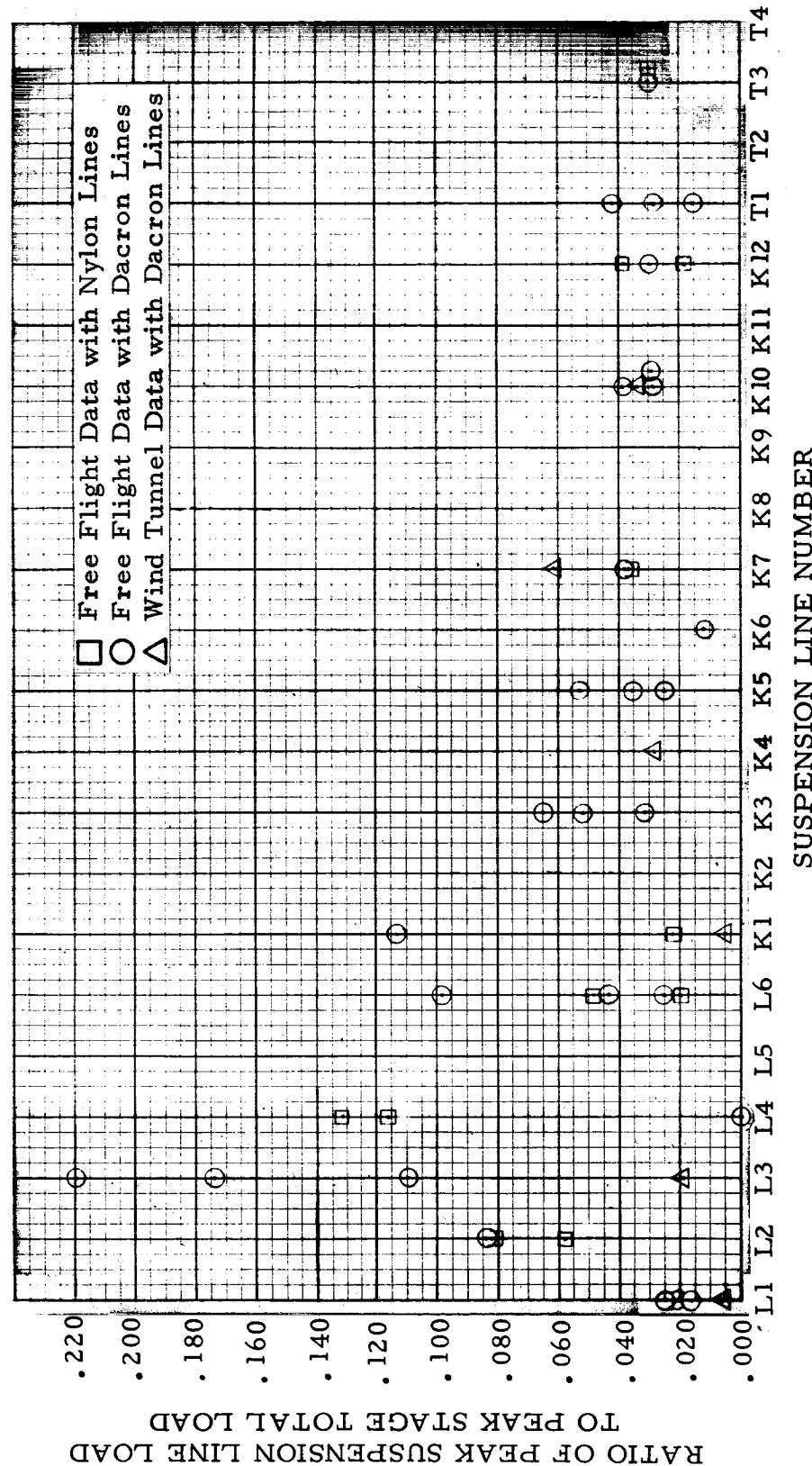
The data indicate large variations in the measured loads for particular suspension lines. Because of the random nature of the opening process of flexible wings such as the parawing, such variations are to be expected. Despite this, general trends of suspension line load distribution (related to location on the wing) are apparent. In the discussion which follows, line locations indicated by L, K and T refer to leading edge, keel and trailing edge, respectively.

Single Keel Stage 1: Lowest loads were recorded at the nose for both the leading edge and keel lines (see Figure 83). Highest loads were obtained near the center of the leading edge and the center of the keel. This load distribution relates to the canopy area distribution during this stage of inflation. The top center of each lobe during stage one is located in the area between leading edge lines 3 and 4 and keel lines 5 and 8.



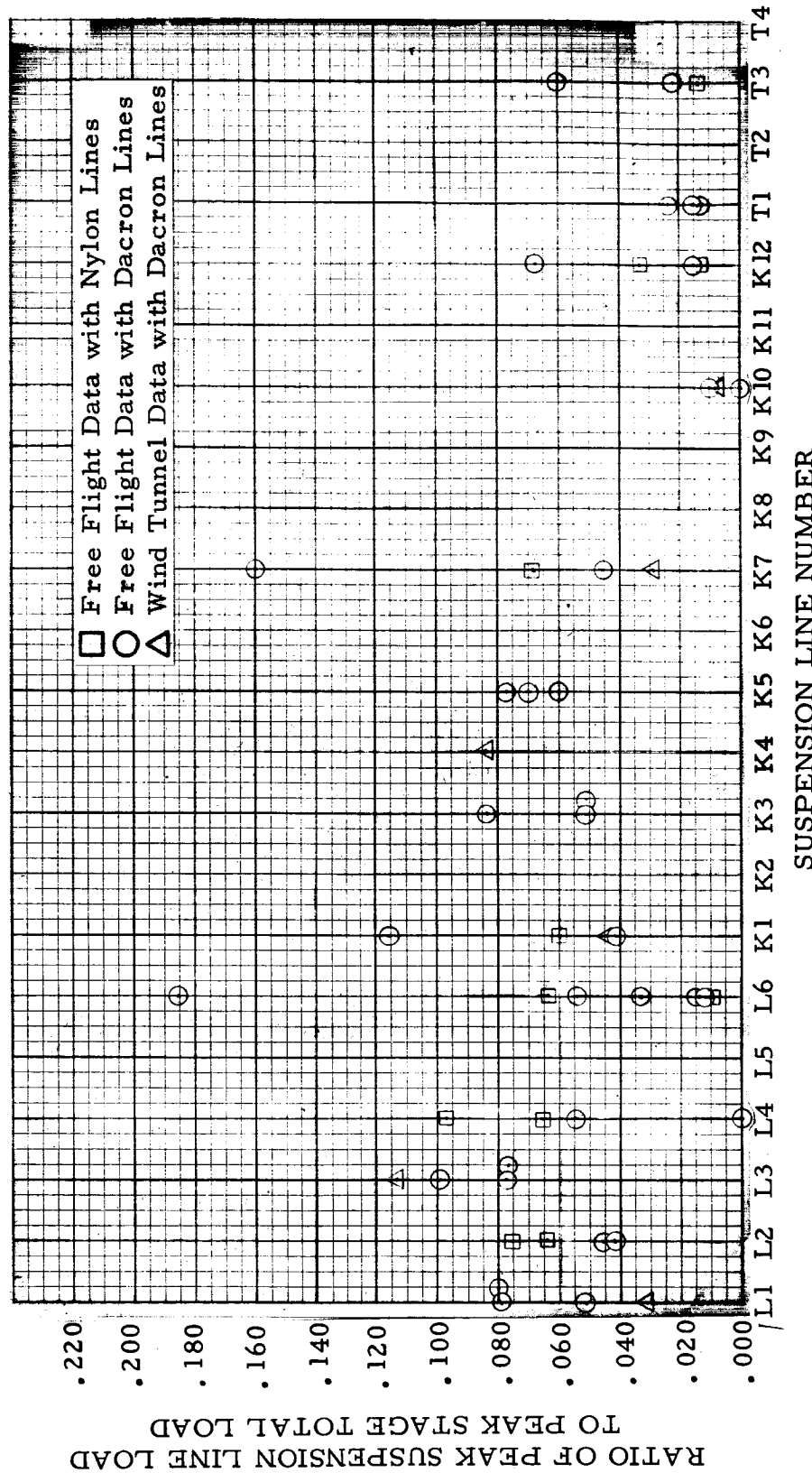
Note: For suspension line numbers L, K, and T, refer to leading edge, keel and trailing edge respectively.

Figure 87. Single Keel, Stage 1 Suspension-Line Load-Ratio Data



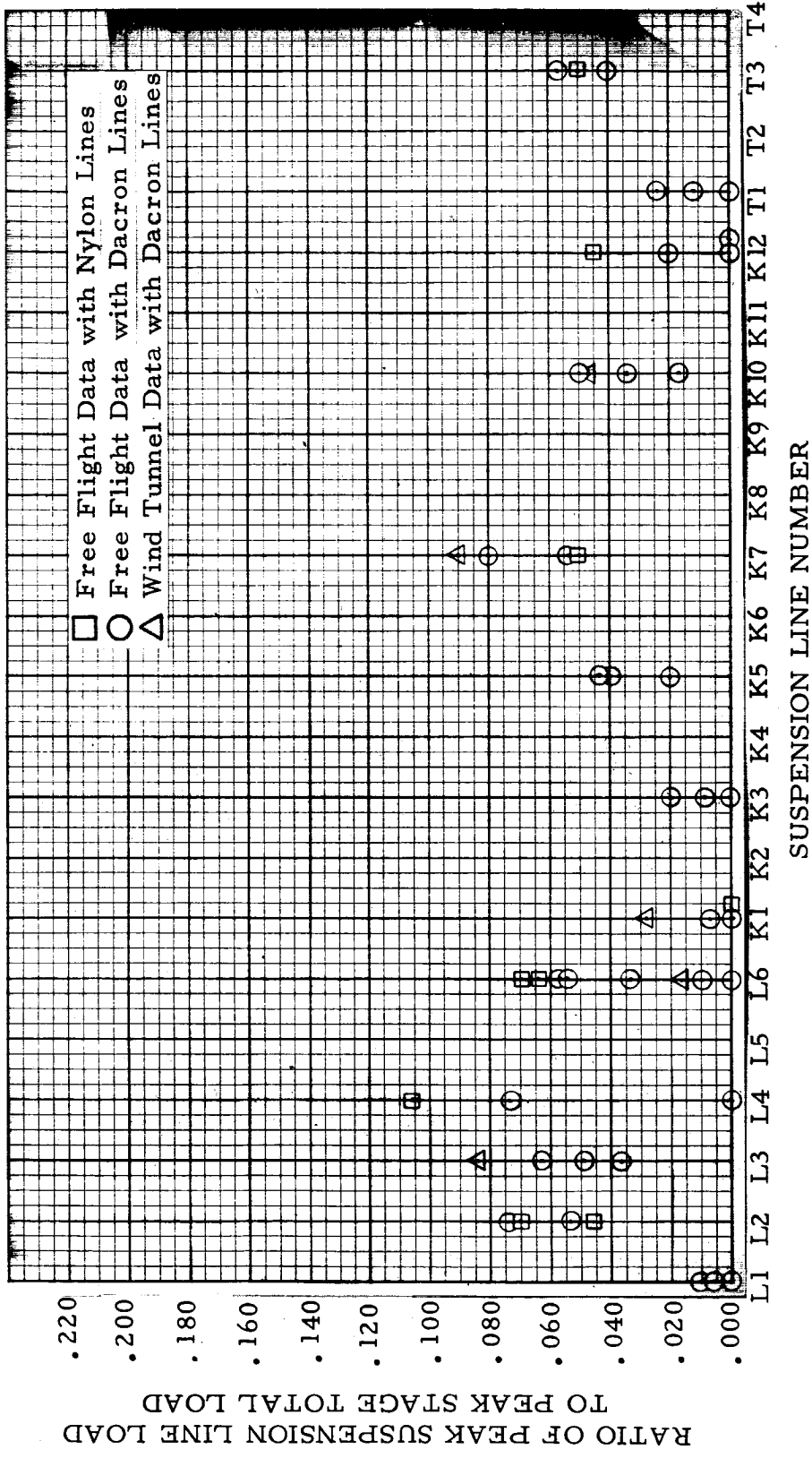
Note: For suspension line numbers L, K, and T, refer to leading edge, keel and trailing edge respectively.

Figure 88 . Single Keel, Stage 2 Suspension-Line Load-Ratio Data



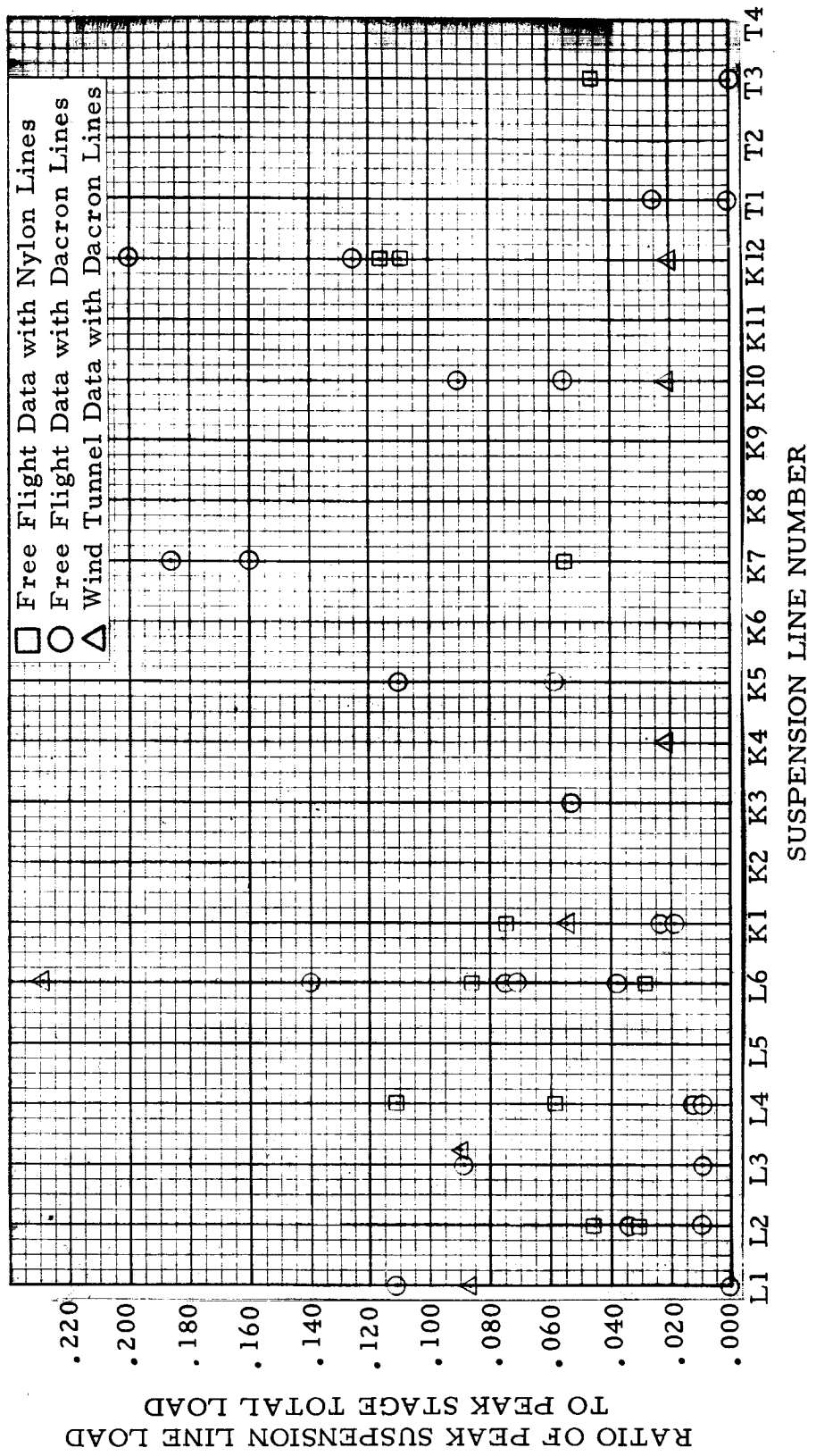
Note: For suspension line numbers L, K, and T, refer to leading edge, keel and trailing edge respectively.

Figure 89. Single Keel, Stage 3 Suspension-Line Load-Ratio Data



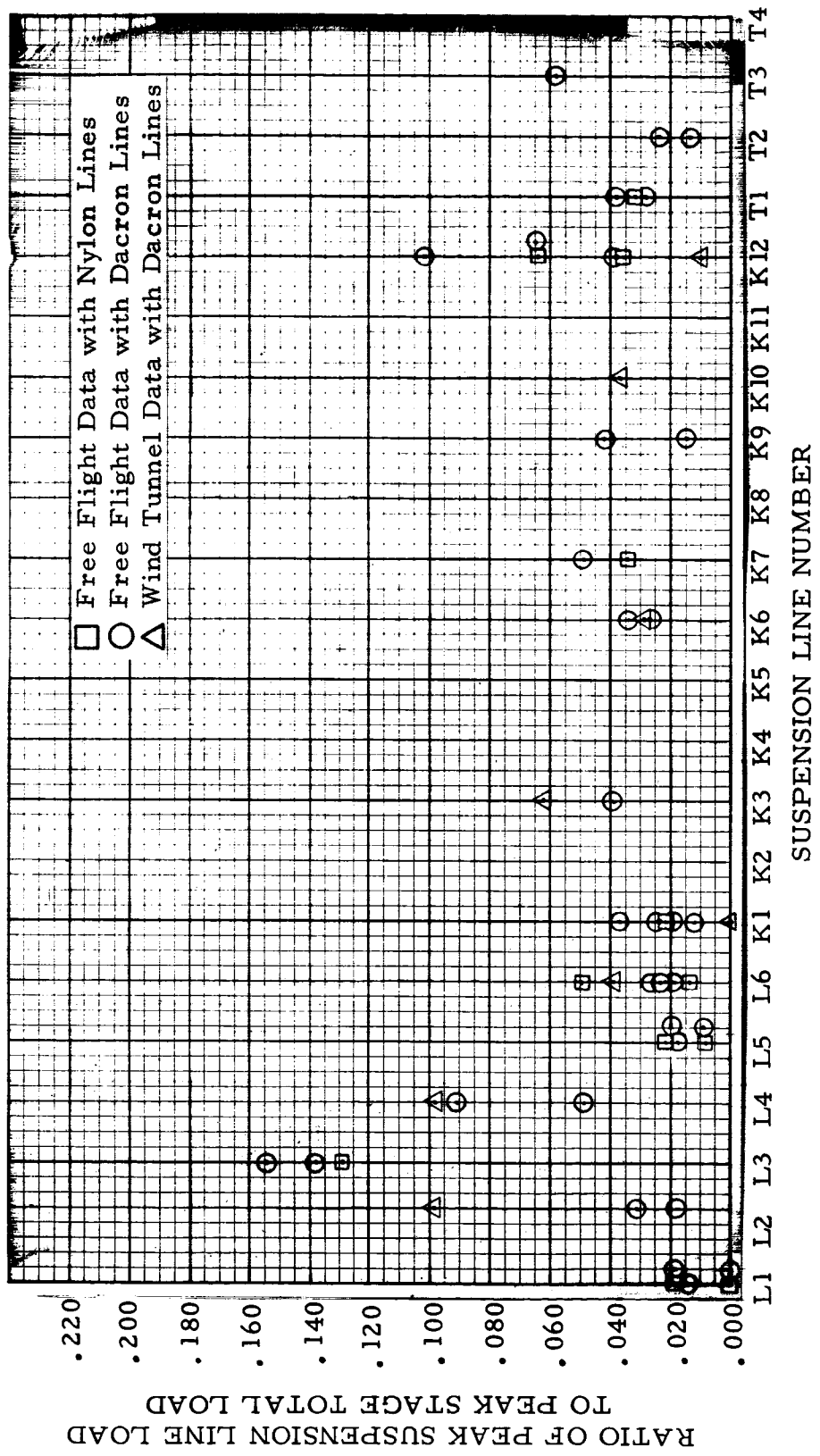
Note: For suspension line numbers L, K, and T, refer to leading edge, keel and trailing edge respectively.

Figure 90. Single Keel, Stage 4 Suspension-Line Load-Ratio Data



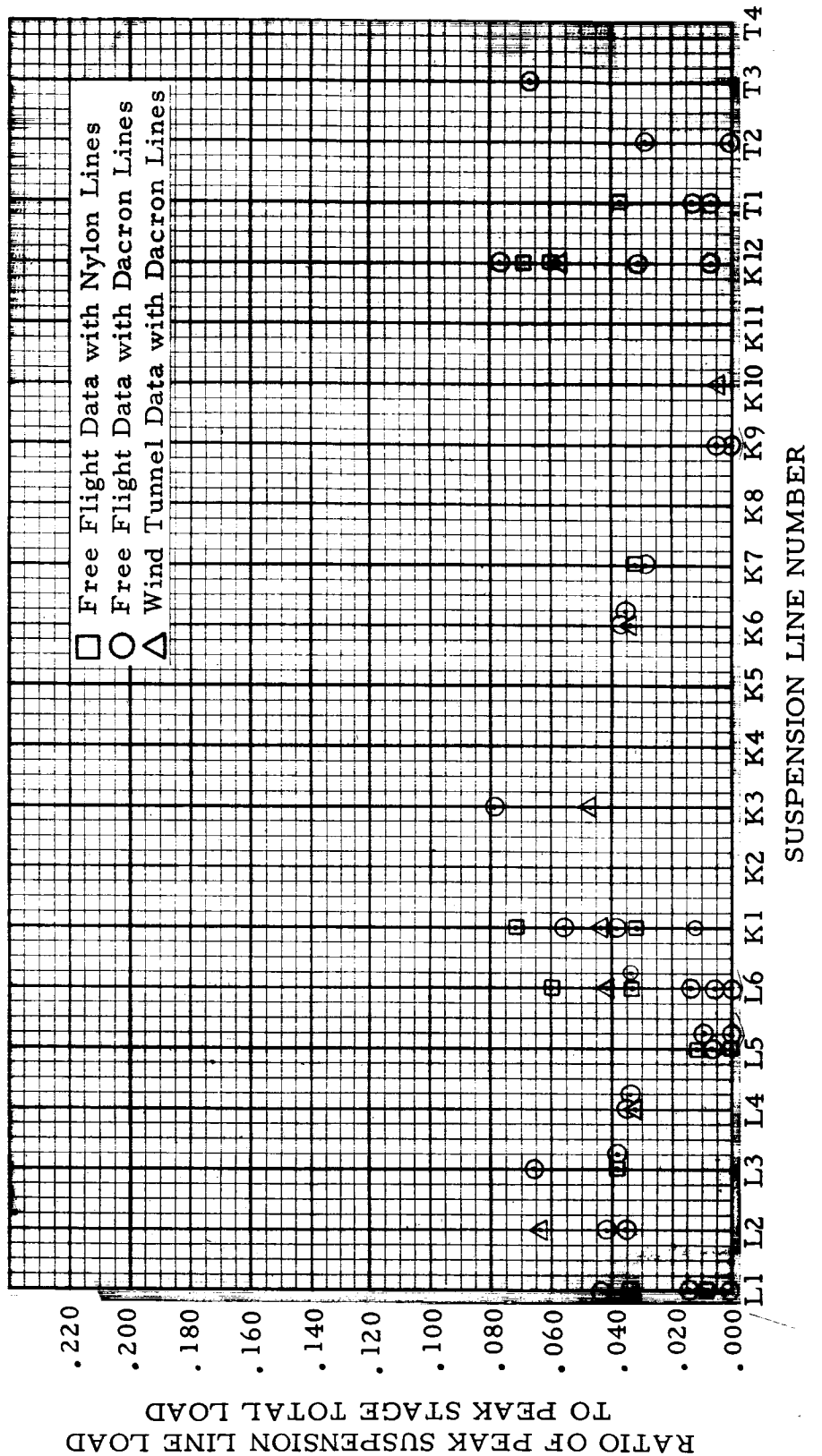
Note: For suspension line numbers L, K, and T, refer to leading edge, keel and trailing edge respectively.

Figure 91. Single Keel, Stage 5 Suspension-Line Load-Ratio Data



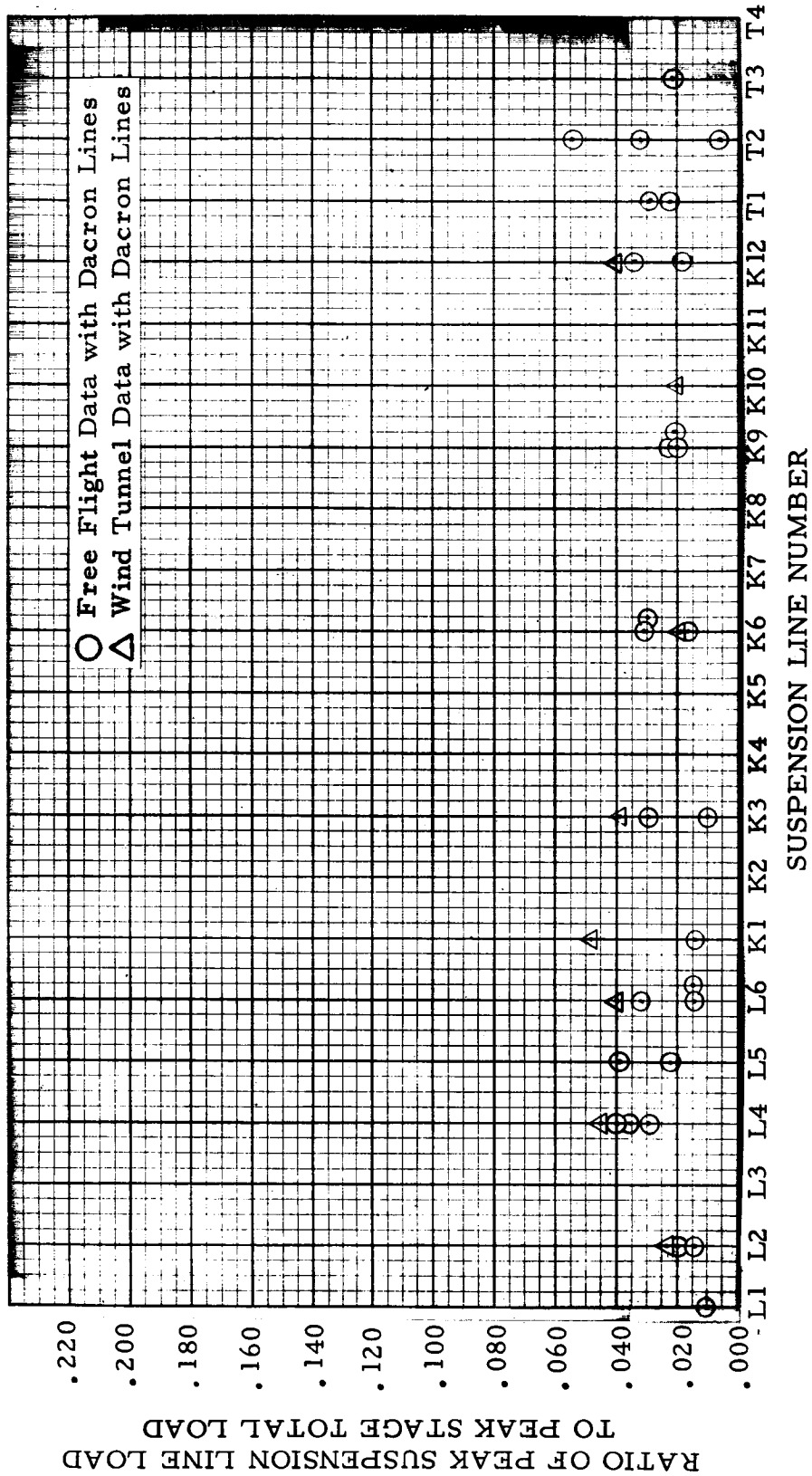
Note: For suspension line numbers L, K, and T, refer to leading edge, keel and trailing edge respectively.

Figure 93 • Twin Keel, Stage 2 Suspension-Line Load-Ratio Data



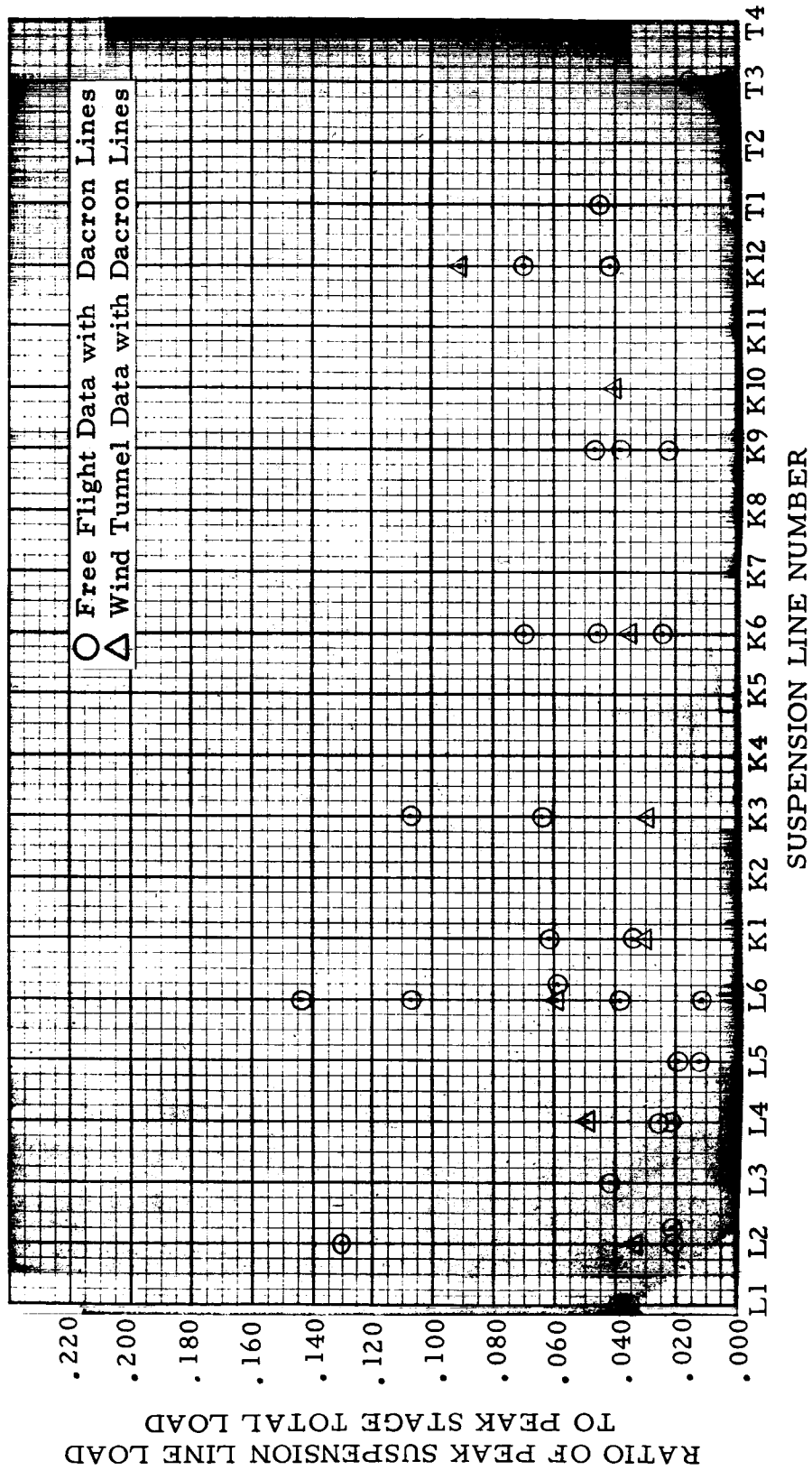
Note: For suspension line numbers L, K, and T, refer to leading edge, keel and trailing edge respectively.

Figure 94. Twin Keel, Stage 3 Suspension-Line Load-Ratio Data



Note: For suspension line numbers L, K, and T, refer to leading edge, keel and trailing edge respectively.

Figure 95. Twin Keel, Stage 4 Suspension-Line Load-Ratio Data



Note: For suspension line numbers L, K, and T, refer to leading edge, keel and trailing edge respectively.

Figure 96. Twin Keel, Stage 5 Suspension-Line Load-Ratio Data

Single Keel Stage 2: During second stage the cloth distribution was basically the same as stage one, ~~one~~, except that the canopy inlet areas (leading edges) were allowed to open further. This produced the same type of load distribution as shown for stage one (see Figure 84).

Single Keel Stage 3: During third stage the keel was released, allowing the forward portion of the wing surface to inflate (the trailing edges remained gathered). The highest loads were measured on the suspension lines in the nose area of the wing (see Figure 85).

Single Keel Stage 4: During fourth stage the trailing edges were released. The leading edges showed a relatively uniform load distribution. The maximum keel line load occurred at Line K7 (see Figure 86).

Single Keel Stage 5: These data show a wide range of scatter for each line, with a relatively uniform distribution over all the suspension lines (see Figure 87).

Twin Keel Stage 1: During first stage, relatively uniform loading was obtained, with some indication of high load distribution in the regions of the centers of the leading edges and keels (see Figure 88).

Twin Keel Stage 2: During second stage, high peak loads were measured at the center of the leading edge (see Figure 89). Also, there was some indication of a peak at the center of the keel, although keel loading appeared to be relatively uniform. With the two lobes formed during stage two, peaks at the centers of the leading edges were expected.

Twin Keel Stage 3: The opening of the center lobe during third stage allowed the leading edge to fully inflate (the trailing edges were still gathered). Consequently, higher loading for the nose area lines was experienced, due to the increased wing area in the forward portion of the wing (see Figure 90).

Twin Keel Stage 4: Suspension line load distribution was relatively uniform in fourth stage (see Figure 91).

Twin Keel Stage 5: Load distribution obtained along the leading edge in fifth stage was relatively uniform except for tip line (L6) (see Figure 92). The L6 peak was probably caused by the fact that L5 was slack during the gliding phase of the flight. High loads were also indicated at the K3 and K12 locations.

Comparison of Wind Tunnel and Free Flight Suspension Line Load Data. - In addition to free flight suspension line load data, Figures 87 through 96 show data obtained during the Langley wind tunnel test program. The wind tunnel data in general are comparable to the data obtained during free flight and show generally the same load distributions. Therefore, wind tunnel data may be used for design purposes.

Effect of Suspension Line Elongation During Deployment on Gliding Flight Characteristics. - A secondary objective of the deployment tests was to evaluate the effect on flight trim of suspension line elongation resulting from deployment loads. Nylon and dacron cord having different elongation characteristics were both considered as candidate materials for use in larger scale parawings. Accordingly, four of the sixteen small scale

deployment tests were conducted with wings having nylon suspension lines. These were Tests 102T, 102S, 107T and 107S. The other twelve tests utilized models having dacron lines. In all sixteen tests the deployment loads applied to the lines were small percentages of the strength of the suspension lines. Consequently, loads did not cause sufficient line stretch to result in out-of-trim flight in any of the tests. Therefore, no evidence was obtained from which conclusions could be drawn regarding the effect of suspension line material elongation on gliding flight trim.

Reefing Line Loads

Table 23 gives the reefing line load data obtained during the free flight deployment tests. This table shows the data as ratios of maximum reefing line load for each reefing line to maximum total load. As with the suspension line load ratios, these data show a great deal of scatter. Because of the small sample size and the historical evidence that the inflation process of non-rigid devices such as parachutes or parawings is a random process, the data presented in Table 23 should be considered as showing order of magnitude loads for reefing line design.

Table 23. Reefing Line Load Ratio Data

Test	Stage 1			Stage 2			Stage 3		
	SRL	CRL	RRL	SRL	CRL	RRL	SRL	CRL	RRL
100T	.080	.087	*	0	.213	*	0	0	*
103T	.175	ND	*	0	ND	*	0	0	*
105T	ND	.067	.072	0	.152	.130	0	0	.079
100S	.111	.045	.055	0	.093	.150	0	0	.085
103S	.075	.068	*	0	ND	*	0	0	*
105S	.013	.026	*	0	.156	*	0	0	*

NOTES:

SRL - Side lobe reefing line

CRL - Center lobe reefing line for twin keel, keel reefing line for single keel

RRL - Trailing edge gathering line

ND - Data not readable

* - This reefing line not instrumented for these data

CONCLUDING REMARKS

Based on the results of the small scale test phase of the program, the following conclusions are drawn:

1. The maximum lift-to-drag ratio measured in the wind tunnel (with the line rigging used in test) was 2.7 for the single keel parawing and 3.4 for the twin keel parawing. Free flight maximum L/D was lower than that measured in the wind tunnel. Maximum free flight L/D was 2.97 for the twin keel parawing and 2.30 for the single keel parawing.
2. Maximum L/D is significantly affected by the tip suspension line lengths and by wing loading. Also, L/D performance is greatly influenced by the inflated shape of the nose area of the wing. Distortions of the nose area, due either to canopy structural design or variations in suspension line lengths in the nose area, can seriously reduce L/D capability.
3. A limited number of suspension lines added to the leading edges and the keels of the twin keel models generally did not degrade L/D performance. This is also true for the single keel models, provided the added lines were of sufficient length that the canopy shape, particularly in the nose area, was not distorted from the shape obtained with the basic single keel parawing line rigging.
4. L/D modulation capability, using rear keel line(s) retraction, appears limited to a reduction of approximately 0.5 from maximum L/D, both for single and twin keel models.

5. First stage opening loads during the scale tests varied from 4.0 g's to 5.8 g's for the single keel parawing and 3.9 g's to 6.8 g's for the twin keel parawing. The ranges of reefing ratios tested during the scale tests were .116 to .201 for the single keel parawing and .141 to .219 for the twin keel parawing.

During deployment stages two, three, four and five the average opening loads were 3.60 g's, 2.13 g's, 1.55 g's and 1.96 g's, respectively, for the single keel parawing and 3.22 g's, 2.92 g's, 2.00 g's and 2.65 g's, respectively for the twin keel parawing.

6. Suspension line load distribution varied considerably from stage to stage as a result of non-uniform area growth from stage to stage. Scatter of individual line load data in any given stage was due to random variations in the mechanics and dynamics of the reefing stages.
7. A characteristic two-slope drag area time history was obtained in first stage inflation during the wind tunnel deployment tests and the free flight deployment tests.
8. First stage filling time was inversely proportional to inlet area during both the Langley wind tunnel tests and the flight tests.
9. During ground controlled flight tests, the twin keel design was easier to control than the single keel design. The twin keel wings would maintain a directional heading, whereas the single keel wings would not.
10. The single keel models required less control line travel to obtain a given rate of turn than the twin keel. Turn rate was a linear function of control line

movement for single tip control inputs. Turn rates of up to 125 degrees per second with the single keel parawing and 110 degrees per second with the twin keel parawing were obtained using single tip control inputs. Differential tip control was tested with the twin keel parawing, and turn rate using this method was not a linear function of the differential tip control input. Turn rate was apparently limited by canopy distortion during the differential control input tests.

APPENDIX A

TEST VEHICLES
AND INSTRUMENTATION

The test vehicles and instrumentation used in the small scale parawing flight tests at the El Mirage and El Centro test sites are described in this Appendix.

Test Vehicles for Free Flight
Gliding Performance Tests

The weight vehicle used during the initial aerial verification of parawing rigging had no instrumentation or provisions for control. This phase of the test program was identified as Phase IA. A controllable vehicle, capable of producing variations in parawing tip and aft keel line lengths during glide descent, was used in the later controlled flight tests. These tests were identified as Phase IB.

Weight Vehicle. - The weight vehicle consisted of a welded steel box equipped with four harness attachment fittings, a removable top cover plate and a set of ballast bars. This vehicle is schematically illustrated in Figure 97. A set of ballast plates permitted variation of the vehicle weight over a range from 159 to 583 pounds in increments of approximately 20 pounds. In addition to the four parawing harness attachment fittings, four suspension panel attachment fittings were provided on the vehicle side plates. Two triangular fabric suspension panels were attached to the vehicle by means of these fittings. The suspension panels were used to suspend the vehicle from the helicopter drop aircraft.

Controllable Vehicle. - The controllable vehicle consisted of a structural framework, landing-impact attenuation skids and

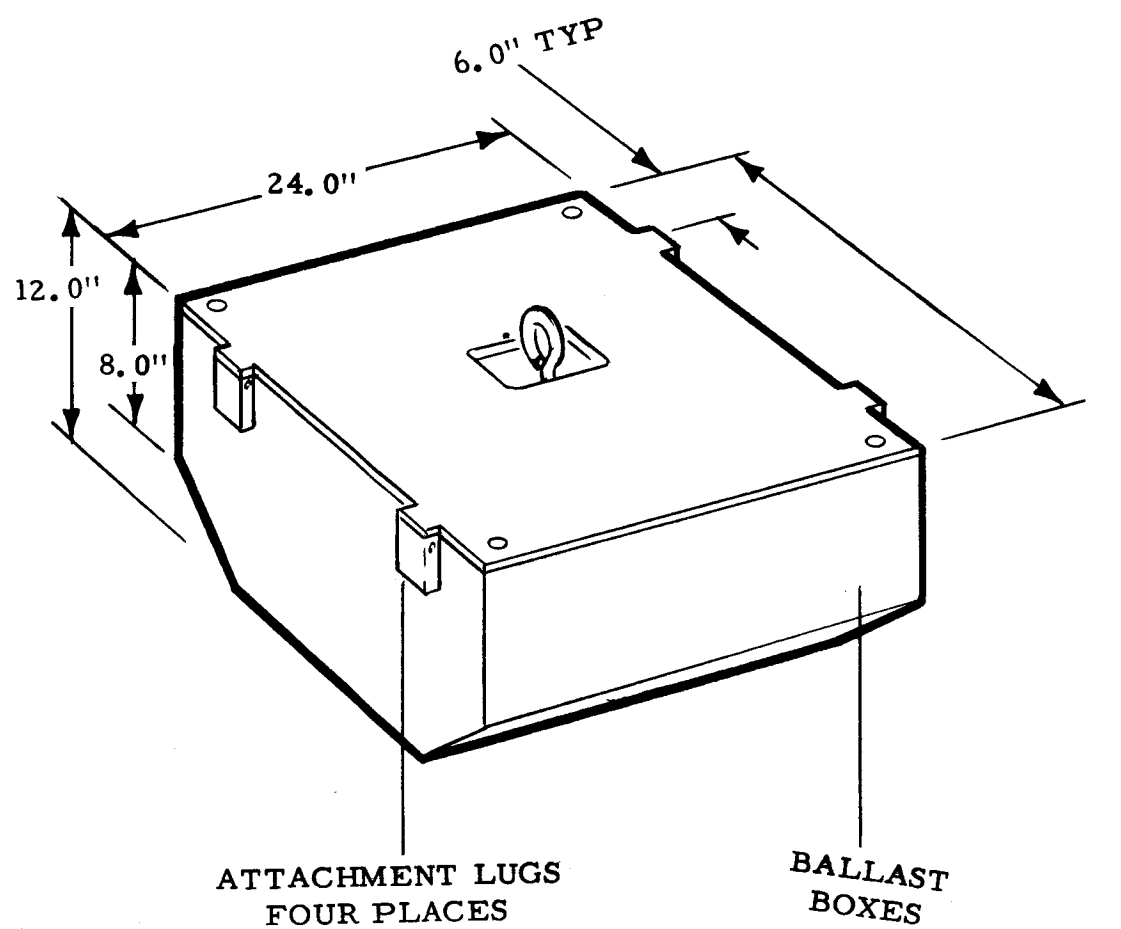


Figure 97. Weight Vehicle

ballast installations. The vehicle contained data acquisition instrumentation, flight control actuators and radio command receiving and decoding equipment. The controllable test vehicle is shown in Figure 98.

The vehicle weight could be varied from 199 pounds to 479 pounds. The basic vehicle structure provided mountings for the keel and wing tip control mechanisms, an L/D indicator boom, and a four channel telemetry unit. The landing/impact skids and styrofoam landing-shock-attenuation blocks were secured to the underside of the vehicle structure. The parawing harness and fabric carrier-suspension flaps were secured to four attachment points provided on the top periphery of the structural frame. The vehicle frame was covered with a thin sheet metal skin for internal equipment protection. The vehicle exterior was painted black and white in a pattern designed to aid in determining vehicle attitude during the tests.

During tests, the two parawing tip lines were connected to cables which in turn were attached to the turn control winch. The aft keel line(s) were connected to the L/D modulation control winch. These control units (turn and L/D modulation) were controlled by inputs from the ground radio command unit.

Instrumentation for Free Flight Gliding Performance Tests

L/D Performance Tests. - The instrumentation used for the L/D performance tests measured flight path angle relative to the earth, changes in rear keel suspension line(s) length, and changes in the magnitude of tip control line lengths. Flight path angle was obtained with an instrument which measured angle of attack of the L/D indicator relative to the airstream and attitude of the L/D indicator relative to the earth. This was done by means of a wind vane in the pitch plane which measured

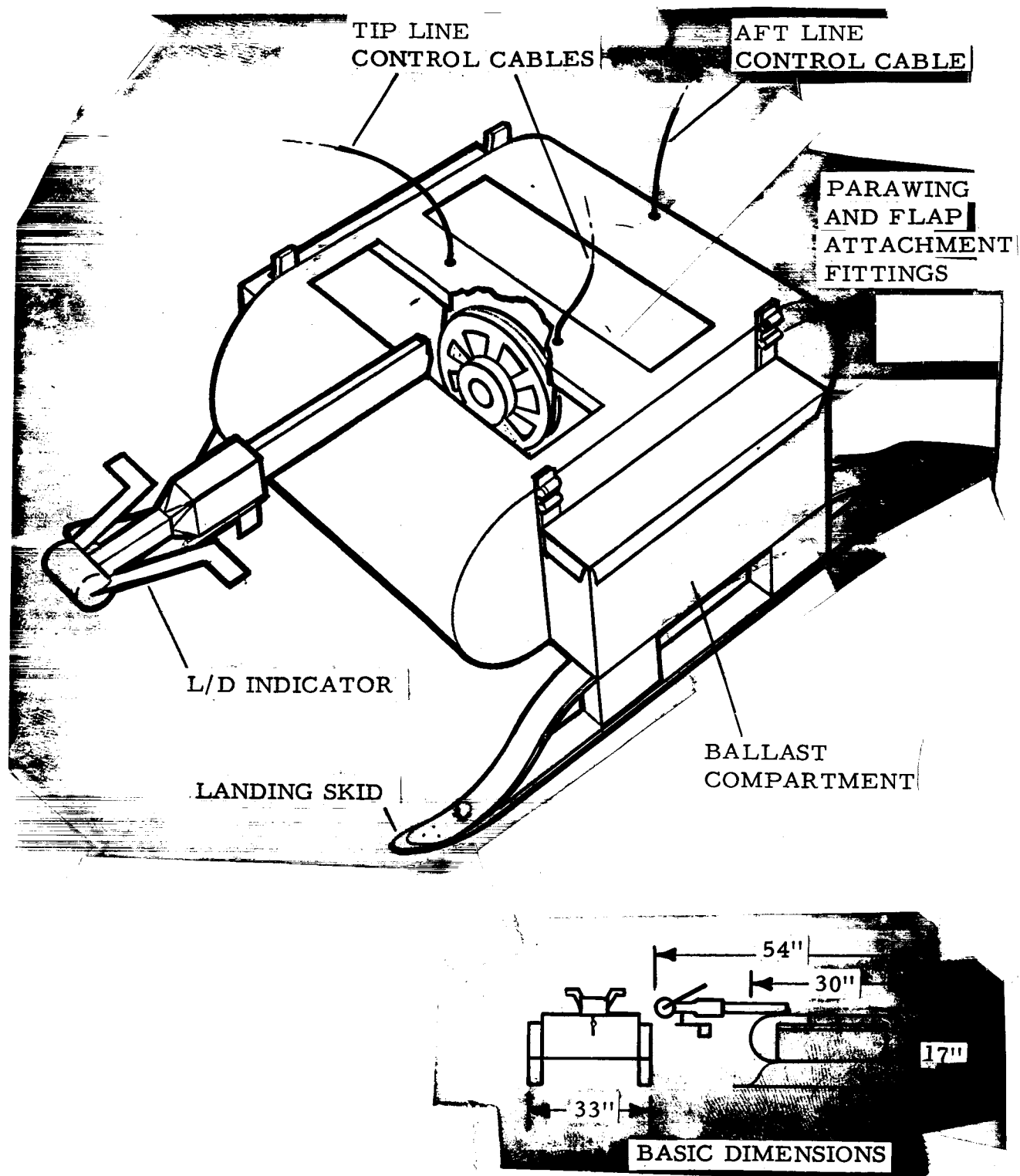


Figure 98. Controllable Vehicle - El Mirage Tests

angle of attack and a pendulum, also in the pitch plane, which provided an earth oriented vertical reference. For unaccelerated flight, the sum of the angle of attack of the wind vane and a vertical reference angle gave the flight path angle which in turn determined L/D. Figure 99 shows a three view layout of the L/D indicator.

The pitch vane and its external counterweight were mounted in low friction bearings. A high-resolution, low-friction potentiometer was driven by the vane and was the mechanical-to-electrical transducer in the system.

The vertical reference was a self-contained unit, utilizing a damped pendulum and a potentiometer as the indicating and readout elements. This unit was mounted parallel to the longitudinal axis of the vehicle in the rear housing of the indicator assembly.

At 8 ft per second IAS the pitch indicator was accurate to ± 0.25 degrees. The vertical reference was accurate to ± 0.25 degree. The L/D indicator had the capability of indicating flight path angle with an accuracy of ± 0.5 degrees.

The positions of the rear keel control line and tip control lines were monitored by potentiometers keyed to the cable drums. The outputs from these potentiometers and those in the L/D indicator were telemetered to a ground receiving station, where the signal was decoded and the data recorded on strip chart recorders.

Turn Rate Tests. - The data telemetered to the ground during the turn rate tests consisted of changes in flight heading and tip control line positions. Changes in flight heading were obtained by use of a directional gyro. Tip control settings were obtained by the same method used for the L/D performance tests.

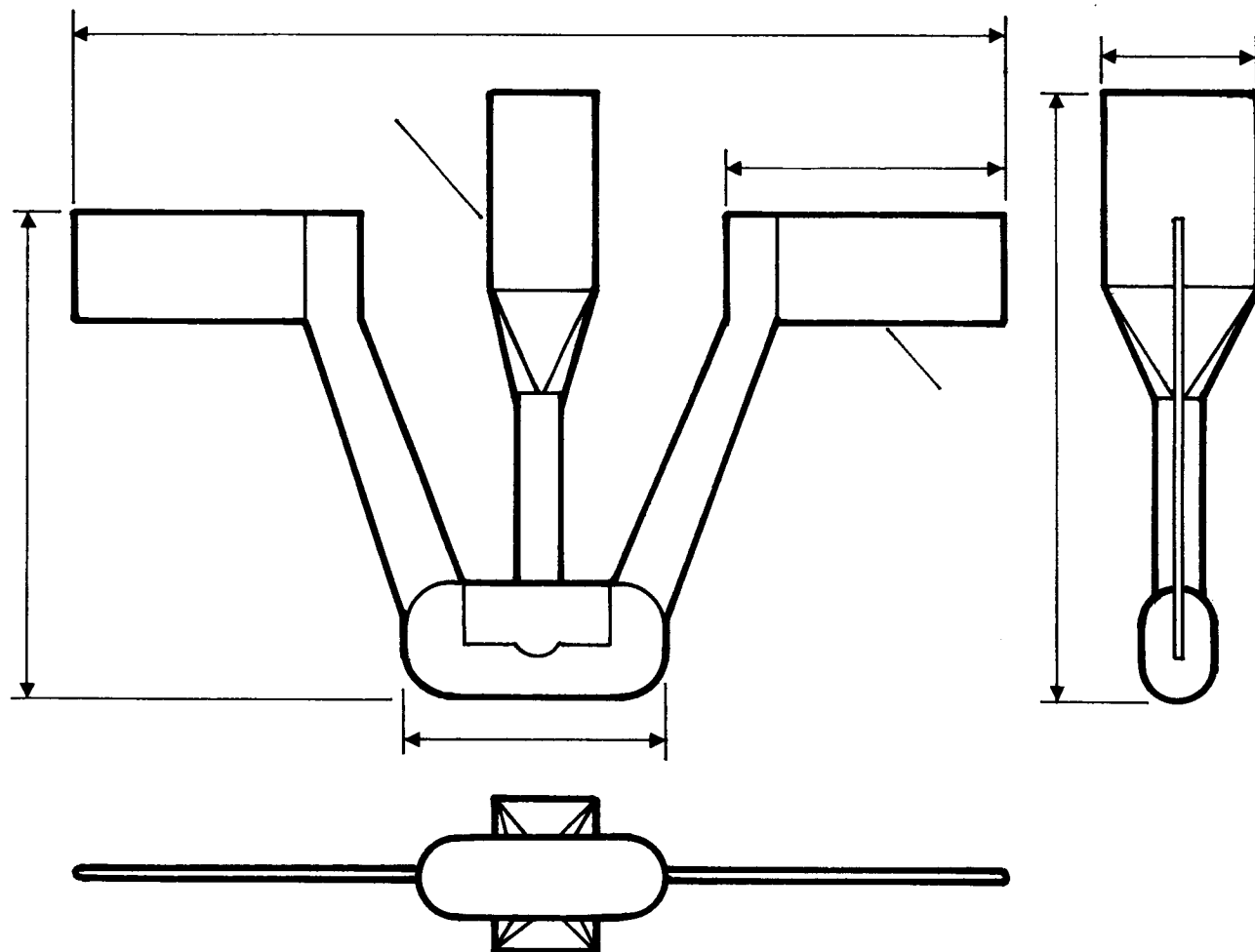


Figure 99. L/D Indicator

Test Vehicles for Deployment Tests

The two functional verification tests conducted at El Mirage employed the same weight vehicle ("weight bucket") used for the free flight performance test, as shown in Figure 97, with the addition of a sequencing subsystem. This sequencing subsystem consisted of dual, independent lanyard operated arming switches, time delay relays, and batteries. The parawing pack was rigged on top of the vehicle in the same manner used for the free flight performance tests. The system was then suspended from the helicopter cargo-release hook by the suspension flaps.

A bomb-type test vehicle was used in the reefed deployment tests at El Centro. It consisted of a cylindrical structure with a flared external aft section and a removable conical nose. The vehicle was designed for launch from either a C-130 or a B-66 carrier aircraft. Launches from a C-130 were made from the rear of the cargo compartment with the aid of an inclined ramp. B-66 launches were made from the bomb bay by use of launch lugs mounted on the centerline of the bomb. Large variations in vehicle weight were obtained by attaching ballast bars externally. Smaller adjustments were made by adding lead shot to ballast compartments in the vehicle nose. The vehicle contained a compartment in the aft end to accommodate the packed parawing, programmer parachute, pyrotechnically operated programmer parachute disconnects, high speed motion picture camera, and system safety switches. The forward section of the bomb contained a telemetry (TM) and sequencer module. By removing the vehicle nose, the sequencer and TM module could be extracted for checkout and resetting. Figure 100 shows the vehicle external envelope.

Instrumentation for Deployment Tests

Instrumentation used in the deployment tests included a total load link which measured the total loads applied to the

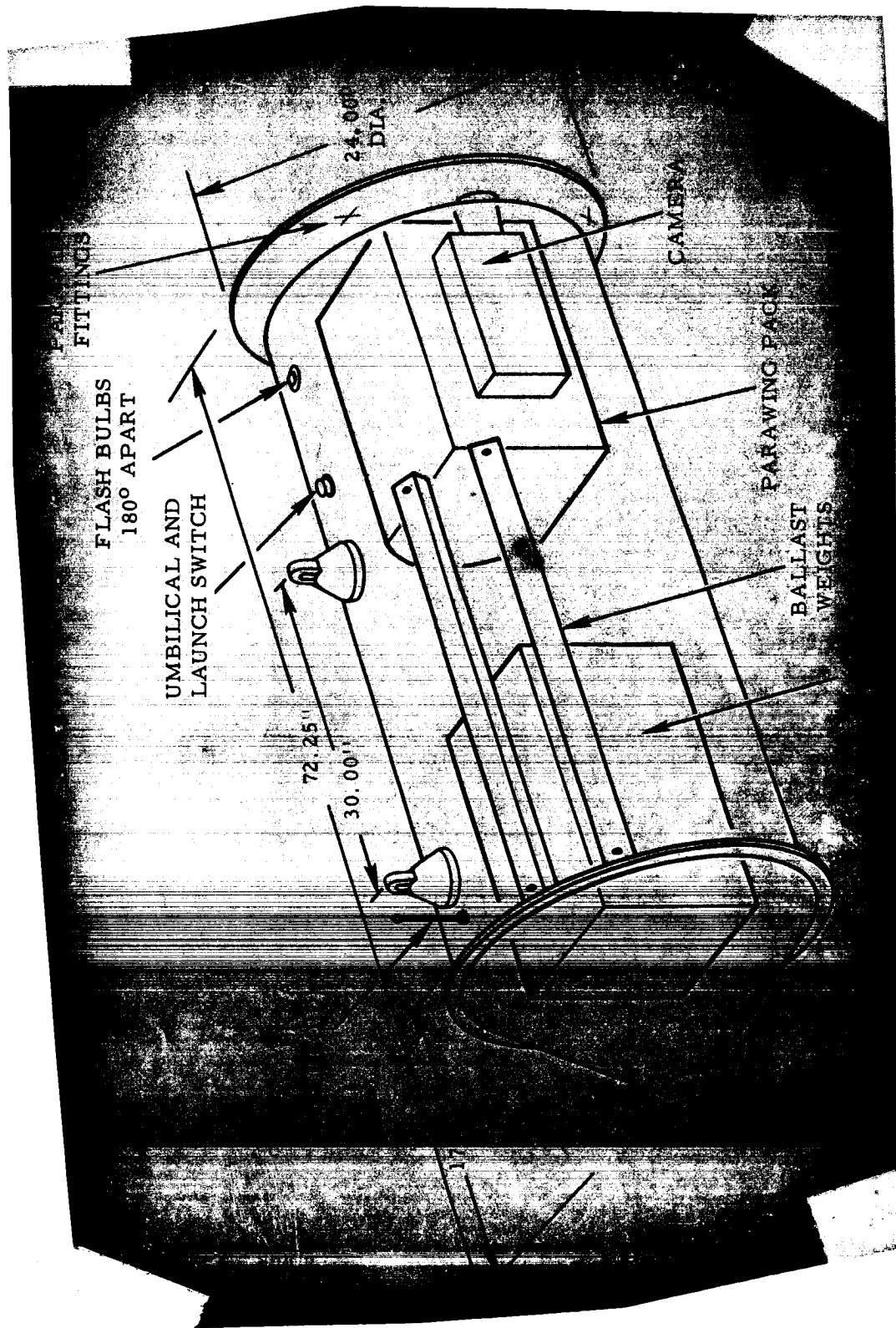


Figure 100. Small Scale Bomb Vehicle - El Centro Tests

test vehicle by the parawing model, linear accelerometers to measure acceleration felt by the test vehicle along the three vehicle body axes, and load links to measure individual suspension line loads. In certain of the tests, reefing-line-load links were mounted in the parawing model and their output read in lieu of the output from certain of the accelerometers. The information measured by these transducers was telemetered to a ground receiving station and recorded.

In addition to the telemetered information, an on-board camera recorded the parawing deployment-and-opening portion of the flight. Air-to-air and ground-to-air motion picture coverage of the flight was also obtained. These films were used in conjunction with the TM and on-board camera data to obtain event times plus qualitative information on parawing deployment and inflation behavior. Trajectory parameters such as dynamic pressure, flight path angle, etc., were obtained from Askania phototheodolite space position measurements.

REFERENCES

1. Naeseth, Rodger L; and Fournier, Paul G.: Low-Speed Wind Tunnel Investigation of Tension Structure Parawings. NASA TN D-3940, June 1967
2. Bugg, Frank M; and Sleeman, William C., Jr.: Low-Speed Tests of an All-Flexible Parawing for Landing a Lifting-Body Spacecraft. NASA TN D-4010, June 1967
3. Gainer, Thomas G.: Investigation of Opening Characteristics of an All-Flexible Parawing. NASA TN D-5031, Feb. 1969
4. Ware, George M.: Wind-Tunnel Investigation of the Aerodynamic Characteristics of a Twin-Keel Parawing. NASA TN-D-5199, May 1969
5. Libbey, Charles E.; Ware, George M.; and Naeseth, Rodger L.: Wind-Tunnel Investigation of the Static Aerodynamic Characteristics of an 18-Foot (5.49 Meter) All Flexible Parawing. NASA TN-D-3856, 1967
6. Barton, Richard L.: Scale Factors for Parachute Opening. NASA TN D-4123, Sept. 1967
7. Eichblatt, David L.; Moore, Robert H., and Barton, Richard L.: Experimental Verification of Scale Factors for Parawing Opening Characteristics. NASA TN D-4665, Aug. 1968
8. Waters, M. H. L.: Elementary Estimates of Parachute Opening Forces. Technical Note: Mech. Eng. 238, Royal Aircraft Establishment, Farnbrough, Hants.